Government of Western Australia

Department of
Industry and Resources

RECORD
2004/16

GOLD AND NICKEL DEPOSITS IN THE ARCHAEAN NORSEMAN–WILUNA GREENSTONE BELT, YILGARN CRATON, WESTERN AUSTRALIA — A FIELD GUIDE

compiled by P. Neumayr, M. Harris,
and S. W. Beresford

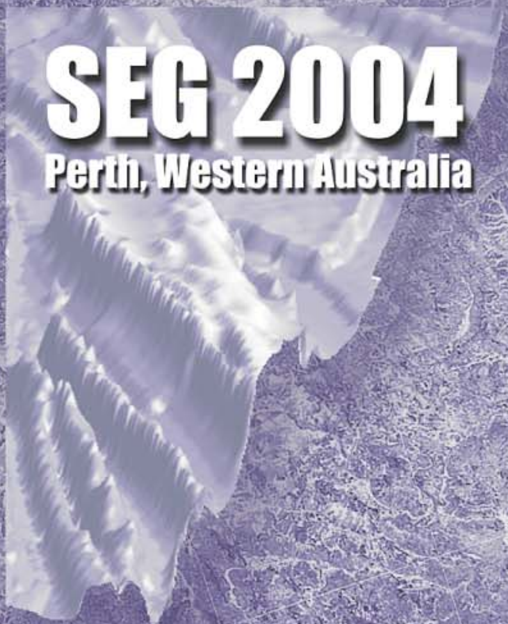

Geological Survey of Western Australia

SEG 2004
Predictive Mineral Discovery Under Cover

Presented by

Society of Economic Geologists

Geoconferences (WA) Inc.

Society for Geology Applied to Mineral Deposits

Platinum sponsors

AngloGold Ashanti Australia Limited

Barrick Gold of Australia Limited

LionOre Australia

Perilya Limited

Rio Tinto Exploration Pty Limited

WMC Resources Limited

Gold sponsors

Anglo American Exploration (Australia) Pty Ltd
BHP Billiton
CSIRO Exploration and Mining
De Beers Australia Exploration Limited
Gold Fields Australasia Pty Ltd
GSA Specialist Group in Economic Geology
Independence Group NL
MPI Mines Ltd
Newcrest Mining Limited
Newmont Australia Limited
Placer Dome Asia Pacific
Resolute Mining Limited
Sons of Gwalia Limited
Teck Cominco Australia Pty Ltd

Silver sponsors

Anvil Mining Limited
Cryptodome Pty Ltd
Gnomic Exploration Services Pty Ltd
Newexco Mining and Exploration Services
Southern Geoscience Consultants
Spatial Analysis Services
SRK Consulting
Terra Search Pty Ltd
UTS Geophysics

Backpack sponsors

Centre for Global Metallogeny
CODES Special Research Centre
CRC LEME
EGRU, James Cook University
Geological Survey of Western Australia
Geoscience Australia
*pmd*CRC*

Official publication

Gold & Minerals Gazette

Icebreaker sponsor

Fugro Airborne Surveys Pty Ltd

Sundowner sponsors

CSA Australia
Fractal Technologies
GPX Services Pty Ltd
RSG Global

GEOLOGICAL SURVEY OF WESTERN AUSTRALIA

Record 2004/16

GOLD AND NICKEL DEPOSITS IN THE ARCHAEAN NORSEMAN–WILUNA GREENSTONE BELT, YILGARN CRATON, WESTERN AUSTRALIA — A FIELD GUIDE

compiled by
P. Neumayr[1], M. Harris[2], and S. W. Beresford[3]

[1] The University of Western Australia
[2] Cryptodome Pty Ltd
[3] Monash University

Perth 2004

Disclaimer:
The book 'Gold and nickel deposits of the Archaean Norseman–Wiluna greenstone belt, Yilgarn Craton, Western Australia — a field guide' is published by the Geological Survey of Western Australia (GSWA) to accompany the field trip of the same name conducted as part of the SEG 2004: Predictive Mineral Discovery Under Cover conference, held in Perth from 27 September to 1 October 2004. Authorship of this book included contributors from academic institutions, mining and exploration companies, and GSWA. All papers were edited to bring them into GSWA house style. The scientific content, resource data, and initial drafting of the figures were the responsibility of the authors

REFERENCE
The recommended reference for this publication is:
NEUMAYR, P., HARRIS, M., and BERESFORD, S. W., compilers, 2004, Gold and nickel deposits in the Norseman–Wiluna greenstone belt, Yilgarn Craton, Western Australia — a field guide: Western Australia Geological Survey, Record 2004/16, 116p.

National Library of Australia Card Number and ISBN 0 7307 8978 0

Unless identified as a local mine or exploration grid or height, grid and height references in this publication refer to the Geocentric Datum of Australia 1994 (GDA94) and Australian Height Datum (AHD), respectively.

Cover image modified from Landsat data, courtesy of ACRES. The conference logo is based on a vectorial fuzzy logic prospectivity image generated by Spatial Analysis Services.

Printed by Digital Documents, Perth, Western Australia

Published 2004 by Geological Survey of Western Australia

Further details of geological publications and maps produced by the Geological Survey of Western Australia are available from:

Information Centre
Department of Industry and Resources
100 Plain Street
EAST PERTH, WESTERN AUSTRALIA 6004
Telephone: +61 08 9222 3459 Facsimile: +61 8 9222 3444

www.doir.wa.gov.au/gswa/onlinepublications

Contents

Gold and nickel deposits in the Archaean Norseman–Wiluna greenstone belt, Yilgarn Craton, Western Australia — an introduction

by

P. Neumayr[1], M. Harris[2], and S. W. Beresford[3]

Introduction

This field guide provides background technical information on the mines and localities to be visited during an excursion associated with the SEG 2004: Predictive Mineral Discovery Under Cover conference, held in Perth in September–October 2004. It covers world-class gold and nickel deposits in the extremely well endowed and deeply weathered Kalgoorlie Terrane, and investigates the main stratigraphic and structural features controlling the localization of hydrothermal (orogenic) gold and magmatic (komatiitic) nickel mineralization. The itinerary includes older established mines and recently discovered deposits, starting in the Kalgoorlie–Norseman district and then travelling 500 km north to the Wiluna–Leinster district.

The individual contributions address topics such as:

1. regional geology of the Eastern Goldfields Province of the Yilgarn Craton;
2. geological setting of several major gold and nickel ore deposits;
3. principle mineral assemblages in these gold and nickel deposits;
4. structural and lithological controls on gold and nickel mineralization;
5. principle alteration styles associated with the orogenic gold deposits;
6. exploration procedures that led to the discovery of each deposit;
7. future directions for predicting the discovery of these deposit types under cover.

The excursion first visits the main gold and nickel mines around and to the south of Kalgoorlie, such as the Golden Mile, Kanowna Belle, and Kundana gold mines, the St Ives gold camp, and the Miitel–Wannaway and Kambalda – Long Shaft nickel orebodies. The second part of the excursion visits the Thunderbox gold mine, and the Mount Keith, Cosmos, Honeymoon Well, and Waterloo nickel mines between Leonora and Wiluna. Presentations at the mine sites will include the latest mining information, detailed geological and structural settings, and most recent research results on ore deposit formation and controls on the location of mineralization. Representative diamond drillcore of host rocks, hydrothermal alteration, and mineralization styles will be examined in company core farms.

The excursion also visits the Joe Lord Core Library of the Geological Survey of Western Australia (GSWA). This facility archives diamond drillcore that is representative of the geology and mineralization of the Eastern Goldfields Province.

Modern history of gold and nickel exploration, and mining in the Yilgarn Craton

Gold

The modern gold rush in Western Australia commenced in the middle to late 1970s, when higher gold prices stimulated exploration. Exploration expenditure for gold in Western Australia is concentrated within the Yilgarn Craton, and particularly within the Eastern Goldfields Province. Expenditure rose from almost nothing to a peak of around A$500 million in the years 1987–88 (Flint and Abeysinghe, 2001). Both established miners and junior explorers re-evaluated all of the historic mining districts, including Southern Cross, Mount Magnet, Cue, Meekatharra, Norseman, Kalgoorlie, Menzies, Leonora, Laverton, Agnew, and Wiluna. Most developments were based on opencut mining of lower grade haloes left by earlier phases of mining. Several major camps were discovered from ‘greenfields’ exploration, including Plutonic, Boddington, Granny Smith, and Mount McClure.

[1] Centre for Global Metallogeny, School of Earth and Geographical Sciences, The University of Western Australia, Nedlands, W.A. 6009, Australia
[2] Cryptodome Pty Ltd, Post Office Box 7135, Shenton Park, W.A. 6008, Australia
[3] Department of Earth Sciences, Monash University, Victoria 3800, Australia

After a brief decline in exploration expenditure following the stock market crash of October 1987, a new peak of just over A$500 million was reached in 1996–97, and gold production increased steadily to a peak of 220 t in 1996 (Flint and Abeysinghe, 2001). In the 1990s, a more optimistic outlook and a change in exploration methods resulted in the discovery of more greenfields deposits. Deposits were discovered buried beneath Tertiary or Quaternary transported laterite cover, salt lakes, or both, including Bronzewing, Nimary–Jundee, Thunderbox, Kanowna Belle, Sunrise Dam – Cleo, Mount Pleasant, Bounty, and Yilgarn Star.

A new phase of exploration began in 1997–98 when a rapid weakening of the gold price led to a 40% decrease in exploration expenditure. During this period, greenfields exploration was largely abandoned and near-mine 'brownfields' targets were drilled to feed central treatment plants. A trend of amalgamation and take-overs resulted in fewer and bigger companies. Notable successes in brownfields exploration include deep extensions of Granny Smith, Gwalia, Mount Magnet, Kanowna Belle, and Ghost Crab. Near-mine 'blind' discoveries were made at Centenary at Darlot mine, Bellisle at Kambalda – St Ives, and Kundana near Kalgoorlie. The Laverton Tectonic Zone emerged as an even larger gold camp at the turn of the 21st century, with significant discoveries at Sunrise Cleo, Granny Smith, Red October, Chatterbox, and Wallaby.

Western Australia currently produces 8% (210 t) of annual global gold output, but production is set to decline unless major new deposits are discovered in the next three years. However, the steady increase in the gold price from 2001 onwards to the latest high of about US$427 in April 2004 has improved investors' confidence in gold as a hedge commodity. There has been even more consolidation of ownership in the last five years, such that the only remaining wholly Australian-owned companies with significant gold production are Newcrest Mining Limited and Sons of Gwalia Limited (recently entered voluntary administration). Nevertheless, a raft of new junior explorers with promising gold prospects has recently listed on the Australian Stock Exchange (ASX) and some, such as Siberia Mining Corporation Limited, are already in production.

Nickel

In 1992, Australia contributed 887 200 t or 6.5% of world nickel production (Department of Minerals and Energy, Western Australia, 1994). In that year, it was ranked as the world's sixth-largest producer of nickel behind the former Soviet Union, which contributed 24.8% of total production, Canada (21.7%), New Caledonia (11.3%), Indonesia (8.7%), and Botswana (6.7%).

In 2002, Western Australia produced 187 000 t of nickel, which was shipped as concentrates and refined product. Of this, about 60 000 t of metal was produced directly from lateritic nickel ores at Murrin Murrin.

Before the discovery of high-grade nickel sulfide ore at Kambalda in 1966, Western Australia had virtually no nickel reserves (Department of Minerals and Energy, Western Australia, 1994). However, rising world nickel prices and a prolonged strike at The International Nickel Company of Canada Limited's mine at Sudbury, Canada, meant that the discoveries made at Kambalda were developed rapidly, and the famous 'nickel boom' of 1967–71 ensued. During this period, many discoveries were made in a belt between Norseman and Wiluna, which is now recognized as one of the world's major nickel provinces.

Nickel ores in the Yilgarn Craton of Western Australia are divided into sulfide and lateritic ores. Nickel sulfide deposits associated with volcanic ultramafic rocks (komatiites) make up the largest proportion of the sulfide resource, and are also the most important economically. Current and future nickel sulfide production in the Yilgarn Craton comes from mines at Kambalda, Widgiemooltha, Silver Swan, and Carnilya in the Kalgoorlie district; Maggie Hayes – Emily Anne and Forrestania in the Lake Johnston – Southern Cross district; and Leinster, Mount Keith, Cosmos, Honeymoon Well, and Waterloo–Amorac in the Agnew–Wiluna district.

Current and future Archean gold and nickel research programs in Western Australia

Due to the substantial value of mine production for Australia, and with mineral resource exports comprising 78% of all exports in Western Australia, there is a significant focus of research into understanding the genesis of mineral deposits and the geological controls on their location.

The federal (Geoscience Australia, GA) and state government (GSWA) geological authorities are responsible for the acquisition and interpretation of broad-scale data, which are made available to the public.

Geoscience Australia has invested significant resources into terrane- to craton-scale geophysical surveys and the construction of three- and four-dimensional models of the Eastern Goldfields Province. Foundation mapping at local, district, and terrane scales is provided by GSWA. It has also compiled geochemical data at a district scale, and published mineral occurrence data. Reports such as Witt (1993) provide district-scale descriptions and interpretations of mineralization. GSWA also documents all company reports relating to exploration on Western Australian mining tenements.

Apart from the government authorities, significant research is undertaken by publicly and corporately funded organizations, including universities, the Commonwealth Scientific and Industrial Research Organisation (CSIRO), and AMIRA International.

The Centre for Global Metallogeny (CGM) at The University of Western Australia (UWA) was founded as a Key Centre for Teaching and Research in Strategic Mineral Deposits in the late 1980s by Professor David

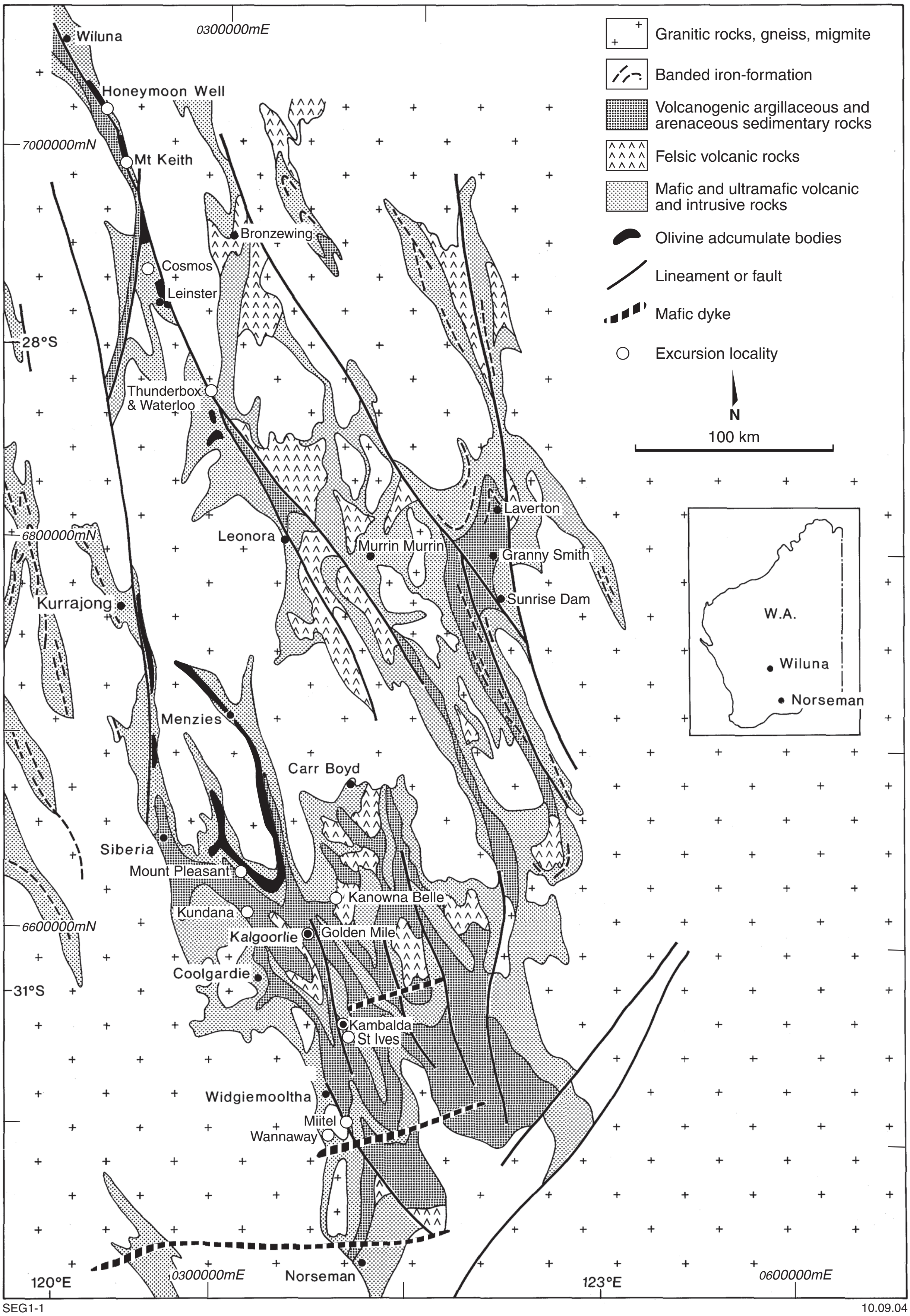

Figure 1. Simplified geological map of the Norseman–Wiluna greenstone belt showing excursion localities (adapted from Hill et al., 2001, fig. 1)

Groves. It has produced numerous research theses at Honours, Masters, and Doctoral levels on Australian and overseas deposits. Studies range from detailed mine-scale projects, to camp- and terrane-scale research on the fundamental controls on orogenic gold and komatiitic nickel deposits in the Yilgarn Craton and worldwide. The pertinent research on mineral deposits has attracted sponsorship and support from many international and national exploration and mining companies.

Despite a threefold increase in exploration expenditure over the past 30 years, the low rate of discovery of large, high-quality orebodies has become unsustainable. Although part of the problem is the ineffective use of available exploration funds, the increasing difficulties of discovering mineable deposits under cover is even more problematic. This has focused an Australian-wide research push into predictive mineral discovery under cover, and the financial resources of the federal government and a large number of industry sponsors were pooled to fund the Predictive Mineral Discovery Cooperative Research Centre (pmd*CRC), which consists of seven core partners (AMIRA International, CSIRO, GA, James Cook University, Monash University, The University of Melbourne, UWA). The centre aims to generate a fundamental shift in exploration practice and cost-effectiveness by improved understanding of mineral processes and four-dimensional understanding of the geological evolution of mineralized terranes. Research fields include enabling technologies, and detailed studies of mineralized terranes at all scales ranging from oreshoot through mine–camp to terrane.

In recent years, nickel research in Australia has been headed by collaborative Monash University and CGM studies. Studies have focused on detailed mine-scale volcanic and structure studies, ore remobilization, camp-scale mineral and whole-rock lithogeochemical vectors, terrane-scale volcanic and intrusive architecture, and strategic studies of recent brownfields and greenfields discoveries. This research has been supported by the Western Australian mineral industry, in particular.

Future nickel research directions include understanding the camp-scale 'fertility' of Western Australia's large nickel mining camps; fundamental controls on sulfur solubility, including the roles of pressure and volatiles; mobilization of sulfide magmas; platinum group element (PGE) and mantle heterogeneity; and fertility indicators including resistate minerals and whole-rock lithogeochemical vectors.

Technological advances over the past 20 years have been instrumental in some of the gold and nickel discoveries. At Kanowna Belle, for example, geochemical sampling and analytical procedures available in commercial laboratories have enabled the accurate and precise low-level detection of gold to parts per billion. Downhole electromagnetic surveying of the Forrestania nickel deposit has enabled the precise targeting of dense nickel-sulfide concentrations at great depths.

Organization

The field guide is organized so that camp and deposit descriptions follow the excursion route (Fig. 1). The first section covers the 'southern' nickel deposits in the Widgiemooltha area and Kambalda Dome, as well as gold deposits in the St Ives camp, and at Kanowna Belle, the Golden Mile, and Kundana. A short paper on the Joe Lord Core Farm explains the purpose of the facility. The second section of the guide describes nickel deposits in the 'northern' part of the excursion area, such as Waterloo, Mount Keith, Honeymoon Well, and Cosmos. It also describes the geological setting of the Thunderbox gold deposit.

Specific excursion stops are difficult to plan in active mining environments, so most papers cover detailed geological and structural settings, as well as hydrothermal alteration and ore mineral assemblages, rather than referring to precise stops. The excursion stops in mines will be determined shortly before the excursion arrives, and will depend on the mine schedule. Additional information will be provided to excursion participants upon arrival on site.

Acknowledgements

The excursion leaders acknowledge the support of the local mining community and GSWA in presenting this excursion and accompanying field guide.

References

FLINT, D. J., and ABEYSINGHE, P. B., 2001, Western Australia mineral exploration and development for 1999 and 2000: Western Australia Geological Survey, 35p.

DEPARTMENT OF MINERALS AND ENERGY, WESTERN AUSTRALIA, 1994, Fact sheet 21, nickel: Western Australia, Western Australia Geological Survey, 4p.

HILL, R. E. T., BARNES, S. J., and DOWLING, S. E., 2001. Komatiites of the Norseman–Wiluna greenstone belt, Western Australia — a field guide: Western Australia Geological Survey, Record 2001/10, 71p.

WITT, W. K. 1993, Gold mineralization in the Menzies–Kambalda region, Eastern Goldfields, Western Australia: Western Australia Geological Survey, Report 39, 165p.

Komatiite-hosted Ni–Cu–PGE deposits of the Kambalda nickel camp — an overview

by

S. W. Beresford[1] and W. E. Stone[2]

Introduction

Kambalda is the type location for type 1 komatiitic-hosted nickel–sulfide deposits (Lesher, 1989). The pre-mined reserve of about 35 Mt at 3% Ni (Stone and Masterman, 1998) indicates that Kambalda is a world-class mining district for nickel sulfide.

Kambalda Dome is a doubly plunging antiform located in the south-central part of the Norseman–Wiluna greenstone belt, Yilgarn Craton, Western Australia (Stone and Masterman, 1998). It is adjacent to the major north-northwesterly trending Boulder–Lefroy fault system, and is folded about the Kambalda Anticline, cored by a granitoid pluton, and flanked by major thrust ramps (Fig. 1). The nickel deposits in the Kambalda Dome area (Fig. 1) are most closely associated with Lunnon Basalt (footwall) and the Kambalda Komatiite (host rock and hangingwall). The volcanic–sedimentary rock section formed at c. 2.7 Ga (Claoué-Long et al., 1988), and has been subjected to complex polyphase structural deformation, lower amphibolite metamorphism (Barrett et al., 1977; Bavinton, 1979), and granitoid intrusion (Cowden and Roberts, 1990).

The deformation sequence at Kambalda is described as separate events, termed D_1–D_4 (Cowden and Archibald, 1987; Cowden and Roberts, 1990):

- D_1 is thrusting directed south to north;
- D_2 thrust-folding is directed south-southwest to north-northeast, and is the peak deformation event;
- D_3 is doming and related faulting during granitoid intrusion and peak metamorphism;
- D_4 is oblique north-northeasterly trending strike-slip faulting and retrogressive metamorphism.

During progressive deformation and metamorphism, the komatiitic rocks were hydrated to serpentine–chlorite–magnetite assemblages, and subsequently carbonated to talc–carbonate–chlorite assemblages (Cowden and Roberts, 1990).

The Kambalda Komatiite shows systematic upsection asymmetry and lateral symmetry (Gresham and Loftus-Hills, 1981; Cowden and Roberts, 1990; Lesher and Arndt, 1995; Beresford et al., 2002). Three to six komatiitic peridotite flows up to 100 m thick at the base (Silver Lake Member) pass upsection to multiple <10 m-thick spinifex-textured flows at the top of the section (Tripod Hill Member). The basal komatiitic peridotite flows overlie and intercalate with carbonaceous to albitic sedimentary units, except in the ore environment. Laterally away from individual oreshoots, komatiitic flows decrease in thickness, and contact and interflow sedimentary units are present, but significant nickel sulfides are absent. The flow thickness and degree of olivine enrichment decrease laterally, suggesting a lateral transition from channelized to sheet flow facies. These volcanic and stratigraphic variations define elongate prisms of distinctive komatiite flow sequences, and imply a strong volcanic control on ore localization (Gresham and Loftus-Hills, 1981; Cowden and Roberts, 1990; Beresford et al., 2002).

The nickel sulfide deposits are restricted mainly to the base of the lowermost channel facies flow (termed contact ore; type 1 deposits) and, more rarely, to the base of overlying flows (termed hangingwall ore) and in crosscutting structures as offset ore (Gresham and Loftus-Hills, 1981). Contact ore constitutes 80% of the resources and forms tabular to ribbon-like linear oreshoots up to 2500 m long, 300 m wide, generally <5 m thick, and <0.6 to about 10 Mt in size (Marston and Kay, 1980). Individual sulfide orebodies comprising pyrrhotite–pentlandite–pyrite–chalcopyrite are zoned, with a layer of massive sulfide, up to 2 m thick, at the base overlain in sequence by matrix sulfide to 2 m thick, then disseminated sulfide. The massive sulfide has fabrics, such as monomineralic layering and foliated pyrite lenses (Ostwald and Lusk, 1978), that preserve the entire deformation sequence (Cowden and Archibald, 1987).

The volcanic and stratigraphic controls on the nickel deposits, and the deformation and alteration characteristics of the ore suggest original formation via magmatic processes (Ross and Hopkins, 1975; Lesher, 1989). The generally accepted model (Huppert et al., 1984; Huppert and Sparks, 1985; Lesher, 1989; Hill et al., 1995; Williams et al., 1998) is based on a distal komatiite eruption and

1 Department of Earth Sciences, Monash University, Victoria 3800, Australia
2 Geoinformatics Exploration Canada Ltd, Suite 1280, 625 Howe Street, Vancouver, British Columbia V6C 2T6, Canada

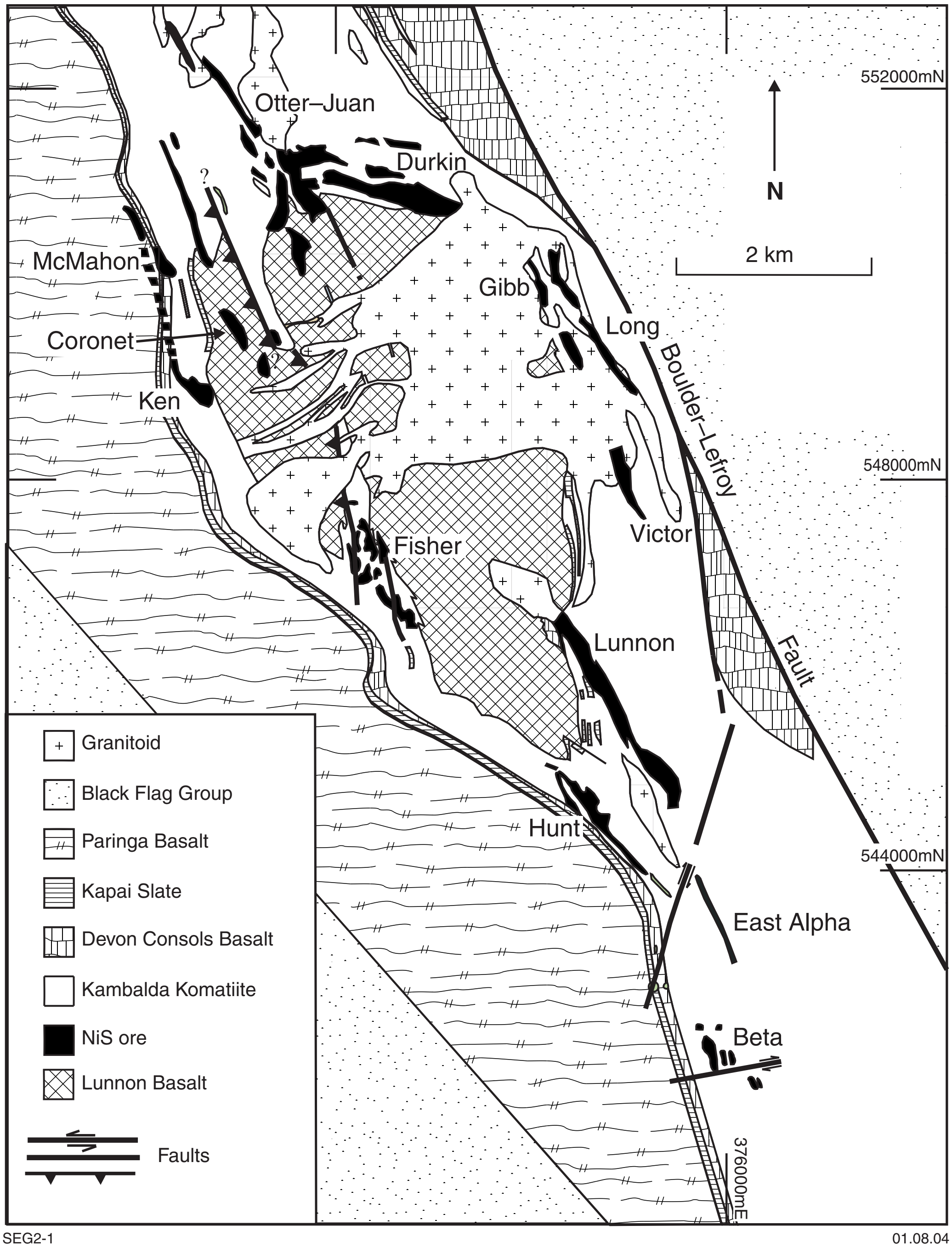

Figure 1. Geological map of Kambalda Dome showing nickel sulfide orebodies (adapted from Gresham and Loftus-Hills, 1981)

flow, channeling by thermal erosion, assimilation of sulfidic sedimentary substrate by sulfur-undersaturated lava, and deposition of Fe–Ni sulfides on the channel floor. Significant systematic differences in tenor (nickel content in 100% sulfides) between individual deposits (Marston and Kay, 1980; Cowden and Woolrich, 1987) are attributed to variations in R-factor (Lesher and Burnham, 2001) and fO_2/fS_2 within the sulfide-silicate system during lava emplacement and ore genesis (Cowden and Woolrich, 1987).

Integrated structural and volcanic studies

Recent integrated structural and volcanic studies provide new insights into the geological controls on the geometry and configuration of komatiite-hosted nickel sulfide deposits at Kambalda. Analysis of a three-dimensional model of the Kambalda exploration database reveals oreshoot-scale controls consistent with the superimposed

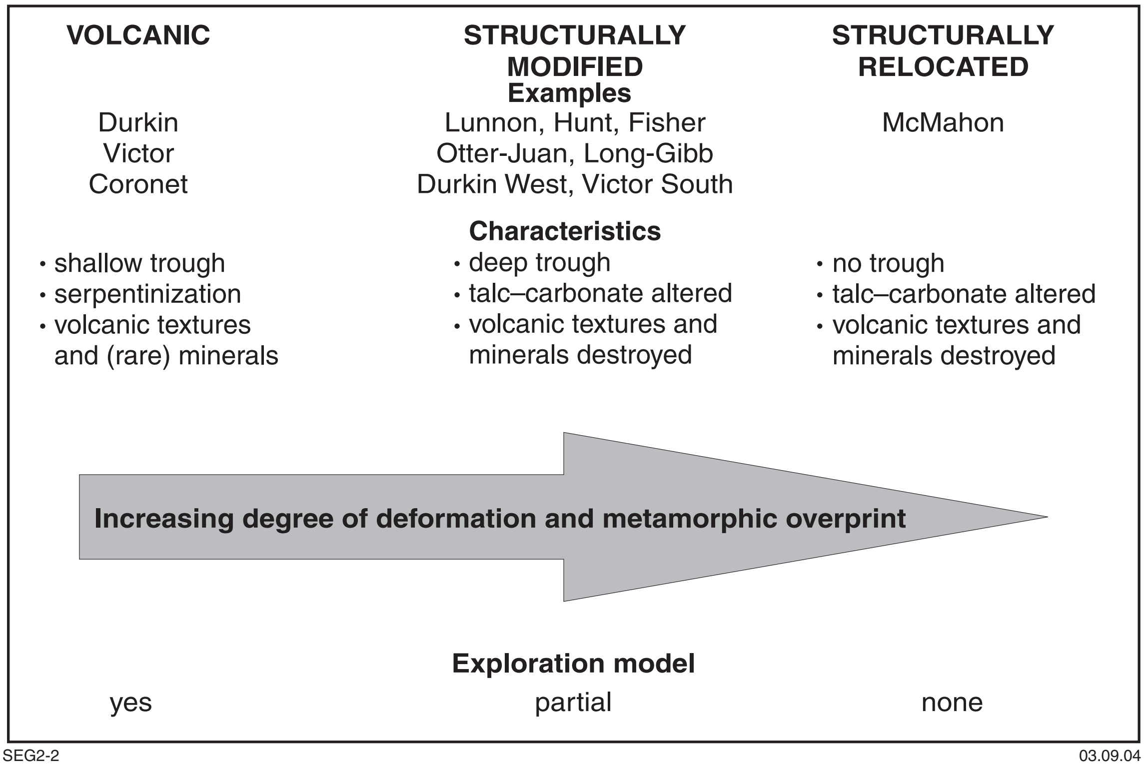

Figure 2. Structural continuum model (adapted from Stone et al., in press a)

effects of post-volcanic deformation and metamorphism (Stone and Archibald, 2004; Stone et al., in press a,b). The troughs are generally asymmetric, with most having re-entrant downdip margins and upright updip margins, consistent with fold-related thrusting (Stone and Archibald, in press a). Moreover, some troughs confine volcanic channels, but others transgress and truncate channels (Lunnon and Fisher shoots). Troughs that are <5 m deep contain serpentine-altered komatiitic with relict cumulate textures and matrix-disseminated sulfide oreshoots. Deeper troughs (up to 50 m) are remarkably linear, defined by discrete tectonic boundaries, and contain talc–carbonate with or without significant massive sulfide.

The integrated results of these multidisciplinary studies confirm the distinction of volcanic channels and trough structures, and demonstrate that oreshoots are generally associated with channels, but not with deep troughs. The asymmetric trough geometries, truncation of channels, and associated talc–carbonate alteration indicate that the deep troughs are tectonic in origin, formed by D_1–D_2 thrust-folding and D_3 doming and related faulting during the tectono-metamorphic evolution of Kambalda Dome. These troughs do not reflect thermally eroded channels.

Various volcanic-depositional and tectonometamorphic features are present on the Kambalda Dome, reflecting a continuum of Kambalda oreshoots from a mainly volcanic controlled endmember (three of 15 shoots; shallow troughs, serpentinized hangingwall, dominated by matrix–disseminated sulfide) through structurally modified (11 of 15 shoots; deep troughs, talc–carbonated hangingwall, dominated by massive sulfide) to a structurally controlled endmember (one shoot, tectonically emplaced in hangingwall; Stone et al., in press a; Fig. 2).

Stone et al. (in press b) reviewed tenor variations from 14 deposits in the Kambalda nickel camp, and illustrated significant intrashoot tenor variations that were difficult to reconcile with solely magmatic processes. The striking relationship of increasing Ni content with secondary phase abundance, such as pyritization, indicates a strong role for metamorphic modification of tenor variation.

Primary contact relations, geochemistry, and textural and vesicle distribution of the primary komatiitic facies variation are consistent with emplacement of komatiite lava flows under laminar flow conditions (Cas et al., 1999). However, the absence of sedimentary units beneath komatiites with coherent flow tops in ore environments seems contradictory, and suggests both turbulent and passive laminar emplacement, respectively (Beresford et al., in press). The absence of platinum group element (PGE) depletion in the host komatiite crust (and core; Lesher et al., 2001) and sediment–ore antithetism, suggests that the komatiite lava was initially turbulent and probably open-channel fed. Nickel sulfides were deposited during this initial stage. As the flow evolved, widened and thickened, laminar flow conditions prevailed and the komatiites are inferred to have flowed through the development of interior magma tubes (Beresford et al., in press). The constant lava flow-through or recharge is consistent with the ore–lava geochemical disequilibrium (Lesher and Arndt, 1995).

Primary whole rock and grain-scale trace element and isotopic geochemistry (when screened through significant alteration effects) indicate limited (<3%) to no silicate assimilation. However, the absence of sedimentary units in the ore environment implicates syn-emplacement erosion.

Acknowledgements

This paper is the result of a recently completed WMC–Monash collaborative research project. We acknowledge Ray Cas, Yann Lahaye, Mary Jane, David Lambert, Chris Banasik, Peter Bewick, Craig Reddell, Jon Hronsky, and the staff at Kambalda Nickel Operations for support and discussions.

References

BARRETT, F. M., BINNS, R. A., GROVES, D. I., MARSTON, R. J., and McQUEEN, K. G., 1977, Structural history and metamorphic modification of Archean volcanic-type nickel deposits, Yilgarn Block, Western Australia: Economic Geology, v. 77, p. 1195–1223.

BAVINTON, O. A., 1979, Interflow sedimentary rocks from the Kambalda ultramafic sequence: their geochemistry, metamorphism and genesis: The Australian National University, PhD thesis (unpublished).

BERESFORD, S. W., CAS, R. A. F., LAHAYE, Y., and JANE, M., 2002, Facies architecture of a komatiite-hosted Ni-sulphide ore deposit, Victor, Kambalda, Western Australia: implications for komatiite emplacement: Journal of Volcanology and Geothermal Research, v. 118, p. 57–75.

BERESFORD, S. W., STONE, W. E., CAS, R. A. F., LAHAYE, Y., and JANE, M. J., in press, Volcanic controls on the localization of a komatiite-hosted Ni–Cu–(PGE) deposit, Coronet, Kambalda, Western Australia: Economic Geology.

CAS, R. A. F., SELF, S., and BERESFORD, S. W., 1999, The behaviour of the fronts of komatiite lavas in medial to distal settings: Earth and Planetary Science Letters, v. 172, p. 127–139.

CLAOUÉ-LONG, J. C., COMPSTON, W., and COWDEN, A. C., 1988, The age of the Kambalda greenstones resolved by ion-microprobe: implications for Archaean dating methods: Earth and Planetary Science Letters, v. 89, p. 239–259.

COWDEN, A. C., and ARCHIBALD, N. J., 1987, Massive-sulfide fabrics at Kambalda and their relevance to the inferred stability of monosulfide solid-solution: Canadian Mineralogist, v. 25, p. 37–50.

COWDEN, A., and ROBERTS, D. E., 1990, Komatiite-hosted nickel sulphide deposits, Kambalda, *in* Geology of the mineral deposits of Australia and Papua New Guinea *edited by* F. E. HUGHES: The Australasian Institute of Mining and Metallurgy, Monograph 14, v. 1, p. 567–582.

COWDEN, A., and WOOLRICH, P., 1987, Geochemistry of the Kambalda iron-nickel sulfides: implications for models of sulfide–silicate partitioning: The Canadian Mineralogist, v. 25, p. 21–36.

GRESHAM, J. J., and LOFTUS-HILLS, G. D., 1981, The geology of the Kambalda nickel field, Western Australia: Economic Geology, v. 76, p. 1373–1416.

HILL, R. E. T., BARNES, S. J., GOLE, M. J., and DOWLING, S. E., 1995. The volcanology of komatiites as deduced from field relationships in the Norseman–Wiluna greenstone belt, Western Australia: Lithos, v. 34, p. 159–188.

HUPPERT, H. E., and SPARKS, R. S. J., 1985, Komatiites I. Eruption and flow: Journal of Petrology, v. 26, p. 694–725.

HUPPERT, H. E., SPARKS, R. S. J., TURNER, J. S., and ARNDT, N. T., 1984, Emplacement and cooling of komatiite lavas: Nature, v. 309, p. 19–22.

LESHER, C. M., 1989, Komatiite-associated nickel sulfide deposits: Reviews in Economic Geology, v. 4, p. 45–101.

LESHER, C. M., and ARNDT, N. T., 1995, REE and Nd isotope geochemistry, petrogenesis, and volcanic evolution of contaminated komatiites at Kambalda, Western Australia: Lithos, v. 34, p. 127–157.

LESHER, C. M., and BURNHAM, O. M., 2001, Multicomponent elemental and isotopic mixing in Ni–Cu–(PGE) ores at Kambalda, Western Australia: The Canadian Mineralogist., v. 39, p. 421–446.

LESHER, C. M., BURNHAM, O. M., KEAYS, R. R., BARNES, S. J., and HULBERT, L., 2001, Trace-element geochemistry and petrogenesis of barren and ore-associated komatiites: The Canadian Mineralogist, v. 39, p. 673–696.

MARSTON, R. J., and KAY, B. D., 1980, The distribution, petrology and genesis of nickel ores at the Juan Complex, Kambalda, Western Australia: Economic Geology, v. 75, p. 546–565.

OSTWALD, J., and LUSK, J., 1978, Sulfide fabrics in some nickel sulfide ores from Kambalda, Western Australia: Canadian Journal of Earth Sciences, v. 15, p. 502–515.

ROSS, J. R., and HOPKINS, G. M. F., 1975, Kambalda nickel sulphide deposits, *in* Economic geology of Australia and Papua New Guinea *edited by* C. L. KNIGHT: The Australasian Institute of Mining and Metallurgy, Monograph 5, v. 1, p. 100–120.

STONE, W. E., and ARCHIBALD, N. J., 2004, Structural controls on nickel sulphide ore shoots in Archaean komatiite, Kambalda, WA: the volcanic trough controversy revisited: Journal of Structural Geology, v. 26, p. 1157–1171.

STONE, W. E., BERESFORD, S. W., and ARCHIBALD, N., in press a, Towards an holistic model for Kambalda-style NiS deposits: Economic Geology.

STONE, W. E., HEYDARI, M., and SEAT, Z., in press b, Nickel tenor variations between Archaean komatiite-associated nickel sulphide deposits, Kambalda ore field, Western Australia: the metamorphic modification model revisited: Contributions to Mineralogy and Petrology.

STONE, W. E., and MASTERMAN, E. E., 1998, Kambalda nickel deposits, *in* Geology of Australian and Papua New Guinean mineral deposits *edited by* D. A. BERKMAN and D. H. MacKENZIE: The Australasian Institute of Mining and Metallurgy, Monograph 22, p. 347–356.

WILLIAMS, D. A., KERR, R. C., and LESHER, C.M., 1998, Emplacement and erosion by Archean komatiite lava flows at Kambalda: revisited: Journal of Geophysical Research, v. 103, p. 27533–27549.

Long nickel mine, Kambalda

by

C. Bonwick[1] and S. Sheppard[1]

Acquisition of the Long nickel mine

Independence Group NL's wholly owned subsidiary Lightning Nickel Pty Ltd (Lightning) acquired its first operation, the Long nickel mine, from WMC Resources Ltd in September 2002. This acquisition will provide a significant cash flow to the company over many years, with good prospects for further mine life extensions.

Lightning paid A$15 million to WMC Resources for the asset, funded by a combination of debt (A$10 million) and equity funds from the August 2002 A$7 million capital raising. The company also secured A$5.3 million in capital equipment financing, a A$3 million working capital facility, and a facility for up to A$2 million in environmental bond bank guarantees.

Apart from the tenure and reserves, Lightning also acquired a headframe and winders, office complex, underground communications system, air compressors, dewatering pumps, seismic monitoring system, and mining equipment valued at over A$4 million. This resulted in a considerable reduction in the capital required to bring the mine back into production.

Lightning has employed a highly skilled workforce at the Long nickel mine, most of whom have many years of underground experience in the Kambalda region.

The mine was successfully commissioned during the year and is now producing at an annualized rate of 160 000 t of ore. As well as getting the mine into full production, exploration and development activities have resulted in the discovery of an additional year of reserves (at current nickel prices and production rate) and, more importantly, have increased resources by 20% in terms of contained nickel tonnes.

Research and development studies to extract mine pillars outside reserves, and exploration success at Long South also have the potential to significantly increase the mine life.

[1] Independence Group NL, Level 3, 72 Melville Parade, South Perth, W.A. 6151, Australia

Kambalda history

In January 1966, Western Mining Corporation (WMC) intersected nickel sulfide mineralization in a drillhole near the abandoned gold-mining town of Kambalda. This discovery led to the development of a world-class nickel province, which has produced more than 1 million tonnes of nickel metal over a period of 30 years.

As a result, the Kambalda region is well serviced by established infrastructure, including grid power, sealed highways, and potable water supplies, and extensive mining industry support is available locally in the form of contract mining, haulage, engineering, and technical support services. A large and highly skilled labour pool is available in both Kambalda and Kalgoorlie.

Long nickel mine history

The Long shoot was first intersected by diamond drilling in 1971, with subsequent drilling indicating the presence of significant mineralization within both the Long and Victor nickel orebodies, collectively known as the Long Complex (Fig. 1).

Underground development commenced at Long in 1975 with the sinking of a vertical shaft to a depth of 971.4 m. Ore production began in 1979. The Victor decline was started in 1989 to access the Victor orebody and, by 1994, had provided mechanized access to the deeper levels of the Long nickel mine. After the mine was placed on care and maintenance in April 1999, WMC Resources maintained the underground infrastructure, shaft, and headframe in excellent condition for a planned resumption of mining. WMC Resources also refurbished the mine, undertook additional exploration, and completed a mine-operating plan, which was later used by Lightning.

Past production from Long shaft and Victor decline represents the second largest concentration of nickel in the Kambalda region, and qualifies Long as one of WMC's longest operating nickel mines, with a 21-year mine life. Total production to closure in 1999 was 5.43 Mt at an

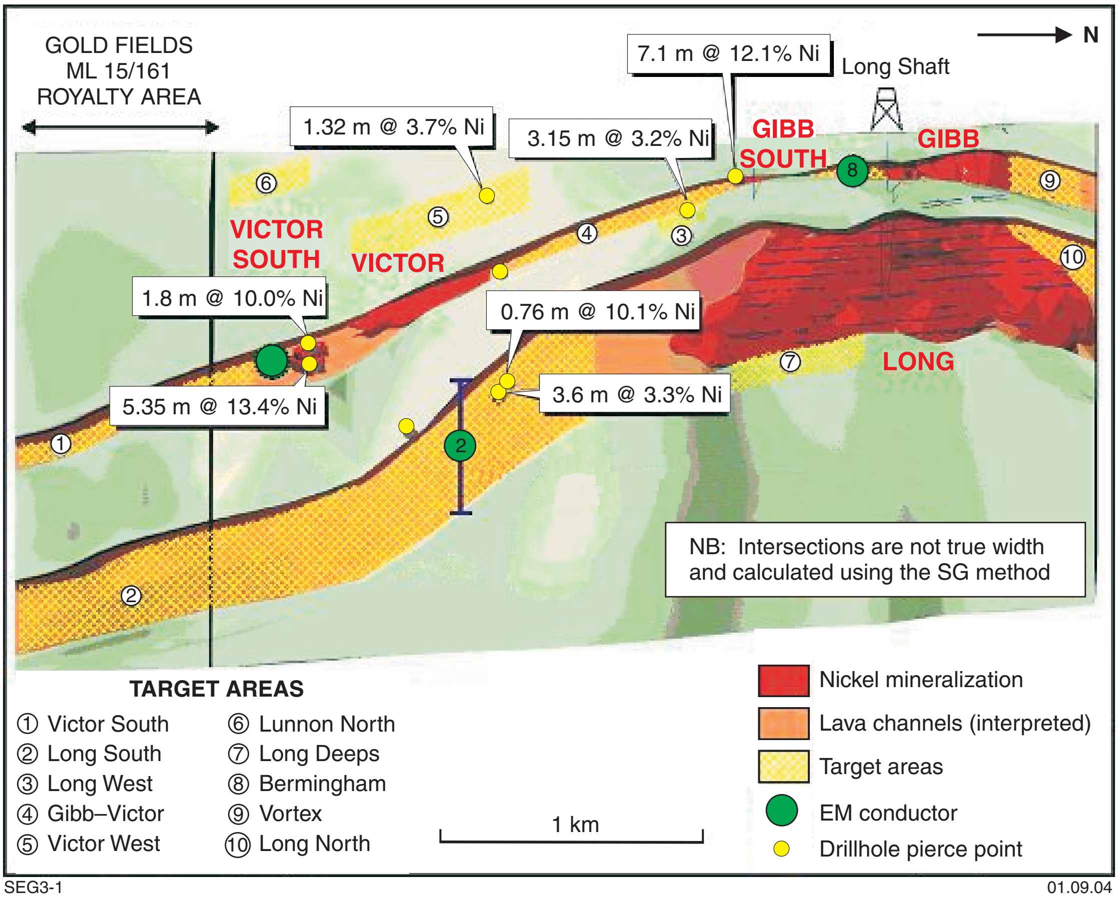

Figure 1. Interpretive long section for the Long Complex showing nickel orebodies

average reconciled grade of 3.7% nickel (>200 000 nickel tonnes).

Tenure

The Long Complex assets are located on three Western Australian Mining Act (1904) Mineral Leases (ML15/158, 159, and 160), and a portion of East Location 48 leased to Independence for ten years. Location 48 is one of a number of freehold land grants created in the Coolgardie district in 1890. Independence also has access, via a nickel royalty agreement, to mine nickel on five Gold Fields Australia Pty Ltd (Gold Fields) Mineral Leases (ML) to the east and south of the operation.

WMC Offtake Agreement

Lightning has an agreement with WMC Resources whereby the ore produced from the mine is delivered to the adjacent WMC Kambalda Nickel Concentrator for toll treatment and production of nickel concentrates, which are then sold to WMC Resources on terms set out in that agreement. The agreement expires on 27 February 2010, with WMC Resources having the option to extend for another nine years.

Ground conditions and seismicity

The risks of 'mine-induced' seismicity are well known and understood at Long. The orebody is disrupted by a swarm of crosscutting porphyries, some of which are stressed. These bodies have reacted in a consistent and predictable geotechnical fashion. When mining the discrete ore blocks that constitute the Long mining inventory today, the procedures to manage these events are built into the operating standards of Lightning, and are well understood by mining personnel.

Ground support

A combination of mesh and rock-bolting, cone and cable bolting, and shotcrete forms the standard practice for excavations of varying size and accessibility. No person is allowed to perform their duties beyond safe and secure overhead support.

Consultants

Lightning has retained the expertise of BFP Consultants Pty Ltd (Melbourne), and Dempers and Seymour Pty Ltd

(Perth), and received advice from Professor Will Bawden (Canada), to ensure that the mining methods, ground support, and sequence of activities at Long provide a low-risk workplace for employees while enabling optimum extraction of the orebodies.

Kambalda Nickel Royalty Agreement

Lightning reached agreement with Gold Fields to mine underground nickel extensions on ML 15/161, 167, 168, 169, and 170, south and east of the Long and Victor deposits. Gold Fields retains tenement ownership and the right to gold, both at the surface and underground.

The royalty payable to Gold Fields is on a sliding scale, and depends on the Australian dollar (A$) price received on nickel produced from the related area. This ranges from 0% when the price per nickel pound is less than A$5.00, to 5% when the price per nickel pound is A$8.30 or greater.

Mine work force

Lightning currently employs 72 full-time staff. Many employees, including the General Manager, are ex-WMC Kambalda employees, who brought an immediate pool of sound operating knowledge, experience, and skills to the project. The mining team has a combined underground experience of 1240 man years (average 19.4 years), with 240 years previously spent at Long.

Lightning's work force has been very stable, with a 99% retention rate, since the commencement of mining in October 2002. All miners, apart from the handheld team, are on salary, and a gain-share bonus scheme was introduced during the 2003–04 financial year to reward the mining team when safety, teamwork, and cost targets are achieved.

Mine production

Production was initially scheduled over a period of five years commencing in October 2002, using a variety of mining techniques designed to safely accommodate changes in orebody attitudes, thicknesses, and geometry.

Mining methods range from longhole open stoping with mullock or sand backfill, to mechanized Jumbo flatback stoping. A handheld mining team has also been established to extract remnant blocks in the upper levels of the mine, and in narrow stopes not suitable for mechanization. Wherever possible, non-entry, mechanized mining methods are employed for safety reasons and to maximize productivity. The spacing of stoping sublevels and other aspects of the mining methods have been designed to minimize opportunities for dilution.

From first firing on 24 October 2002 to the end of the March 2004 quarter, over 5000 t of nickel metal (Ni tonnes) have been produced by Lightning, as shown in Table 1.

Table 1. Reserves for Lightning's Long nickel mine from first firing on 24 October 2002 to 30 March 2004

	Tonnes ore	*Grade % Ni*	*Nickel tonnes*
Outside reserve	31 767	4.6	1 457
Inside reserve	90 101	4.3	3 858
Reserve estimate [(a)]	71 305	3.7	2 626
Total	**121 868**	**4.4**	**5 316**

NOTES: (a) expected ore reserve grade and tonnes as defined by the area mined 'inside reserves'

Production from the start-up reserve of 26 800 Ni tonnes was estimated to result in an A$60 million cash flow after tax and debt repayment, based on an exchange rate for A$/USD of 0.55 and a nickel price of US$6950 per tonne (A$12 636 per Ni tonne).

Development

Long mining blocks

During 2002–2003, development costs that were capitalized related to the initial access into Gibb South and Victor South. Mining at Long shaft involved re-establishing reserve blocks, which in some cases had not been in operation for more than a decade. The rehabilitation of these areas involved extensive shotcreting, re-meshing, and cone and cable bolting. Thus 2002–03 was a year of preparing the reserve blocks for safe extraction of ore.

Gibb South

To date, a total of 19 143 t ore at 7.1% Ni (1365 Ni tonnes) has been mined from Gibb South (June 2003 reserve: 28 000 t at 3.7% Ni; 1000 Ni tonnes). Gibb South's ore grade averages 7.1% Ni, significantly higher than the reserve grade. Mining has defined additional high-grade nickel ore outside the June 2003 ore reserve boundary. South of the current ore reserve block, transient electromagnetic (TEM) surveys have located new conductors, which the company plans to develop.

Victor South

Capitalized decline development to access the high-grade Victor South deposit commenced in July 2003. Victor South contains 5900 Ni tonnes in reserve, and an additional 14 900 Ni tonnes in resources. Ore reserve definition drilling has commenced, using the drill drive over the orebody, to convert existing resources to reserves by increasing drill density. Drilling will also test for extensions to the south (open) and around the open 5.35 m at 13.4% Ni drillhole intercept in shoot 3 (not in the mining schedule).

Ore reserves and resources

Cube Consulting Pty Ltd (resource consultants) and BFP Consultants Pty Ltd (mine reserve consultants) were used to estimate the Long resources and reserves based on industry best practice.

Ore tonnages and grades have been calculated at a 1% nickel cutoff on the basis of the new resource model, which takes into account the high value of the ore, its mode of occurrence, the geotechnical considerations to ensure successful and safe mining in the geological environment, and the depths at which the operations will be conducted. The resource was calculated using the 2D metal accumulation of grade, thickness, and density interpolated by ordinary kriging into 20 m × 20 m blocks for each mineralized surface, followed by subtraction of porphyry pillars and mining depletion.

The reserve, at 2% nickel cut-off, has been estimated by creating stoping block models and adding appropriate dilution according to the mining methods.

The Long Complex also contains significant resources and exploration targets that could considerably extend the current five year mine life.

A large geophysical and drilling program aimed at increasing the nickel reserves to 50 000 Ni tonnes for Lightning's Long nickel mine commenced during the March 2004 quarter. The program, which could take 12 months to complete, comprises:

- a systematic geophysical survey testing the Long, Gibb South, and Victor South ore positions using the company's proprietary EM Torch to locate and define new massive and matrix nickel sulfides up to 100 m from existing mine workings;
- a >10 000 m diamond drilling program, using up to five underground drill rigs on two shifts, to convert existing resources to reserves and test new targets defined by the EM Torch and geological studies;
- downhole TEM surveys.

It is anticipated that about 22 000 of the Ni tonnes defined in the June 2003 reserves will remain unmined by the end of the current financial year. An additional 28 000 t will be targeted from:

- existing mine resources outside reserves (60 000 Ni tonnes at June 2003);
- mine pillars outside reserves and resources (27 200 Ni tonnes at June 2003);
- new near-mine discoveries, which can be cheaply mined using existing underground infrastructure.

New ore blocks outside ore reserves continue to be defined in the upper and lower levels of the mine. To date, 31 767 tonnes of ore at 4.6% Ni have been mined outside reserve blocks this financial year, predominantly from previously unknown remobilized massive nickel sulfide hangingwall and footwall surfaces, mainly on the 15 and 16 levels. More importantly, these new surfaces are open in many directions, which should add further to the reserve base.

Remnant pillars

About 44 000 Ni tonnes were contained in mine pillars when Lightning purchased Long, which, based on previous handheld mining techniques, were thought to be unextractable. A total of 10 400 pillar Ni tonnes has been added to resources during the year.

Geophysics

The first underground trials of the portable underground EM system (EM Torch) have been completed and minor finetuning is in progress. The system, analogous to a large metal detector, is being used to produce real-time massive and matrix nickel sulfide location information, providing a vector to the mineralization. This will significantly reduce the cost of drilling, allow more accurate mine design, reduce expensive 'exploration' development, and locate missed oreblocks adjacent to existing workings. Lightning is applying for a Commonwealth Government Start Grant, which could provide 50% of the funding to refine the EM Torch, and other geophysical equipment and procedures.

Exploration

Nickel sulfide formation

The Long and Victor deposits are typical Kambalda-style nickel deposits, consisting of narrow, steeply dipping, shallowly plunging, ribbon-like accumulations of massive or semimassive sulfides, and located at the base of komatiitic ultramafic flows at the contact with an underlying basalt unit. Massive sulfide is overlain by matrix and then disseminated mineralization, with the bulk of the ore expected to be massive and matrix. The orebodies average 2.6 m in thickness.

The Long nickel oreshoots consist of shallowly plunging channels (therefore high tonnes per vertical metre), and the high nickel tenor of massive sulfides compared to many other deposits means that even small incremental discoveries can have a significant positive impact on the project's profitability.

Long nickel mineralization is associated with Archaean ultramafic lava channels (analogous to river channels), where molten liquid nickel sulfides pooled at specific points along the channel. Subsequent folding has tilted the channels to a 60° dip to the east, and also resulted in the remobilization of some of the original sulfides into new structurally controlled positions (Victor South). During these deformation events and resultant sulfide remobilization, the massive sulfide can be thought to behave like a tube of toothpaste when squeezed, with weak massive sulfides squeezed into surrounding country rocks under extreme pressure. To date, two channels have been recognized:

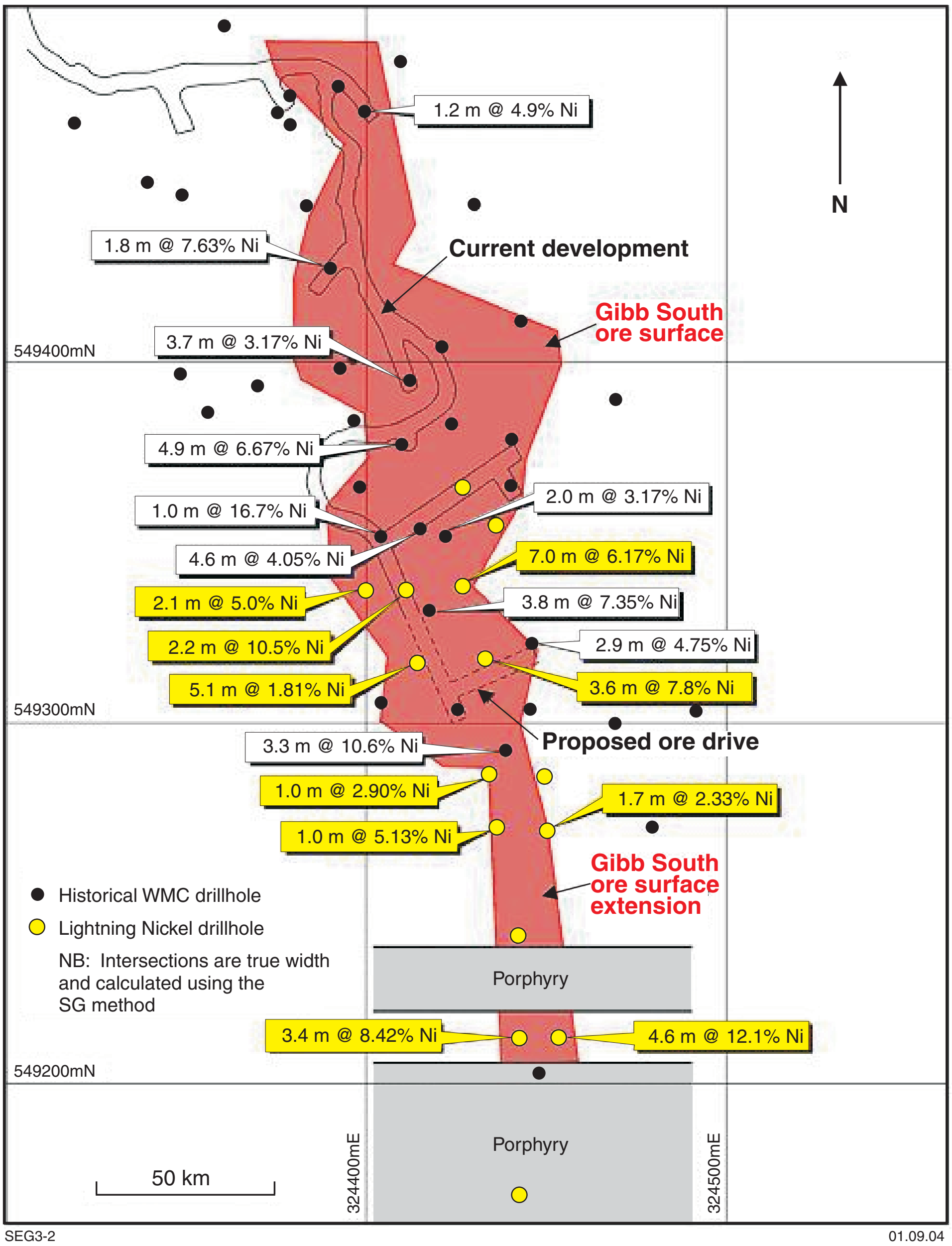

Figure 2. Plan showing ore intercepts in Gibb South

- Channel 1 — the upper, high-tenor nickel channel is interpreted to contain, from north to south, the Gibb, Gibb South, Victor, and Victor South deposits;
- Channel 2 — the lower, wider, moderate-tenor nickel channel contains the Long deposit and nickel sulfides to the south.

Strategy

Exploration at Long is divided into two categories:

- incremental ore targets — targets that could replace depleting reserves or resources in and around known orebodies;
- long-life targets —targets that have the potential to significantly enhance overall project parameters, such as doubling mine life at twice the capacity, and require major new development.

Lightning's exploration team is focusing on both target types using the integration of geological mapping, structural studies, and magnetic and EM geophysical surveys to produce a three-dimensional picture of the ultramafic stratigraphy. To date, exploration has been very successful, given the small (A$0.33 million) exploration expenditure in 2002–03. The 2003–04 Long exploration budget has been increased to about A$2 million.

Incremental ore targets

Gibb South

Infill and extension drilling was completed during 2003 year to test for additional ore extensions and successfully convert resources to reserves (Fig. 2). Drilling and downhole EM surveys indicate the Gibb South sulfides are terminated at 549 200N, where the Gibb South lava channel is crosscut by a large felsic porphyry intrusion. However, ground magnetic highs south of the porphyry suggest a possible continuation of the untested channel ultramafic units that requires further exploration.

Long 11–12 level

Underground drilling at the southern end of the 11 level in 2003 returned a number of significant intersections in a previously undrilled section of the mine. These intersections added new reserves to the Long orebody, and confirmed the potential for additional discoveries and reserves within the proximal mine environment.

Re-interpretation of the felsic intrusive model has also lead to the discovery of more high-grade nickel sulfides above the 11 level, in an area previously thought to be stoped out by intrusions.

Long-life targets

Long South

Drilling to test for a possible repetition of the 1.6 kilometre long and 0.5 kilometre high Long orebody (past production: 4.66 Mt at 3.7% Ni; 173 600 Ni tonnes) beneath Victor and Victor South has commenced. Previous WMC drilling intersected 0.76 m at 10.09% Ni in drillhole KD6067B, 0.7 km south along strike from the most southerly known point of the Long orebody. No previous drilling has effectively tested the 1.2 km of prospective Long lava channel south of this hole.

Drillhole KD6067B was re-entered and a new hole drilled to test the area just south of the previous WMC hole. This wedge hole, KD6067BW7, intercepted the prospective contact about 24 m south of the original intercept, and returned 3.6 m at 3.3% Ni, including thin, high-tenor massive sulfide units assaying 0.29 m at 14.6% Ni.

Follow-up underground diamond drillhole LSU001 was drilled to 869 m depth in late 2003. The hole was drilled from the footwall at a low angle to the interpreted position of the prospective ultramafic–mafic contact in order to give maximum downhole geophysical coverage over the prospective contact. The drillhole ended in footwall pillowed mafic basalt after passing through a narrow interval of faulted ultramafic rocks containing significant concentrations of disseminated sulfides. Geological interpretation suggests a slightly higher degree of structural complexity in the area, with a resultant flattening of the main target contact. The hole failed to reach the prospective ultramafic–mafic contact because the drilling rig reached the limits of its capacity. The hole has been surveyed by downhole EM from the surface to 756 m. The remaining 113 m closer to the prospective contact remains to be surveyed, and an off-hole EM anomaly has been defined. The anomaly is currently being followed up with an updip wedge off drillhole LSU-001.

Victor South extensions

Significant potential exists at Victor South to define additional high-grade ore along strike and downdip from the known mineralization. To date, the Victor South reserves and resources are contained in three shoots. WMC Resources intersected 5.35 m at 13.4% Ni in shoot 3. This intersection is open along strike and downdip, and follow-up drilling is planned. Reinterpretation of WMC Resources downhole geophysical logs has defined numerous conductors outside the current resource areas. These targets will be followed up after the Victor South decline development has been completed, and drill cuddies established to provide better drilling angles and shorter drilling distances.

Drilling to test for shoot 1 and 2 extensions to the north of the current Victor South resource outlines in 2004 has been successful, possibly extending both shoots 40 m north.

Long Deeps

Reinterpretation of the lower levels of the Long orebodies suggests the potential for additional nickel sulfide shoots below the southern end of the deposit, in an area structurally complicated by thrust faulting.

The Miitel and Wannaway nickel sulfide deposits, Widgiemooltha Dome, Kambalda

by

J. S. Reeve[1]

Introduction

The Widgiemooltha Dome is located some 40 to 70 km by road southwest of Kambalda (Fig. 1). Soon after the discovery of nickel at Kambalda in January 1966, the mafic–ultramafic stratigraphy surrounding the granitoid centre of the Widgiemooltha Dome was recognized as being similar to the Kambalda host stratigraphy (Fig. 2), and this area became the focus of an intense exploration effort that lasted through to the mid-1970s. The then-major global mining houses were actively involved in this area, and a number of small but significant discoveries were made. In the southern and western part of the Dome, a joint venture between Anaconda Australia and CRA Exploration discovered Redross and Wannaway. At the northern end, a joint venture between BHP Minerals and Inco discovered the Mount Edwards ('26N') deposit. Further north, but in the same stratigraphic succession, Selection Trust (Seltrust) discovered a number of orebodies, of which the Spargoville 5D was the most significant. Each of these explorers also located other significant occurrences, and many are still the focus of ongoing evaluation today.

Unfortunately, the collapse of the nickel price in the early 1970s meant that many of the discoveries were not brought into production at the time. Those that were developed (Redross and Seltrust) struggled economically, before closing prematurely in the prolonged low price environment. Shafts were also sunk at Wannaway and Mount Edwards, but production plans were shelved. By the early 1980s, Western Mining Corporation (WMC) had gained control of most of the prospective leaseholdings in the Widgiemooltha area, and these were consolidated into the Kambalda operation.

Largely because of low nickel prices, all nickel mines in the Widgiemooltha area were closed by 1999. At this point, WMC embarked on a progressive sell-off of its nickel assets in the Widgiemooltha and Kambalda areas. The Miitel–Mariners–Redross block on the eastern side of the Widgiemooltha Dome was purchased by Mincor Resources in February 2001, and production commenced from the Miitel mine in the following month. Production has continued ever since, at the rate of 18 000 t of ore per month. In mid-2001, Mincor also purchased the Wannaway block (on the western side of the Widgiemooltha Dome), and commenced production in October 2001, at a rate ramping up to15 000 t of ore per month.

Assisted by the strong nickel price, Mincor has, since mid-2003, implemented development plans for three new ventures in the area:

- an access decline to the North Miitel orebody;
- commencement of a decline into the remaining orebody at Redross;
- dewatering and rehabilitation of the Mariners mine.

All three developments will be in production by the end of 2004.

Mincor also maintains an aggressive exploration program on its leaseholdings in the Widgiemooltha area

The total cumulative production to date of all nickel mines in the Widgiemooltha Dome area is listed in Table 1.

Miitel orebody

The Miitel nickel deposit is located on the eastern side of the Widgiemooltha Dome, about 55 km by road southwest of Kambalda (Figs 1 and 2). The deposit was discovered by WMC Resources in the early 1990s, as a result of following up low-grade occurrences (about 0.5–1.0% Ni) in drilling from the late 1960s and early 1970s, carried out by Anaconda–CRA, the original nickel explorers in this area. The deposit was purchased by Mincor Resources, and brought into production in March 2001. Production to end of June 2004 is 697 000 t at 3.95% Ni. A further 370 000 t at 3.00% remains in ore reserves at Miitel, and 465 000 t at 2.65% at North Miitel, along the northern extension of the same ore channel. The deposit is open to the north and south, and further significant additions are expected. Currently, mineralization is known over a plunge length of 2300 m.

[1] Mincor Resources NL, 1 Havelock Street, West Perth, W.A. 6005, Australia

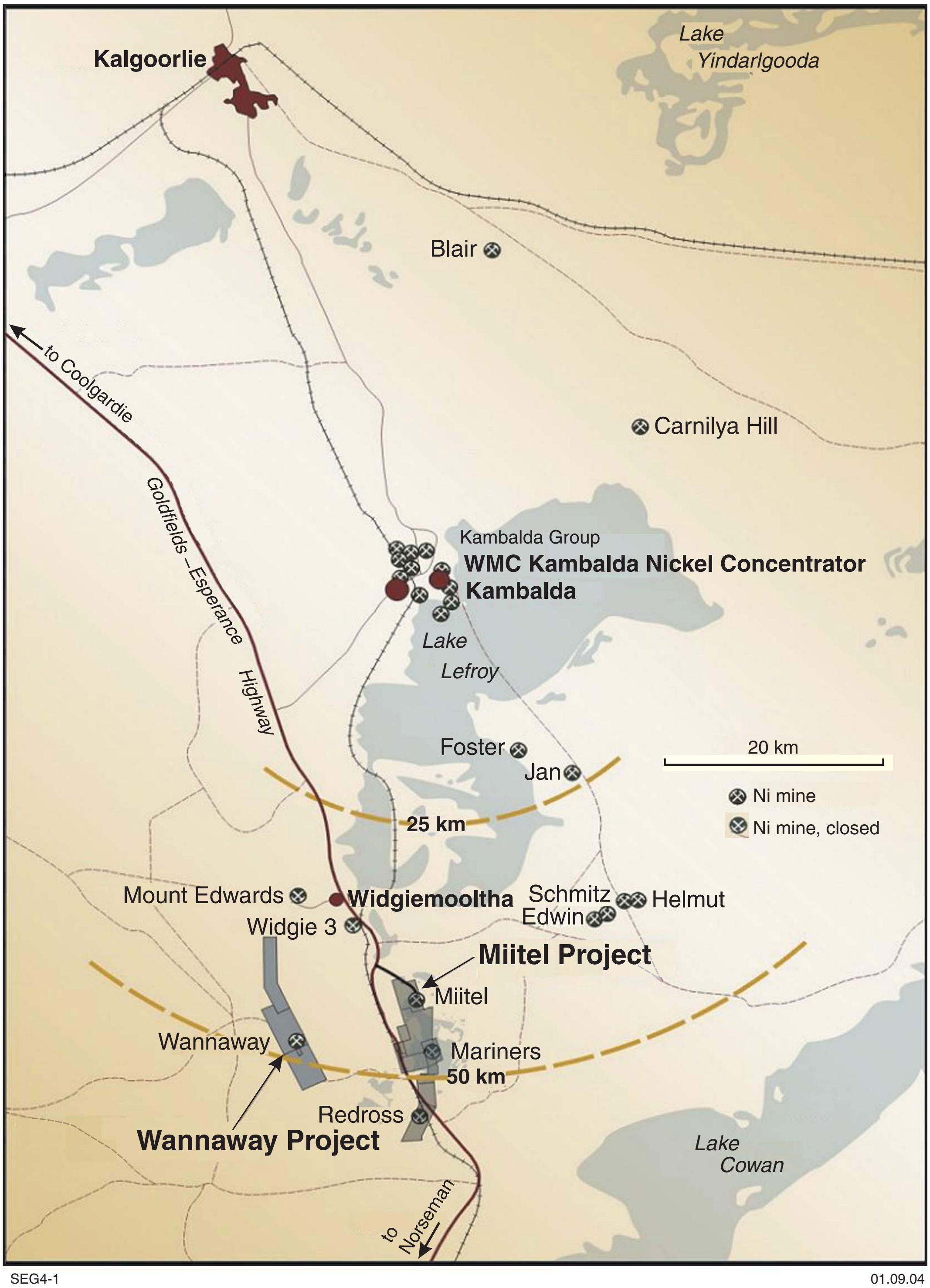

Figure 1. Location of Miitel and Wannaway nickel deposits

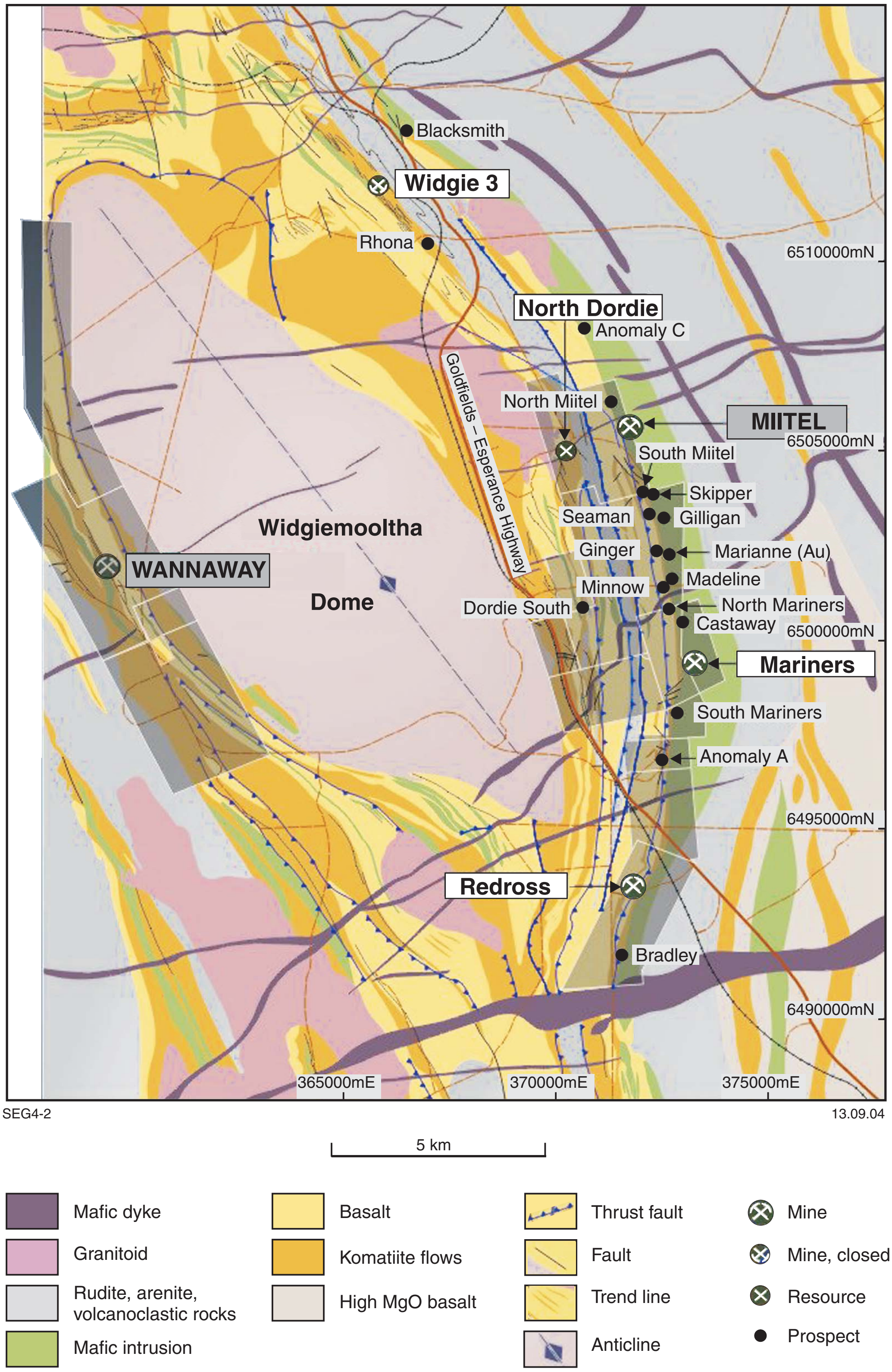

Figure 2. General geology of the Widgiemooltha Dome

Table 1. Total cumulative production to June 2004 of all nickel mines in the Widgiemooltha Dome area

Mine	*Years*	*Company and extraction method*	*Tonnes and nickel grade*	*Current status*
Redross	1971–78 1989	(Anaconda–CRA, underground) (WMC, openpit)	438 000 t @ 3.25% 97 600 t @ 2.43%	Being brought into production by Mincor Resources
Wannaway	1984–98 2001–04	(WMC, underground) (Mincor, underground)	646 600 t @ 2.30% 397 000 t @ 3.25%	Still in production by Mincor Resources
Mariners	1991–98	(WMC, underground)	1 114 700 t @ 2.53%	Being brought into production by Mincor Resources
Miitel	2001–04	(Mincor underground)	697 000 t @ 3.95%	Still in production by Mincor Resources
Mount Edwards	1981–95	(WMC, underground)	954 600 t @ 2.72%	Being evaluated by Titan Resources
Widgie 3	1988–91	(WMC, openpit)	82 600 t @ 2.17%	Being evaluated by Titan Resources
132 North	1991–92	(WMC, openpit)	32 200 t @ 3.54%	Being evaluated by Titan Resources
Spargoville 5D	1975–80	(Seltrust, underground)	600 000 t @ 2.50% (estimate only)	Being evaluated by Breakaway Resources
Spargoville 1A	1992–93	(Amalg, underground)	64 000 t @ 2.10% (estimate only)	Being evaluated by Breakaway Resources
Spargoville 5A	1997–98	(Amalg, openpit)	20 000 t @ 2.50% (estimate only)	Being evaluated by Breakaway Resources
Total mined to date:			**5.144 Mt @ 2.85%**	

Miitel is a typical Kambalda-style komatiite-hosted deposit. It has a north-northwesterly–south-southwesterly strike, and dips at 70–85° to the east (Figs 3 and 4), in keeping with its position on the eastern flank of the Widgiemooltha Dome. A recent geological description is given by Cairns et al. (2003). Significant features are summarized below.

- The deposit sits on the stratigraphically underlying basalt contact, and exhibits a typical ‘trough’-type channel structure, substantially modified by later structural deformation. The ore environment (the structurally modified channel) plunges flatly to the north (at the northern end), and flatly to the south at the southern end.
- Visually, the underlying basalt does not appear to be particularly strongly deformed relative to other orebody environments. Paradoxically, however, strongly ptygmatic quartz veins are present in some areas of the basalt, just below the contact.
- Five structural events have been defined. A late-stage arsenic mineralization event has resulted in vein structures, interpreted to be associated with D_4.
- Broadly, high grade mineralization occurs in the central ‘channel’ position, with lower grade mineralization on the upper and lower ‘flank’ positions. However, in detail, the picture is far more complex, as a result of superimposed structure. Towards the southern end, the mineralization occurs in a series of pods that are ellipsoidal in long-section.
- The ore profile is typical of Kambalda-type deposits, with massive sulfide (12–13% Ni) at the base, overlain by matrix mineralization (5–7% Ni), which is then overlain by disseminated sulfides (0.5–1.5% Ni) in talc–magnesite host. The higher-than-average grade for the Miitel deposit is a result of the relatively high tenor (nickel content of 100% sulfide equivalent), the overall thickness of the profile (averaging 1.5–2.0 m), and the relatively high proportion of massive sulfide in the total ore profile. All sulfide ores are pyrrhotite–pentlandite, with minor pyrite and chalcopyrite. There is some metre- to 10 m-scale remobilization of massive sulfide, resulting in a massive-sulfide-only profile in attenuated basalt–basalt ‘pinchout’ positions.
- Sedimentary rocks are essentially absent from the mine environment.
- Overlying ultramafic units are very high in Mg (reflecting the original olivine-rich cumulate), and are entirely altered to a talc–magnesite assemblage, with no serpentinite minerals recorded. Flow margins are observed, but original textures, such as cumulate and spinifex textures, appear to have been largely destroyed.

Wannaway orebody

The Wannaway nickel deposit is situated on the western side of the Widgiemooltha Dome, about 60 km southwest of Kambalda. Wannaway was discovered in 1970 by Anaconda–CRA, as a result of follow-up of a soil geochemistry anomaly. Although an exploration shaft was sunk at the time, and metallurgical bulk samples taken, the deposit was not brought into production until 1984, after it had been purchased by WMC. Between 1984 and 1998, 647 000 t at 2.3% Ni was mined. Towards the end of this period, WMC geologists located an adjacent ore position, known as the N02 orebody, just south of the mined orebody (designated the N01).

Mincor purchased the Wannaway property from WMC in mid-2001, and brought the N02 orebody into production in October of that year. Total production from this period to June 2004 is 397 000 t at 3.25% Ni. Remaining tonnages are largely lower grade material in the lower areas of both the N01 and N02 orebodies, and total about 150 000 t at 2.1% Ni. Exploration of the mine environment is continuing, however, and there are promising signs of further extensions.

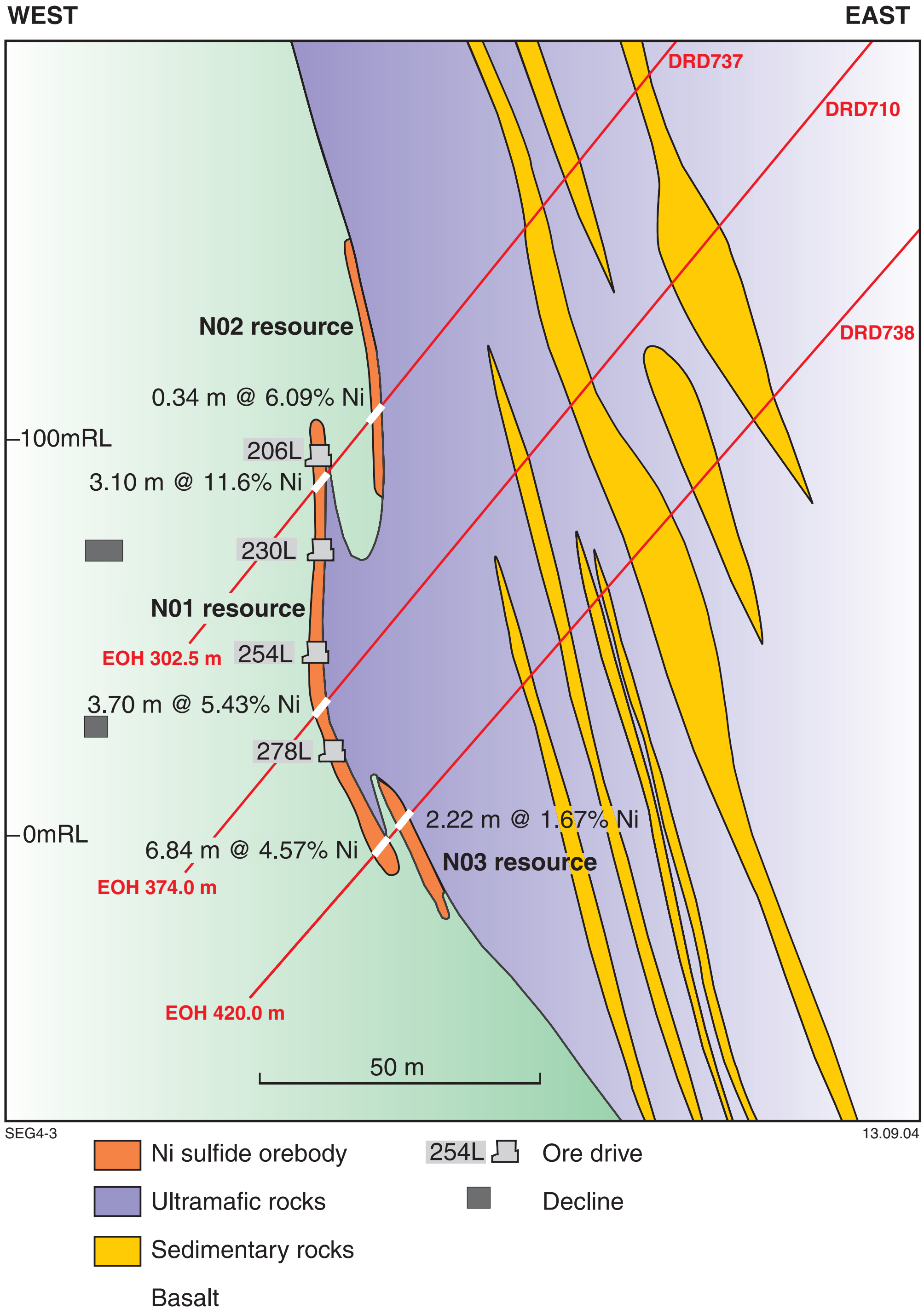

Figure 3. Cross section of the Miitel nickel deposit at 6505050N

Geologically, Wannaway has some unusual features and is less typical of a Kambalda-style deposit. A recent description is given by Daddow et al. (2003), and the geological features of Wannaway are summarized below.

- The orebody consists of two subparallel oreshoots (designated the N01 and N02 shoots; Fig. 5), which dip to the west at 60°, strike northerly, and plunge at 70° to the north-northwest.
- The upper part of the orebody sits above the basalt contact, with a small thickness (?2–10 m) of ultramafic rock sandwiched between the ore zone and the contact. In this area, sedimentary rocks sit on the contact. However, most of the orebody (approximately the lower three-quarters) directly abuts the underlying basalt contact, with no sedimentary units present.
- The orebody does not have a defined 'trough' or channel structure in the underlying basalt. This is very

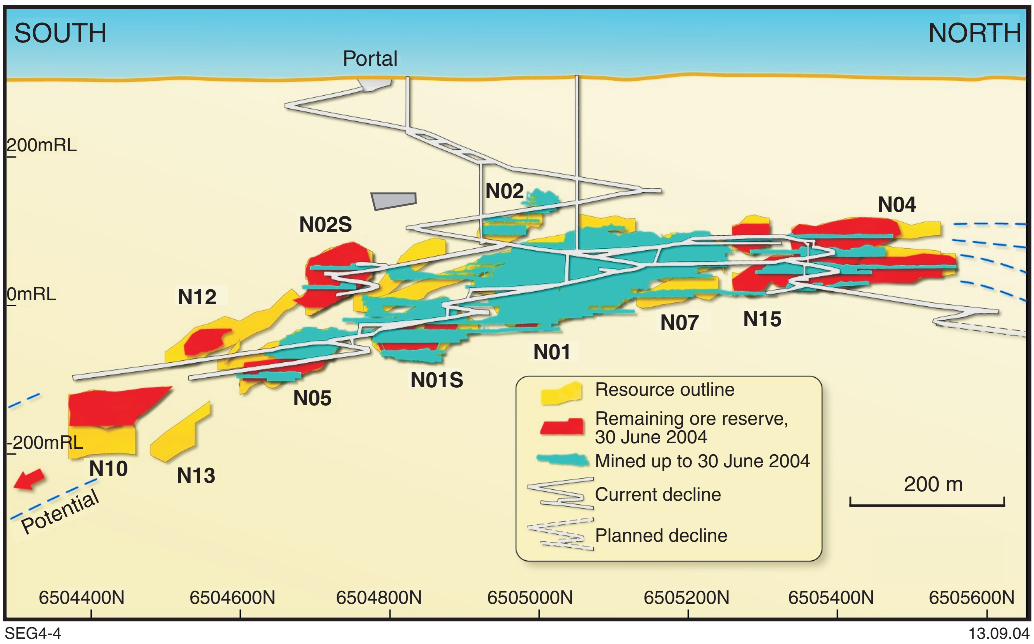

Figure 4. Long section of the Miitel nickel deposit showing distribution of ore

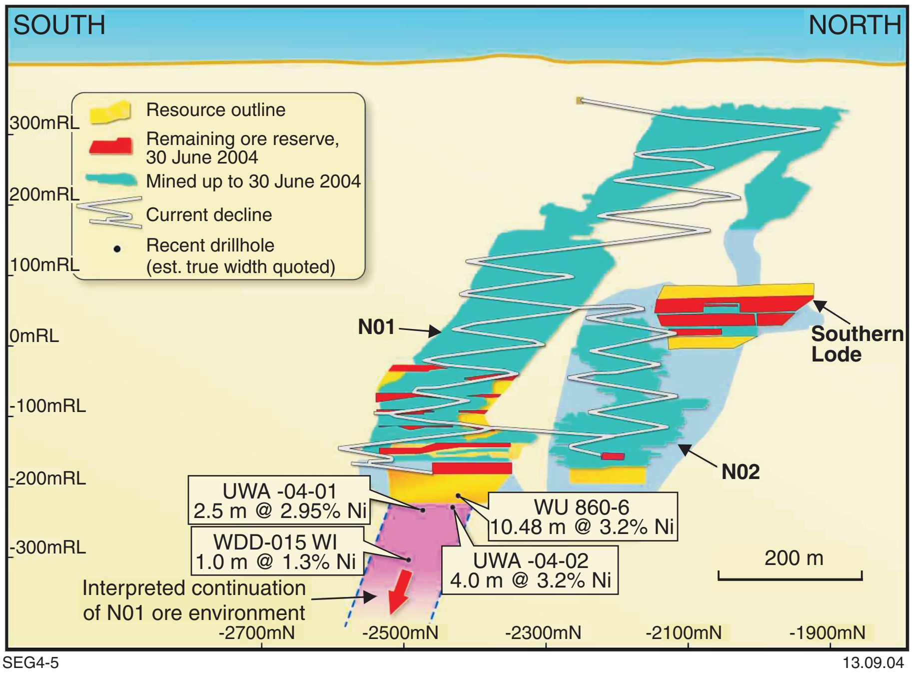

Figure 5. Long section of the Wannaway nickel deposit (local mine grid)

unusual for orebodies of the Kambalda district. At Wannaway, the basalt contact exhibits a broadly curviplanar morphology, with only minor small-scale 'pinchout'-type structures.

- The underlying basalt is strongly pillowed (at least in the upper 20 m). Pillows are invariably strongly deformed, exhibiting elongation and stretching from structural deformation (whereas for the Kambalda Dome orebodies, pillows in the basalt generally appear undeformed).
- The overlying ultramafic unit is a black serpentinite, with essentially no talc–magnesite alteration. This is unique in the Kambalda area, where ore-environment ultramafic rocks are always strongly or completely altered to talc–magnesite (with only remnant serpentinite areas). Relict cumulate textures are preserved in the Wannaway serpentinite.
- The lower margins of both the N01 and N02 oreshoots are characterized by interaction with sedimentary units along the basalt contact. Here, the massive sulfide and matrix sulfide ore types become progressively lower in tenor (as low as 4% Ni), as the pentlandite content decreases. Concurrently, the true sedimentary rock (usually a typical Archaean laminated black sulfidic 'shale') contains a high proportion of nickel — commonly up to 1–2%. In places, discrete zones of massive sulfide and matrix sulfide are interlayered with sedimentary units. However, the detailed relationships are highly variable and inconsistent. In some areas, the magmatic sulfides overlie the sedimentary units, whereas in others, the sulfides underlie these units and are in direct contact with basalt. Elsewhere, sulfides are enclosed by sedimentary rocks.
- The N01 and N02 oreshoots have different characteristics. The N01 oreshoot has a lower tenor (8–10% Ni), and only a very thin component of massive sulfide in its ore profile. Much of this ore zone is a relatively narrow width of matrix ore, leading to an overall low mined grade of 2.30% Ni, even using narrow-vein mining techniques. The N02 oreshoot has a relatively high tenor of 12–13% Ni, and a higher proportion of massive sulfide, giving the higher average mined grade of 3.25% Ni.
- Massive sulfide in the N02 oreshoot has apparently undergone significant local remobilization. Within this orebody, there are two relatively small (25 m × 50 m in long section) 'pods' of massive sulfide, where the thickness is up to 8 m. This is interpreted as local structural thickening associated with reverse movement.

The Wannaway orebody is interpreted an endmember representative of the Kambalda-style deposit. Low-angle reverse structural movement is interpreted to have thrust the upper part of the orebody off the contact, while also juxtaposing the lower sedimentary unit with the lower margin of the orebody.

Acknowledgements

The author acknowledges the work of all geological personnel who have documented the geology of these orebodies over the years. This description is published with the permission of Mincor Resources NL.

References

CAIRNS, C. P., MAPLESON, D. B., BEWSHER, A. W., and McCUAIG, T. C., 2003, Understanding the structural controls on arsenic mineralisation and ore distribution at the Miitel nickel mine, Widgiemooltha, Western Australia, *in* 5th International Mining Geology Conference, Bendigo, Victoria, 2003, Proceedings: Melbourne, Victoria, The Australasian Institute of Mining and Metallurgy, p. 61–72.

DADDOW, B., McCUAIG, T. C., and MAPLESON, D. B., 2003, Structural controls of the Wannaway nickel sulphide deposit, Widgiemooltha, Western Australia, *in* 5th International Mining Geology Conference, Bendigo, Victoria, 2003, Proceedings: Melbourne, Victoria, The Australasian Institute of Mining and Metallurgy, p. 101–112.

Gold mineralization in the St Ives camp near Kambalda

by

P. Neumayr[1], J. Walshe[2], K. Connors[3], S. Cox[4], R. S. Morrison[3], and E. Stolz[3]

Introduction

This contribution describes the geological and structural settings, and structural controls on gold mineralization, as well as camp- to deposit-scale hydrothermal alteration footprints in the St Ives gold camp (Fig. 1). The aim of the visit to St Ives is to show:

- the structural architecture of the camp;
- the structural and stratigraphic setting of gold deposits,
- typical mineralization styles;
- different alteration styles and alteration footprints in the camp.

Subject to mine schedules, the excursion will visit the Argo and Greater Revenge deposits, and excursion participants will have the opportunity to examine representative diamond drillcore showing mineralization and alteration styles.

Discovery and mining history

The St Ives gold camp is located about 55 km south-southeast of Kalgoorlie (Fig. 1). St Ives Gold Mining Company, a wholly owned subsidiary of Gold Fields Ltd, is currently the second-largest gold-mining operation in Australia, producing about 500 000 ounces of gold per annum.

Gold was discovered at Kambalda (the 'Red Hill Camp') in 1897 and, between 1897 and 1907, the gold workings of the area supported a small township. Other gold-bearing locations, such as Victory, were discovered at this time. A total gold production of 31 000 ozs is recorded for this period, mostly from the Red Hill group of mines. Thereafter, the area attracted only intermittent attention of prospectors until 1919, when a significant new discovery was made at St Ives. Another small town was constructed, but soon abandoned when the mine closed in about 1926.

Gold prospecting activity continued until Fe–Ni sulfides were discovered in 1966 near the old Red Hill mine. Gossanous outcrop collected by uranium prospectors in 1954 was brought to the attention of Western Mining Corporation (WMC) in 1964. The ground was acquired by WMC, and geological mapping, and geochemical and geophysical surveys were completed in the area of the Kambalda Dome. Several anomalies and gossans were identified at the basal contact of the ultramafic unit. Drilling (diamond drillhole KD-1) of the gossan near Red Hill commenced at the end of 1965, and resulted in the discovery of the Lunnon shoot in January 1966. This orebody, and others discovered shortly thereafter, formed the resource base of Kambalda Nickel Operation (KNO). A mining and milling operation was developed rapidly, and transport of nickel concentrates from Kambalda commenced in mid-1967. Production increased rapidly and exceeded 30 000 t of nickel metal in 1970–71. This production represented about 8% of the western world production. WMC constructed a refinery at Kwinana in 1970, and a smelter at Kalgoorlie in 1972. A major new industry had been established. Total historical production for the greater Kambalda nickel mining district from 1967 to 1996 is about 34 Mt at 3.1% nickel, for more than 1 Mt of nickel metal in concentrate.

An increase in the price of gold in the late 1970s provided the impetus for re-evaluation of the old gold prospects in the Kambalda area. It was soon recognized that significant gold mineralization remained, particularly in the Victory area, and exploration effort substantially increased in the early 1980s. Gold production recommenced in 1981 and has since expanded with the construction of a 3 Mt per annum mill at St Ives. Annual gold production reached 400 000 ozs in 1996. From commissioning until May 1998, the plant processed almost 27 Mt of ore to produce just over 3 million ounces (Moz) of gold.

[1] pdm*CRC; Centre for Global Metallogeny, The University of Western Australia, 35 Stirling Highway, Crawley, W.A. 6009, Australia

[2] pmd*CRC; Division for Exploration and Mining, CSIRO, 26 Dick Perry Avenue, Kensington, W.A. 6151, Australia

[3] St Ives Gold Mining Company Pty Ltd, Post Office, Kambalda, W.A. 6444, Australia

[4] Research School of Earth Sciences and Department of Geology, The Australian National University, Canberra, A.C.T. 2600, Australia

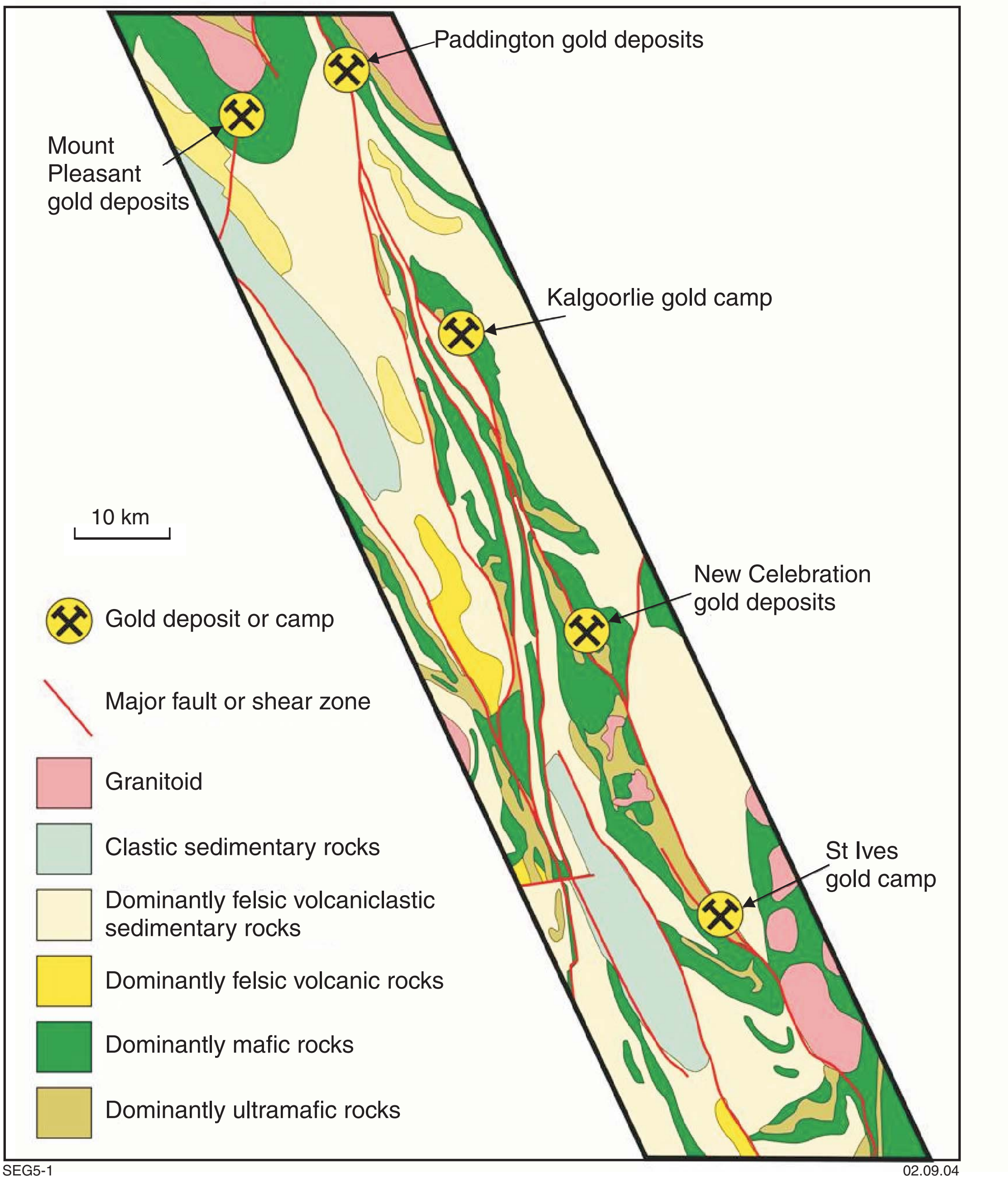

Figure 1. Location of the St Ives gold camp

Since Gold Fields purchased the properties for US\$232 million in 2001, the camp has seen an unprecedented exploration effort, mainly in the Greater Revenge, Argo, and Intrepide complexes, and a total of A\$30 million was spent on reserve replacement and reserve expansion work in the 2003 financial year. In late 2003, Gold Fields announced plans to construct a new A\$125 million, 4.5 Mtpa gold-processing facility at St Ives. At present, St Ives Gold Mining Company operates three underground mines (Junction, Argo, and Leviathan) and two openpit complexes (Greater Revenge and Argo). In the 2003 financial year, 513 000 oz of gold were produced from the camp.

Geological setting of the St Ives gold camp

Introduction

The St Ives gold camp is located in the Archaean Norseman–Wiluna greenstone belt of the Yilgarn Craton of Western Australia (Figs 1 and 2). The Norseman–Wiluna greenstone belt (Gee, 1979; Gee et al., 1981) is a north-northwesterly trending belt that extends about 200 km in width and 800 km in strike length, and is part of the Eastern Goldfields Province (McNaughton and

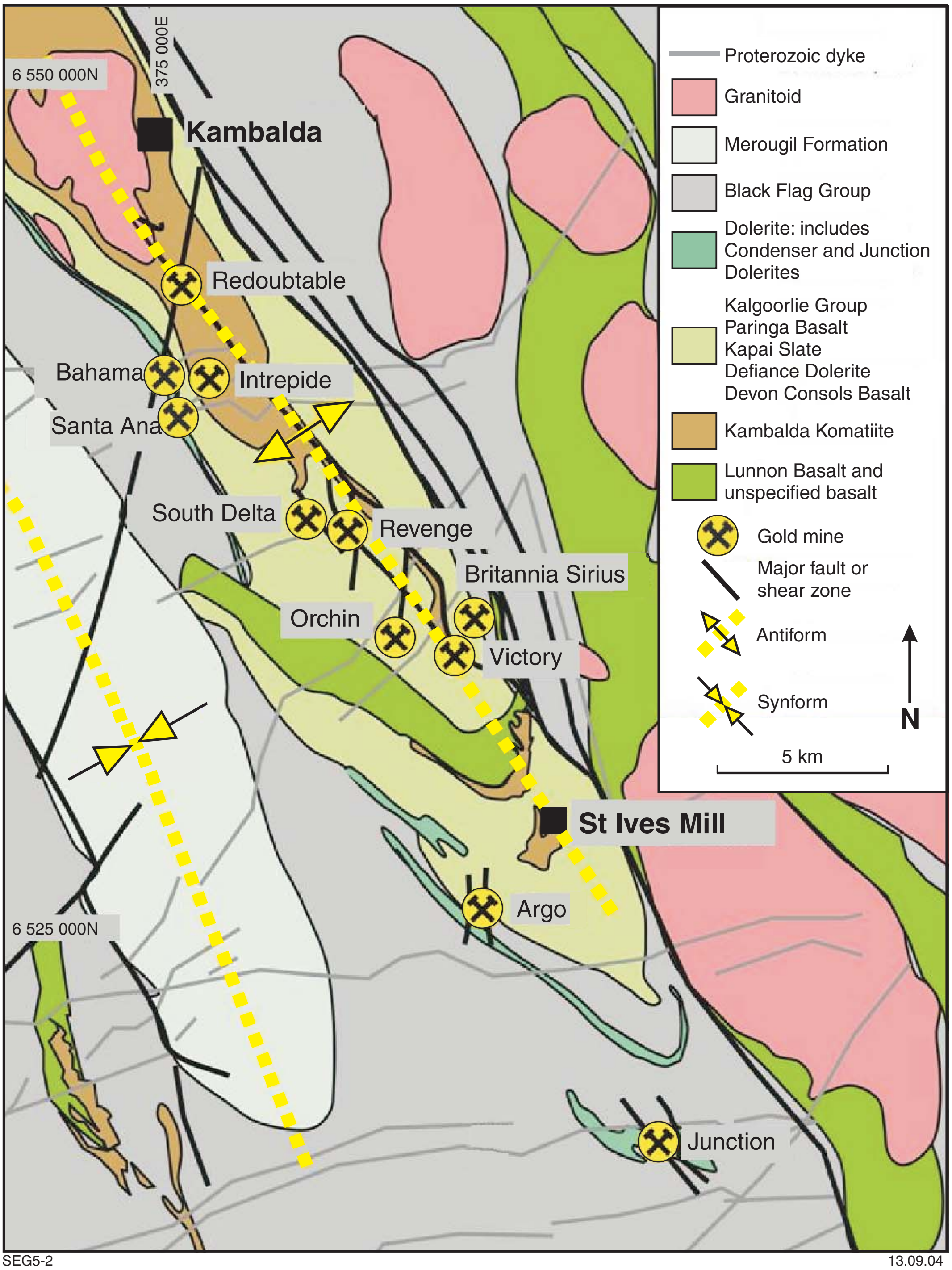

Figure 2. Geology and location of gold deposits in the St Ives gold camp

Dahl, 1987). It comprises successions of tholeiitic and komatiitic volcanic rocks, felsic–intermediate intrusive rocks, and volcanoclastic and epiclastic sedimentary rocks (Gee, 1979; Gee et al., 1981). The belt is intruded by numerous granitoids and porphyry swarms, and is characterized by the absence of banded iron-formation (BIF) marker horizons. The Norseman–Wiluna greenstone belt hosts over two-thirds of Australia's known Archaean gold endowment (Woodall, 1990).

Stratigraphy

Stratigraphic sequence

In the Kambalda – St Ives area, the Norseman–Wiluna greenstone belt consists mainly of mafic–ultramafic lavas and intrusions (Figs 2, 3, and 4; Table 1), and is bound by the Lefroy Fault to the east and the Merougil Fault to the west (Nguyen et al., 1998). In the following descriptions,

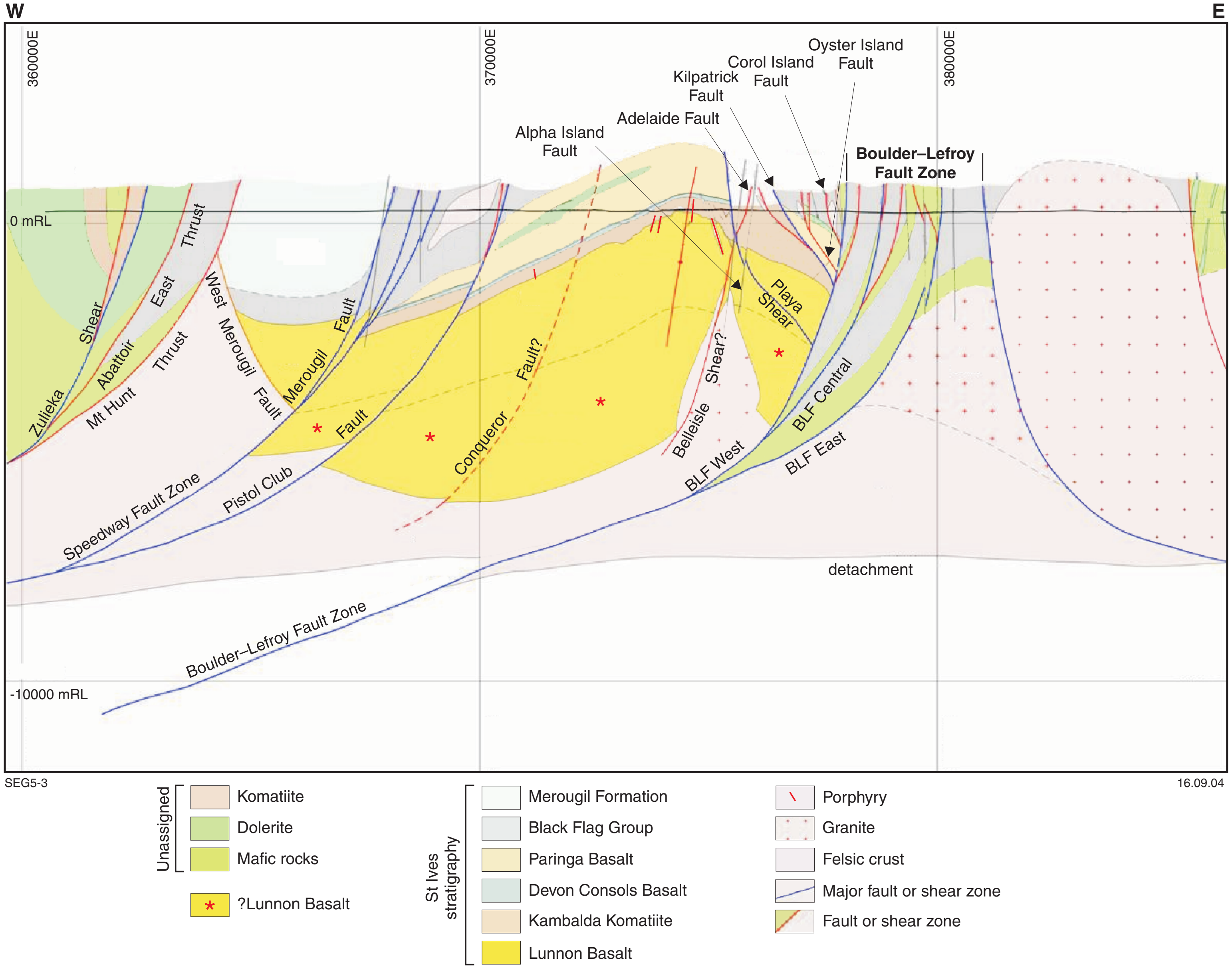

Figure 3. Cross section at 6545020N in the Intrepide area showing geological and structural setting of the St Ives gold camp

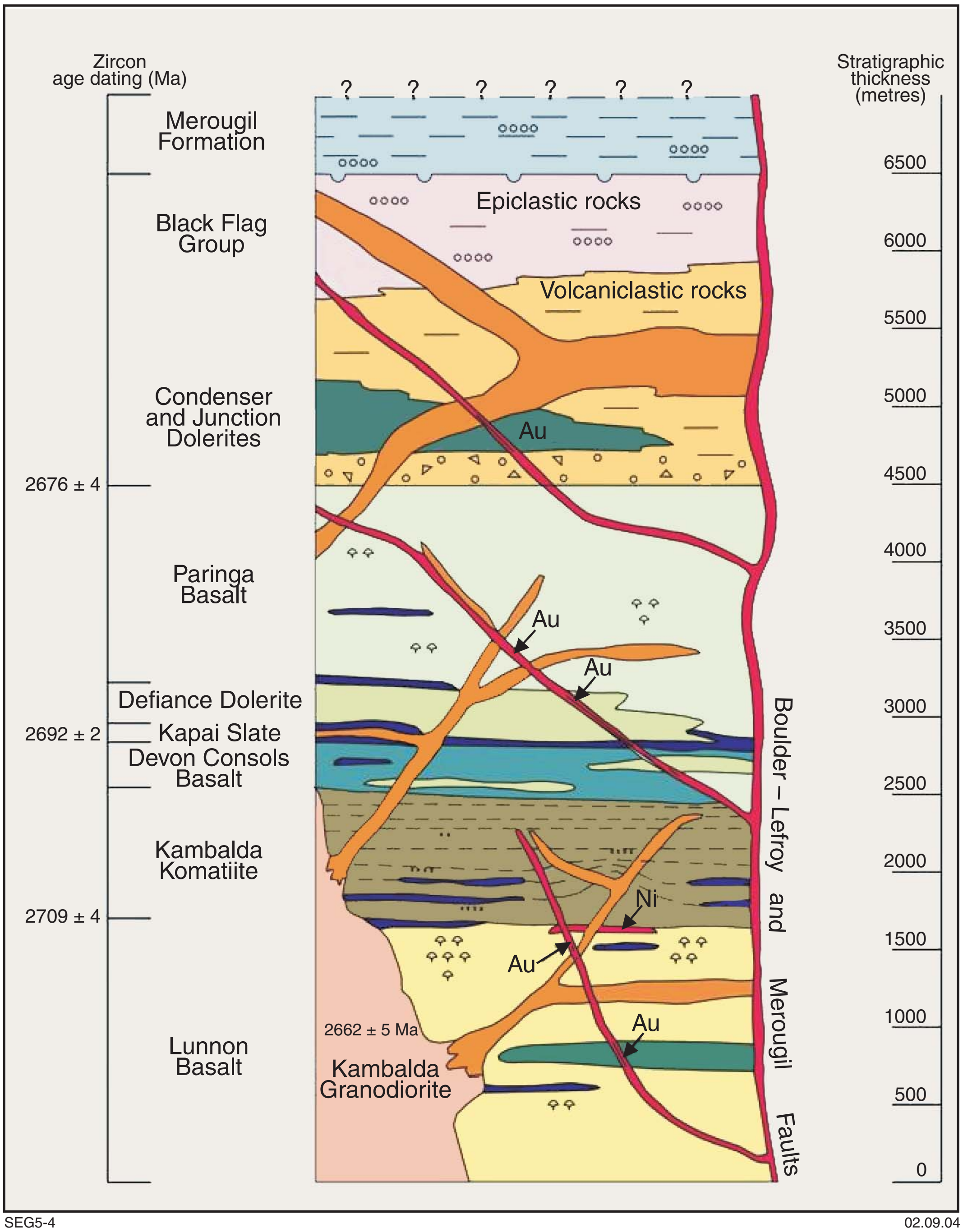

Figure 4. Stratigraphic relationships in the St Ives gold camp, based on the Kambalda–Tramways stratigraphy (after Cowden and Archibald, 1987)

Table 1. Summary of main stratigraphic units in the Kambalda–Kalgoorlie region

Group	*Formation*	*Age (Ma)*	*Notes*
	Merougil Formation	2664 ± 6	Hand (1996)
Black Flag Group	Morgans Island Epiclastic Formation	2666–2669	Hand (1996); locality just south of Kalgoorlie but most Black Flag Group must predate D_1 deformation at c. 2675 Ma, consistent with the 2676 ± 4 Ma age of a crystal tuff unit from the Kambalda area (quoted in Connors et al., 2003)
	Newton Felsic Formation		
Kalgoorlie Group	Paringa Basalt	2690 ± 5	Quoted in Connors et al. (2003)
	Kapai Slate	2692 ± 4	Claoué-Long et al. (1988)
	Devon Consols Basalt	2693 ± 30	Compston et al. (1986)
	Kambalda Komatiite	2709 ± 4	Quoted in Connors et al. (2003)
	Lunnon Basalt	2726± 30	Chauvel et al. (1985)

all Archaean rocks are metamorphosed, and the prefix 'meta' is omitted but implied.

Kalgoorlie Group

Lunnon Basalt

The Lunnon Basalt is the lowest stratigraphic formation in the Kalgoorlie Group. It is a thick (>2000 m, and up to 5 km based on three-dimensional gravity models) tholeiitic basalt sequence that consists of thin (2–3 m) lava flows, minor interflow sedimentary rocks, and concordant dolerite dykes (Watchorn, 1998). Pillowed zones are common in the basalt, but vesicles (varioles) are rare. The basalt is a low-magnesium pillow basalt, with MgO content ranging from 6 to 7% at the Foster Thrust (Nguyen, 1997). The formation is conformably overlain by the Silver Lake Member of the Kambalda Komatiite.

Kambalda Komatiite

The Kambalda Komatiite is a 100 to >1200 m-thick sequence of high-MgO ultramafic flows (Watchorn, 1998). The sequence has been subdivided into the lower Silver Lake Member and the upper Tripod Hill Member (Gresham and Loftus-Hill, 1981). The volcaniclastic sedimentary unit near the base of the komatiite has been dated at 2709 ± 4 Ma (Claoué-Long et al., 1988). The massive-sulfide nickel orebodies of the Kambalda area occur at the basal contact of the Silver Lake Member with the Lunnon Basalt. The Silver Lake Member consists of one or more, 10–100 m-thick, komatiite flows, which are subdivided into a lower cumulate zone, with up to 48% MgO, and an upper spinifex-textured zone. Numerous lenticular interflow sedimentary rocks are interleaved with the komatiite lavas. The Tripod Hill Member consists of thin (<0.5 to 10 m) komatiite lava flows, which reach a combined thickness of up to 700 m. The upper komatiite flows are more differentiated than those of the Silver Lake Member, and contain less abundant interflow sedimentary rocks.

Devon Consols Basalt

The contact of the Devon Consols Basalt with the underlying Tripod Hill Komatiite is typically gradational (interfingering) but locally sharp (Gresham and Loftus-Hill, 1981; Cowden and Roberts, 1990). The unit, previously documented as being 60–100 m thick, has been noted at over 150 m thick in the Greater Revenge area. It is composed of pillowed and massive variolitic lava flows and thin differentiated synvolcanic dolerites (Victory and Trafalgar Dolerites). The Victory Dolerite is internally zoned, with an ultramafic pyroxenite base to ophitic gabbro, but granophyre is absent and there is no evidence for systematic Fe-enrichment (MacGeehan, 1984).

The Devon Consols Basalt pillowed sections are distinctively variolitic. Field exposures typically have a nodular, warty appearance due to differential weathering of the varioles. The varioles are up to 2 cm in diameter, felsic (white to pale yellowish-green), and are concentrated in the central zones of pillows. Aphyric hyaloclastite fragments occupy interpillow spaces. The differentiated units comprise fine-grained basaltic upper zones and coarse-grained gabbroic lower zones. The major metamorphic mineral assemblage of the Devon Consols Basalt is actinolite–chlorite–zoisite–albite, with about 30% actinolite.

Geochemically, the Devon Consols Basalt has been divided into two types (Redman and Keays, 1985): (1) high-Si, low-Mg basalts (52–60% SiO_2, 4–6% MgO); and (2) low-Si, high-Mg basalts (47–52% SiO_2, 9–16% MgO). The two geochemical types have Al_2O_3/TiO_2 ratios of about 20 and are enriched in LREE ($[La/Sm]_n$ ratio = 1.2–1.3). The Nd isotopic data of ε_{Nd} range from +1.2 to -3 (Foster, 1993), and indicate melt derivation from a long-term depleted source (Lesher and Arndt, 1995). These rocks are considered by Lesher and Arndt (1995) to be komatiitic basalts formed from crustally contaminated komatiitic melt. This interpretation is consistent with the presence of xenocrystic zircons older than 3400–3100 Ma in the Victory Dolerite (Compston et al., 1986; Claoué-

Long et al., 1988). The morphology of the zircons suggests derivation from felsic granulite (Compston et al., 1986). All the data suggest that the Devon Consols Basalt parental melts interacted with very old felsic granulite basement, or eroded products thereof, and were contaminated by up to 5–7% continental crust (Lesher and Arndt, 1995).

Kapai Slate

The Kapai Slate marks the boundary between the underlying Devon Consols Basalt and the overlying Paringa Basalt, and occurs throughout the Kambalda Dome – St Ives – Tramways area. The Kapai Slate is up to 10 m thick, but is typically intruded by intermediate to felsic sills.

Siliceous sedimentary facies of the Kapai Slate are considered to represent a combination of tuffaceous debris from distal felsic volcanic eruptions, and minor chemical deposition from silica-rich exhalations. In an alternative interpretation, these zones have been silicified after their deposition. The interpretation of a tuffaceous component is consistent with the presence of 2692 ± 4 Ma magmatic zircons in these rocks (Claoué-Long et al., 1988). Rare xenocrystic zircons as old as 3450 Ma have been identified, and could indicate pre-existing continental crust (Claoué-Long et al., 1988). Carbonaceous facies of the Kapai Slate probably originated from non-photosynthetic bacteria and cyanobacteria inhabiting quiescent sea-floor environments. A sulfide-rich facies is interpreted by Marsh (1988) to have been deposited in an active extensional basin where sea-floor hydrothermal alteration was intense.

Paringa Basalt

The Paringa Basalt is 500–1500 m thick, and consists of thin variolitic, pillowed flows and thick, differentiated dolerite units, such as the Defiance Dolerite (Carey, 1994).

Basalt facies

Pillows display 2–3 cm-thick rinds and chlorite-rich varioles. The varioles are markedly less prominent than in the Devon Consols Basalt (see above). Interpillow breccias are common and broad zones of hyaloclastite breccia are developed close to the base. Thin, laminated interflow cherty sedimentary units are present close to the base of the unit (Balkau, 1989).

The metamorphic assemblage of the Paringa Basalt is actinolite–chlorite–biotite–albite–epidote–clinozoisite–quartz and Fe–Ti oxides. Where igneous textures are preserved, the basalts appear to have been clinopyroxene-phyric. Clinopyroxene is replaced by biotite, chlorite and actinolite.

Geochemically, the Paringa Basalt has high magnesium (12–16% MgO) and silica (49–57% SiO_2) contents (Redman and Keays, 1985). The Al_2O_3/TiO_2 ratios average about 20. Thicker differentiated flows or sills contain coarse-grained gabbroic (6–8% MgO) upper parts and ultramafic (22–24% MgO) lower parts. The Paringa Basalt has $[La/Sm]_n$ ratios of 2.5–2.8 and negative ε_{Nd} values, which together have been interpreted to indicate up to 25% crustal contamination (Lesher and Arndt, 1995). Sensitive high resolution ion microprobe (SHRIMP) U–Pb analyses of magmatic zircons derived from interflow chert (drillhole TD 1323, 214 m) high in the Paringa Basalt provided a date of 2690 ± 5 Ma (quoted in Connors et al., 2003; Clout, 1991).

Dolerite facies

The Defiance Dolerite occurs at the base of the Paringa Basalt and is up to 300 m thick, but is variable in thickness, being thin or absent in many areas of the camp (i.e. Intrepide to the Dome). The dolerite is distinctly zoned in areas where it is thick and well preserved. The unit is interpreted to have fractionated in situ to produce five internal zones:

- *Zone 1*: Directly overlies the Kapai Slate and has an average thickness of 55 m in the Victory mine area. It is an equigranular dolerite at the base, grading upwards into a medium-grained orthopyroxene orthocumulate with <10% feldspar. The bulk composition is about 18% MgO.
- *Zone 2*: Porphyritic dolerite consisting of glomero-porphyritic clusters of orthopyroxene altered to amphibole, in an equigranular pyroxene–plagioclase matrix.
- *Zone 3*: Equigranular dolerite with tabular plagioclase and lacking mafic phenocrysts. Granophyric intergrowths of albite and quartz comprise 10% of the groundmass, and form irregular patches up to 3 mm in diameter.
- *Zone 4*: Granophyric or oxide gabbro zone. It is defined by an increase in quartz-granophyre content to more than 10%, the presence of fine-grained subhedral magnetite, and the development of bladed pyroxene. Up to 70% spherulitic granophyre can be present in the centre.
- *Zone 5*: This is an upward gradation of Zone 4 into a medium- to fine-grained dolerite, which contains bladed ex-pyroxene with <10% granophyre. The upper chill zone contains radiating clusters of elongate branching pyroxene forming a quench texture.

The parental magma composition has been estimated by analysing chilled border zones and calculating the weighted average of all the internal zones. The interpreted parent magma composition is about 53% SiO_2 and 9.6–11.4% MgO, similar to the siliceous, high-Mg Paringa Basalt.

Black Flag Group

The contact between the Black Flag Group and the underlying Paringa Basalt is unconformable. The Black Flag Group consists of a lower sequence of mafic conglomerates, and felsic and intermediate volcanic rocks, and an upper sequence of felsic pyroclastic rocks and conglomerates, calcareous wackes, siltstones, and shales (McCall, 1969; Balkau, 1989). The sequences are called the Newtown Felsic Formation and the Morgans Island Epiclastic Formation, respectively.

Merougil Formation

The Merougil Formation outcrops on the west shores of Lake Lefroy, where it unconformably overlies the Black Flag Group. The formation is composed of lensoidal, monomictic to increasingly polymictic conglomerate units, and massive to stratified sandstones (Hand, 1996). The basal unconformity, which is typically faulted, marks a drastic change from a deep-water environment to a proximal braided river system. The formation is subdivided into a lower conglomerate-dominant facies and an upper sandstone-dominant facies (Bader, 1994).

Dolerites and gabbros

The stratigraphy is intruded by numerous mafic intrusions of varying thickness and displaying varying degrees of differentiation. Most are similar in geochemical composition to the lavas they intrude, and are therefore interpreted to be synvolcanic sills (e.g. Defiance Dolerite). However, the Junction and Condenser Dolerites are geochemically distinct from any known lavas in the area, and intrude the Black Flag Group.

The Condenser and Junction Dolerites are up to 500 m thick and are considered to be lateral equivalents of the very highly mineralized Golden Mile Dolerite at Kalgoorlie. They are internally zoned as follows:

- *Zone 1*: Weak pyroxene cumulate dominated by amphiboles and quartz, and containing less abundant feldspar. Ilmenite is the dominant oxide.
- *Zone 2*: Porphyritic dolerite containing amphiboles and an increased plagioclase content as distinct laths and an interstitial phase. Ilmenite and titanomagnetite are present.
- *Zone 3*: Quartz–plagioclase granophyre comprising up to 25% of the rock. Blue quartz is characteristic of this zone. Tabular plagioclase is common, and amphibole forms elongate acicular crystals. The oxide concentration is highest in this zone, consisting of co-existing ilmenite and magnetite.
- *Zone 4*: 'Bladed' dolerite with elongate to tabular amphiboles, and plagioclase as laths as well as an interstitial phase. Ilmenite is the dominant oxide.

Parental magma compositions are estimated by analysing chilled border zones or calculating the weighted average of all the internal zones. The Condenser and Junction Dolerites are Fe-rich tholeiites (50.6–51.1% SiO_2, 1.2–1.6% TiO_2, 12.7–14.5% FeO, and 5–7% MgO), very different in composition from the Defiance Dolerite (high-Mg basalt), but similar to the stratigraphically equivalent Golden Mile Dolerite. The Condenser and Junction Dolerites formed by the in situ differentiation of a tholeiitic magma. SHRIMP analyses of magmatic zircons from a pegmatite patch in the gabbro zone of the Condenser Dolerite gave a date of 2680 ± 8 Ma (Carey, 1994).

Granitoids

The Kalgoorlie and Black Flag Groups are intruded by intermediate to felsic granitoid stocks, dykes, and sills ranging from diorite to trondhjemite to rhyolite in composition (Roberts and Elias, 1990). Three major granitoid associations have been described:

1. Small intermediate to mafic intrusions that are aphyric and fine grained, deformed, and either bound by shear zones or forming layer-parallel bodies. A possible example is the Loreto Aplite (post D_1), dated at 2687 ± 4 Ma (quoted in Connors et al., 2003).

2. Large and subconcordant xenolithic sills, mainly of intermediate composition with rare felsic differentiates. Sills abound within the Kambalda Komatiite and are up to 300 m thick, possibly forming composite bodies; thinner felsic and intermediate sills intrude the Kapai Slate. The compositions of these rocks range from dioritic to granitic, with intermediate endmembers being hornblende phyric, and felsic members containing embayed quartz and albite phenocrysts in a fine-grained crystalline or glassy groundmass. SHRIMP analyses of magmatic zircons from a quartz–albite felsic porphyry at Victory gave an date of 2673 ± 10 Ma (Clout, 1991; quoted in Connors et al., 2003), whereas a xenolithic diorite and felsic phase from the Revenge mine yielded SHRIMP ages of 2661 ± 2 Ma and 2658 ± 4 Ma, respectively (Nguyen 1997).

3. Kambalda Granodiorite, a trondhjemite intrusion, and associated near vertical felsic dykes. These intrusions are largely massive, discordant to early structures, and are intruded along and deformed by late faults (Clark et al., 1986). The dykes are mainly felsic with quartz and albite phenocrysts, or rare megacrysts, in a glassy to medium-grained groundmass. The felsic dykes have equivocal field relationships with the Kambalda granodiorite. SHRIMP analyses of magmatic zircons from the Kambalda Granodoirite indicated a date of 2662 ± 6 Ma (drillhole LD9188/615, 624 m; Compston et al., 1986).

Four types of 'porphyry' intrusions are recognized in the Kambalda – St Ives area:

1. 'Pietra' porphyritic microgranodiorite, with 15–20% large rounded to lobate transparent quartz phenocrysts and about 25% smaller plagioclase phenocrysts, and hornblende bearing.

2. 'Lapis' porphyritic micromonzodiorite, with about 10% rounded to lobate transparent quartz phenocrysts and about 30% smaller plagioclase phenocrysts, and hornblende bearing.

3. 'Rocca' porphyritic micromonzodiorite, with 10–15% phenocrysts, most of which are feldspars, and lacking hornblende.

4. 'Flames' porphyritic tonalite to granodiorite, with quartz and albite phenocrysts, and alkali feldspar megacrysts. It also contains granite and lamprophyre xenoliths.

Geochemically, the granitoids are felsic to intermediate, with SiO_2 contents of 60–70%; $Na_2O + K_2O$ contents in the range 5–10%; and FeO/MgO ratios in the range 1.3–2.5. The rocks are classified as tonalite (dacite) and granodiorite or quartz-monzodiorite (trachydacite). Their major element compositions are the same, and they are sub-alkaline to calc-alkaline in geochemical affinity.

Lamprophyres

Lamprophyres are dark, strongly porphyritic, igneous intrusions that contain abundant euhedral phenocrysts of mafic minerals such as olivine, clinopyroxene, biotite or phlogopite, and amphibole, set in a felsic, mafic, or intermediate matrix. Important criteria for recognition are a lack of felsic phenocrysts, with feldspar and quartz being restricted to the groundmass. The principal types of lamprophyres in the Kambalda – St Ives area are kersantites and spessartites. SHRIMP analyses of magmatic zircons from kersantite bodies at Hunt and Cave Rocks (drillhole CVK166, 165 m) yielded dates of 2684 ± 6 Ma and 2627 ± 10 Ma, respectively (quoted in Connors et al., 2003).

Lamprophyres form a subordinate group of sills, dykes, and plugs in the Kambalda – St Ives district. Sills several metres thick intrude the Kapai Slate and thin biotite- and hornblende-phyric lamprophyre dykes have been identified associated with felsic dykes in the Lunnon shoot area and to the north of the Durkin shoot (Rock et al., 1990).

Geochemically, the lamprophyres are mafic to intermediate, with SiO_2 contents in the range 53–55%; $Fe_2O_{3\,total}$ contents of 6.3–7.4%; MgO content of of 7–9%; CaO content of 3–7%; and total volatiles in the range 4.0–8.5%. They are enriched in large-ion lithophile elements, with K_2O contents of 1.33–2.7%; Rb contents of 56–83 ppm; and Ba contents of 885–1296 ppm. Most of the incompatible elements, such as Th, Zr, P, and light rare earth elements (LREE), are also enriched relative to mid-ocean ridge basalt (MORB). Compatible elements Cr and Ni are present in moderate to high amounts.

Proterozoic dykes

Unmetamorphosed Proterozoic dolerite dykes intrude fracture sets with four main orientations: east, northeast, east-northeast, and south-southeast. The dykes are subvertical and up to 40 m thick. Proterozoic dykes are distinguished from Archaean dolerites by the presence of olivine, a strongly magnetic character, and abundant epidote on fracture surfaces.

Tectonostratigraphic evolution

The stratigraphic sequence shows the effects of four phases of post-volcanic compressional deformation (D_1–D_4), and a number of deformation schemes have been proposed. More recent interpretations of the structural history have recognized the importance of several episodes of extensional deformation and basin formation in the development of the early fault architecture, which, in turn, has had a significant influence on the later history of compressional deformation.

Nguyen (1997) recognized the same four major compressional events as previous workers, but also included an early episode of basin development during formation of the Kambalda stratigraphy (D_{e1}), and an early D_3 stage of northeasterly to east-northeasterly subhorizontal extension associated with deposition of the Merougil Formation and emplacement of quartz–albite dykes. More recent geochronology suggests that the Merougil Formation was deposited during the later stages of D_2 compression (see below), and that the extension event noted by Nguyen (1997) probably occurred between D_1 and D_2 (D_{e3} in Table 2, rather than between D_2 and D_3). Workers in other parts of the Yilgarn Craton have recognized an additional period of extensional deformation (D_{e2} in Table 2, Fig. 5) between the two noted by Nguyen (1997), and this is associated with felsic magmatism, and Black Flag Group sedimentation and volcanism. Seismic data suggest that some structures, such as the Abbatoir Shear, were active during this event.

D_{e1} mafic–ultramafic volcanism

The tectono-stratigraphic history of the Eastern Goldfield Province started with a period of mafic–ultramafic volcanism (D_{e1}) at 2720–2690 Ma (Barley et al., 2002). The mafic to ultramafic volcanic rocks were deposited in basins formed within older continental crust, which appears to be largely felsic, based on the seismic reflection data and gravity modelling (Goleby et al., 1993). This older crust is locally exposed at the southern end of the Eastern Goldfield Province at Norseman, where the rocks have been dated at c. 2930 Ma (Hill et al., 1992). The stratigraphic units in the St Ives area that formed during this period are collectively termed the Kalgoorlie Group and include the:

- Lunnon Basalt;
- Kambalda Komatiite (2709 ± 4 Ma, U–Pb zircon SHRIMP; Claoué-Long et al., 1988);
- Devon Consols Basalt (2693 ± 30 Ma, U–Pb zircon SHRIMP; Compston et al., 1986);
- Kapai Slate (2692 ± 4 Ma, U–Pb zircon SHRIMP; Claoué-Long et al., 1988);
- Defiance Dolerite;
- Paringa Basalt (2690 ± 5 Ma, U–Pb zircon SHRIMP; Clout, 1991).

The faults that originated during this deformation event are interpreted to include many of the major north-northwesterly trending structures previously interpreted as being D_3. Significant across-structure stratigraphy variations indicate that these structures were probably involved in basin development during this event.

D_{e2} felsic magmatism

The second major depositional event (D_{e2}) occurred from c. 2690 to 2660 Ma (Barley et al., 2002), involved north-northwesterly–south-southeasterly extension (based on extensional fabrics in c. 2680 Ma granitoid domes; Williams and Whitaker, 1993), and was associated with felsic magmatism, sedimentation, and local mafic magmatism (Condenser, Defiance, and Junction Dolerites; 2680 ± 8 Ma). This event resulted in deposition of the

Table 2. Compilation of the deformation history for Kambalda region. See text for references

Deformation event	*Major features*	*Orientation*	*Approximate age (Ma)*
D_{e1}	Mafic–ultramafic volcanism	Approximately east–west 'extension'	2720–2690
D_{e2}	Felsic magmatism, Black Flag sedimentation	North-northwest–south-southeast extension with southeast side down	2690–2660
D_1	Thrust faults, major stratigraphic repetitions; ?gold at Golden Mile (pre-D_2)	North–south shortening	c. 2660
D_{2a}	Folds and cleavage (early D_2 folds cut by late basins, e.g. Kurrawang and Pig Well)	East-northeast–west-southwest shortening	unknown
D_{e3}	Late Basin sedimentation (Merougil); felsic magmatism (switch high Ca to low Ca)	Approximately northeast–southwest extension in strike slip setting	<2657
D_{2b}	Folds and thrust faults; Au at Wallaby c. 2650 Ma (post late basins, but early D_{2b})	East-northeast–west-southwest shortening	c. 2650–2645
D_{2x} [(a)]	Structures in granites, minor northeasterly trending folds overprinting D_2 northwesterly trending folds, reactivation of D_1 thrusts with possible development of new thrust faults	Approximately northwest–southeast shortening	c. ?2645
D_3	Folds and faults; gold at St Ives (dated at 2631 ±5 Ma and 2627 ± 7 Ma)	East-southeast–west-northwest shortening	c. ?2645–2630
D_4	Northeasterly to northerly trending faults, reactivation of earlier faults	Northeast–southwest shortening	c. 2630–2625

NOTE: (a) Geoscience Australia work: Blewett et al. (2004)

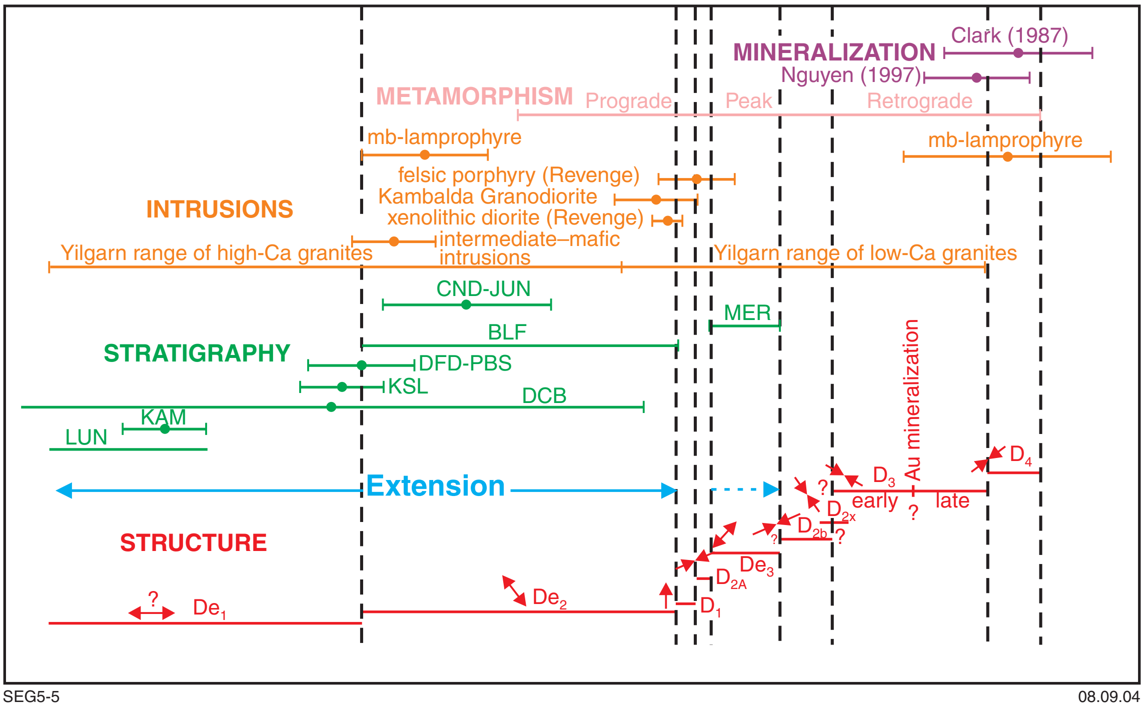

Figure 5. Temporal and structural framework for the Kambalda–Tramways corridor. BLF = Black Flag Group, CND–JUN = Condenser and Junction Dolerites, DCB = Devon Consols Basalt, DFD–PBS = Defiance Dolerite and Paringa Basalt, KAM = Kambalda Komatiite, KSL = Kapai Slate, LUN = Lunnon Basalt, MER = Merougil Formation, mb-lamprophyre = biotite lamprophyre

extensive Black Flag Group. The basins related to this stage of extension generally deepen to the south, implying southeast-side-down displacement (Hayward, N., 2001, pers. comm.). Intrepretation of seismic data in the St Ives area suggests that the Boulder–Lefroy Fault dips east and formed as an extensional fault during deposition of the Black Flag sequence.

D_1 north–south thrusting

D_{e2} sedimentation and felsic magmatism were followed closely by D_1 thrust faulting at c. 2657 Ma, which involved north–south compression and inverted the basins developed during D_{e2}. This event resulted in development of westerly trending thrust faults, and recumbent folds. Some of the best-documented D_1 thrusts within the Yilgarn Craton occur in the St Ives area, including the Foster, Tramways, and Republican Thrusts. Swager and Griffin (1990) interpreted these thrust faults as part of a megaduplex, which formed in response to northwards thrusting and could have linked into the Feysville Thrust. Other well-documented D_1 thrusts occur in the Kanowna and Dunnsville areas.

D_{2a} east-northeasterly–west-southwesterly shortening

Early north-northwesterly trending D_{2a} folds are truncated by the late basins (D_{e3} sedimentation) in both the Pig Well (Blewett et al., in press) and Kurrawang areas. This implies that a stage of east-northeasterly–west-southwesterly shortening had initiated prior to the extensional event related to deposition of the late basins.

D_{e3} late basin sedimentation and felsic magmatism

A third major depositional event occurred post c. 2655 ± Ma, based on the youngest zircons found in any of the late basins (Krapez et al., 2000). However, the ages of these basins vary across the Eastern Goldfield Province (Blewett et al., in press). Age dating in the St Ives area suggests that the widespread felsic to intermediate porphyries and the Kambalda Granodiorite were emplaced during or just before this event. The Kambalda Granodiorite, which is exposed in the dome area, has been dated at 2662 ± 4 Ma (U–Pb zircon SHRIMP; Compston et al., 1986), whereas the porphyries have been dated at 2660 ± 6 Ma and 2658 ± 4 Ma (U–Pb zircon SHRIMP; Nguyen, 1997), and 2680 ± 12 Ma (U–Pb zircon; Clark, 1987). There are few data to indicate the extension direction during this event but, given the dominant northwesterly–southeasterly trend of the porphyries in much of the St Ives area, it is considered most likely that the extension direction was about northeast–southwest.

The fluvial rocks of late basins such as the Merougil Formation (and equivalents including Jones Creek Conglomerate and Yandal Sandstone) are interpreted to have been deposited in elongate, localized basins, in contrast to the widespread turbidite fan deposits of the Kurrawang Formation (Barley et al., 2002).

D_{2b} main stage of east-northeasterly–west-southwesterly shortening

D_{2b} east-northeasterly–west-southwesterly shortening is interpreted to have occurred late syn- to post-granite intrusion (Archibald, 1985; Nguyen, 1997) at c. 2650 Ma or later. This event represents the major period of crustal shortening within the Eastern Goldfield Province, and is readily recognized throughout the Yilgarn Craton, including the Southern Cross Province. D_2 shortening is associated with large-scale north-northwesterly trending folds and abundant north-northwesterly trending thrust faults. This event resulted in inversion of the extensive basins of mafic–ultramafic rocks that developed during D_{e1}. Peak metamorphic conditions are interpreted to have been reached broadly synchronous with D_2 in the St Ives region (Archibald, 1985; Nguyen, 1997). However, it has been suggested that peak conditions were reached at a later time at depth (Hayward, N., 2001, pers. comm.). If this is the case, then it allows for the involvement of metamorphic fluids in D_3 mineralization.

D_2 involved the generation of open upright folds such as the Kambalda and Widgiemooltha Domes, the development of the main upright cleavage (S_2 foliation), and M_2 greenschist metamorphism, possibly synchronous with the main phase of granitoid intrusion. The D_2 folds are roughly parallel with the major north-northwesterly striking fault systems of the Yilgarn Craton, but most of these faults, such as the Boulder–Lefroy Fault and Zuleika Shear, are interpreted to have formed during earlier D_{e1} or D_{e2} extensional deformation. At a regional scale, the folds are components of large north-northwesterly trending anticlinoria (Kalgoorlie – Kambalda – St Ives and Depot Rocks – Widgiemooltha – Pioneer corridors) and synclinoria (Kurrawang and Merougil Basins). In the seismic studies of Goleby (1993) and Williams (1993), the regional anticlinoria and synclinoria appear as openly folded, imbricately stacked wedges bounded by north-northwesterly striking anastomosing faults, which could be stacked listric thrusts and backthrusts linked in a flat basal decollement at 6 km depth.

Regional S_2 foliations are defined by peak metamorphic mineral assemblages, which indicate that peak regional metamorphism accompanied this phase of crustal shortening and thickening. In addition, many of the elongate, foliated syntectonic granitoid plutons are interpreted to have intruded into anticlinal hinge zones at this time. The occurrence of telescoped metamorphic grade changes across D_2 faults (Archibald, 1979; Hayward, 1988) and the abundance of retrogressive chlorite–calcite alteration halos around them suggest D_2 thrusts remained active following peak metamorphism. The general lack of economic gold mineralization associated with D_2 thrusts suggests that the post-peak metamorphic carbonation event considered by many to be intimately associated with gold mineralization actually predates mineralization (Bennet, 1995).

D_{2x} northwest–southeast shortening

Recently, workers from Geoscience Australia have documented evidence for a period of northwesterly–southeasterly shortening after D_2 and before D_3 (Blewett et al., 2004). The main lines of evidence for this event are:

- the results of a detailed study of granitoids in the Laverton area showing the presence of structures related to this event;
- minor 'refolding' of northwesterly oriented D_2 folds by northeasterly oriented folds, resulting in variations in plunge direction;
- some 'D_1' thrusts at St Ives and Kanowna Belle appear to cut D_2 folds and are not folded by this event, as previously interpreted;
- the D_1 Republican thrust at St Ives cuts a northwesterly trending fault, which, in turn, cuts the major Boulder–Lefroy Fault.

At present it is uncertain whether D_1 thrusts have simply been reactivated during the D_{2x} northwest–southeast shortening event, or whether the faults originated at this time.

D_3 east-southeast–west-northwest shortening

D_3 east-southeast–west-northwest shortening represents a return to the broadly east–west shortening direction of D_2. The east-southeast–west-northwest shortening direction for the St Ives area is confirmed by sinistral reverse movement on numerous northerly trending faults, in contrast to the east-northeast–west-southwest D_3 shortening direction in the Kalgoorlie area. D_3 deformation resulted in the tightening of D_2 folds and local development of new folds overprinting D_2 structures, as well as reactivation of old faults and development of new faults, largely as subsidiary structures to the pre-existing north- to northwesterly trending faults. The timing of the change from east-northeast to east-southeast shortening is not well constrained, but is likely to have been c. 2645 Ma (or later).

The later stages of D_3 east-southeast–west-northwest shortening, which coincided with gold mineralization at St Ives, must have pre-dated 2632 Ma, the age of a post-tectonic granite cutting the Ida Fault (Bateman, 2001). This age represents a minimum age for any major deformation including D_4. Age dating at St Ives suggests that the Victory and Revenge gold mineralization formed during the final stages of D_3 deformation.

D_4 shortening

D_4 deformation is generally interpreted as northeast–southwest shortening that resulted in reactivation of various faults and development of brittle northeasterly and northwesterly trending faults (Nguyen, 1997). In general, this event does not appear to be very significant but it could be associated with the final stages of mineralization. At St Ives, the Redoubtable deposit has been interpreted as synchronous with D_4 deformation, given that it is associated with the Alpha Island Fault, which has been considered to be D_4 in age. However, observations during this study suggest that the fault is older.

Metamorphic setting

The style of metamorphism at Kambalda appears to be static, with good preservation of volcanic textures. Peak metamorphic conditions during D_2 ranged from upper greenschist to lower amphibolite facies in the Kambalda Dome, to mid-amphibolite facies in the Widgiemooltha and Carnilya Hill areas (Bavinton, 1979; Archibald, 1985; Perriam, 1985; Goodgame, 1997). Peak metamorphic conditions are estimated at 520 ± 20°C and 1–4 kbar in the St Ives camp (Bavinton, 1979; Donaldson, 1983; Archibald, 1985). Higher metamorphic temperatures were reached in the contact aureole of the Kambalda Granodiorite (Wong, 1986). Retrograde greenschist facies metamorphism extended from D_3 to D_4.

Camp- to deposit-scale hydrothermal alteration footprints

Camp-scale hydrothermal alteration zonation

In the St Ives camp, a range of alteration styles is documented (Clark, 1987; Neall and Phillips, 1988; Clark et al., 1989; Nguyen, 1997; Polito et al., 2001; Neumayr et al., 2003). The alteration styles are the result of several metasomatic events related to different deformation events, and are telescoped. Documented styles are:

1. carbonate associated with deformation along the transcrustal structure (Lefroy);
2. epidote–calcite–magnetite–pyrite–chalcopyrite–quartz,
3. magnetite halo around gold-bearing structures (interpreted as oxidized hydrothermal fluid);
4. pyrrhotite(–pyrite) alteration flanking oxidized domains on a camp scale (interpreted as reduced hydrothermal fluid);
5. zoned chlorite–biotite–feldspar–carbonate–pyrite quartz alteration associated with gold.

For gold mineralization, styles 3, 4, and 5 are the most important, and are discussed here in more detail.

Gold-associated sulfide and oxide minerals indicate a zonation with respect to ore-fluid chemistry within the St Ives gold camp (Fig. 2). Oxide and sulfide assemblages are correlated to reduced and oxidized conditions using fO_2–$\alpha\Sigma S$ diagrams at 400°C and 2 kbar. Deposits in the southwest of the camp, such as Argo and Junction, contain arsenopyrite–pyrrhotite and pyrrhotite–pyrite assemblages, respectively. These assemblages indicate dominant relatively reduced hydrothermal fluids. The deposits in the ‘central corridor’ of the St Ives gold camp are characterized by pyrite–magnetite and pyrite–hematite assemblages, indicating dominant relatively oxidized hydrothermal fluids. Deposits in the northwest, close to the Kambalda dome, typically contain pyrite as the main sulfide mineral.

In the central corridor, two main domains are distinguished with respect to the redox conditions of the hydrothermal alteration (Fig. 6; Neumayr et al., 2003):

- reduced (pyrrhotite–pyrite and pyrrhotite assemblages);
- oxidized (pyrite–magnetite and pyrite–hematite assemblages).

The domain mapping is not completed as yet, but preliminary data indicate a distinct distribution pattern. Domains with oxidized alteration assemblages are focused, and are best mapped by hydrothermal magnetite in sedimentary rocks, such as the Kapai Slate. Magnetite in Kapai Slate is present around the Victory–Defiance deposits and to the southeast of, and locally within, the Greater Revenge area. These domains with magnetite–pyrite assemblages are aligned along some major structures, such as the northwesterly trending, northeasterly dipping Playa fault, and domains with magnetite–pyrite also rim two pronounced gravity lows centred around the Victory–Defiance deposits, and to the west of the Revenge deposits (Fig. 7). The gravity lows extend for several kilometres in diameter, and are interpreted to represent abundant magmatic intrusions at a depth of about 500–1000 m below present surface. Abundant felsic intrusions are also interpreted from seismic data in a cross section across Victory–Defiance (Fig. 8). Domains with reduced alteration assemblages (pyrrhotite–pyrite) flank those with oxidized assemblages to the northeast and southwest of the Victory–Defiance and Greater Revenge deposits. and are also present locally between oxidized domains in the Greater Revenge deposits.

Deposit-scale hydrothermal alteration in oxidized deposits

At a deposit scale, hydrothermal alteration mineralogy depends mainly on the host rock composition. Therefore, any comparison of hydrothermal alteration between deposits has to take into account the host rock types. Hydrothermal alteration is discussed here mainly for mafic host rocks, as exemplified by the Revenge and Conqueror gold deposits. In the Conqueror deposit, most distal hydrothermal alteration assemblages are pyrrhotite–pyrite. Gold lodes are rimmed by a >100 m-wide halo of hydrothermal, fine-grained magnetite, which is best monitored via variations in the magnetic susceptibility. However, the gold lodes themselves are characterized by low magnetic susceptibility and less abundant magnetite. Hydrothermal magnetite proximal to gold lodes is overprinted by the typical zoned gold-associated alteration (chlorite, chlorite–biotite, and feldspar–carbonate–pyrite). The most distal zone of gold-associated alteration contains hydrothermal chlorite, and less abundant biotite and dolomite (Clark et al., 1989; Neumayr et al., 2003). The intermediate alteration zone, proximal to the gold lodes, comprises hydrothermal biotite, carbonate, and lesser albite and pyrite, with traces of magnetite. The most proximal areas to the gold lodes are bleached zones adjacent to hydrothermal quartz veins, and these contain albite, ankerite, dolomite, quartz, and pyrite, as well as less abundant biotite, muscovite, and calcite. Gold-associated pyrite grains contain magnetite inclusions in their cores and hematite inclusions in their rims.

Deposit-scale hydrothermal alteration in reduced deposits

Both reduced deposits in the camp (Argo and Junction) are hosted in dolerite near the contact of the mafic succession and the Black Flag Group. Three distinct

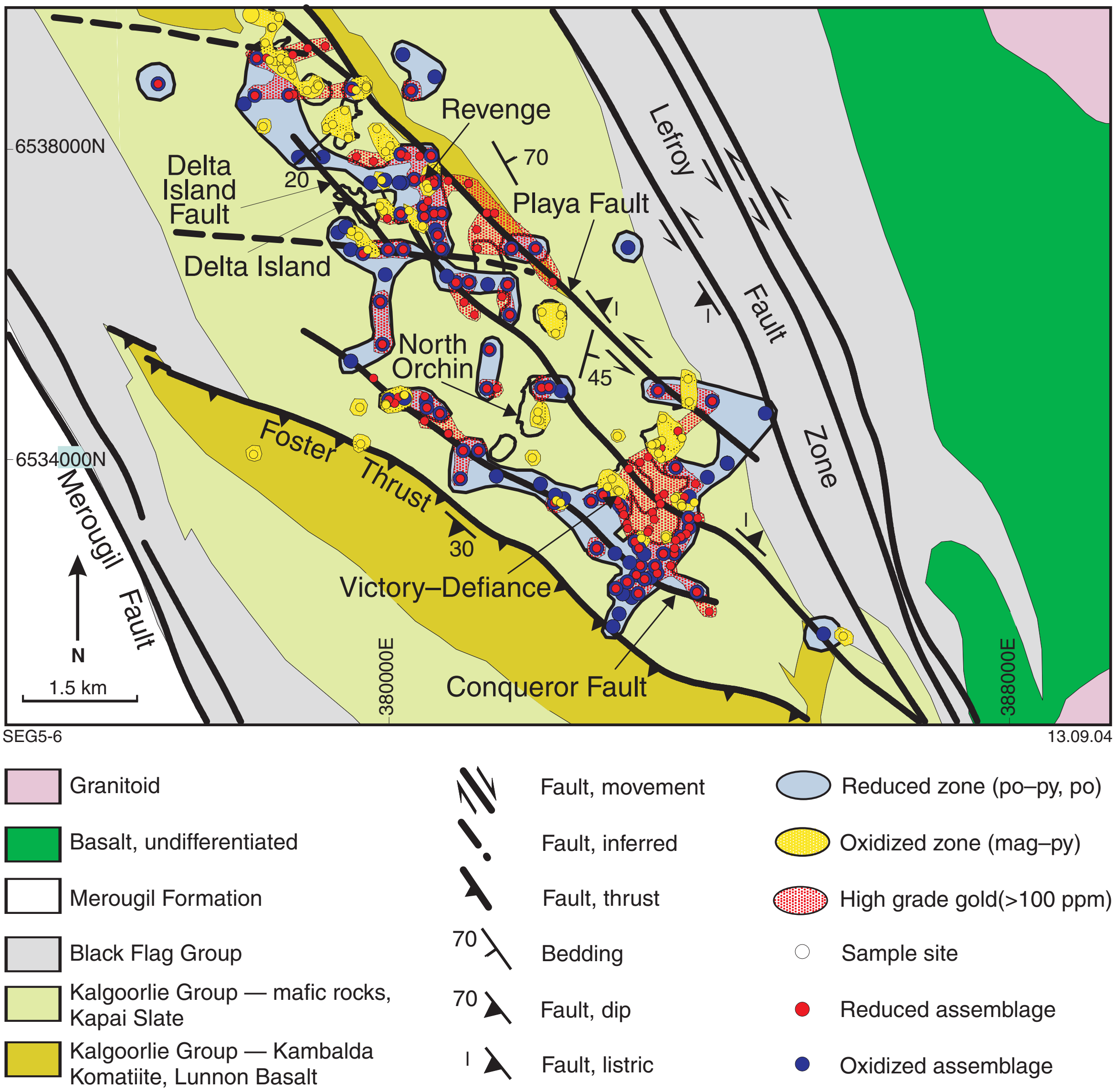

Figure 6. **Simplified geology, main deposits, and redox mineral assemblages in the St Ives gold camp. The figure shows the main distribution of reduced (pyrrhotite–pyrite) and oxidized (magnetite–pyrite) assemblages in the camp. Note that high grade (>100 ppm) gold intersections are located at the boundary between reduced and oxidized domains**

mineralization styles contribute to gold mineralization at the Argo A1 orebody. The first is represented by the intensely sheared mylonite, which has three distinct alteration halos:

- the distal alteration halo is defined by a chlorite–calcite–pyrrhotite assemblage;
- the intermediate alteration zone is characterized by the assemblage biotite–chlorite–plagioclase;
- proximal alteration zone is reflected by the increased modal abundance of albite–quartz(–dolomite or ankerite).

The sulfide assemblage in the proximal zone is pyrrhotite–arsenopyrite–chalcopyrite–pyrite. The main development of alteration halos is replaced in the centre of the proximal zone by the reactivation and subsequent brecciation. Late brittle quartz-rich veins overprint the mylonitic shear zone and the breccia.

Controls on gold mineralization

Host rock controls

Gold mineralization in the St Ives camp can be subdivided into three distinct types with respect to their host rocks. The Junction group comprises two main deposits: Junction and Argo. These deposits are hosted by the Condenser and Junction Dolerites.

Gold deposits in the Victory–Defiance complex are hosted in several rock types, including Kambalda Komatiite, Paringa Basalt and Defiance Dolerite, Flames porphyry, and Kapai Slate. The Intrepide deposit group includes two main deposits, Intrepide and Redoubtable, and an old working mine, Red Hill. These deposits are mainly associated with porphyry–ultramafic contacts.

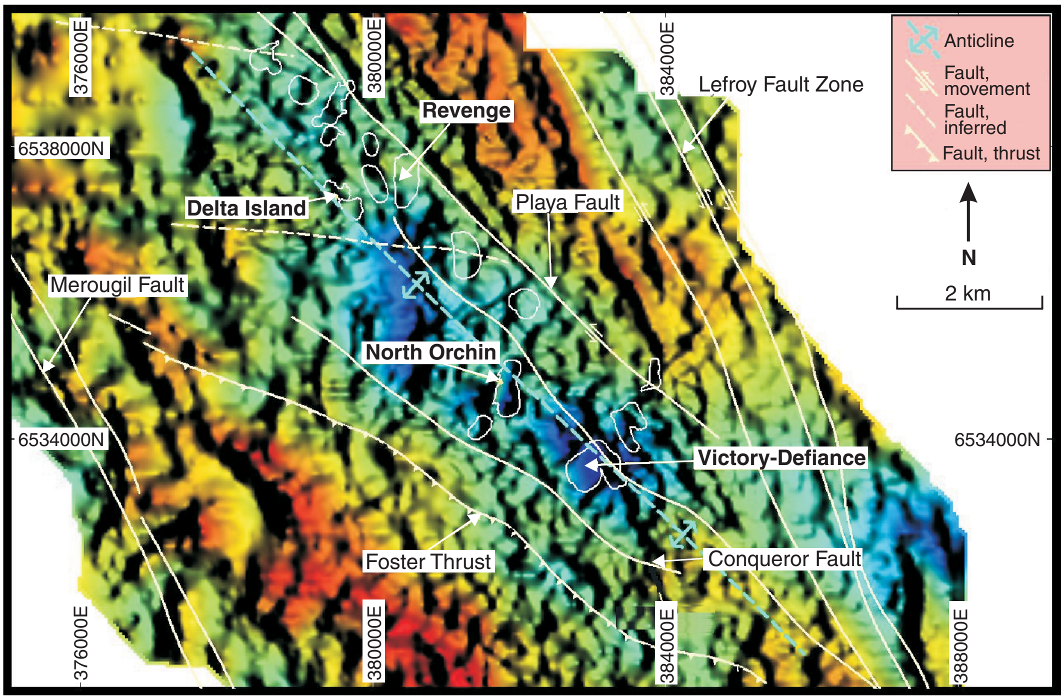

Figure 7. Detailed gravity image of the St Ives gold camp showing main structures and location of gold deposits. Note the distinct gravity lows in the Victory–Defiance area and southwest of the Revenge deposit

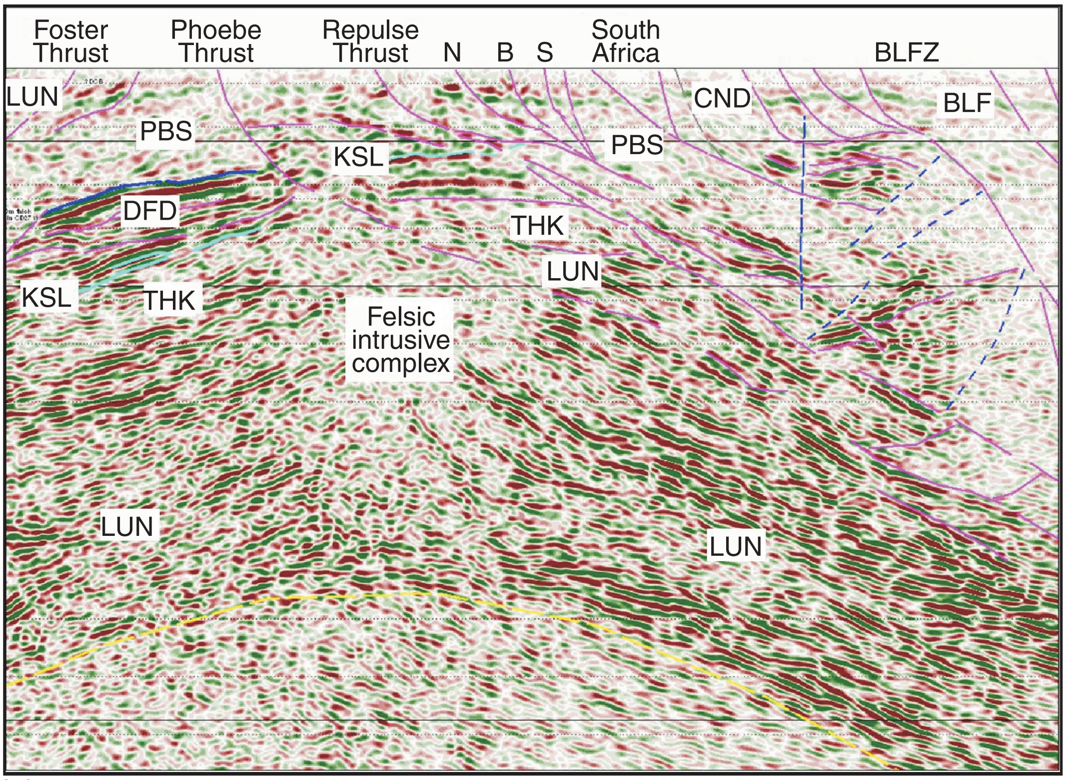

Figure 8. Seismic cross section across the Victory–Defiance gold deposits. The image shows main rock types and structures. Note the seismic response and location of the felsic intrusive complex beneath Victory–Defiance. B = Britannia Thrust, BLFZ = Boulder–Lefroy Fault Zone, N = Nautilus Thrust, S = Sirius Thrust, THK = Tripod Hill Komatiite. Other abbreviations as in Figure 5

Shearing is controlled by the mechanical contrast between brittle porphyry and ductile ultramafic rocks. The ultramafic rocks are typically foliated whereas quartz vein stockworks are developed in the porphyry.

Dolerite, including the Defiance and Junction Dolerites, is currently considered the most favourable host rock for the St Ives camp because it hosts the largest gold deposits (Junction, Defiance, Revenge, Argo, Conqueror, Orchin, North Orchin), and accounts for about 70% of pre-mining reserves (Roberts and Elias, 1990; Nguyen et al., 1992), although this could change with recent and current drilling in the Revenge complex. High-grade gold mineralization is mainly associated with thick magnetite-rich granophyric zones of the dolerite (Nguyen, 1997). Basalt, including the Lunnon, Devon Consols, and Paringa Basalts, currently accounts for about 20% of the pre-mining reserves. The magnetite-bearing chert facies within the Kapai Slate typically hosts high grade but low tonnage orebodies. Felsic intrusions are commonly poorly endowed but, adjacent to ultramafic rocks, the competency contrast between brittle felsic and ductile ultramafic rocks has localized gold mineralization (Intrepide, Redoubtable, and Formidable).

Structural controls

The following description of the structural controls on gold mineralization in the St Ives camp is summarized from Cox and Ruming (2004). Gold mineralization at St Ives formed during D_3. Many of the gold deposits are hosted by faults and shear zones that are spatially and kinematically related to D_3 displacement on the Playa Fault (Fig. 9). These deposits occur in low displacement brittle–ductile shear zones, which are interpreted as splays and linked fault–shear networks in a 2 km-wide zone west of the Playa Fault (Figs 9 and 10). The total displacement on the northwesterly trending Playa Fault is poorly constrained, but could be up to several kilometres.

In contrast, ore-hosting structures in individual deposits such as Revenge, North Orchin, Argo, and much of the Victory area, are mainly northerly striking, moderately to gently east- or west-dipping reverse faults and shear zones with maximum displacements of a few tens of metres. Strike lengths of ore-hosting structures are rarely more than about 1 km. The orientations of stretching lineations, curvature of shear zone foliations, associated gently dipping extension veins, and stratigraphic separations all indicate a reverse slip sense for most D_3 ore-hosting structures, especially in the Argo–Victory–Revenge area. The geometries of faults and associated extension veins indicate formation in a stress regime in which the far-field maximum principal stress was approximately east–west and horizontal.

In the Victory–Defiance area, ore is localized along an apparently imbricate series of moderately to gently dipping, low displacement thrusts. The Playa Fault here (known locally as the Repulse Fault in the Victory–Defiance mine area) has a ramp–flat–ramp geometry. Where it is more gently dipping, a number of low displacement, ore-hosting thrusts splay from the Playa Fault into its hangingwall. To the west, where the Playa Fault forms a more steeply dipping ramp, low displacement, ore-hosting thrusts occur in the footwall of the Playa (Repulse) Fault, and host the Defiance and Conqueror lodes. The geometry and kinematics of the Victory thrust complex, and its geometric relationship with the Playa Fault indicate that the thrust complex developed within a jog on the Playa Fault, to the northwest of where it splays from the Boulder–Lefroy Fault. The overall northwesterly trend and predominantly sinistral shear sense on the Playa Fault, as well as the thrust to oblique-thrust sinistral shear sense on low displacement faults within the imbricate thrust complex, are interpreted to indicate that gold mineralization here is localized within a kilometre-scale contractional jog that was active during D_3, and the contemporaneous hydrothermal alteration and gold mineralization.

Similarly, the orientation and reverse shear sense of the low displacement, ore-hosting structures on the western side of the Playa Fault, for more than 5 km northwest of the jog (Victory–Revenge area), are also interpreted as contractional structures (Cox and Ruming, 2004), whose formation is kinematically related to mainly sinistral slip on the Playa Fault during D_3. Accordingly, the gold deposits in the Orchin to Revenge areas are interpreted to have formed in a low displacement contractional damage zone generated by strain accommodation around the Victory jog (Figs 10 and 11). Northwest of the Revenge area, several gold deposits and prospects occur within the Playa Fault, or west of this structure.

The Delta and Santa Ana deposits are localized in northwesterly trending fault zones west of the Playa Fault. The Formidable, Redoubtable, and Intrepide deposits are located within the Playa Fault, or strands of this structure. The Minotaur, Mars, and Agamemnon deposits are associated with shear zones that are likely to be link structures between the Playa Fault and the Delta Fault north of the Delta deposit.

The Argo and Junction deposits are spatially separated from the other St Ives deposits, and located south of the Victory jog and west of the Boulder–Lefroy Fault. Argo occurs within a moderately westerly dipping, brittle–ductile, reverse shear zone. The Junction deposit is located along an easterly dipping, north-northwesterly trending, reverse or sinistral shear zone. Maximum displacement on these latter structures is between 50 and 100 m.

Displacement on ore-hosting structures in the St Ives goldfield involved both ductile and brittle processes. Hydrothermal alteration and associated gold mineralization were synchronous with deformation along the ore-hosting network of shear zones. In many deposits, ductile shearing was punctuated by repeated brittle slip events, which produced breccias and shear veins, especially in jogs and dilatant bends in shear zones.

By analogy with modern seismogenic systems, the low displacement structures that localized fluid flow and gold mineralization in the St Ives goldfield are interpreted by Cox and Ruming (2004) as aftershock structures whose development and distribution was controlled by major slip events on the Lefroy Fault. For a number of years, seismologists have been successfully using analysis of

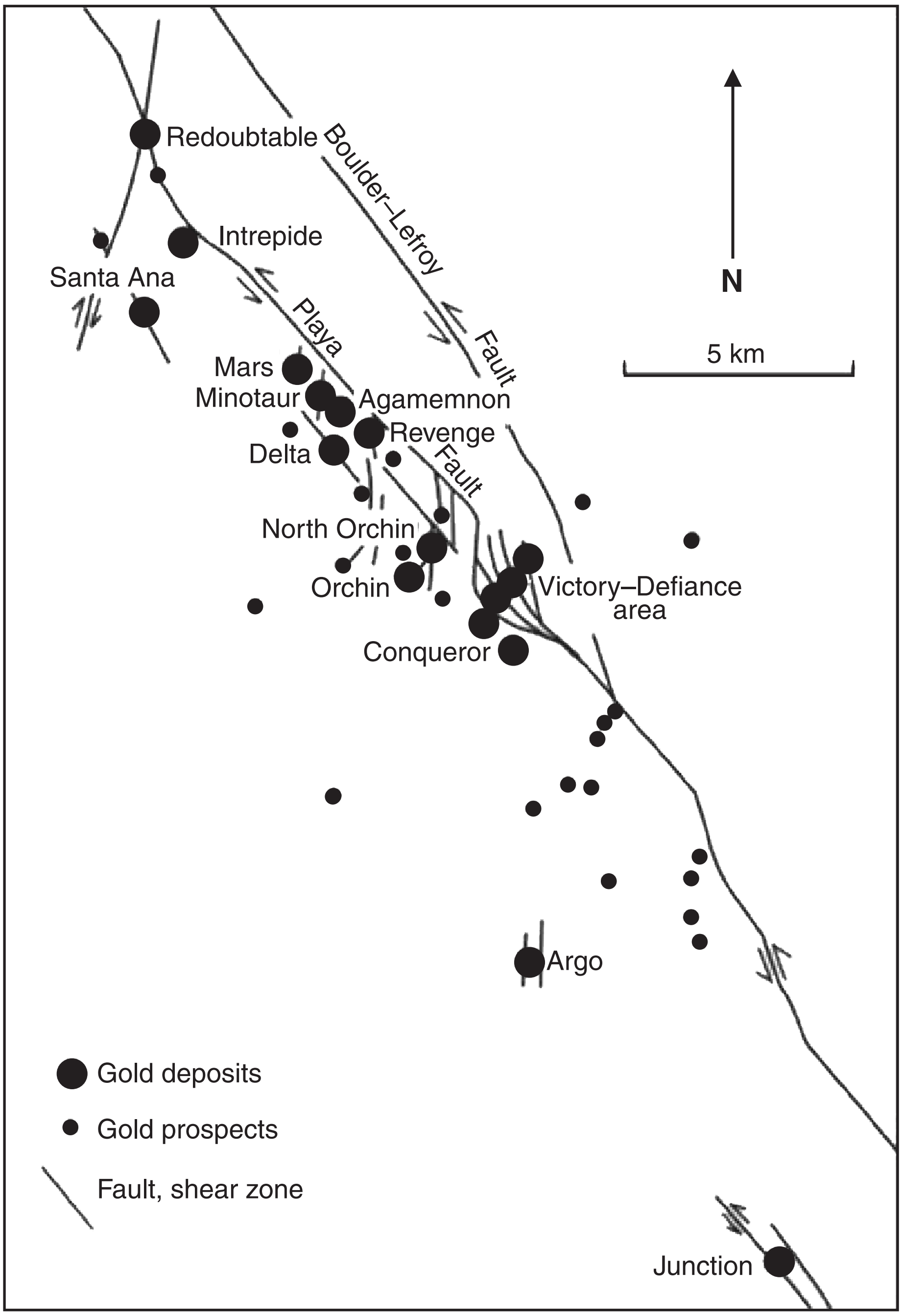

Figure 9. Simplified map illustrating the geometry and distribution of D_3-active faults and shear zones, including the Boulder–Lefroy Fault, the Playa Fault and various lode-hosting faults in the Kambalda region (modified after Cox and Ruming, 2004). Major gold deposits in the St Ives goldfield are also shown

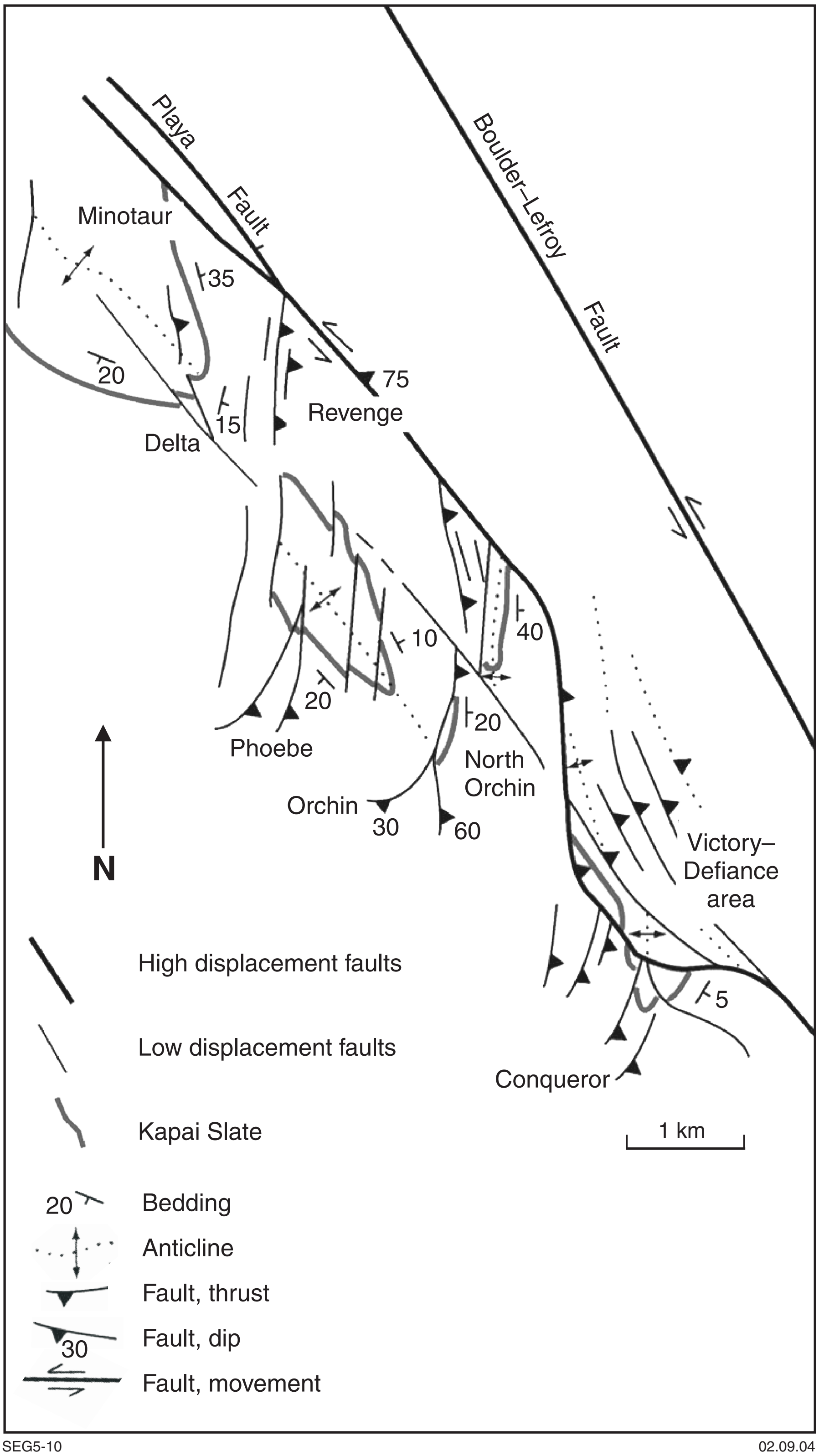

Figure 10. Fault geometry and distribution in the central part of the St Ives goldfield (modified after Cox and Ruming, 2004). The deposits of the Victory–Defiance area are located in an imbricate thrust complex developed within a contractional jog on the largely sinistral Playa Fault. Other deposits are localized mainly on northerly trending reverse faults in a contractional domain northwest of the Victory jog

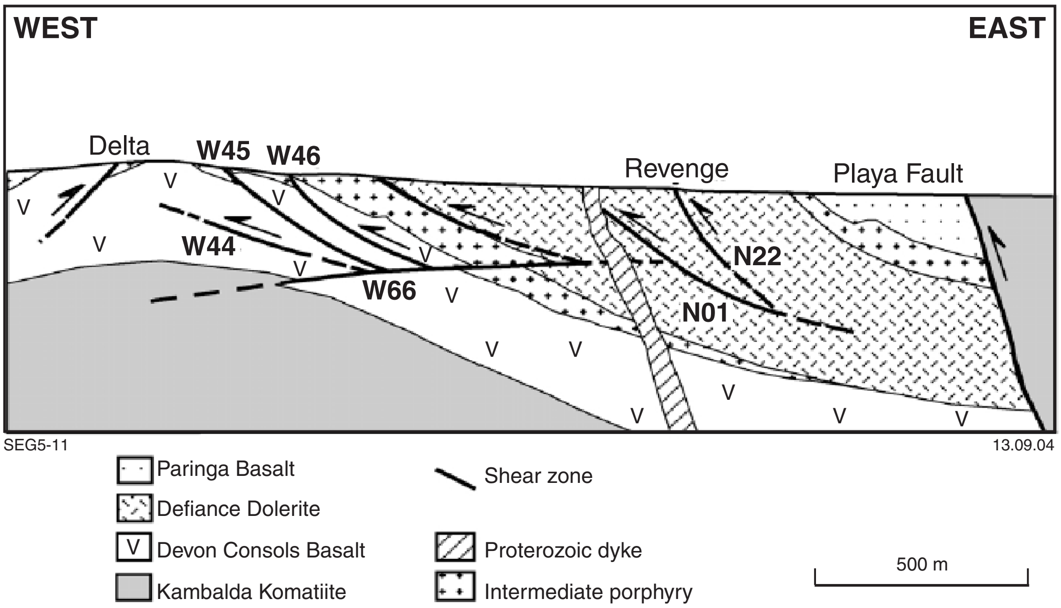

Figure 11. Simplified east–west cross section of the Revenge mine area. Orebodies (numbered) are hosted in conjugate thrusts just west of the Playa Fault (after Nguyen et al., 1998)

stress changes induced by mainshock earthquake ruptures (stress transfer modelling) to predict where, in active fault systems, aftershocks are most likely to occur. On this basis, Cox and Ruming (2004) have used stress transfer modelling to test if the location of the St Ives goldfield within the Boulder–Lefroy Fault has a relationship to the structure of the fault system.

It was found that, for large slip events (magnitude 6.5) on the Lefroy Fault, the predicted aftershock footprint produced by mainshock rupture arrest at the Victory jog very closely matches the location and geometry of the St Ives goldfield. The modelling supports an interpretation that aftershock networks can form a high permeability damage zone that localizes fluid flow and gold mineralization within particular parts of crustal-scale fault systems. The aftershock concept provides one explanation for the long-known relationship that gold deposits hosted by faults or shear zones tend to occur in low displacement structures up to several kilometres from the associated crustal-scale shear zones.

Both co-seismic stress transfer and time-dependent changes in fluid pressures, during post-seismic fluid redistribution, are implicated in driving the growth of low displacement, gold-hosting fault networks in the St Ives goldfield. Stress transfer modelling can be applied to area selection in exploration programs targeting mesothermal gold systems. Clustering of deposits hosted by aftershock fracture networks is favoured by the presence of major, long-lived jogs or bends, which can repeatedly arrest ruptures propagating along high displacement faults.

Chemical controls

Chemical controls are described for the oxidized deposit groups because these are the best documented to date (Clark et al., 1989; Neumayr et al., 2003). Whereas Clark et al. (1989) documented conditions of hydrothermal alteration and chemical changes during alteration, recent camp-scale studies identified camp-scale hydrothermal alteration footprints and distinct chemical controls on the location of high-grade gold mineralization (Neumayr et al., 2003).

On a camp scale, two main domains of sulfide–oxide mineral assemblages (pyrrhotite–pyrite, magnetite–pyrite) are identified and are best interpreted to relate to two hydrothermal fluids, one a reduced system and the other oxidized, respectively (Neumayr et al., 2003). Oxidized mineral assemblages, as well as felsic to intermediate porphyry intrusions, are centred around the Greater Revenge and Victory–Defiance mines. This suggests that oxidized mineral assemblages are genetically related to the porphyry intrusions. Reduced mineral assemblages are located outboard of the oxidized domains, and flank these domains to the northeast and southwest. High grade (>100 ppm) gold intersections are preferentially located at the border, or in overlapping zones, between reduced and oxidized domains, but within the oxidized domain (Figs 6 and 12). This indicates a chemical control on the precipitation of high-grade gold mineralization.

Currently, there are two competing genetic models to explain the oxide–sulfide mineral assemblage. The first model assumes that two hydrothermal fluids of different redox state infiltrated the rock volume progressively. The second fluid interacted with hydrothermal alteration that had precipitated from the earlier fluid. Large differentials in the redox state between the new fluid and alteration from the first fluid provided a powerful gold precipitation mechanism.

In the second model, interaction of two contemporaneous fluids of grossly different redox state is assumed.

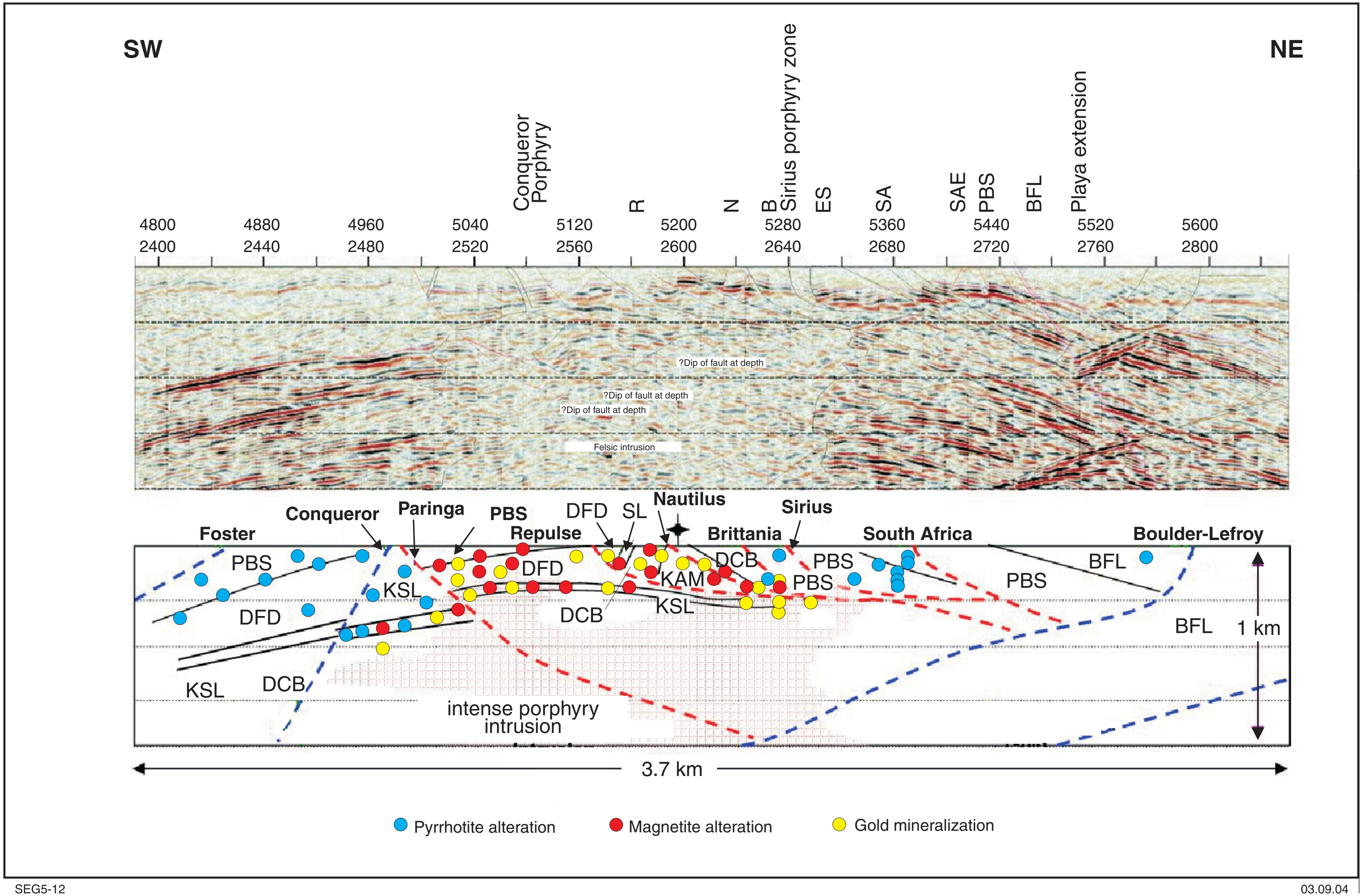

Figure 12. Cross section showing seismic data, and location of reduced and oxidized mineral assemblages, and gold mineralization. ES = East Sirius Thrust, R = Repulse Thrust, SA = South Africa Fault, SAE = South Africa East Fault. Other abbreviations as in Figures 5 and 8

This model requires that the two fluids migrate along different fluid conduits. Linking structures between these conduits provide zones where these fluids with grossly different redox conditions mixed. During the mixing process, the redox conditions of the hydrothermal fluid changed rapidly and resulted in gold precipitation, explaining the location of high-grade gold mineralization in the mixing zones. It is assumed that other gold precipitation mechanisms, such as phase separation in the hydrothermal fluid and fluid-wallrock interactions, took place but played a subordinate role in producing high grade oreshoots.

Excursion route

Introduction

It is difficult to plan the exact excursion route in advance in an active mine environment. However, it is likely that the excursion will visit the Argo mine and a mine in the Greater Revenge area, and these deposits are described below. The excursion will also inspect typical diamond drillcore showing hydrothermal alteration and ore mineral assemblages.

Argo gold deposit

Introduction

Argo is owned by the St Ives Gold Mining Company, a wholly owned subsidiary of Gold Fields. The Argo gold deposit was discovered in 1991 from aircore drilling targeting a distinct break in the airborne magnetic data over an interpreted dolerite unit. Follow-up drilling delineated a significant mineralized north-northeasterly trending structure referred to as the Argo Shear. Definition drilling commenced and an ore reserve was delineated by 1993. The deposit is currently being mined as both an openpit and underground operation. Past production and current reserves total 5 Mt at 5.8 g/t for about 930 000 ounces of gold, with a mineral resource of 7.2 Mt at 5.89 g/t for 1.38 Moz of gold as at July 2002. There is significant potential to increase the reserve and resource with increased exploration from underground.

Deposit geology and controls on mineralization

The Argo gold deposit is positioned on the western limb of the Kambalda – St Ives Antiform, to the west of the Boulder–Lefroy Fault, a major crustal-scale wrench fault system. The Condensor Dolerite, a 500 m-thick subvertical to southwesterly dipping differentiated sill, hosts the mineralization at Argo. The sill intruded along the contact between the Paringa Basalt and Black Flag Group.

The Argo deposit is a structurally complex, large mineralized shear system, which consists of the Argo Shear and a series of subsidiary mineralized shears. Gold mineralization at Argo is mainly confined to the Argo Shear, which strikes north and dips west, and extends over 800 m downdip. The shear system extends over a strike length of 1 km, and attenuates at the contact with the Paringa Basalt to the north, and the Black Flag Group to the south. Two easterly trending subvertical Proterozoic dolerite dykes crosscut the system. The Argo Shear is accompanied by a number of mineralized satellite structures. These include large, subparallel structures such as the H1 hangingwall shear, and lesser shallower dipping structures in the footwall positions (F2, and C1–3). The subhorizontal structures contain dilation vein sets, whereas steeper structures have a dominant (reverse fault) mylonitic component. The subparallel Apollo (A2 and A3) Shear bounds the eastern margin of the Argo system. The A2 Shear links with the Argo Shear at depth. Little is known about zones of mineralization beyond the H1 structure to the west, and the A2 and A3 structures to the east. The southern end of the deposit is covered by a sequence of Tertiary sediments, which are up to 60 m thick.

Three types of gold mineralization are evident at Argo:
- high-grade placer-style deposit hosted by quartz gravel at the base of the Tertiary cover sequence;
- supergene mineralization within the Tertiary sedimentary units and Archaean regolith;
- primary shear-hosted mineralization.

Greater Revenge deposits

Introduction

The Greater Revenge gold complex is almost entirely blind. The Revenge deposit itself was discovered beneath lake sediment cover in 1984 from diamond drilling to test magnetic anomalies in a favourable structural and stratigraphic setting. It was mined from 1989 to 1998. Subsequent discoveries have come from a lake exploration strategy using track-mounted aircore rigs for anomaly definition programs. However, credit must be given to ‘old timers’ (late 1890s) who were responsible for workings on Delta Island, which provide the only surface clue to mineralization in the area. Exploration of the Greater Revenge area, measuring 4.5 × 2.5 km, was started in 1994 and identified supergene gold anomalies. From 1997, progressive exploration delineated supergene pittable resources and significant primary ore. The >1 Moz potential of the system was recognized in 1998, but it was not until 2001 that the scale of the opportunity was appreciated, and programs were initiated to realise the full potential of the Greater Revenge area. From this time, accelerated exploration has added over 4 Moz to the inventory of modelled mineralization, above a cutoff of 0.8 g/t Au. The post-mined modelled inventory (total mineralization that has been captured in a model above a specified cutoff grade) above a 0.8 g/t cutoff has grown from 50 thousand ounces in 1998 to over 6.9 Moz in September 2003. About 3.7 million ounces of this was added between June 2002 and September 2003. The mineralized complex remains open to the north, south, and west, and at depth.

Deposit geology and controls on mineralization

The distribution of rocks in the area is controlled by the Delta Island Anticline, itself a segment of the Kambalda Anticline, which formed as a result of D_2 and subsequent minor D_3 folding events. The anticline is a gently plunging feature with a northwesterly striking D_2 major axis, and a northeasterly striking minor axis. The Tripod Hill Komatiite is situated within the core of the anticline, with conformably overlying and progressively younger Devon Consols Basalt, Kapai Slate, Defiance Dolerite, and Paringa Basalt. The numerous fractionated intermediate to felsic intrusions are dominantly concordant to subconcordant sills in the Greater Revenge area, and are folded with the stratigraphy, in contrast to more common steeply dipping dykes elsewhere in the field. The Tertiary lake sediments vary from being absent to 100 m thick. The dominant structural features in the Revenge area are the second order Playa, Belleisle, and Delta Shears. These structures strike north-northwest, but the Belleisle and Delta Shears dip westwards whereas the Playa Shear dips eastwards. Third-order reverse shears are shallow to steep, easterly or westerly dipping, and vary in strike from northwest to northeast. These third-order structures are the main hosts to mineralization, and include the Minotaur, Agamemnon, Mars, W66, N01, Delta, North Revenge, Kapai, West Revenge, and W series structures.

References

ARCHIBALD, N. J., 1979, Tectonic–metamorphic evolution of an Archaean terrain: a study of the Norseman–Widgiemooltha granitoid–greenstone belt, Eastern Goldfields Province, Western Australia: The University of Western Australia, PhD thesis (unpublished).

ARCHIBALD, N. J., 1985, The stratigraphy and tectono-metamorphic history of the Kambalda–Tramway area, Western Australia: Western Mining Corporation (unpublished).

BADER, K., 1994, Geology of the Merougil Formation, Kambalda, Western Australia: Monash University, BSc Honours thesis (unpublished).

BALKAU, J., 1989, Exploration history, Junction gold orebody: Western Mining Corporation (unpublished).

BARLEY, M. E., BROWN, S. J., KRAPEZ, B., and CAS, R. A. F., 2002, Tectono-stratigraphic analysis of the Eastern Yilgarn Craton: an improved framework for exploration in Archaean terrains: Australian Mineral Industry Research Institute, Final Report for AMIRA P437, 200p.

BATEMAN, R., 2001, Archaean gabbros and basalts (Kalgoorlie); geochemistry and tectonics in time, *in* Fourth International Archaean Symposium extended abstracts *edited by* K. F. CASSIDY, J. M. DUNPHY, and M. J. VAN KRANENDONK: AGSO – Geoscience Australia, Record, no. 2001/37, p. 124–126.

BAVINTON, O. A., 1979, Interflow sedimentary rocks from the Kambalda ultramafic sequence: their geochemistry, metamorphism and genesis: The Australian National University, PhD thesis (unpublished).

BENNET, M. A., 1995, The structure and timing of gold mineralization in the Victory area and its relationship to regional deformation in the eastern Goldfields: Western Mining Corporation (unpublished).

BLEWETT, R. S., CASSIDY, K. F., CHAMPION, D. C., and WHITAKER, A. J., 2004, The characterisation of granite deformation events in time across the Eastern Goldfields Province, Western Australia: Geoscience Australia, Record, no. 2004/10 (CD-ROM).

BLEWETT, R. S., CASSIDY, K. F., CHAMPION, D. C., HENSON, P. A., GOLEBY, B. S., JONES, L., and GROENEWALD, P. B., in press, The Wangkathaa Orogeny: an example of episodic regional 'D_2' in the late Archaean Eastern Goldfields Province, Western Australia: Precambrian Research.

CAREY, M. C., 1994, Petrography and geochemistry of selected sills from the Kambalda–Kalgoorlie region, W.A.: The Australian National University, BSc Honours thesis (unpublished).

CHAUVEL, C., DUPRE, B., and JENNER, G. A., 1985, The Sm–Nd age of Kambalda volcanics is 500 Ma too old!: Earth and Planetary Science Letters, v. 74, 315-324.

CLAOUÉ-LONG, J. C., COMPSTON, W., and COWDEN, A. C., 1988, The age of the Kambalda greenstones resolved by ion-microprobe: implications for Archaean dating methods: Earth and Planetary Science Letters, v. 89, p. 239–259.

CLARK, M. E., 1987, The geology of the Victory gold mine, Kambalda, Western Australia: Queens University, PhD thesis (unpublished).

CLARK, M. E., ARCHIBALD, N. J., and HODGSON, C. J., 1986, The structural and metamorphic setting of the Victory gold mine, Kambalda, Western Australia, *in* Proceedings of Gold '86 *edited by* A. J. Macdonald: Toronto, Canada, Konsult International, p. 243–254.

CLARK, M. E., CARMICHAEL, D. M., HODGSON, C. J., and FU, M., 1989, Wall-rock alteration, Victory Gold Mine, Kambalda, Western Australia: processes and P–T–X(CO_2) conditions of metasomatism, *in* The geology of gold deposits: the perspective in 1988 *edited by* R. R. KEAYS, W. R. H. RAMSAY, and D. I. GROVES: Economic Geology Monograph 6, p. 445–456.

CLOUT, J. M. F., 1991, Geochronology of the Kambalda–Kalgoorlie area: a review: Western Mining Corporation (unpublished).

COMPSTON, W., WILLIAMS, I. S., CAMPBELL, I. H., and GRESHAM, J. J., 1986, Zircon xenocrysts from the Kambalda volcanics: age constraints and direct evidence for older continental crust below the Kambalda–Norseman greenstones: Earth and Planetary Science Letters, v. 76, p. 299–311.

CONNORS, K., DONALDSON, J., MORRISON, R., and DAVY, C., 2003, Internal technical note TN SIG0329: the stratigraphy of the Kambalda – St. Ives district. Gold Fields Ltd (unpublished).

COWDEN, A. C., and ARCHIBALD, N. J., 1987, Kambalda–Kalgoorlie stratigraphy: evidence of volcanic cycles and structural repetition in Archaean greenstones: Western Mining Corporation (unpublished).

COWDEN, A. C., and ROBERTS, D. E., 1990, Komatiite hosted nickel sulphide deposits, Kambalda, *in* Geology of the mineral deposits of Australia and Papua New Guinea *edited by* F. E. HUGHES: The Australasian Institute of Mining and Metallurgy, Monograph 14, v. 1, p. 567–581.

COX, S. F., and RUMING, K., 2004, The St Ives mesothermal gold system, Western Australia — a case of golden aftershocks?: Journal of Structural Geology, v. 26, p. 1109–1125.

DONALDSON, M. J., 1983, Progressive alteration of barren and weakly mineralised Archean dunites: a petrological, mineralogical and geochemical study of some intrusive dunites from Western Australia: The University of Western Australia, PhD thesis (unpublished).

FOSTER, J. G., 1993, Applications of rare earth element (REE) and Re–Os isotope geochemistry to the exploration for komatiite hosted nickel sulphide deposits: Western Mining Corporation (unpublished).

GEE, R. D., 1979, Structure and tectonic style of the Western Australian Shield: Tectonophysics, v. 58, p. 327–369.

GEE, R. D., BAXTER, J. L., WILDE, S. A., and WILLIAM, I. R., 1981, Crustal development in the Archaean Yilgarn Block, Western Australia, *in* Archaean geology, Second International Symposium, Perth, 1980 *edited by* J. E. GLOVER and D. I. GROVES: Geological Society of Australia, Special Publication, no. 7, p. 43–56.

GOLEBY, B. R., RATTENBURY, M. S., SWAGER, C. P., DRUMMOND, B. J., WILLIAMS, P. R., SHERATON, J. W., and HEINRICH, C. A., 1993, Archaean crustal structure from seismic reflection profiling, Eastern Goldfields, Western Australia: Australian Geological Survey Organisation, Record, no. 1993/15, p. 54.

GOODGAME, V. R., 1997, The distribution and origin of arsenic and platinum group element mineralisation in the Mariners nickel deposit, Widgiemooltha, Western Australia: University of Oregon, PhD thesis (unpublished).

GRESHAM, J. J., and LOFTUS-HILL, G. D., 1981, The geology of the Kambalda nickel field, Western Australia: Economic Geology, v. 76, p. 1373–1416.

HAND, J., 1996, Mineralised volcanic and sedimentary environments in the Eastern Goldfields: Western Mining Corporation (unpublished).

HAYWARD, N. L., 1988, Geology of the Widgiemooltha area and exploration progress to February 1988: Western Mining Corporation (unpublished).

HILL, R. I., CHAPPELL, B. W., and CAMPBELL, I. H., 1992, Late Archaean granites of the southeastern Yilgarn Block, Western Australia: age, geochemistry and origin: Transactions of the Royal Society of Edinburgh, Earth Sciences, v. 83, p. 211–226.

KRAPEZ, B., BROWN, S. J. A., HAND, J., BARLEY, M. E., and CAS, R. A. F., 2000, Age constraints on recycled crustal and supracrustal sources of Archaean metasedimentary sequences, Eastern Goldfields Province, Western Australia: evidence from SHRIMP zircon dating: Tectonophysics, v. 322, p. 89–133.

LESHER, C. M., and ARNDT, N. T., 1995, REE and Nd isotope geochemistry, petrogenesis, and volcanic evolution of contaminated komatiites at Kambalda, Western Australia: Lithos, v. 34, p. 127–157.

MacGEEHAN, P. J., 1984, Internal zonation: Victory Dolerite: Western Mining Corporation (unpublished).

MARSH, S., 1988, Origin of the magnetite-rich facies Kapai Slate, Kambalda, Western Australia: The University of Western Australia, PhD Honours thesis (unpublished).

McCALL, G. J. H., 1969, The Archaean succession to the west of Lake Lefroy: Journal of the Royal Society of Western Australia, v. 52, p. 119–128.

McNAUGHTON, N. J., and DAHL, N., 1987, A geochronological framework for gold mineralisation in the Yilgarn Block, Western Australia, *in* Recent advances in understanding Precambrian gold deposits *edited by* S. E. HO and D. I. GROVES: Geology Department and University Extension, The University of Western Australia, Publication, no. 11, p. 29–49.

NEALL, F. B., and PHILLIPS, G. N., 1988, Fluid-wall rock interaction in an Archean hydrothermal gold deposit: a thermodynamic model for the Hunt mine, Kambalda: Economic Geology, v. 82, p. 1679–1694.

NEUMAYR, P., HAGEMANN, S. G., WALSHE, J., and MORRISON, R. S., 2003, Camp- to deposit-scale zonation of hydrothermal alteration in the St Ives gold camp, Yilgarn Craton, Western Australia: evidence for two fluid systems?, *in* Mineral exploration and sustainable development, Seventh Biennial SGA Meeting, Athens, 2003, abstracts: Athens, Greece, Society for Geology Applied to Mineral Deposits, p. 799–802.

NGUYEN, T. P., 1997, Structural controls on gold mineralization at the Revenge Mine and its tectonic setting in the Lake Lefroy area, Kambalda, Western Australia: The University of Western Australia, PhD thesis (unpublished).

NGUYEN, T. P., COX, S. F., HARRIS, L. B., and POWELL, C. M., 1998, Fault-valve behaviour in optimally oriented shear zones: an example at the Revenge gold mine, Kambalda, Western Australia: Journal of Structural Geology, v. 20, p. 1625–1640.

NGUYEN, T. P., GOODWIN, D., WILKINSON, C., and WITHERS, J., 1992, Kambalda gold targeting criteria: Western Mining Corporation (unpublished).

PERRIAM, R. P. A., 1985, The tectonic evolution of the Mt Martin – Carnilya Hill district of the Eastern Goldfields, Western Australia: The University of Western Australia, MSc thesis (unpublished).

POLITO, P. A., BONE, Y., CLARKE, J. D. A., and MERNAGH, T. P., 2001, Compositional zoning of fluid inclusions in the Archaean Junction gold deposit, Western Australia: a process of fluid–wall-rock interaction?: Australian Journal of Earth Sciences, v. 48, p. 833–855.

REDMAN, B., and KEAYS, R. R., 1985, Archaean basic volcanism in the Eastern Goldfields Province, Yilgarn Block, Western Australia: Precambrian Research, v. 30, p. 113–152.

ROBERTS, D. E., and ELIAS, M., 1990, Gold deposits in the Kambalda–St Ives region, *in* Geology of the mineral deposits of Australia and Papua New Guinea *edited by* F. E. HUGHES: The Australasian Institute of Mining and Metallurgy, Monograph 14, v. 1, p. 479–491.

ROCK, N. M., TAYLOR, W. R., and PERRING, C. S., 1990, Lamprophyres, *in* Gold deposits of the Archaean Yilgarn Block, Western Australia: nature, genesis and exploration guides *edited by* S. E. HO, D. I. GROVES, and J. M. BENNETT: Geology Department (Key Centre) and University Extension, The University of Western Australia, Publication, no. 20, p. 128–135.

SWAGER, C. P., and GRIFFIN, T. J., 1990, An early thrust duplex in the Kalgoorlie–Kambalda greenstone belt, Eastern Goldfields Province, Western Australia: Precambrian Research, v. 48, p. 63–73.

WATCHORN, R. B., 1998, Kambalda – St Ives gold deposits, *in* Geology of Australian and Papua New Guinean mineral deposits *edited by* D. A. BERKMAN and D. H. MacKENZIE: The Australasian Institute of Mining and Metallurgy, Monograph 22, p. 243–254.

WILLIAMS, P. R., and WHITAKER, A., 1993, Gneiss domes and extensional deformation in the Archaean Eastern Goldfields Province, Western Australia: Ore Geology Reviews, v. 8, p. 141–162.

WONG, T., 1986, Metamorphic patterns in the Kambalda area and their significance to Archaean greenstone belts of the Kambalda–Widgiemooltha area: The University of Western Australia, BSc (Honours) thesis (unpublished).

WOODALL, R., 1990, Gold in Australia, *in* Geology of the mineral deposits of Australia and Papua New Guinea *edited by* F. E. HUGHES: The Australasian Institute of Mining and Metallurgy, Monograph 14, v. 1, p. 45–67.

Kanowna Belle gold mine

by

J. R. Rogers[1], K. A. Joyce[1], G. J. Masterman[1], S. W. Halley[1], and J. L. Walshe[2]

History of exploration and mining

Exploration in the Kanowna district commenced in 1895 with the discovery of gold near the historic Kanowna townsite. About 0.5 million ounces of gold (Moz) was produced in the early part of the twentieth century, primarily from quartz reef (e.g. White Feather – Reward trend) and 'deep lead' palaeochannel deposits. Modern exploration for gold, nickel, and base metals (volcanogenic massive sulfides) commenced in the late 1970s. A series of widely spaced rotary airblast (RAB) drilling and soil sampling programs were carried out in the vicinity of the Kanowna Belle deposit between 1983 and 1989. These programs targeted the historic 'deep lead' deposits with the aim of locating a shallow supergene gold resource. 'Target 11' was a coincident gold anomaly in soils (350 m-diameter bullseye anomaly with a peak value of 150 ppb) and RAB drilling (2 m at 11 g/t Au from 52 m, 4 m at 3 g/t Au from 28 m) at the western edge of the target area. Follow-up reverse circulation (RC) drilling of this anomaly in late 1989 revealed economic mineralization beneath a 40 m-deep zone of gold-depleted saprolite. By September 1991, a resource of 11.2 Mt at 5.2 g/t had been determined by RC and diamond drilling, and openpit feasibility studies had commenced. By 1993, drilling on 80 × 80 m spacings had been completed to a depth of 1000 m, and proved a pre-mining resource of 21.4 Mt at 5.7 g/t Au (4 Moz) for the Kanowna Belle deposit. Openpit mining was completed in 1998 to a depth of 220 m, with a total production of 8.87 Mt at 4.4 g/t Au. Mining of the decline commenced in 1995, with underground production beginning in July 1998. Total gold production from Kanowna Belle to 31 December 2003 totals 2.6 Moz. The remaining resources and reserves are listed in Table 1.

Kanowna Belle and the Golden Mile are the only known refractory pyritic orebodies in the Yilgarn Craton where arsenopyrite is not a major sulfide phase. Gold in the Kanowna Belle deposit occurs mostly as fine grained (<10 µm) inclusions in pyrite or as invisible gold located in arsenic-rich growth zones in pyrite (Guest, 2002; typical ore assemblage contains 0.5–1.5% S and 40 ppm As). Processing is by jaw crushing, primary semi-autogenous grinding (SAG) milling, and secondary ball milling, followed by sulfide flotation. The pyrite and arsenopyrite concentrate is treated by roasting followed by carbon-in-leach (CIL) to extract the gold. The nameplate capacity of the Kanowna Belle plant is 1.35 Mtpa, but it is currently operating at 1.85 Mtpa. Mill feed is in excess of the mine production (1.3 Mtpa) and is supplemented from openpit stockpiles. The average gold recovery in 2003 was 89.3%.

Geological and structural setting

The following section is extracted from Davis (2000). Kanowna Belle occurs in the Boorara Domain subdivision of the Kalgoorlie Terrane, Eastern Goldfields. Mineralization is hosted in a sequence of conglomeratic and felsic volcaniclastic rocks (2668 Ma), which have been intruded by a porphyritic granodiorite (Kanowna Belle Porphyry; 2655 Ma) and minor felsic intrusions (Fig. 1). An intense zone of structural disruption separates the deposit into hanging- and footwall structural domains, and has a close spatial association with mineralization (Figs 1 and 2).

Initial deformation that controlled deposit architecture occurred in response to northerly directed thrusting during north–south shortening. This produced a mylonitic fabric (Fitzroy mylonite), variation in the strike of rocks in the foot- and hangingwalls, and was instrumental in localizing

Table 1. December 2003 resource and reserve statement for Kanowna Belle

	Mt	*Au g/t*	*Million oz*
Reserves	15.7	4.5	2.25
Additional resources (M+I)	11.1	4.5	1.59
Total reserves + resources	26.8	4.5	3.84

NOTES: M+I = Measured and Indicated Ore Reserves

[1] Placer Dome Asia Pacific, Post Office Box 1907, West Perth, W.A. 6872, Australia

[2] CSIRO Division of Exploration and Mining, Underwood Avenue, Floreat, W.A. 6014, Australia

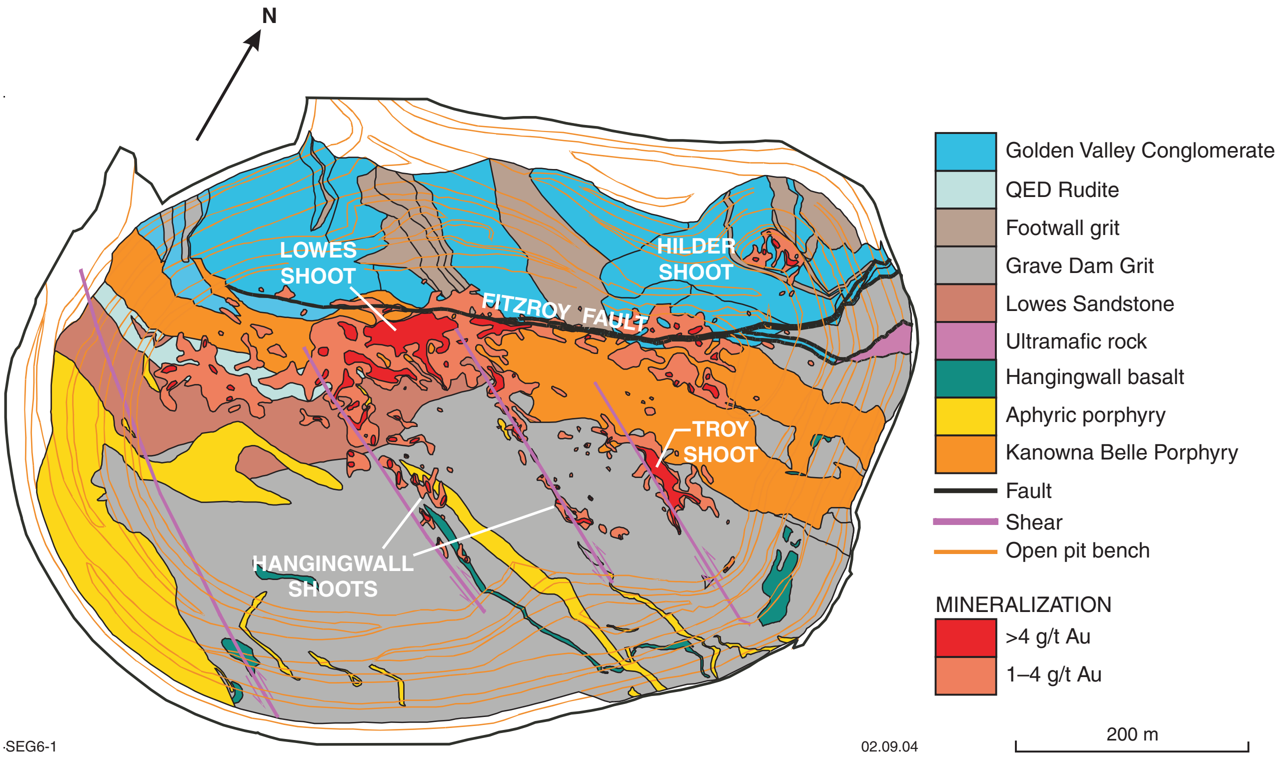

Figure 1. Geology of the Kanowna Belle openpit (map is orientated on KB mine grid; mine grid north = 330° TN; centre of pit is located at about MGA 363514E 6612745N)

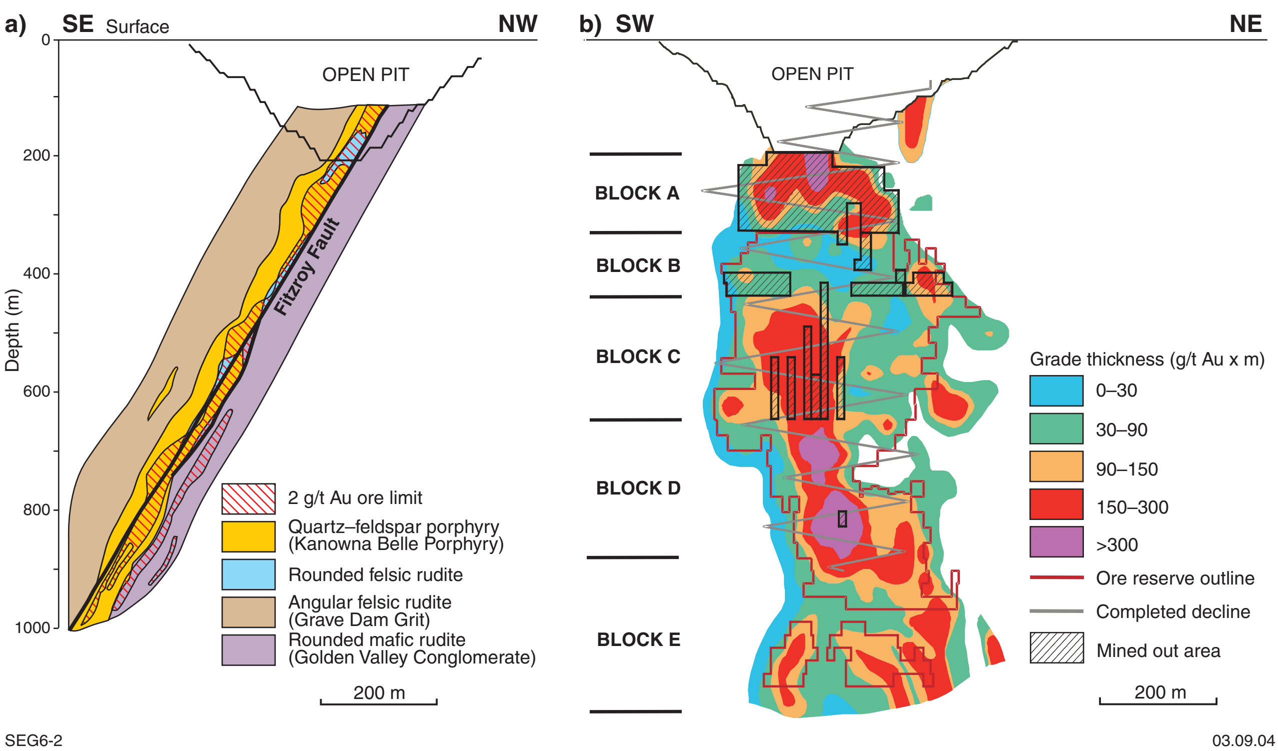

Figure 2. Sections through Kanowna Belle gold mine. a) northwest–southeast cross section (looking west). b) long section (looking northwest in the plane of the Fitzroy Shear Zone)

Table 2. Kanowna Belle alteration stages

Timing	*Proximal assemblage*	*Distal assemblage*
Early	Ankerite–sericite	Ankerite–sericite along regional structures, hematite alteration of porphyry intrusions
Late (gold-bearing hydrothermal fluids)	Alkali feldspar–dolomite Phengite–dolomite–pyrite	Muscovite–ankerite–pyrite

subsequent emplacement of the tabular Kanowna Belle porphyry. A short tectonic hiatus is inferred during emplacement of the Kanowna Belle porphyry, followed by resumption of north–south shortening. This resulted in the formation of an extensive zone of brittle–ductile deformation, characterized by fault splays that bound zones of intense foliation, all of which have accommodated steeply directed reverse movement. This zone is termed the Fitzroy Shear Zone. The Fitzroy mylonite and Fitzroy Shear Zone are interpreted to have formed during regional D_1.

A switch in far-field stress axes to an east-northeasterly–west-northwesterly orientation caused sinistral reactivation of the Fitzroy Shear Zone. This imparted sigmoidal geometries to pre-existing Fitzroy Shear Zone structures, and produced a shallow lineation on pre-existing structures in response to subhorizontally directed shearing. Emplacement of mineralization is interpreted to have been contemporaneous with sinistral reactivation of the Fitzroy Shear Zone (c. 2650 Ma), and is hosted by carbonate breccias, carbonate vein stock-works, quartz–carbonate veins, siliceous breccias, and sulfide–quartz–carbonate veinlets (stringers) and sheeted vein arrays. A synchronously developed, steep, northwesterly trending foliation has locally controlled emplacement of mineralization. Fitzroy Shear Zone reactivation, cleavage formation, and emplacement of mineralization are all interpreted to have been synchronous with the regional D_2 deformation event.

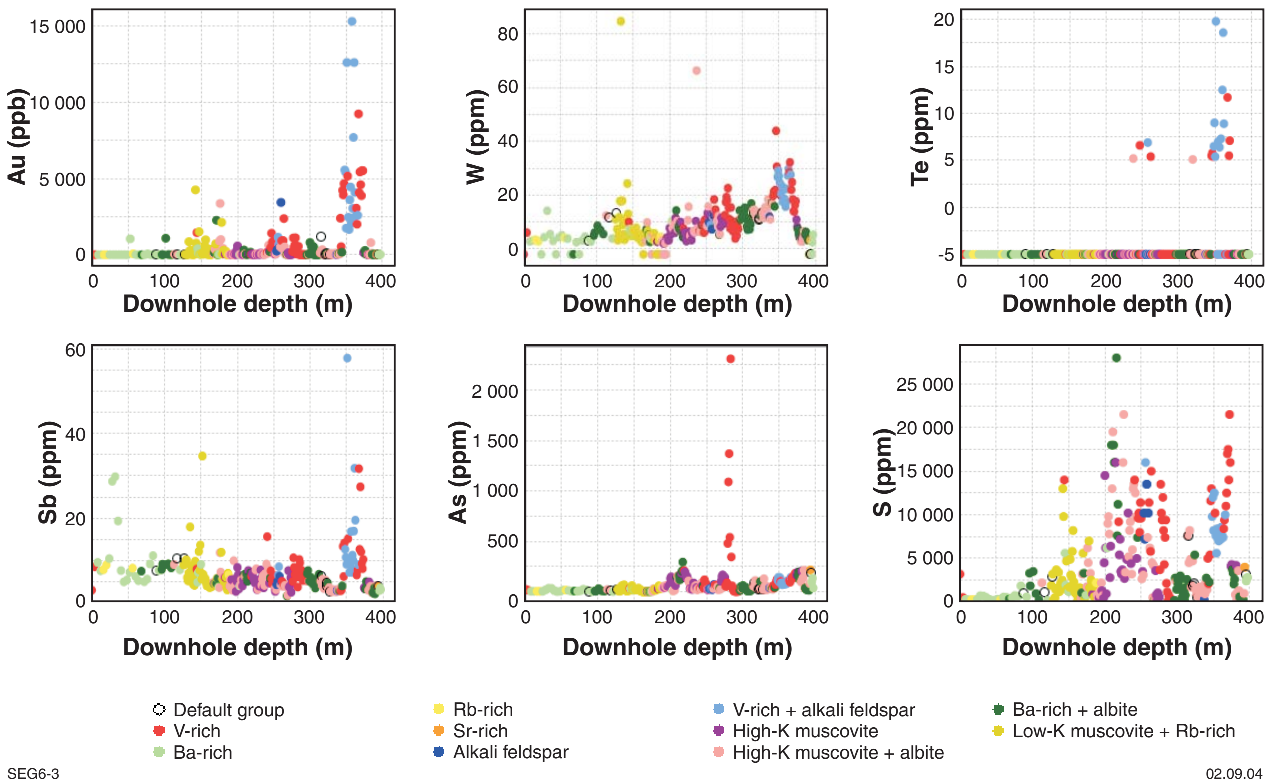

Figure 3. Distribution of pathfinder elements in diamond drillhole GDD438 (Lowes shoot). Downhole geology: 0–95 m = quartz grit; 95–130 m = felsic intrusion; 130–270 m = quartz grit and quartz–feldspar porphyry; 270–375 m = Kanowna Belle porphyry; 375 m = Fitzroy Fault; 375–398 m = polymict conglomerate

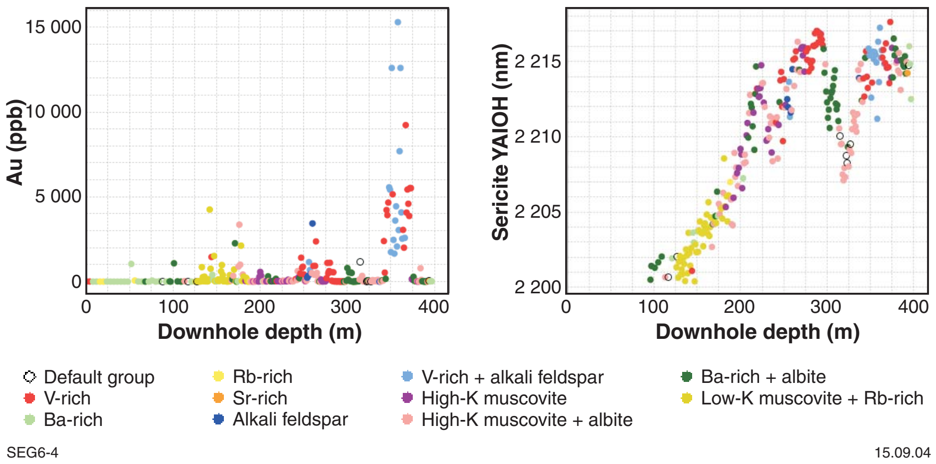

Figure 4. Gold grade and sericite infrared absorption wavelength (measured using PIMA, a portable infrared multispectral analyser) versus downhole depth for diamond drillhole GDD438. Downhole geology as for Figure 3

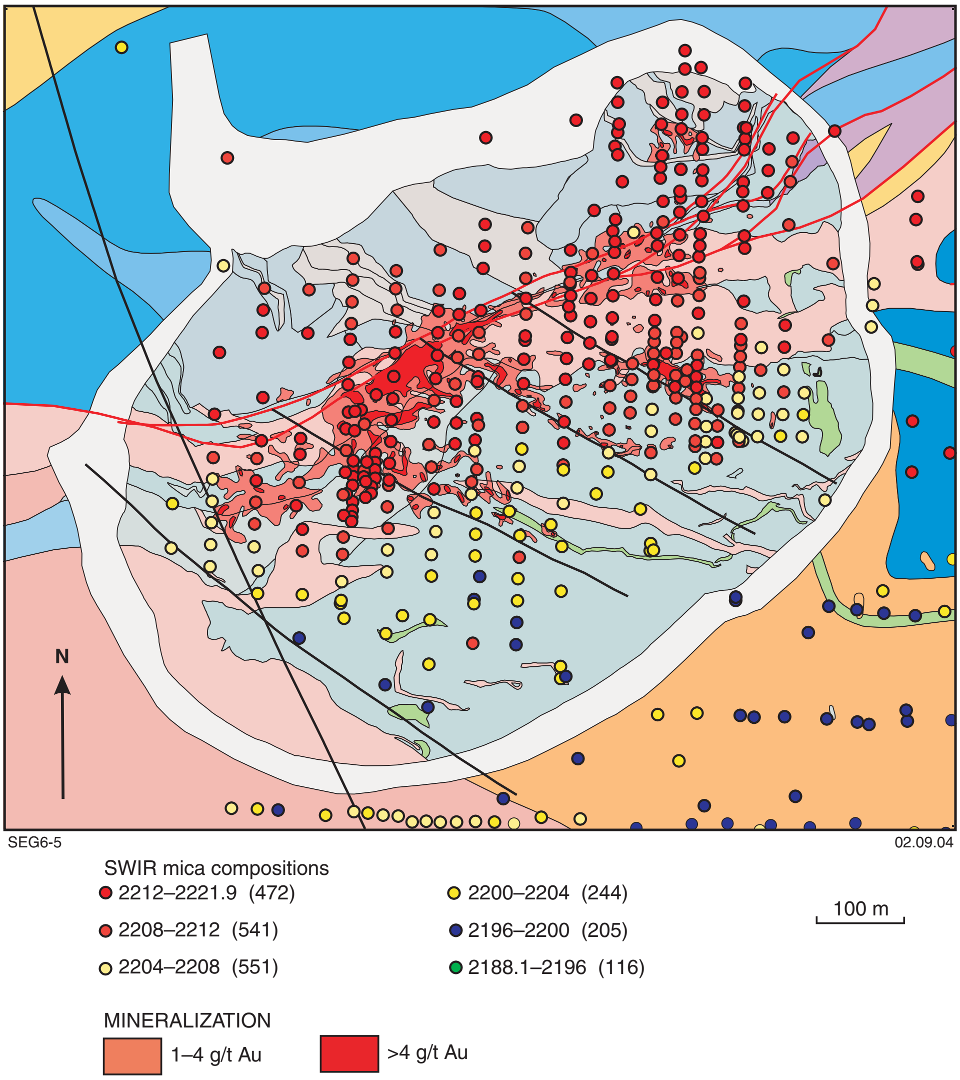

Figure 5. Results of PIMA survey of SWIR white mica compositions across the Kanowna Belle pit. Note correlation of high wavelength micas and gold grade shells

Hydrothermal alteration and gold mineralization

Two temporally and mineralogically distinct styles of gold mineralization are recognized at Kanowna Belle, corresponding to stages III and IV of the vein emplacement history (Aaltonen, 1997). The first, volumetrically minor, style of gold mineralization is represented by a telluride-associated mineralogy, and is restricted to crustiform carbonate(–quartz) veins and breccias (type III veins) near the Fitzroy Shear Zone. Veins show structural overprinting relationships consistent with emplacement synchronous with regional D_2. Telluride–gold mineralization occurs as microfracture and microvug infill. Free gold is associated with altaite, coloradoite, and melonite with rare hessite. No gold tellurides have been noted.

The second style of gold emplacement comprises the bulk of economic mineralization and overprints the telluride-associated style. It is a telluride-absent mineralization phase that displays a strong D_2 control on lode geometry. Gold occurs within pyrite–sericite–quartz–carbonate 'stringers' (type IV veins), which comprise stockwork geometries close to the Fitzroy Shear Zone but become more regularly aligned with the regional S_2 fabric away from the shear zone. Gold forms as inclusions, is located in arsenic-rich growth zones in pyrite, or both. Subordinate free gold occupies D_2 extensional sites adjacent to pyrite crystals.

Several stages of hydrothermal alteration have been recognized at Kanowna Belle (Table 2). The proximal alteration footprint associated with gold mineralization hosted by sedimentary rocks (footwall lodes) and porphyry (Lowes shoot) includes W, Mo, Bi, Te, As, and Sb (Fig. 3). The W halo around Lowes shoot is about 150 m wide and shows a systematic increase towards gold mineralization. Both sedimentary- and porphyry-hosted mineralization styles have alkali halos (K, Na, Rb, and Ba) that are well developed and characterized by alkali feldspar (albite–K-feldspar) altered rocks with a sericite overprint.

Gold in Lowes shoot is mainly found within V-bearing phengite domains, which are characterized by high AlOH short wavelength infrared (SWIR) absorption, near the transition to Ba-rich muscovite, which is characterized by low AlOH absorption wavelengths (Fig. 4). The correlation between gold and white mica gradients is evident at all scales across Kanowna Belle (Fig. 5). The transition from V-rich phengite (oxidized) associated with ore to Ba-rich (reduced) muscovite implies that a redox gradient influenced the composition of the white micas. This gradient is consistent with that inferred from the distribution of sulfur isotope values in ore-related and regional pyrite. The redox gradient observed at Kanowna Belle is interpreted to have resulted from multiple and contrasting fluid types that overlapped temporally and spatially during gold deposition.

References

AALTONEN, A., 1997. The significance of vein and breccia paragenesis to mineralisation at the Knaowna Belle gold mine, Eastern Goldfields Province, Western Australia: The University of Western Australia, Honours thesis (unpublished).

DAVIS, B. K., 2000. The Scotia–Kanowna dome, Kalgoorlie terrane: deformation history, structural architecture and controls on mineralisation: Delta Gold Ltd (unpublished).

GUEST, B., 2002. An investigation into the refractory nature of the Kanowna Belle gold deposit, Eastern Goldfields, Western Australia: Camborne School of Mines, University of Exeter, MSc thesis (unpublished).

Structural architecture and relative timing of Fimiston gold mineralization at the Golden Mile deposit, Kalgoorlie

by

L. Gauthier[1], S. Hagemann[1], F. Robert[2], and G. Pickens[3]

Introduction

The giant Archean Golden Mile gold deposit, which contains over 60 million ounces (Moz) of gold, is located in the southern part of the Archean Norseman–Wiluna greenstone belt, part of the Yilgarn Craton of Western Australia. It is situated on the outskirts of the city of Kalgoorlie. The Golden Mile has been in near-continuous production since the initial discovery of gold in 1893. It has produced over 50 Moz of gold, and the current Super Pit operation still hosts over 12 Moz of gold reserves. Over 10 Moz of gold were produced between 1894 and 1909, with the all-time peak year of production being 1903, when 1.2 Moz of gold was produced at an average grade of 41 g/t Au (Woodall, 1965; Clout et al., 1990). By 1912, the deepest shaft on the Golden Mile was the main shaft of the Boulder Consolidated Gold Mine, already 27 levels deep (-823 m). This led Larcombe (1912) to write that, 'In view of these facts the necessity for a detailed geological examination of the belt, coupled with an exact deciphering of the underground structure, becomes at once evident, for one of the necessary consequence of mining is the destruction of the evidence as to the origin and relation of the ore deposits'.

Historically, numerous mining companies, controlling a patchwork of separate small mining leases, operated several underground operations on the Golden Mile deposit. Operating leases on the Golden Mile were progressively amalgamated through the years until, in 1989, Kalgoorlie Consolidated Gold Mines (KCGM), a current joint venture between Barrick Gold Corporation and Newmont Gold, emerged as the sole owner of the Golden Mile and Mount Charlotte deposits. Underground gold mining effectively ceased in 1990 at the Golden Mile, and current mining operations consist of large scale open-pit mining extending over the entire Golden Mile deposit, complemented by underground mining of the Mount Charlotte deposit. The Super Pit operation recovers gold mostly from low-grade alteration selvedges along mined-out lodes, pillars, and portions of lodes that were uneconomic for underground mining. Underground access on the Golden Mile was maintained until the end of 2003.

The scope of the field trip at the Golden Mile will depend on the progress of mining. The nature and scale of the mining operation at the Golden Mile makes it difficult to visit specific sites of interest in the pit. The visit will probably comprise an overview of the Golden Mile geology from an observation bay near the top of the pit. This will be complemented by a review of drillcore documenting the main mineralization and alteration styles. Nonetheless, this field guide presents detailed mapping of localities in the pit and underground, which are now mined out or inaccessible. The field guide has focused on the documentation of the structural architecture and relative timing of gold emplacement at the Golden Mile, based on field relationships established through underground and pit mapping. More comprehensive overviews of the Golden Mile geology include Travis et al. (1971), Clout et al. (1990), and Bateman et al. (2001).

Structural architecture

Stratigraphy

A good understanding of the host stratigraphy is critical to better define the structural architecture of the Golden Mile deposit. The major and trace element geochemistry of the Paringa Basalt and Golden Mile Dolerite is used in three ways to define the structural architecture:

1. Consistent geochemical fractionation trends within the Paringa Basalt and individual units of the layered Golden Mile Dolerite are used as younging indicators.
2. Major faults are documented by offsets in the fractionation trend of the Paringa Basalt.
3. Early synvolcanic faults are interpreted by abrupt changes in the thickness and composition of the Paringa Basalt and Golden Mile Dolerite.

[1] Centre for Global Metallogeny, School of Earth and Geographical Sciences, The University of Western Australia, Crawley, W.A. 6009, Australia

[2] Barrick Gold Corporation, Level 10, 2 Mill Street, Perth, W.A. 6000, Australia

[3] KCGM Pty Ltd, PMB 27, Kalgoorlie, W.A. 6433, Australia

The Paringa Basalt sequence consists of a 400–700 m-thick accumulation of basaltic flows grading from a high magnesium basalt with ubiquitous variolitic and local spinifex textures at the base, to a gradually more fractionated tholeiitic basalt (Bateman et al., 2001). The upper portion of the Paringa Basalt is characterized by pillow and flow breccia textures, with a general increase of interflow sedimentary rocks. The Paringa Basalt displays a gradual fractionation trend with increasingly more evolved compositions towards the stratigraphic top, characterized by increasing Zr, TiO_2, Al_2O_3, V, and Fe_2O_3 contents, and decreasing MgO, Ni, and Cr contents (Fig. 1). The top 50–100 m section of the Paringa Basalt sequence consists of a high Fe tholeiite in sharp contact with the underlying tholeiitic basalt. It is characterized by high contents of TiO_2, Fe_2O_3, Zr, and P_2O_5, and very low MgO, Ni, and Cr contents. The high Fe tholeiite constitutes an important marker of the stratigraphic top of the Paringa Basalt sequence: this unit itself displays a normal fractionation trend.

The Golden Mile Dolerite is a differentiated layered gabbroic sill about 700 m thick. The intrusion has been subdivided into ten units based on petrographic and geochemical characteristics (Travis et al., 1971). Units 1 and 10 form the basal and upper chill margins, respectively. Units 2 and 3, the basal cumulate units, display very high Cr, Ni, and MgO contents with a decreasing trend upward into the intrusion. Units 4 and 5 consist of medium-grained subophitic gabbro with a generally flat geochemical pattern. Units 6, 7, and 8 are magnetite-rich (10–15 wt % magnetite), and unit 6 displays a very strong enrichment in elements with strong partition coefficients into magnetite, such as V, Cr, Ni, and Cu. These elements are, in turn, strongly depleted in units 7 and 8. Units 6 and 7 display gradual enrichment trends in Zr, TiO_2, and Fe_2O_3 towards unit 8. Unit 8, the granophyric unit, is characterized by high SiO_2, Zr, TiO_2, P_2O_5, and Fe_2O_3 contents. Unit 9 displays a gradual fractionation trend characterized by higher Zr, V, and TiO_2 contents, and lower Cr, Ni, and MgO contents towards the contact with unit 8.

The Golden Mile Dolerite displays important lateral variations in terms of thickness, internal magmatic layering, and geochemistry. The Golden Mile Dolerite on the easterly dipping limb of the upright northwesterly trending Kalgoorlie Anticline is significantly thinner (200 m) than on the westerly dipping limb (700 m), and displays a gradual fractionation trend without the formation of magmatic layering (Figs 2 and 3). The fractionation trend in the thin Golden Mile Dolerite is

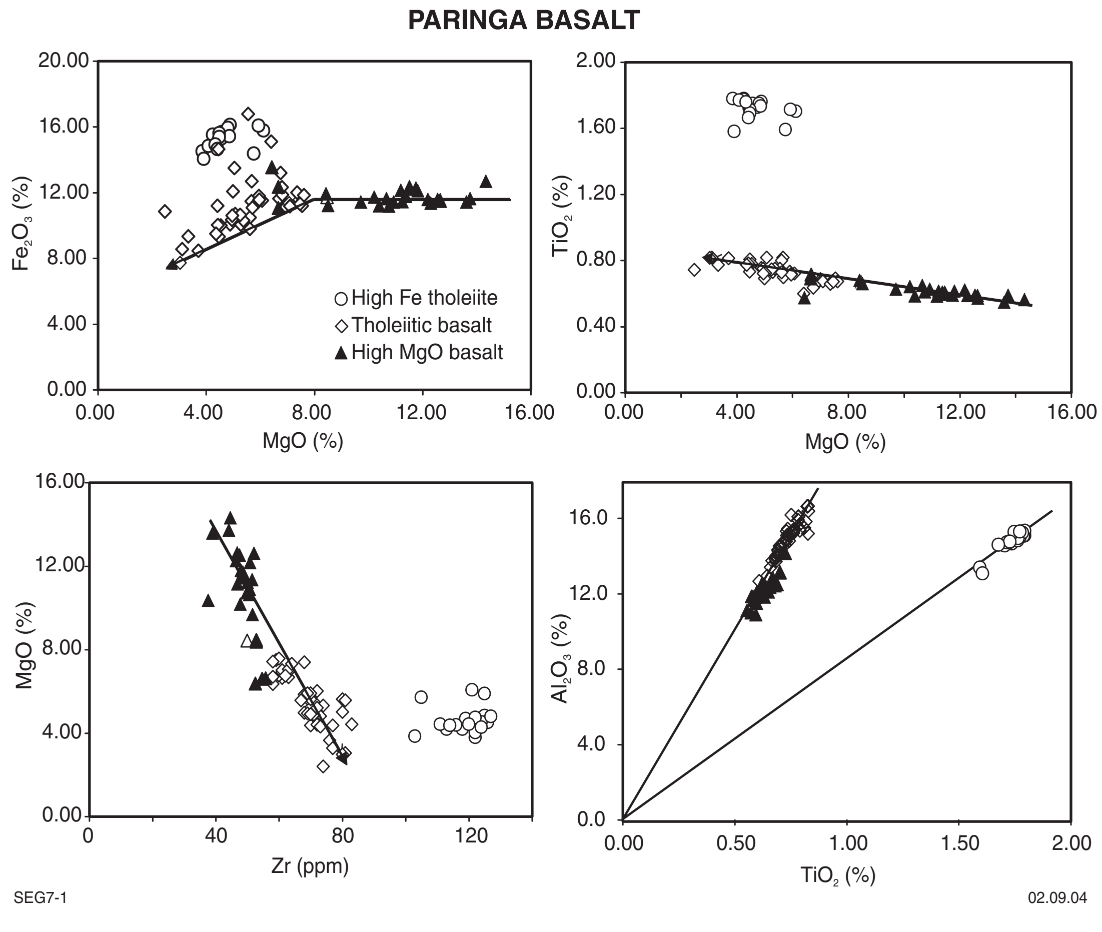

Figure 1. Geochemical variation diagrams of the Paringa Basalt highlighting the progressive fractionation trend from the high MgO basalt at the bottom of the Paringa Basalt sequence to the more fractionated tholeiitic basalts higher in the stratigraphy, and the high Fe tholeiite marker unit at the top of the Paringa Basalt sequence

indicative of a younging direction to the east, which is consistent with the interpretation of this thinner dolerite being on the easterly dipping limb of the Kalgoorlie Anticline. The chemostratigraphy of the underlying Paringa Basalt also supports this interpretation.

South of the Eastern Lode System, the Golden Mile Dolerite is slightly thinner (500 m) and displays less well developed internal magmatic layering, with significantly less abundant magnetite in units 6, 7, and 8. This transition is gradual and not associated with the Adelaide Fault (Travis et al., 1971). In turns, this confirms the equivalence of the Golden Mile and Aberdare Dolerites across the late stage Adelaide Fault (Clout, 1989).

Structure

The continuity of the Golden Mile Dolerite south of the Adelaide Fault establishes the regional continuity of the north-northwesterly trending, upright, and shallowly south plunging Kalgoorlie Syncline–Anticline pair (Fig. 1), which dominates the structural architecture of the Golden Mile (Woodall, 1965; Travis et al., 1971). The Kalgoorlie Syncline is an asymmetric fold, with the western limb being subvertical whereas the eastern limb dips at 30° to the west. Geochemical studies have further highlighted a consistent internal chemostratigraphy in the Paringa Basalt, which provides an additional marker for precisely locating the Kalgoorlie Anticline. The anticline plunges at about 20° south, which results in progressively older units being exposed along its axis towards the northwest. The Golden Mile Fault, a steeply west-dipping normal fault with substantial displacement, offsets the hinge of the Kalgoorlie Syncline (Woodall, 1965). The Golden Mile Fault forms the eastern contact between a narrow band of Black Flag Group (mudstone–sandstone), and the Golden Mile Dolerite to the east (Figs 2 and 3). The western contact of the Black Flag Group with the Golden Mile Dolerite is intrusive, as indicated by the wide chill margin within the dolerite. The Black Flag Group is itself intruded by numerous feldspar porphyry dykes.

There is a parasitic syncline–anticline fold pair on the western limb of the Kalgoorlie Anticline within the Golden Mile area (Figs 1 and 2). The Paringa Anticline and the Brownhill Syncline are at the northern end of the deposit. The Brownhill Syncline correlates with the Lake View Syncline at the southern end of the deposit (Gustafson and Miller, 1937). The Golden Mile Fault truncates the Brownhill Syncline – Paringa Anticline fold pair, indicating that initiation of the Golden Mile Fault postdates development of the Kalgoorlie Syncline–Anticline pair (Figs 1 and 2). This relationship does not support the interpretation of the Golden Mile Fault as a thrust and the Kalgoorlie anticline as an overturned hangingwall anticline (Swager, 1989).

A regional, steeply west-dipping, north-northwesterly oriented foliation (N140°/80°W) overprints the Kalgoorlie Syncline–Anticline pair and smaller subsidiary folds. This is well documented in the southern part of the Super Pit

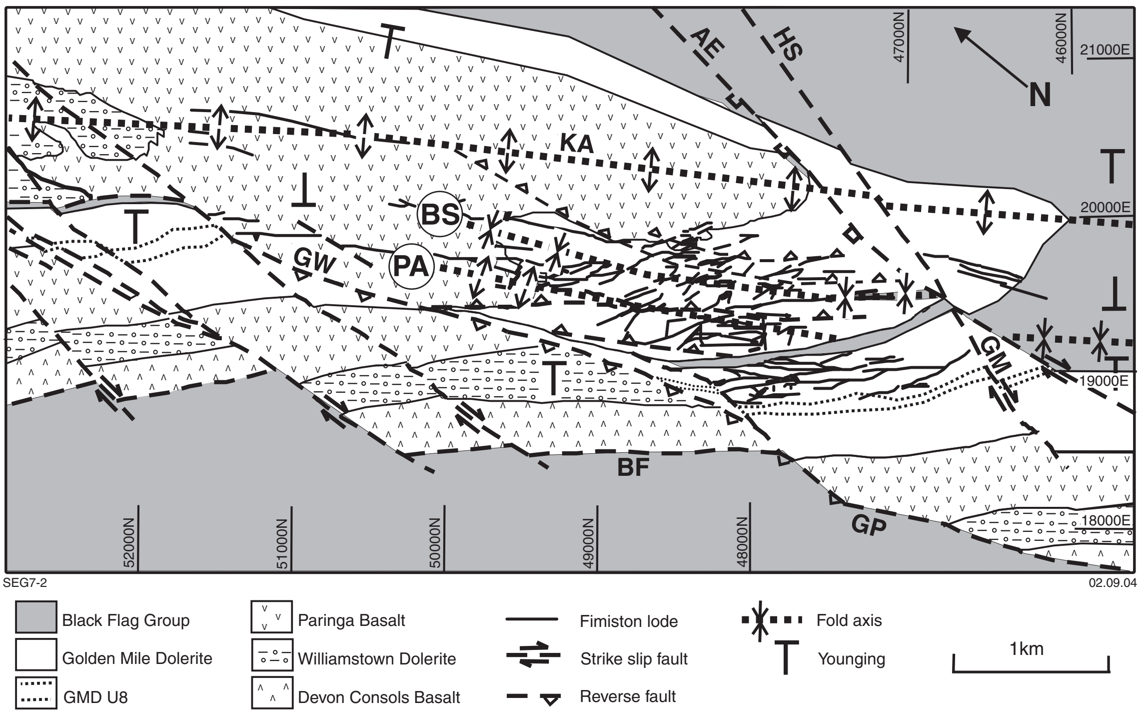

Figure 2 . Map of Golden Mile deposit area, modified after Bateman (2001), Clout (1989), and Gustafson and Miller (1937). AE = Adelaide Fault, BF = Boulder Fault, BS = Brown Hill Syncline, GM = Golden Mile Fault, GMD U8 = Golden Mile Dolerite unit 8, GP = Golden Pike Fault, GW = Golden Mile Dolerite 'wedge', KA = Kalgoorlie Anticline, KF = Kalgoorlie Fault, HS = Hannan Star Fault, PA = Paringa Anticline. Note that a local grid is used

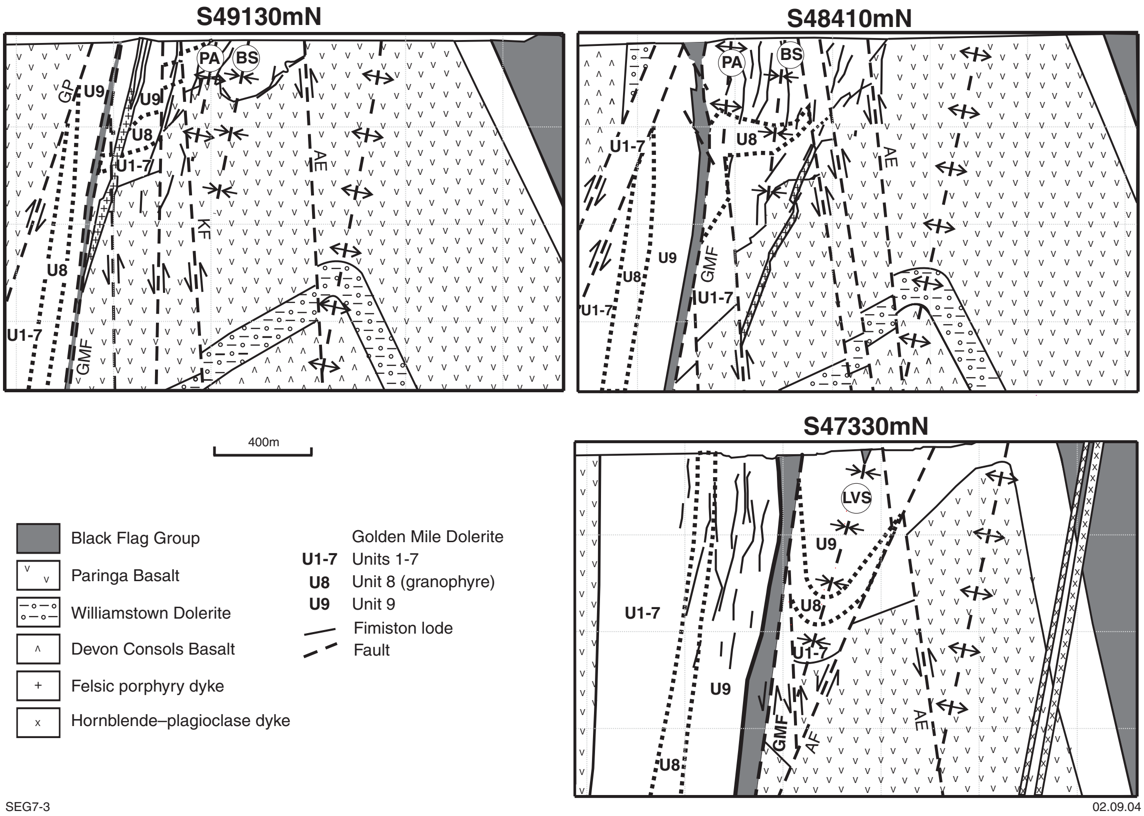

Figure 3. Geological cross sections, oriented local grid east–west looking local grid north, interpreted from compilation, relogging, and geochemical data. Abbreviations as for Figure 2, plus LVS = Lake View Syncline

where the Lake View syncline is exposed in the pit wall (Fig. 4). In that location, interbedded mudstone and siltstones of the Black Flag Group define a tight syncline. Individual beds within the Black Flag Group can be traced continuously across the hinge of the syncline. The upper chill margin of the Golden Mile Dolerite (unit 10) underlies the Black Flag Group. The syncline is also well documented within the underlying Golden Mile Dolerite. The reversal of younging direction in the Golden Mile Dolerite, from the western to the eastern hinge of the fold, is indicated by a reversal of the geochemical fractionation trends within unit 9. In the pit wall exposure of the Lake View Syncline, the regional north-northwesterly trending foliation cuts both limbs of the fold with the same anti-clockwise discordant relationship, indicating that the fabric postdates the fold.

Relative timing relationships

A swarm of feldspar porphyry dykes, centered on the deposit, transects both limbs of the Kalgoorlie fold pair, indicating the dykes were emplaced after this regional folding event and most likely in an upright position (Fig. 2; Golding, 1978; Mueller et al., 1988).

The dykes are, in turn, overprinted by the regional north-northwesterly trending foliation. The feldspar porphyry dykes are also overprinted by Fimiston-style gold mineralization, consisting of narrow vertically and laterally extensive lodes (up to 1200 m vertically and 1000 m along strike) of carbonate–quartz–pyrite wallrock disseminations, accompanied by variably developed carbonate–quartz–pyrite breccias and quartz veinlets. The feldspar porphyry dykes and Fimiston lodes are spatially associated and share three common orientations, historically known as Main (N140°/80°W), Caunter (N115°/65°W), and Cross (N050°/85°N–S). Hornblende porphyry dykes, of alkaline affinity, are also present and share the same orientations. These hornblende porphyry dykes crosscut the feldspar porphyry dykes and, locally, clearly cut the Fimiston lodes.

The north-northwesterly trending regional foliation is preferentially developed within weak layers such as mudstone beds and sericite-rich Fimiston lode selvedges. The constant orientation of the north-northwesterly trending foliation in lode selvedges across a wide range of lode orientations, including the northeasterly trending Cross Lodes and the shallowly dipping Caunter Lodes, provides clear evidence that the foliation overprints the lode selvedges, rather than being related to shearing synchronous with lode formation (Clout, 1989; Swager, 1989). The north-northwesterly trending regional foliation is also axial planar to small-scale buckle folds of Fimiston veins, and dykes, which is consistent with their east-northeast–west-southwest bulk shortening.

The stratigraphy, porphyry dykes, and Fimiston lodes are offset by a network of north-northwesterly trending reverse shear zones comprising a dominant steeply northeasterly dipping and steeply southwesterly dipping sets. The shear zones are particularly abundant in the Eastern Lode System (Figs 1 and 2). The Kalgoorlie Fault, one of the most extensive shear zones of this set, displays a 175 m reverse offset of the stratigraphy, feldspar porphyry dykes, and Fimiston lodes. The Fimiston lodes are commonly transposed within these shear zones, and the shears typically contain boudins of lode material. A conjugate network of shallowly dipping shear zones commonly postdates the steep reverse shear zones (Wells, 1964). These two sets of shear zones are reactivated by a later dextral strike-slip transcurrent deformation event, as indicated by ubiquitous shallowly plunging mineral lineations and slickensides within fault planes (Finucane, 1941).

The Adelaide Fault is a regional-scale, south-southeasterly trending, steeply west-dipping dextral fault, which terminates in the southern part of the Eastern Lode System in a south-southwesterly trending releasing bend that dips 70° west (Fig. 1). In the releasing bend, the fault displays a normal movement with an offset of about 300 m. The Australia East Fault, a steeply east-dipping reverse fault offsetting the Fimiston Lodes, is itself crosscut and offset by the Adelaide Fault (Fig. 2). Late northerly to north-northeasterly trending steeply dipping dextral faults form the latest set of faults at the Golden Mile. The Hannans Star Fault dextrally offsets the Morrisson lode, part of the Western Lode System, by about 40 m. The Hannans Star Fault also offsets the Adelaide Fault.

Quartz–carbonate veins and breccias, typical of the Mount Charlotte vein style mineralization, are associated with both late steeply dipping, and shallowly dipping reverse fault sets. The veins and breccia cut the Fimiston lodes, and contain fragments of these lodes with randomly oriented, foliated, sericite alteration selvedges. This implies that these late veins and some of the shallowly dipping and steeply dipping reverse faults postdate the north-northwesterly trending regional foliation.

A small wedge of Golden Mile Dolerite west of the Golden Pike Fault displays a geochemical signature similar to the thin, 200 m-thick Golden Mile Dolerite on the eastern limb of the Kalgoorlie Anticline and south of the Adelaide Fault (Figs 1 and 2). The thinner Golden Mile Dolerite is fractionated but does not display the magmatic layering typical of the thicker Golden Mile Dolerite (Travis et al., 1971). This suggests that the Golden Pike Fault influenced emplacement of the Golden Mile Dolerite and is an early structure, albeit reactivated by later deformation events. In turn, it is possible that the early

SEG7-4 02.09.04

Figure 4. Wall at the southern end of the Super Pit, looking south. Black Flag Group (dark) forms the core of the Lake View Syncline flanked on either side by Golden Mile Dolerite (orangish-brown). The north-northwesterly trend of the regional foliation is highlighted (S_2) and clearly overprints the syncline

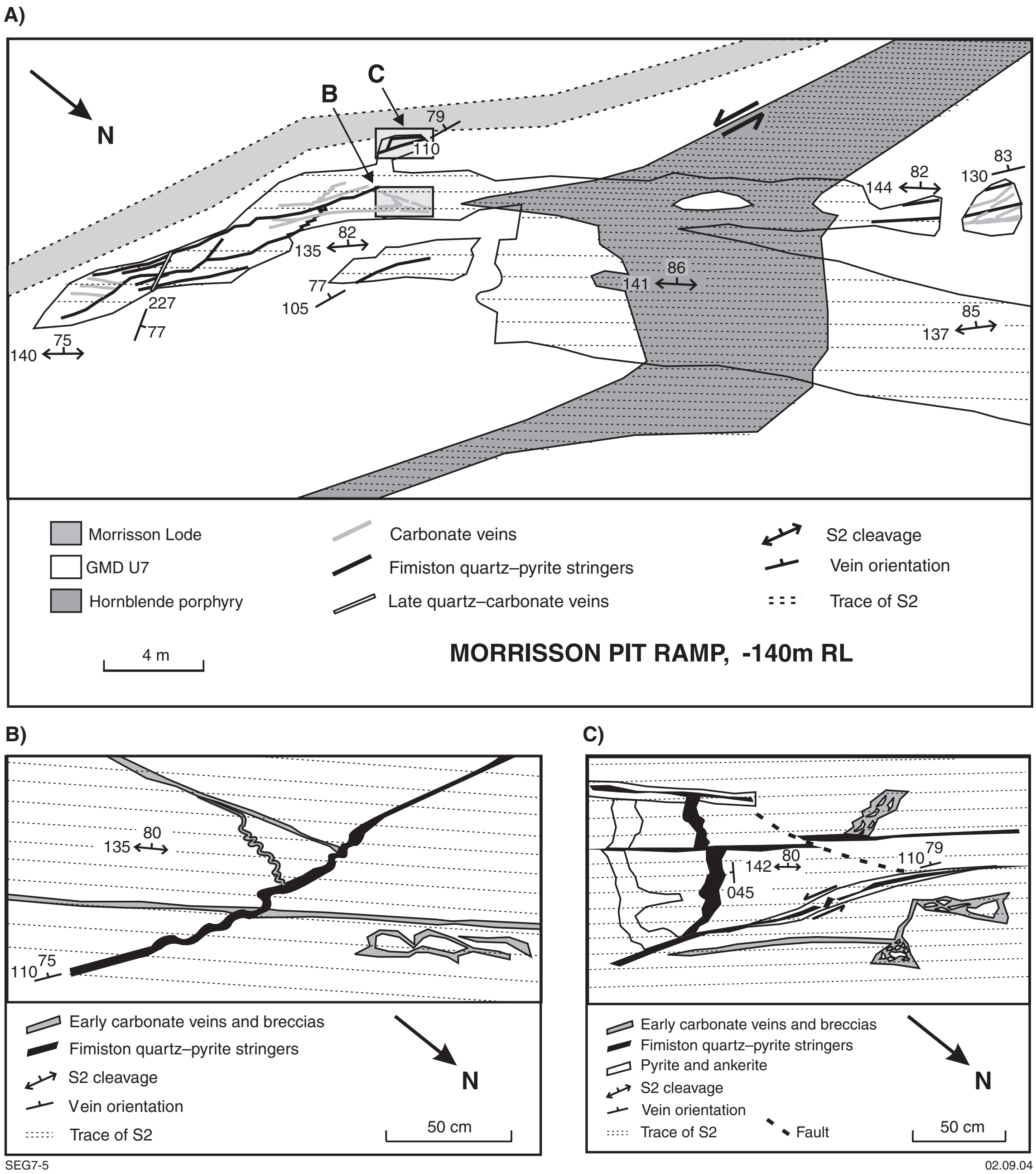

Figure 5. Detailed map of the northern margin of the Morrisson lode, at the bottom and middle of the Morrisson pit. The lode is situated in the southern part of the Western Lode System

Golden Pike Fault had a major control on the localization of the Golden Mile deposit by setting up a favourable geometry.

Field documentation

Some of the key field relationships and structural observations synthesized above are illustrated by a detailed map of the eastern margin of the Morrisson lode within the Morrisson pit (Fig. 5) and an underground sketch of the Black Flag Group between the Western and Eastern Lode Systems (Fig. 6).

Morrisson lode

The Morrisson lode map documents the northeastern margin of the Morrisson lode, located along the ramp towards the bottom of the Morrisson pit, within the southern part of the Western Lode System. The detailed map area contains abundant small Fimiston quartz (–carbonate–pyrite) stringers hosted within unit 7 of the Golden Mile Dolerite, along the northeastern margin of the Morrisson lode (Fig. 5).

A hornblende porphyry dyke is strongly sericite–carbonate altered and overprinted by a penetrative foliation. This foliation is much less well developed within the more competent unit 7. The foliation is axial planar to an S-shaped fold within the hornblende porphyry dyke. The southern margin of the dyke displays a steeply dipping sinistral fault, as indicated by slickensides and mineral lineations plunging shallowly southeast that are observed just west of the map area. The folding, sinistral faulting, and pervasive foliation developed in the strongly sericitized hornblende porphyry dyke are consistent with the transposition of a weak layer affected by bulk shortening directed east-northeast–west-southwest (Poulsen and Robert, 1990; Hanmer and Passchier, 1991).

The Fimiston quartz stringers crosscut carbonate veins and carbonate breccias within unit 7, indicating a phase of carbonate alteration pre-dating the main phase of Fimiston gold mineralization (Bartram, 1969). The Fimiston stringers display the three main orientations of lodes observed at the Golden Mile (Main, Caunter, and Cross), suggesting that the three orientations of ore zones are contemporaneous.

Figure 5B documents a Fimiston quartz stringer crosscutting carbonate veinlets. The Fimiston quartz stringer, oriented at N110°, displays S-shaped buckle folds, whereas the carbonate stringer, oriented at N020°, at a sharp angle to the S_2 foliation, displays Z-shaped buckle folding. This is consistent with a moderate bulk shortening directed east-northeast–west-southwest (Ramsay, 1983).

Figure 5C documents Fimiston quartz stringers in the three main orientations typical of Golden Mile lodes. The Fimiston quartz stringers have pyritic selvedges and crosscut early carbonate breccias. The quartz stringer oriented parallel to the Cross Lode orientation displays buckle folds consistent with weak bulk shortening. The Caunter-oriented quartz stringer displays a minor sinistral shearing, as the pyritic selvedge acted as a less competent layer compared to the quartz stringer. These features are consistent with a weak component of east-northeast–west-southwest bulk shortening associated with the north-northwesterly trending regional foliation.

A small Mount Charlotte-style quartz–carbonate vein in the southeastern part of the map area clearly crosscuts Fimiston quartz stringers. Furthermore, although the vein is almost orthogonal to the S_2 foliation, it does not display any folding, suggesting that its emplacement postdated the bulk shortening event associated with the S_2 foliation.

Black Flag Group

Figure 6 represents the western wall of an underground drive on the 20 level (-667 m) cutting through the Black Flag Group between the Western and Eastern Lode Systems. The section presented is along the western margin of the Black Flag Group.

The Black Flag Group consists of well-bedded mudstone and fine-grained sandstones, and has well developed foliation oriented at N145°/65°W. The bedding planes are subvertical, with graded bedding and crossbedding indicating a younging direction to the east. Small-scale folds of the bedding planes are axial planar to the north-northwesterly oriented foliation planes, and the fold axes plunge shallowly.

A feldspar porphyry dyke along the western end of the drive displays a very irregular contact with the Black Flag Group and is clearly discordant to the bedding planes. The dyke contains 5–10% plagioclase and hornblende phenocrysts, as well as quartz-filled vesicles, within a fine-

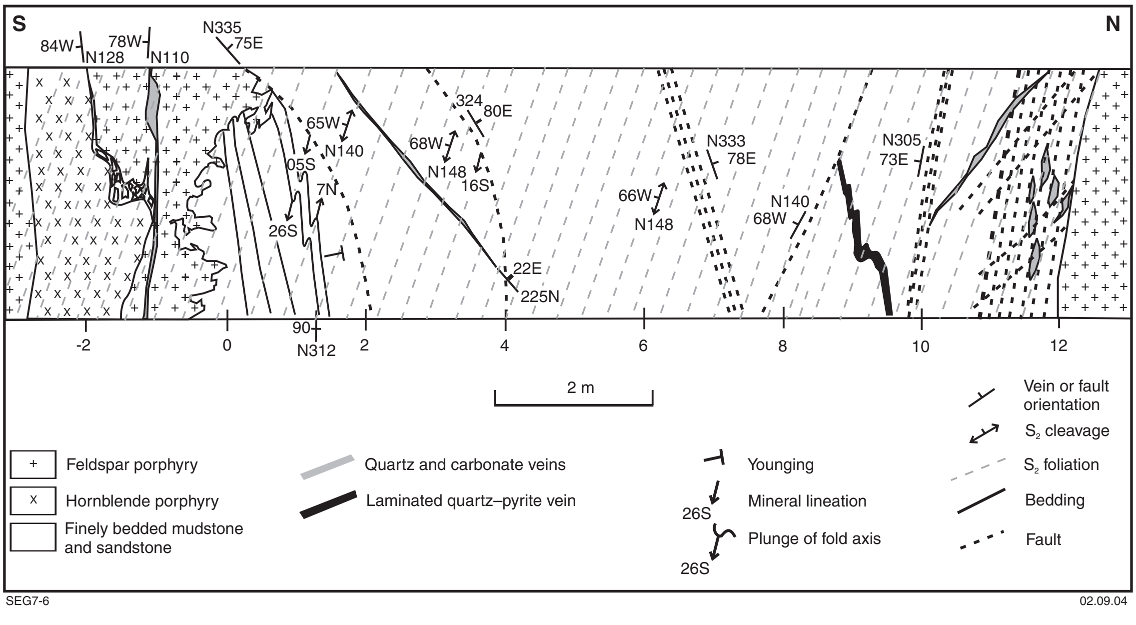

Figure 6. Sketch of underground drive northeast of the Chaffers shaft on level 20 (-667 m RL). Western end of the Black Flag Group separating the Western and Eastern Lode Systems, view of the west wall of the drive, which is oriented north–south

grained quartzofeldspathic groundmass overprinted by a sericite–carbonate assemblage. A hornblende porphyry dyke transects the feldspar porphyry dyke, clearly establishing the relative chronology of dyke emplacement. The hornblende porphyry dyke contains about 20% coarse-grained hornblende phenocrysts, and is also overprinted by intense sericite–carbonate alteration.

Towards the eastern end of the section, there is a small laminated quartz–carbonate vein with pyrite concentrated along the selvedges. Such veins are characteristic of the late stage of the Fimiston ore paragenesis. The vein displays buckle folds that are axial planar to the north-northwesterly trending foliation planes, consistent with bulk shortening associated with the foliation.

The Black Flag Group is cut by several narrow steeply easterly and westerly dipping oblique faults. The faults have a component of reverse offset, but display shallowly plunging mineral lineations and slickensides, which are generally well developed within the sedimentary rocks, and indicate a dextral component of movement. They are interpreted to be reverse faults with a late component of dextral movement, and offset the laminated Fimiston quartz–carbonate vein and feldspar porphyry dykes.

A few coarse-grained carbonate veins and quartz veins within the Black Flag Group, although at sharp angle to the foliation, do not display any buckle folds, and locally crosscut steeply dipping fault planes, such as shown in the eastern portion of Figure 6. These veins are interpreted to be late stage, postdating the north-northwesterly trending foliation, and are probably associated with the late, steeply dipping, oblique faults.

References

BARTRAM, G. D., 1969, Wall rock alteration associated with auriferous lodes at Kalgoorlie: The University of Western Australia, PhD thesis (unpublished).

BATEMAN, R. J., HAGEMANN, S. G., McCUAIG, T. C., and SWAGER, C. P., 2001, Protracted gold mineralisation throughout Archean orogenesis in the Kalgoorlie camp, Yilgarn craton, Western Australia: structural, mineralogical, and geochemical evolution: Western Australia Geological Survey, Record 2001/17, p. 63–98.

CLOUT, J. M. F., 1989, Structural and isotopic studies of the Golden Mile gold–telluride deposit, Kalgoorlie, W.A.: Monash University, PhD thesis (unpublished).

CLOUT, J. M. F., CLEGHORN, J. H., and EATON, P. C., 1990, Geology of the Kalgoorlie gold field, *in* Geology of the mineral deposits of Australia and Papua New Guinea *edited by* F. E. HUGHES: The Australasian Institute of Mining and Metallurgy, Monograph 14, p. 411–431.

FINUCANE, K. J., 1941, East dipping strike slip faults on the Boulder belt, Kalgoorlie: Proceedings of the Australasian Institute of Mining and Metallurgy, v. 124, p. 203–215.

GOLDING, L. Y., 1978, Mineralogy, geochemistry and origin of the Kalgoorlie gold deposits, Western Australia: University of Melbourne, PhD thesis (unpublished).

GUSTAFSON, J. K., and MILLER, F. S., 1937, Kalgoorlie geology reinterpreted: Proceedings of the Australian Institute of Mining and Metallurgy, v. 106, p. 93–125.

HANMER, S., and PASSCHIER, C., 1991, Shear sense indicators; a review: Geological Survey of Canada, Paper, no. 90-17, 72p.

LARCOMBE, C. O. G., 1912, The geology of Kalgoorlie: Australian Institute of Mining Engineering, Transactions, no. 14, p. 1–327.

MUELLER, A. G., HARRIS, L. B. and LUNGAN, A., 1988, Structural control of greenstone-hosted gold mineralisation by transcurrent shearing: a new interpretation of the Kalgoorlie mining district, Western Australia: Ore Geology Reviews, v. 3, p. 359–387.

POULSEN, K. H., and ROBERT, F., 1989, Shear zones and gold: practical examples from the southern Canadian Shield, *in* Mineralization and shear zones *edited by* J. T. BURSNALL: Geological Association of Canada, Short Course Notes, v. 6, p. 239–266.

RAMSAY, J. G., and HUBER, M. I., 1983, The techniques of modern structural geology, Volume I: Strain analysis: New York, U.S.A., Academic Press, 700p.

SWAGER, C. P., 1989, Structure of Kalgoorlie greenstones — regional deformation history and implications for the structural setting of the Golden Mile gold deposits: Western Australia Geological Survey, Report 25, p. 59–84.

TRAVIS, G. A., WOODALL, R. W., and BARTRAM, G. D., 1971, The geology of the Kalgoorlie Goldfield, *in* Symposium on Archaean rocks *edited by* J. E. GLOVER: Geological Society of Australia, Special Publication, no. 3, p. 175–190.

WELLS, A. A., 1964, Western Lode structures and southward extensions on the Boulder Mining Belt: Proceedings of the Australasian Institute of Mining and Metallurgy, v. 211, p. 181–192.

WOODALL, R. W., 1965, Structure of the Kalgoorlie Goldfield, *in* Geology of Australian ore deposits *edited by* J. McANDREW: Melbourne, Victoria, 8th Commonwealth Mining and Metallurgical Congress, and The Australasian Institute of Mining and Metallurgy, p. 71–79.

Rubicon gold mine, Kundana mining centre

by

G. Tripp[1]

Introduction

The Rubicon open pit mine is located in the Kundana mining centre, about 22 km northwest of Kalgoorlie. The mine exposes mafic volcanic rocks of the Grants Patch Group and sedimentary rocks of the Black Flag Group in the Ora Banda Domain. Mineralization is hosted in a 0.5–0.8 m-thick laminated quartz vein along a mafic–sedimentary rock contact. Grants Patch Group mafic rocks in the hangingwall are intensely sheared, with partitioned high-strain zones that trend at a low angle to the main ore vein. Sedimentary rocks in the footwall are folded, with penetrative axial plane foliations.

Other vein arrays are associated with the main vein, including flats, footwall stockworks, and splay veins that affect the grade and location of high grade oreshoots. The main vein is best mineralized in areas where it is most disrupted by other vein intersections and microfaulting of the vein fabrics. Foot- and hangingwall veins, and vein stockworks are also potential exploration targets. Shear zones that intersect the main ore vein at an angle produce an intersection lineation plunging steeply south, and could control the geometry and distribution of high grade oreshoots.

Cross faults disrupt the main ore vein, with displacements of up to 11 m in the open pit. These faults have displaced the vein laterally, and can result in a loss of the ore horizon in underground ore drives. A major cross fault (White Foil Fault) produces the greatest offset of the ore vein, whereas several smaller faults have variable displacements and kinematics.

Kundana mining centre

Geology

Hadlow (1990) described the geology of the Kundana mining centre in detail, and much of the local geology presented here is drawn from that study. The location and geology of the mining centre are presented in Figures 1 and 2.

[1] Placer Dome Asia Pacific, Mount Pleasant Gold Mine, Post Office Box 1162, Kalgoorlie, W.A. 6433, Australia

Rock types

The Kundana mining centre covers the interpreted position of the Zuleika Shear Zone and adjacent areas in the Ora Banda and Coolgardie Domains. The eastern part of the area lies on the north-northwesterly trending Kurrawang Syncline, and the western part is on the eastern limb of the south-southeasterly trending Powder Sill Syncline. In the east, the stratigraphy consists of high-Mg basalt and dolerite (Bent Tree Basalt), feldspar-phyric basalt (Victorious Basalt), graphitic black shale, intermediate

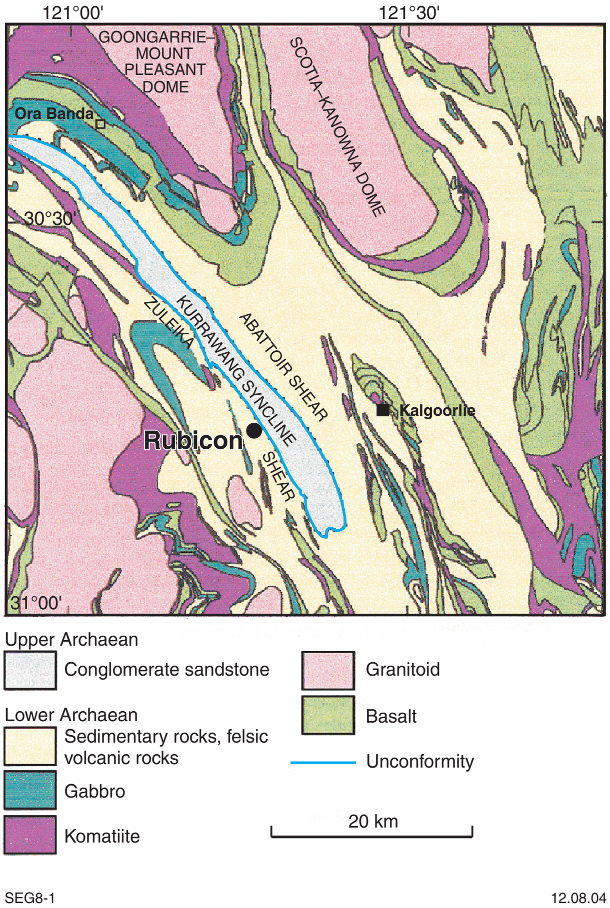

Figure 1. Regional geological setting of the Rubicon gold mine (after Goleby et al., 2000)

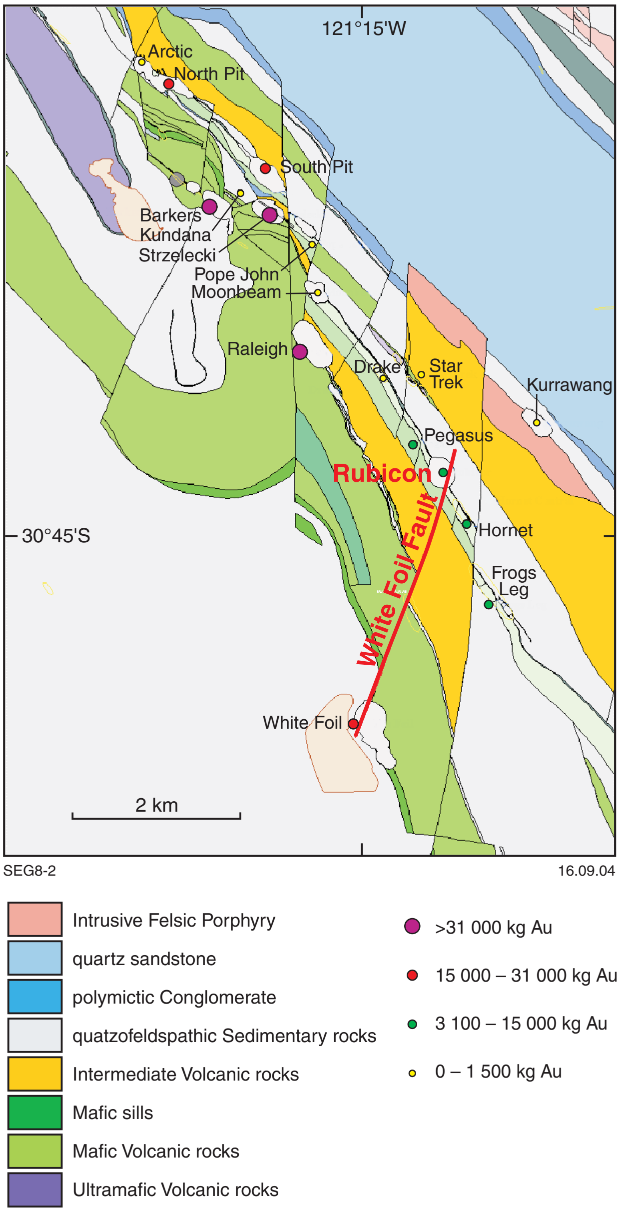

Figure 2. Local geological setting of the Rubicon mine

volcaniclastic rocks, dolerite sills, and polymictic conglomerate (Kurrawang Formation). This sequence contrasts with komatiite, felsic sedimentary rocks of the Spargoville Formation, and the layered, differentiated Powder Sill dolerite in the west. Graphitic shales and andesite–dolerite contacts are of particular interest since they are the primary sites hosting laminated auriferous quartz veins. Shear reactivation of the stratigraphic contacts produced strike-persistent shear zones that localized hydrothermal fluids.

Structure

Rocks in the Kundana mining centre record three main deformation events including folding, shearing, and brittle faulting. Folding in the eastern part of the area produced a slightly overturned sequence, which was interpreted as an isoclinal anticline between the Powder Sill and Kurrawang Synclines (Hadlow, 1990). A small but important northerly plunging anticline at the eastern extension of the Powder Sill could have formed a rigid body that affected the subsequent partitioning of strain during the regional shortening. Ductile shearing produced partitioned zones of flattening and simple shear strain with a dominantly down-dip stretching lineation. Plagioclase phenocrysts in the Victorious Basalt are stretched into rodlike shapes, with axial ratios up to 7:1, and X>>Y=Z indicating an apparent constriction. Exposures in the Arctic open pit show elongation in the XY and XZ planes, whereas the phenocrysts exhibit orthorhombic symmetry in the YZ plane. The orientation of the Zuleika Shear Zone is variable about the vertical, and most exposures show a steep dip, which varies from vertical in the North pit to mostly easterly dipping in the Kundana north outcrops. Reverse kinematics is suggested by asymmetric boudinage of syntectonic quartz veins in a westerly dipping foliation viewed in plan section. The stretching lineation is subparallel to the fold axes of open-tight chevron folds in metasedimentary rocks that also plunge steeply north (interpreted F_2).

Gold deposits

Gold mineralization at Kundana comprises quartz veins that were emplaced into several graphitic shale horizons and along lithological contacts. The deposits are discussed in detail by Lea (1998) and only pertinent structural features are discussed below. The Kundana mines contribute significantly to the total gold endowment of the region, with an estimated historic production plus resources of about 217 t. This endowment is contained within three large deposits — Strzelecki (1.8 Moz), Barkers (0.9 Moz), and Raleigh (0.9 Moz) — and many other smaller deposits, including South pit (0.7 Moz) and North pit (0.5 Moz). The Strzelecki and Barkers orebodies are well developed, and provide clear information on the timing and control of gold mineralization within sheared rock contacts.

Vein thickness and geometry

Veins in the Strzelecki and Barkers orebodies trend about 65°/220° (strike 310°). Underground mine geologists have indicated that the ore grade decreases where the strike orientation of the vein moves away from this trend toward 300°. Small kinks in the vein localize high-grade portions and thick vein intersections. As shown in Figure 3, the thickest portions of the veins form semicontinuous steeply (60°–65°) southeast-pitching pipes where the vein is >0.5 m thick.

Vein kinematics

Veins in the Kundana mines display a well developed, shallowly north-plunging slip lineation that is manifested as slickenside grooving on the vein surface. At one locality underground at the Barkers mine, this lineation pitches 25°–35°N in the plane of the vein, and this orientation is observed throughout the mines (Fig. 3). The slip vector of the veins is about orthogonal to the trend of the thickest

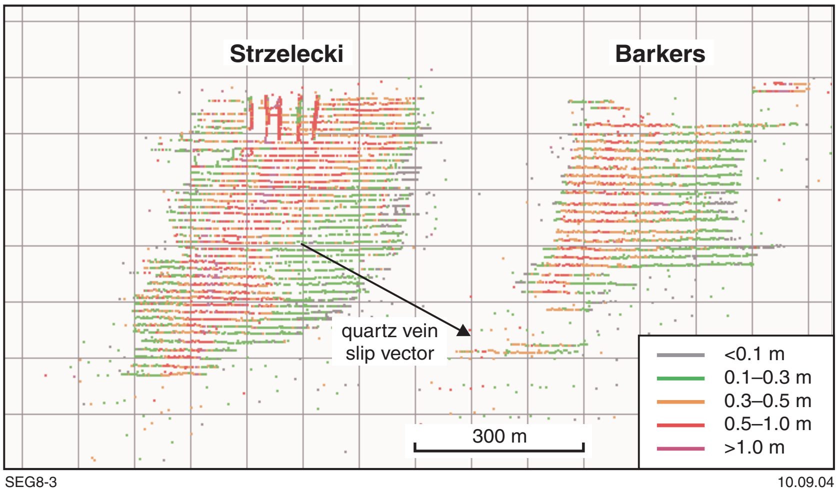

Figure 3. Plot showing variation of vein thickness (m) for the Strzelecki and Barkers orebodies

portion of the veins, suggesting that most quartz veins were emplaced with oblique movement sense (Fig. 3). Dilation and high-grade development at kinks where the vein orientation changes from 300° to 310° suggest a dextral movement sense during the vein formation. However, the sense of offset is equivocal, and clear kinematic indicators are lacking (Hadlow, 1990). Preferential opening along the fault produced a dilational jog and probably facilitated thick quartz precipitation at 90° to the slip vector, with minor development of breccia and fault cataclasite typical of extremely high fluid pressures (Sibson, 1987).

Gold distribution

The distribution of gold grade is erratic in the Barkers and Strzelecki veins (Fig. 4), and, whereas the very high grades apparently show no direct relationship to vein thickness, the presence of gold grades >10 g/t correlates with a vein thickness of >0.1 m. There are small, localized, very high grade shoots with steep to vertical northerly pitches (Fig. 4) in the extreme northern and southern ends of both orebodies. This orientation of the highest grades does not appearto be related to the ductile shearing even though the high grades are subparallel to the principal stretching lineation in the Zuleika Shear Zone. In several areas in the Barkers mine, small thin shear bands transgress the laminations within the ore vein, suggesting a later timing for the shear bands. Microstructural analysis confirms the siting of gold in these early and late shear laminations, and reveals crucial timing relationships for the vein emplacement, ductile shearing, and ore deposition.

Importantly, the orebodies do not occur within the Zuleika Shear Zone, but are totally contained within

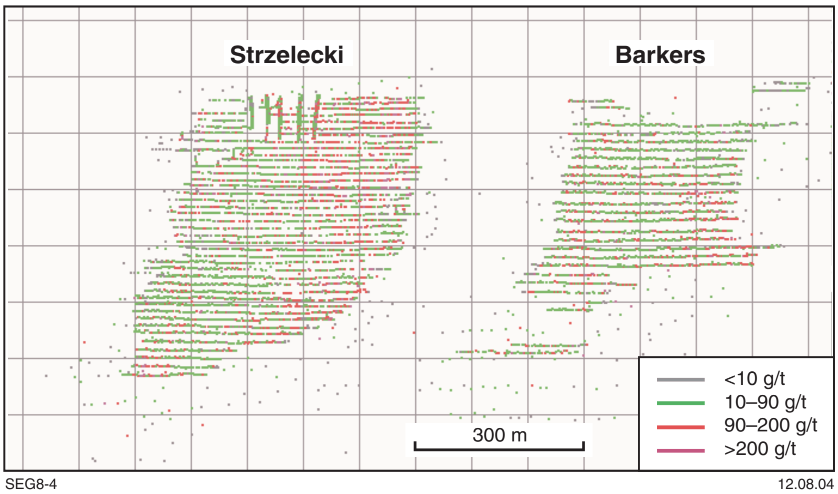

Figure 4. Plot showing variation of gold grade (g/t Au) for the Strzelecki and Barkers orebodies

andesite–dolerite contacts in the wallrocks of the shear zone (Barkers and Strzelecki) or graphitic shales very close to the shear zone (South and North pits). This distinction may seem irrelevant, but the vein kinematics and emplacement geometry (Barkers and Strzelecki) indicate that mineralization either pre- or postdates the ductile shearing. Also, the orientation of the Zuleika Shear Zone is subvertical to easterly dipping, whereas the andesite–dolerite contacts dip moderately southwest. Clearly, the stratigraphic horizons would have failed in a ductile fashion during reactivation (e.g. enforced shearing; Robert et al., 1994), and the emplacement of veins during such movements would have produced the characteristic brittle–ductile deformation style. The South and North orebodies could have had a closer relationship to the Zuleika Shear Zone since they are developed in veins on sheared black shale contacts near the high strain zone. The orebodies are therefore located in structures that almost certainly failed during the ductile deformation, yet this early failure was not necessarily related to their formation. The lack of coincidence between the thickest portions of the veins and the highest grade areas indicates that some other factor controlled the location of the high grade oreshoots. Later shear laminations that crosscut the veins could provide this connection.

Hadlow (1990) advanced an alternative hypothesis, observing that the highest grade portions of the South pit were located where 345°–350°-trending intense foliation zones intersected the main vein or contact. These foliation zones appear to be approximately axial planar to shallowly south-plunging tight to isoclinal folds in the wallrocks of the South pit (Fig. 5). The folds in this exposure are developed in black shale and chert, and plunge 20°→150°. This fold orientation is parallel to the regional F_2 folds, and the folds are the same generation as those observed in the Arctic open pit that plunge steeply north near the Zuleika Shear Zone. From these observations, it is interpreted that the east-northeast–west-southwest shortening of D_2 produced upright F_2 folds that were progressively rotated into parallelism with the principal extension direction of the finite strain ellipsoid as strain was partitioned into ductile shear zones. These folds could have induced anisotropy at the mine scale, localizing the high grade oreshoots in the veins. At a regional scale, the small anticline in the Powder Sill could have induced the anisotropy that altered regional strain and fluid flow patterns, and focused fluids into the actively deforming black shale horizons.

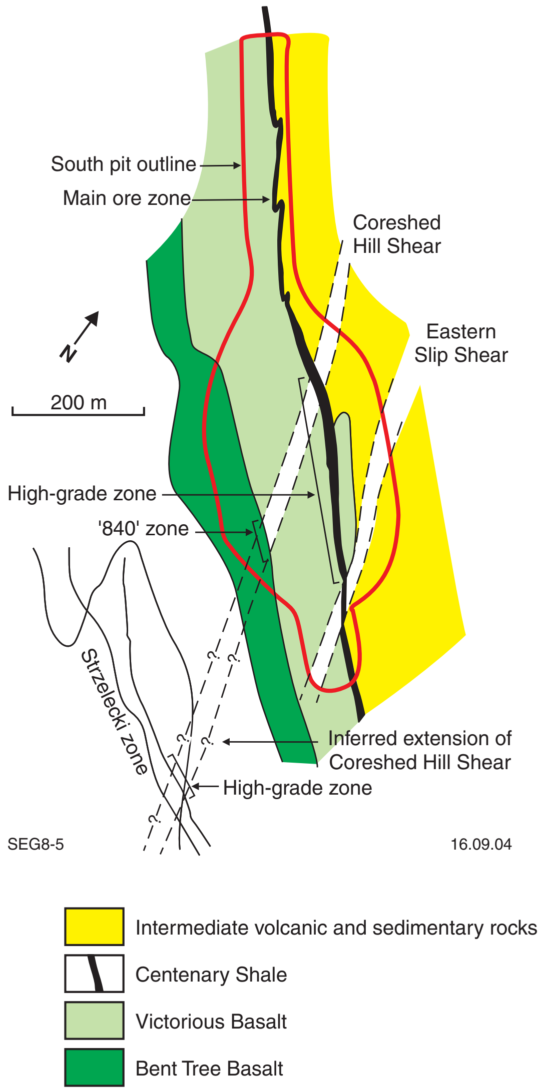

Figure 5. Schematic diagram of the South pit showing the intersection geometry of the Coreshed Hill Shear with the main ore zone, producing a localized high-grade shoot. Diagram oriented to local grid (from Hadlow, 1990)

Rubicon mine geological setting

Stratigraphy

The stratigraphy preserved at Rubicon (Table 1) represents a transition from mafic volcanism to sedimentation and felsic–intermediate volcanism. Formations exposed in the mine include the Bent Tree and Victorious Basalts of the Grants Patch Group, and the Centenary Shale and Spargoville Formation turbidites of the Black Flag Group. Strata of intermediate composition present in the Spargoville Formation are interpreted as crystal and lapilli tuffs since they grade into adjacent metasedimentary rocks. Major bedding contacts dip steeply to the west (Fig. 6), indicating that the stratigraphic sequence is slightly overturned, with Victorious Basalt geometrically overlying the Black Flag succession.

Bent Tree Basalt

The Bent Tree Basalt is not well exposed in the mine, but is present in the upper reaches of the western wall of the pit. The contact with Victorious Basalt is planar and intensely sheared, locally with dismembered slices of the Centenary Shale (also known as K2 black shale horizon) along the contact. The Bent Tree Basalt is massive, pillowed tholeiitic basalt that is locally doleritic with flow layering.

Table 1. Stratigraphic correlation of rock successions across tectonostratigraphic domains of the Kalgoorlie Terrane (modified from Swager et al., 1990). The red boxes show the sections of regional stratigraphy from Ora Banda and Coolgardie Domains exposed in the Rubicon mine

Stratigraphic succession	Characteristic rock types	Ora Banda Domain	Kambalda Domain	Coolgardie Domain	Boorara Domain
Polymictic conglomerate unit	Polymictic conglomerate, immature sandstone: coarse trough cross beds, graded beds	Kurrawang Formation	Merougil Conglomerate	Absent	Absent
Felsic volcanic and sedimentary unit	Felsic volcaniclaastic sedimentary rocks, ranging from coarse-clastic sandstone to interbedded sandstone or siltstone. Rhyolite to dacite, locally andesite; lava, tuff, agglomerate	BLACK FLAG GROUP Pipeline Andesite Orinda Sill Ora Banda Sill	BLACK FLAG GROUP Junction Dolerite Condenser Dolerite Golden Mile Dolerite Triumph Gabbro	BLACK FLAG GROUP White Flag Formation Powder Sill Spargoville Formation	Felsic unit, volcanic and sedimentary rocks
Upper basalt unit	High-Mg and tholeiitic basalt; massive, pillowed, and vesicular lavas	GRANTS PATCH GROUP Victorious Basalt Bent Tree Basalt Mt Pleasant Sill Mt Ellis Sill or Enterprise Dolerite	KALGOORLIE GROUP Paringa Basalt Defiance Dolerite Williamstown Dolerite	COOLGARDIE GROUP Absent or thin and discontinuous	Absent or thin and discontinuous
Komatiite unit	High-Mg basalt at top then thin komatiite flows with minor interflow sedimentary beds, overlying thicker komatiite flows and/or massive olivine adcumulate	LINGER AND DIE GROUP Big Dick Basalt Siberia Komatiite Walter Williams Formation	Devon Consols Basalt Kambalda Komatiite	Hampton Formation	Highway ultramafics
Lower basalt unit	Thoeliitic and high-Mg basalt flows, subaqueous	POLE GROUP Missouri Basalt Wongi Basalt	Lunnon Basalt	Golden Bar Sill Burbanks Formation Three Mile Sill	Scotia Basalt
References		Witt (1987, 1994) Gregory (1998) Harrison (1983,1984, 1987)	Roberts (1988) Woodall (1965) Langsford (1989) Cowden and Archibald (1991)	Hunter (1983)	Christie (1975) Witt (1994)

SEG8-Table1 17.08.04

Victorious Basalt

The Victorious Basalt is a distinctive regional marker unit of plagioclase-phyric tholeiitic basalt. The rock is distinguished by coarse phenocrysts of white plagioclase (up to 6 cm in diameter) in a dark basaltic groundmass (Fig. 7), and forms a uniform layer up to 100 m thick. Locally, the unit is pillowed with internal igneous flow layering. The upper contact of Victorious Basalt forms the major ore horizon in the mine. The basalt at this contact is sheared, with intense ductile strains recorded by stretched phenocrysts. Other significant shear zones throughout the unit anastomose and link with heterogeneous strain distribution. These shear zones are chlorite rich near the main lode, but contain no significant mineralization.

Centenary Shale (K2)

The Centenary Shale forms a regionally continuous unit, typically 1.5 m thick but up to 10 m thick in places (Fig. 8). The shale is a carbonaceous sedimentary horizon, locally discontinuous, that is replaced by disseminated

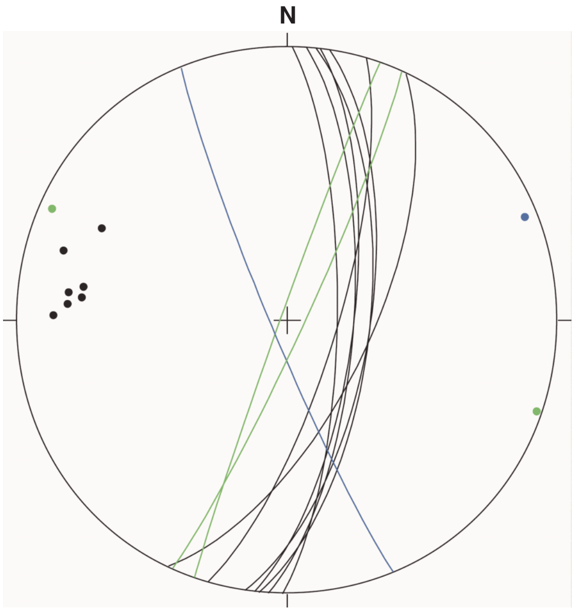

SEG8-6 12.08.04

Figure 6. Stereogram of bedding measurements at Rubicon. Black = S_0 in sedimentary rocks; green = Victorious Basalt – sedimentary rock contact; blue = Victorious Basalt – Centenary Shale contact

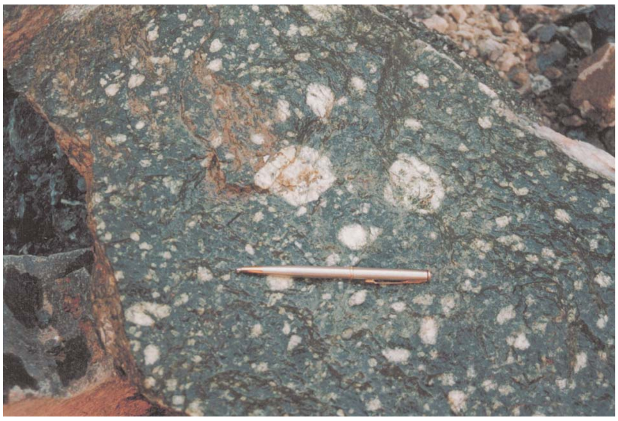

SEG8-7 12.08.04

Figure 7. Plagioclase megagrysts in porphyritic Victorious Basalt

arsenopyrite, pyrrhotite, and biotite with extensive quartz–pyrite vein emplacement, and chlorite alteration near the vein (Fig. 9).

Sections through the shale show discrete thrust faults with mesoscale hangingwall anticlines in pyritic and sedimentary layering, indicating significant thrust movement on the shale. The folds have a penetrative axial planar cleavage, and this cleavage is deformed locally by a spaced crenulation cleavage. Core intersections show layers of pyrite folded and dismembered within an intensely sheared shale matrix. Stacked cross sections show the complexly folded and sheared shale that is locally dismembered and discontinuous on the scale of tens of metres (Fig. 10). This erratic distribution must be carefully considered when extrapolating between intersections of the shale in exploration drillholes.

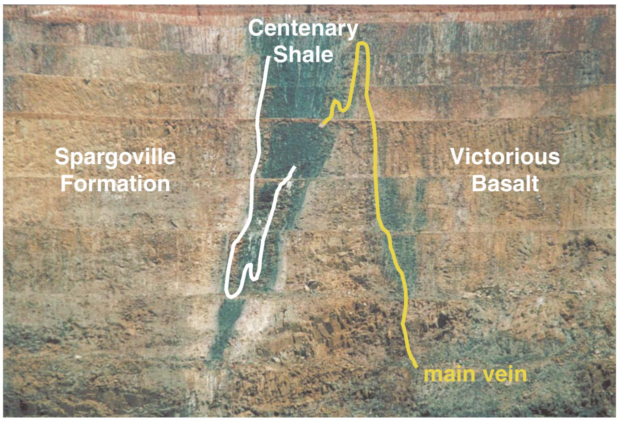

SEG8-8 13.08.04

Figure 8. Infold of Centenary Shale in the footwall of the main stratigraphic contact. The wedge of black shale is within turbidites and contains a section of folded cherty siliceous material that could include fragments of the main vein. The structure is similar to a geometry described in the South Pit by Hadlow (1990)

Spargoville Formation

Spargoville Formation rocks at Rubicon are mostly fine-grained psammopelites, now quartz–chlorite and quartz–biotite schists that are relicts of original finely bedded turbidites; the turbidites also contain rare horizons of black shale (Figs 11 and 12). Primary textures are locally preserved, with graded bedding and scour-and-fill structures. The fine grained rocks also have interbedded crystal-rich tuffs, with plagioclase–hornblende composition, that appear to be intermediate flow rocks in hand specimen, but are polymictic and gradational in contact with the psammopelites, indicating a sedimentary origin (Fig. 13).

SEG8-9 12.08.04

Figure 9. Detail of the chaotic internal structure of intensely sheared and chloritized Centenary Shale near the main vein

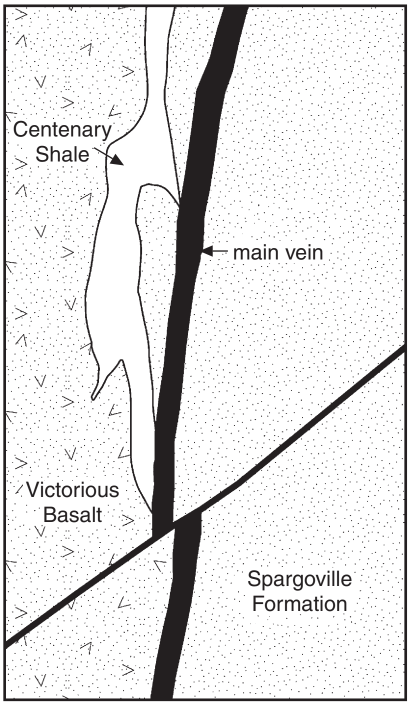

Figure 10. Schematic cross section (looking north) at 5732N (mine grid)

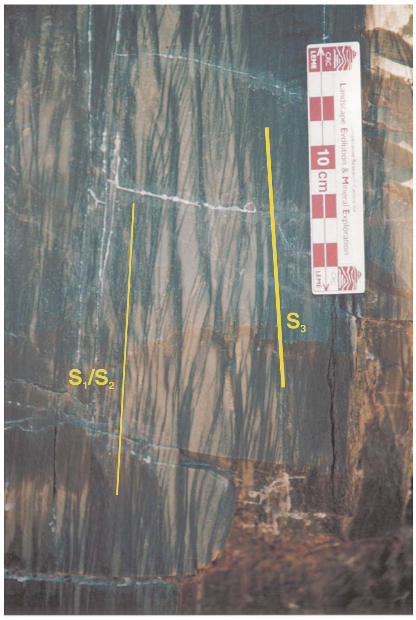

Figure 12. S_1 and S_2 fabrics display minor angular discordance, even using a hand lens, but are cut and reoriented by the S_3 shear bands, which also displace the fold limbs in S_0

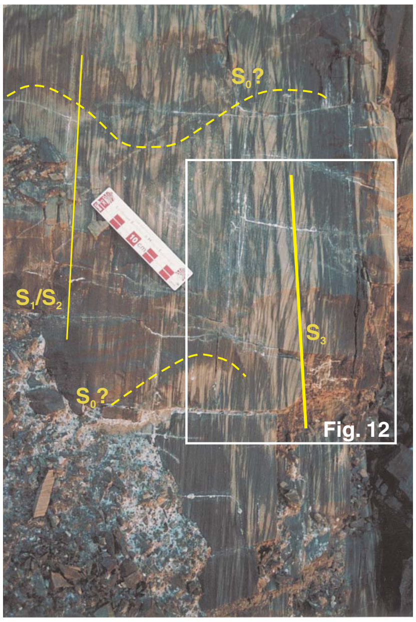

Figure 11. Cleaved metasedimentary rocks with ?bedding S_0 folded into upright folds with S_1/S_2 axial planar cleavage and a later overprinting S_3 discrete shear fabric. Bedding is defined by compositional layers in the rock, possibly remnants of quartz- and mica-rich bedding

Figure 13. Folded carbonate–quartz vein with S_1 axial planar foliation and sericite–carbonate alteration halo. Note the necking and boudinage of the vein in the limbs of the microfold. The polymictic host rock is clastic and of volcaniclastic or ?sedimentary origin; view to the south

Structural geology

Folds

Mesoscopic folds are present but poorly preserved within metasedimentary rocks near the contact with Victorious Basalt. Intrafolial, isoclinal folds indicate significant transposition of bedding into parallelism with the S_1 cleavage, indicating a high degree of shortening of the sequence. These folds, developed on a centimetre scale, are the only folds evident in the pit, with the exception of a large infold of Centenary Shale within the Spargoville Formation turbidites. Mine-scale folding is suggested by folded foliations in the southern pit wall. Cleavage–fold relationships indicate that the mesoscale folding is probably representative of the regional-scale structure.

Foliation

Two main foliations are present in the Rubicon pit. The observations below refer mainly to sedimentary rocks of the Black Flag Group, since the foliation is pervasive in these rocks. The two foliations in the sedimentary rocks are closely related in orientation but have significantly different morphologies. Discrete high-strain zones locally disturb foliations in the Victorious Basalt.

S_1–S_2

S_1 is a continuous cleavage defined by slivers of biotite or chlorite in the psammopelites (Figs 11 and 12). The foliation is penetrative at all scales and defines the gross rock structure where intensely developed, locally forming a slaty cleavage. S_2 is a discrete cleavage that overprints S_1 but, due to the closeness of orientations between the two foliations, does not crenulate S_1. The rocks have a banded appearance in areas where S_2 is well developed, which, on closer inspection, is defined by discrete laminae of biotite or chlorite spaced at about 1–5 mm, at a small angle to S_1. S_2 could represent a stronger partitioning of strain that overprints S_1. The similar orientations of S_1 and S_2 are common throughout the district (Fig. 14), but the two foliations are distinguished by their morphologies.

Shear zones

High strain zones

Several significant high-strain zones are localized within the Victorious Basalt. These zones anastomose and vary from 1 to 20 m in thickness. The shear zones trend 66°/030° on average (Fig. 15), intersecting the main ore contact at an angle of about 20°. This relationship is also observed in diamond drillcore where the immediate wallrocks of the ore zone are sheared, but the shear foliation has an angular relationship with the ore vein: the ore vein cuts the foliation (Fig. 16). These hanging- and footwall shear zones appear to control the emplacement of splay veins that are well mineralized, and their presence in the Rubicon pit where high grades are localized in the main lode is similar to a relationship observed in the South pit by Hadlow (1990).

Shear zones in the Victorious Basalt have strong, steeply north-plunging stretching lineations with an average plunge of 66°→360° defined by elongate plagioclase phenocrysts and mica films on the surface of the foliation (Fig. 17). In one exposure, the S–C fabric relationships indicate a dextral-normal movement sense on the shear zone. Veins within these shear zones are sheared and boudinaged within the ductile fabric, which wraps vein boudin terminations.

Stretched plagioclase phenocrysts have no consistent asymmetry, but are typical of a bulk flattening with ellipsoids in all XYZ sections. Towards the margins of these shear zones, lens-shaped lithons of Victorious Basalt are surrounded by intensely sheared rock as the shear zone tapers into massive basalt. Sheared zones are overprinted by a flat vein array that persists throughout the pit.

Shear vein arrays

Several shear vein arrays are mapped in the open pit (Figs 18 and 19). The arrays have classic sigmoid geometries forming stacked veins sets along a shear plane. The vein tips preserve the original opening orientation of the cracks and the direction of σ_1, but, with subsequent shearing, the central portion of the veins has been

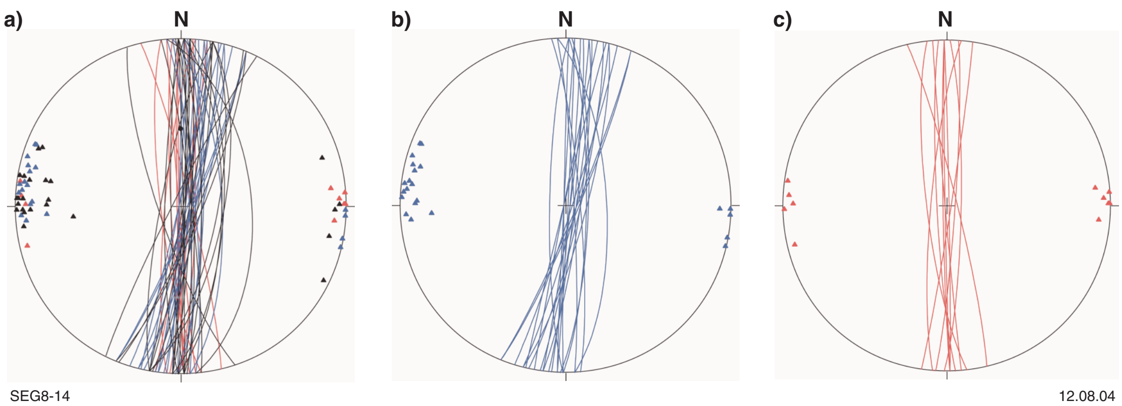

Figure 14. Stereograms showing: a) all foliations; b) S_1 penetrative cleavage; and c) S_2 spaced cleavage. Black = foliation; blue = S_1; red = S_2

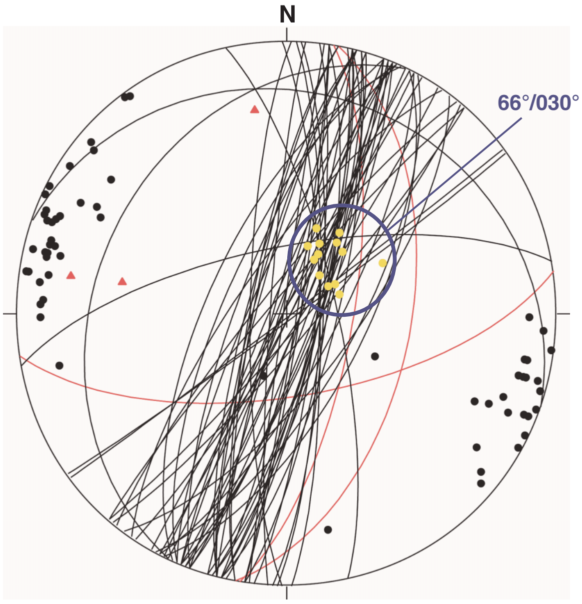

SEG8-15 12.08.04

Figure 15. Stereogram of shear zones measured in the Rubicon pit. The shear zones have a mean orientation of 84°/107°, with strong steeply northeast-plunging stretching lineations (yellow dots) that trend 66°→030° on average

progressively reoriented. Geometric analysis of shear vein arrays allows the shear sense to be determined at the time of deformation of the vein array. Shear vein arrays developed in turbidites in the footwall of the White Foil Fault display a conjugate geometry indicating formation during east–west shortening, which matches that predicted for the formation of the White Foil Fault. The veins are quartz–tourmaline–biotite–pyrite veins, with strong, narrow carbonate–muscovite alteration halos and sigmoid geometry. A small shear vein array in the hangingwall of the orebody deforms the late low-angle vein and fracture set, with a top-to-the-southeast normal shear sense (Fig. 19). This array distorts both the upright shear foliation, and flat veins that crosscut the foliation.

Cross faults

One major cross fault and several minor faults crosscut the ore horizon at high angles. The major cross fault is interpreted, from aeromagnetic imagery (Figs 2 and 20), to be the strike extension of the White Foil Fault.

The White Foil Fault is a zone of brittle–ductile deformation up to 6 m wide, with about 11 m of apparent dextral offset of the main ore horizon in plan view. Apparent offset at the mine is significantly less than the offset of stratigraphy at the camp scale, which is up to several hundred metres, and this indicates a variable displacement along the strike extent of the White Foil Fault (Fig. 2). The offset is sharp and apparently brittle, whereas internally the fault contains a ductile foliation in stretched phenocryst basalt. The mine geologist has confirmed that the fault is not mineralized, and forms a

SEG8-16 12.08.04

Figure 16. Margin of the main vein against sheared, chloritic, and pyritic Centenary Shale

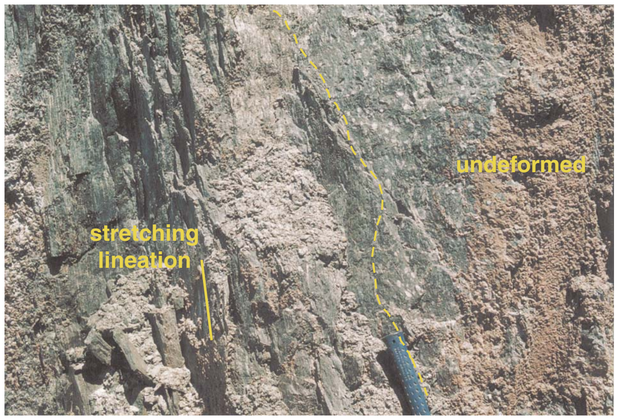

SEG8-17 13.08.04

Figure 17. Intense ductile shear zone in Victorious Basalt. Hammer handle delineates the margin of the shear zone with undeformed porphyritic basalt, showing the highly partitioned nature of the strain. A strong steeply north-pitching stretching lineation is visible on the shear surface

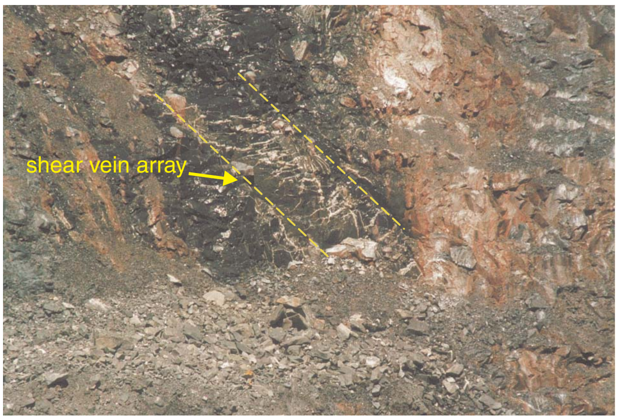

SEG8-18 13.08.04

Figure 18. Shear vein array developed in metasedimentary rocks; the veins are sigmoid in the plane of the wall, hence the view is oblique to the shear plane. The vein geometries indicate a sinistral shear sense in a subvertical plane striking 080°; view to the southeast; field of view about 5 m

SEG8-19 12.08.04

Figure 19. Shear zone deforming flat veins in the Victorious Basalt. The flat veins dip to the south, and are deformed by a shallowly north-dipping shear zone with reverse shear sense; view to the west; field of view about 3 m. The shearing could be a continuation of the same shortening event that led to vein formation

'dead zone' in the ore blocks, hence its timing is probably late with respect to mineralization.

The kinematics is difficult to determine, but the internal foliation contains a lineation pitching 55°→045° and defined by stretched plagioclase phenocrysts. This stretching lineation appears to be developed mostly on S-foliations within the fault, and may not be indicative of the movement vector. Veins and exposed C-planes of the fault have a shallowly east-pitching slickenside and mica lineations that probably indicate the true movement sense. Several cross faults oriented parallel to the White Foil Fault affect the ore. These faults have both sinistral and dextral apparent offsets in plan view, but their offsets are of the order of 1–2 m, indicating that they are not significant at the drive scale.

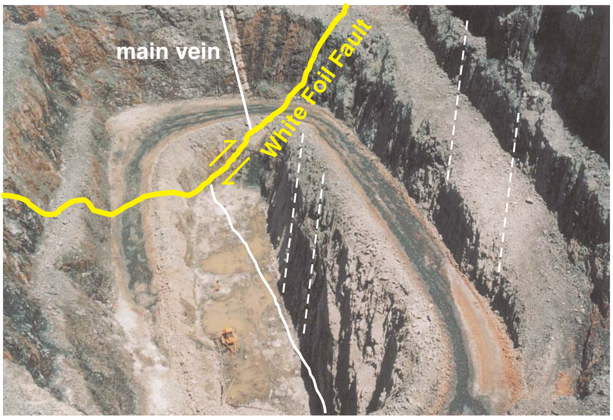

SEG8-20 13.08.04

Figure 20. Location of the White Foil Fault at the southern end of the pit. Note the angular relationship between hangingwall shear zones (delineated by white dashes) in the Victorious Basalt and the main vein

Rubicon mineralization

Main vein

The main vein at Rubicon is a laminated shear vein up to 1.2 m thick, but is generally 0.3–0.8 m in thickness (Fig. 21). The vein dips west and is locally overturned to the east, but maintains a very steep dip of 75–85° (Fig. 22). The foliation in the wallrocks is typically truncated against the vein, but in places the foliation bends into the vein with a reverse deflection sense (Fig. 16). The main vein has laminated margins, with that on the vein footwall being wider and more intense than shear laminations on the hangingwall (Fig. 23).

The ore zone comprises the vein, and mineralized footwall stockwork veins and breccia zones, producing a total width of up to 5 m (Fig. 24). Black shale in contact with the main vein is intensely altered to green chlorite with abundant disseminated, fine-grained pyrite and coarse-grained arsenopyrite. The vein contains coarse-grained disseminated galena, sphalerite, scheelite, and gold. Arsenopyrite in the vein is usually contained within black shale slices that have spalled from the wallrocks during vein formation. The sulfide species (arsenopyrite) reflects the highly reducing nature of the carbonaceous shale, rather than the presence of a distinct ore fluid.

Folding, conjugate microfaulting, and stylolitization deform laminations in the vein. In polished slabs, the gold is located along all of these microstructures, but particularly along those that disrupt laminations, indicating a late timing for gold precipitation (i.e. post vein formation).

Other veins

Several other vein sets are present in the Rubicon pit, including footwall stockwork veins, shear vein arrays, splay veins, and wallrock veins. Shear vein arrays are discussed above (see **Shear zones**).

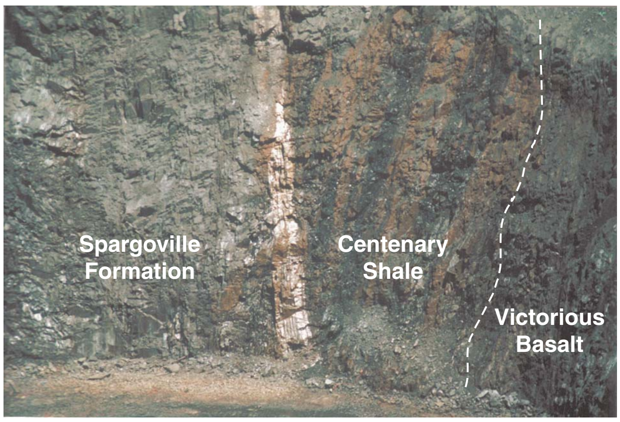

SEG8-21 13.08.04

Figure 21. Main vein at the contact between Centenary Shale and Spargoville Formation sedimentary rocks; view to the south; field of view about 10 m

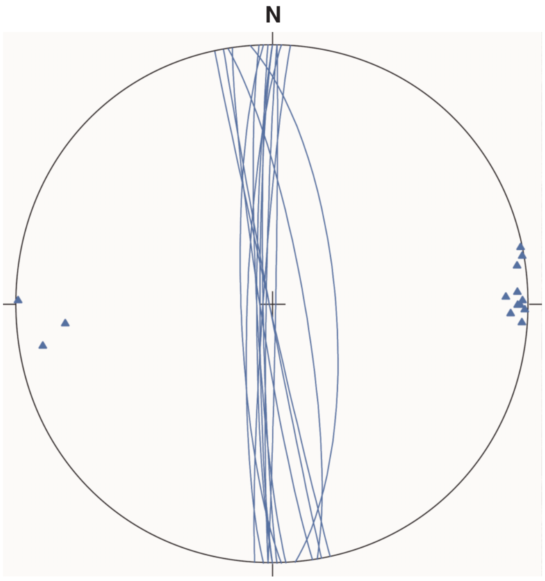

SEG8-22 12.08.04

Figure 22. Stereogram showing the steep westerly orientation of main vein contacts

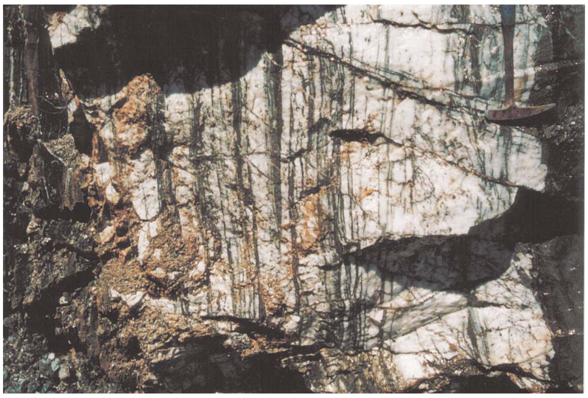

SEG8-23 12.08.04

Figure 23. Laminated main vein. The dark banding is sheared spalls from the Centenary Shale wallrocks included in the quartz vein

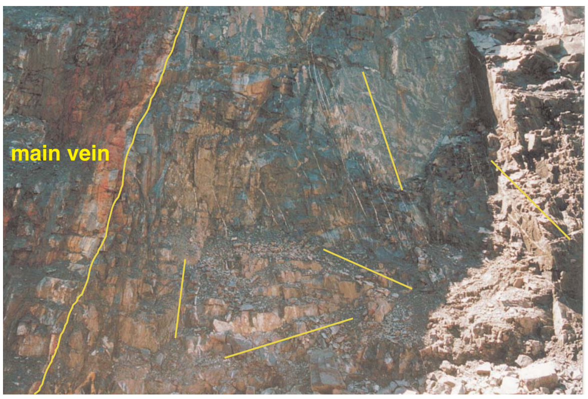

SEG8-24 13.08.04

Figure 24. Stockwork veins (delineated by yellow lines) in the footwall of the Rubicon main vein. Most veins dip steeply east with an angular discordance against the main vein; view to the north; field of view about 6 m

Stockwork veins

Stockwork veins are generally developed in the footwall of the main vein, with several well-defined average orientations (Fig. 25), and comprise crack-fill type veins (with little or no internal structure) and laminated shear veins. Footwall stockwork veins in drillhole URD044 are distributed over 25 m in three main clusters of gold-bearing veins, with a common intersection point of 14°→173° (Fig. 25).

Each cluster represents one of the three main ore-stage orientations, but the recorded veins have mineral assemblages typical of the post-ore stage veins, which are quartz–tourmaline(–actinolite). Throughout the stockwork, the highest gold grades are associated with quartz–tourmaline veins. Hence, there could be more than one phase of tourmaline vein emplacement; i.e. an early stage with gold, and a later stage postdating gold (Fig. 26).

The common intersection point of these three vein sets plunges at about 90° to the average stretching lineation of ductile shear zones in the pit. This relationship suggests that mineralization was synchronous with the shearing that disrupted the main Rubicon ore vein, and generated mineralized footwall stockworks. Such an interpretation fits with observations of the main vein being best mineralized where it is most disrupted at both macro- and microscales. Hence, stockwork formation in the footwall and mineralization was broadly synchronous with the main ore stage at Rubicon.

Flat veins

A significant array of flat veins is present in both the hanging- and footwalls of the Rubicon main vein (Figs 27

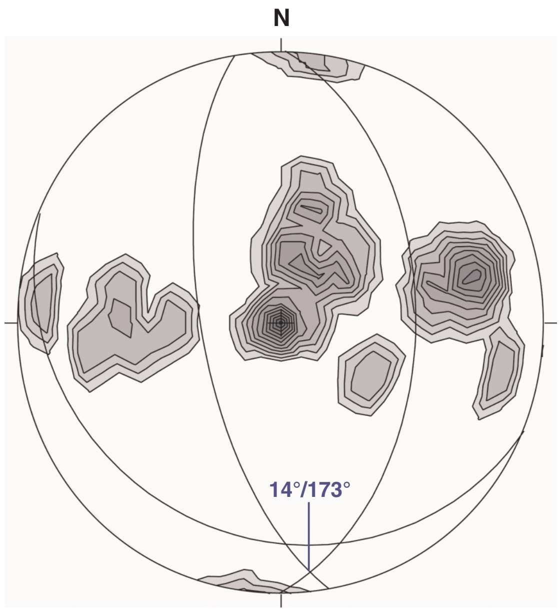

SEG8-25 12.08.04

Figure 25. Contoured stereogram of footwall stockwork veins from drillhole URD044 showing a common intersection direction of 14°→173°

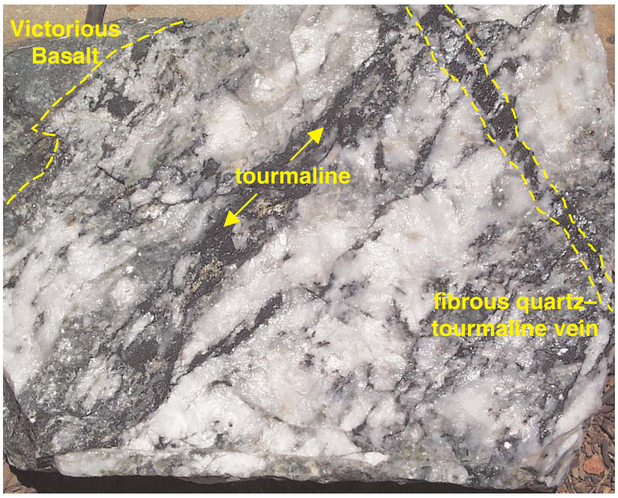

SEG8-26 13.08.04

Figure 26. Slab of main vein showing extensive tourmaline replacement of laminations, and late fibrous quartz–tourmaline veins that cut the main vein fabric at a high angle

and 28). The veins are 0.5–50 mm thick and are crack-fill type, with no evidence of crack-seal texture or lamination. Flat veins form a well-defined set dipping 22°/240°, and have a geometric relationship typical of vein systems hosted by reverse faults. These veins are part of the main ore stage generation containing quartz–tourmaline–?K-feldspar.

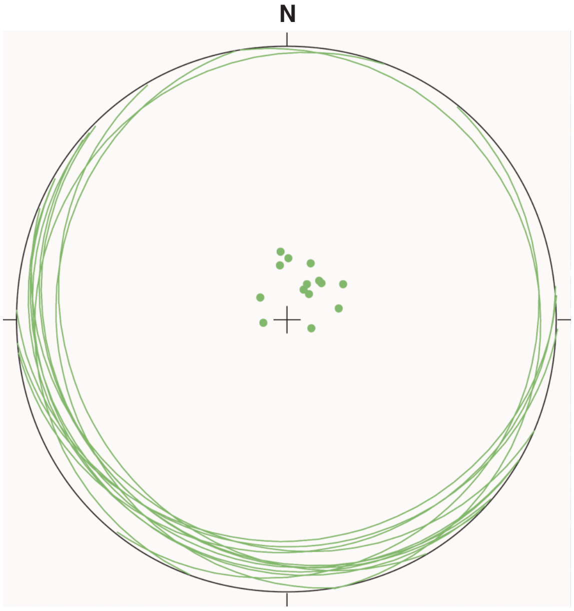

SEG8-27 12.08.04

Figure 27. Stereogram showing the shallowly southward dip of flat veins in the wallrocks of the Rubicon main vein

SEG8-28 12.08.04

Figure 28. Flat veins in Victorious Basalt, spaced at 0.5–1 m; view to the west; field of view about 10 m

Splay veins

Splay veins are developed mostly in the hangingwall of the main vein. They are shear laminated at 10–20 cm in thickness, and splay into the main vein at a small angle (10°–20°). Splay veins are well mineralized and effectively widen the ore zone over small distances.

Wallrock veins

Other wallrock veins include the many shear vein arrays throughout the pit and several thin but remarkably continuous veins that traverse the western wall within Victorious Basalt. Reports from the mining crew indicate some visible gold in these veins, but they are volumetrically minor and do not form mineable ore zones.

Summary

Having multiple vein types and orientations at Rubicon results in a situation where the main laminated vein is not the only ore zone of interest in the system. As a consequence, the ore zone is up to several metres wider than the laminated vein, particularly in areas where splay veins intersect the main vein, or where footwall stockworks are particularly dense. A shallow southerly plunge of the footwall stockwork intersection results in a subhorizontal oreshoot that should be investigated for exploration potential underground away from the main ore horizon. Exploration drilling indicates that these oreshoots have a small to moderate size (i.e. less than 80 × 80 m).

Structural timing and interpretation

The timing and paragenetic history suggest continuous regional shortening and vein deformation, punctuated by episodes of fluid overpressure. Kinematic interpretations do not indicate major reorientations of the principal shortening direction between deformation phases. It is possible that earlier formed structures were reactivated at each successive phase of regional shortening because the shortening direction was apparently consistent: this reactivation could include foliation reactivation, fold tightening, and fault or shear reactivation, and further vein deformation.

Summary and conclusions

The location of the main Rubicon ore vein was controlled by a complex sequence of events. Significant shortening of the rock sequence and deformation of the K2 black shale horizon pre-dates emplacement of the main vein. Subsequent deformation of the vein appears to coincide with the mineralization events in several stages. Strain partitioning and fabric intersection appear to be major controls on the preparation of the ore structures and subsequent location of high grade oreshoots. Cross faults have a late timing, lack gold and alteration, and probably had no significant influence on the location of the main vein.

Stratigraphic facing indicates an overall eastward-younging, slightly overturned sequence in the Rubicon pit. The Victorious and Bent Tree Basalts are significantly thinner in this exposure than elsewhere in the Ora Banda Domain: thin stratigraphic units could reflect structural thinning or original unit thickness at the basin margin. Infolded black shale and chert structures are common in the location of ore zones along the K2 horizon. These infolds appear to coincide with the intersection of high strain zones in the wallrocks with the K2 horizon. It is unclear whether the infolds are produced by strain partitioning in areas where rigid chert bands are present along the K2, or at the shear intersections. Alternatively, the shear zones could have been localized where the infolds cause perturbations in the regional strain field. It is possible that these structures were also instrumental in localizing the later cross faults.

References

CHRISTIE, D., 1975, Scotia nickel sulphide deposit, *in* Economic geology of Australia and Papua New Guinea *edited by* C. L. KNIGHT: The Australasian Institute of Mining and Metallurgy, Monograph 5, v. 1, p. 121–124.

GOLEBY, B. R., BELL, B., KORSCH, R. J., SORJONEN-WARD, P., GROENEWALD, P. B., WYCHE, S., BATEMAN, R., FOMIN, T., WITT, W., WALSH, J., DRUMMOND, B. J., and OWEN, A. J., 2000, Crustal structure and fluid flow in the Eastern Goldfields, Western Australia: Australian Geological Survey Organisation, Record 2000/34, 109p.

GREGORY, M. J., 1998, The geochemistry and petrology of the Enterprise dolerite, Ora Banda, Western Australia: University of Melbourne, BSc thesis (unpublished).

HADLOW, H. R., 1990, Structural controls on mineralization in the Kundana South Pit, Coolgardie Goldfield, WA: The University of Western Australia, MSc (Prelim) thesis (unpublished).

HARRISON, N. M., 1983, Report no. OB17: Geochemistry of the basaltic greenstones and lodes, Gimlet South and Victorious mine areas, Ora Banda Western Australia: BHP Minerals Division Exploration Department (unpublished).

HARRISON, N. M., 1984, Report no. OB52: The influence of volcanic stratigraphy and chemistry on the development of lodes in the basalts and porphyritic basalts at Ora Banda, Western Australia: BHP Minerals Division Exploration Department (unpublished).

HARRISON, N. M., 1987, Report no. OB146: Structural observations on mines and projects in the Ora Banda region and interpretation of the regional controls of gold mineralisation: BHP Minerals Division Exploration Department (unpublished).

HUNTER, W. M., 1993, Geology of the granite–greenstone terrane of the Kalgoorlie and Yilmia 1:100 000 sheets, Western Australia: Western Australia Geological Survey, Report 35, 80p.

LANGSFORD, N., 1989, The stratigraphy of Locations 48 and 50, *in* The 1989 Kalgoorlie Gold Workshops (field volume) *edited by* I. M. GLACKEN: The Australasian Institute of Mining and Metallurgy, Annual Conference and Eastern Goldfields Geological Discussion Group, Kalgoorlie, W.A., 1989, p. B1–B8.

LEA, J. R., 1998, Kundana gold deposits, *in* Geology of Australian and Papua New Guinean mineral deposits *edited by* D. A. BERKMAN and D. H. MacKENZIE: The Australasian Institute of Mining and Metallurgy, Monograph 22, p. 207–210.

ROBERT, F., POULSEN, K. H., and DUBÉ, B., 1994, Structural analysis of lode gold deposits in deformed terranes: Geological Survey of Canada, Open File Report, no. 2850, 140p.

ROBERTS, D., 1988, Kambalda – St Ives area and the Victory–Defiance complex, *in* Western Australia gold deposits, Bicentennial Gold 88 Excursion Guide Book *edited by* D. I. GROVES, M. E. BARLEY, S. E. HO, and G. M. F. HOPKINS: Geology Department and Extension Service, The University of Western Australia, Publication, no. 14, p. 109–113.

SIBSON, R. H., 1987, Earthquake rupturing as a mineralizing agent in hydrothermal systems: Geology, v. 15, p. 701–704.

SWAGER, C. P., GRIFFIN, T. J., WITT, W. K., WYCHE, S., AHMAT, A. L., HUNTER, W. M., and McGOLDRICK, P. J., 1990, Geology of the Archaean Kalgoorlie Terrane — an explanatory note: Western Australia Geological Survey, Report 48, 26p.

WITT, W. K., 1987, Stratigraphy and layered mafic/ultramafic intrusions of the Ora Banda sequence, Bardoc 1:100 000 sheet, Eastern Goldfields, *in* The Second Eastern Goldfields Geological Field Conference, Abstracts and Excursion Guide, 1987 *edited by* W. K. WITT and C. P. SWAGER: Perth, Western Australia, Geological Society of Australia (Western Australian Division), p. 49–63.

WITT, W. K., 1994, Geology of the Bardoc 1:100 000 sheet: Western Australia Geological Survey, Record 1990/14, 50p.

WOODALL, R. W., 1965, Structure of the Kalgoorlie Goldfield, *in* Geology of Australian ore deposits *edited by* J. McANDREW: Melbourne, Victoria, 8th Commonwealth Mining and Metallurgical Congress, and The Australasian Institute for Mining and Metallurgy, p. 71–79.

The Joe Lord Core Library — a valuable resource for mineral exploration

by

P. B. Groenewald[1]

Introduction

The Geological Survey of Western Australia (GSWA) focuses on the provision of high-quality pre-competitive geoscience information for the mineral and petroleum exploration industries. GSWA is principally a field-based organization producing regional geological maps and associated GIS databases. Geophysical surveys are carried out to complement this work, commonly in collaboration with Geoscience Australia, and include airborne magnetic and radiometric surveys, as well as some gravity and seismic projects.

Recent regional mapping programs have covered the granite–greenstone terranes of the Pilbara Craton, the northern part of the Southern Cross granite–greenstone terrane, and the Earaheedy Basin, and current projects include the eastern margins of the Yilgarn Craton, the Capricorn Orogen, and the western Musgrave Complex. Mapping projects in the Murchison and Tanami areas are scheduled to commence in 2004–05. Geological information and associated data are now largely delivered in GIS format, as illustrated by the East Yilgarn 1:100 000 Geological Information Series, which provides seamless geological coverage for over 150 000 km^2 and includes outcrop geology, mineral deposit data, and available satellite and geophysical imagery. Many publications and datasets are now delivered over the internet via the Department of Industry and Resources' website at www.doir.wa.gov.au/gswa/onlinepublications.

Kalgoorlie Regional Office

The Kalgoorlie Regional Office of GSWA consists of the base for five regional mapping geologists and the Joe Lord Core Library. Mapping in the Eastern Goldfields is currently focused on the southeastern margin of the Archaean Yilgarn Craton, a little-explored area of some 15 000km^2 considered to be prospective for gold mineralization. Metamorphosed sedimentary and mafic to felsic volcanic rocks occur in greenstone belts, which occupy more than 10% of this area. The rocks have undergone several periods of Archaean deformation and additional reworking during the Proterozoic Albany–Fraser Orogeny.

Over the next few years, the mapping coverage will be extended to the northeastern limits of the Yilgarn Craton in the Yamarna area, and to the nickel-rich greenstone belts south of Southern Cross and in the Lake Johnston area. The Yamarna area is of particular interest for gold exploration following identification, in a recent deep crustal seismic survey, of structures similar to those associated with major gold deposits elsewhere in the region. Detailed mapping and structural interpretation will assist in highlighting the prospectivity of this area.

The Kalgoorlie office also provides valuable support to the exploration industry in the Eastern Goldfields. A copy of the entire database of open file statutory exploration reports is held in the office, allowing explorers to access the complete exploration history of all mineral tenements in the area.

Joe Lord Core Library

The 1997–98 Western Australian Government initiative to support the mineral and petroleum industries specifically recognized the need to commence systematic collection and curation of a representative suite of mineral exploration drillcore, and to provide facilities for industry geologists to view this material. It was also recognized that access to such a resource would encourage research that would, in turn, enhance exploration and, ultimately, improve the rate of discovery and development of the State's mineral resources. Funding was provided to construct core libraries at Kalgoorlie and Perth.

The core libraries are intended to store 2 to 5% of the 500 000 metres of core drilled each year in Western Australia, and will initially house core selected over the next ten to 15 years. They have been built with provision for expansion to house a further 15 to 30 years of collection. The success of these archival facilities relies on the selection of drillcore that is valuable, in the broadest sense, to the minerals and exploration industries. In order

[1] Geological Survey of Western Australia, Kalgoorlie Regional Office, Post Office Box 1664, Kalgoorlie, W.A. 6430, Australia

to best promote the mineral prospectivity of Western Australia, the core selected for archiving includes the following:

- significant mineral deposits;
- the range of mineral commodities, styles of mineralization, and tectonic settings;
- the geographical distribution of deposits throughout the State;
- localities that could be difficult or expensive to redrill in the future;
- excellent examples of local stratigraphy, significant structural features, or unusual geological features;
- occurrences that have provided type localities for exploration models.

Since opening in July 2000, the Joe Lord Core Library has accumulated more than 110 km of diamond drillcore. This includes 40 km of groundbreaking discovery holes, and heritage minesite holes providing physical records of deposits, such as the Golden Mile, that have been otherwise obliterated through mining. Geologists who take advantage of the facility include those embarking on new exploration ventures and those involved in research projects. It is also useful to universities and high schools for educational purposes, and companies send new staff to examine drillcore that provides fresh examples of the rock types present in their exploration areas.

The drillcore available for inspection at the Joe Lord Core Library during this field excursion is listed below.

Nickel

Kambalda (KD1) — this is the discovery hole that started the Australian nickel boom. It was drilled in December 1965 near the Red Hill gold mine to investigate the nature of sulfides below gossanous outcrops. The massive sulfide body intersected in the hole returned an assay of 8.3% nickel over 2.75 m and was later called the Lunnon shoot.

Silver Swan (SUD821) — this was drilled underground to provide a complete section through the high-grade massive sulfides at the Silver Swan mine. The drillhole was collared in footwall metamorphosed felsic volcanic rocks, and passes through the entire orebody in an area where grades are typically 14–16% Ni. The core exhibits excellent examples of typical massive sulfide textures and mineralogy.

Mount Clifford (MCD408) — this exploration drillhole provides an excellent example of the spinifex and cumulate textures in ultramafic komatiitic lavas associated with the Mount Clifford nickel sulfide mineralization. The Mount Clifford deposit, some 300 km north of Kalgoorlie, comprises several small lenses of high-grade blebby nickel sulfides.

Bulong Ni laterite — the laterite deposits at Bulong comprise over 40 million tonnes containing some 500 000 tonnes of nickel and 38 000 tonnes of cobalt. The core provides a typical profile through the deposit.

Gold

Birthday South (PRD0076) — this core provides a rare record of the Golden Mile, showing the dilational breccias and lode alteration style typical of this major gold deposit.

Binduli (CD28) — this 120 m-long drillhole at Binduli intersected the basal contact to the uppermost metaconglomerate where it overlies metamorphosed felsic epiclastic sedimentary rocks. Quartz veins with abundant gold are present between 60 and 105 m in a variety of structures.

Kanowna Belle (KDU 0058) — this is a representative section through the main host rocks to the gold mineralization at the Kanowna Belle mine, a metamorphosed fine-grained porphyritic intrusion of granodioritic composition, and the surrounding metamorphosed felsic volcaniclastic sedimentary rocks.

Thunderbox gold and Waterloo nickel deposits

by

M. Bennett[1]

Abstract

The Thunderbox gold mine and Waterloo nickel deposit are owned by LionOre Australia, a wholly owned subsidiary of LionOre Mining International. The Thunderbox gold mine was discovered in 1999 and began production in late 2002. It is a blind deposit, being concealed beneath a 25 m-thick sequence of lateritized Tertiary sediments, and has no obvious surface geochemical signature or direct geophysical signature. It is a largely porphyry-hosted mesothermal lode gold deposit, which is currently being mined by openpit methods. The resource comprises 27.8 Mt grading 2.25 g/t gold for more than 2 million contained ounces, and is open at depth beneath the present limit of drilling. It is an atypical mesothermal gold deposit in several ways. Firstly, it is a wide, evenly mineralized deposit rather than a constrained lode style deposit, which is largely due to the shape and rheology of the dacite porphyry host rock. Secondly, it appears to be situated in a major first-order shear zone rather than a second- or third-order structure. Thirdly, many features of the deposit suggest that mineralization was emplaced in multiple incremental episodes over a protracted period, commencing relatively early in the tectonothermal history of the district. These features have implications for models of the formation of mesothermal gold deposits, and the targeting methodologies used in the search for them. The lack of an obvious geophysical and surface geochemical signature at the project–prospect scale also has implications for the methodologies selected at the exploration stage.

The Waterloo nickel deposit was discovered in early 2002 within 5 km of the Thunderbox gold deposit, and is currently at a pre-feasibility stage. Waterloo is a komatiite-hosted magmatic nickel sulfide deposit comprising largely intact matrix and disseminated sulfides, together with local structurally remobilized massive sulfides within a serpentinized olivine mesocumulate or peridotitic ultramafic flow. It is similar in many respects to other komatiitic nickel sulfide deposits in the Archaean Yilgarn Craton of Western Australia, but is unusual in that it does not occur at the basal part of the ultramafic sequence, and it is situated to the east of the Perseverance Fault, a structure previously believed to mark the eastern limit of nickel-prospective stratigraphy. Despite being situated in an area of outcrop, Waterloo is also a blind deposit, commencing at a depth of 100 m and plunging shallowly to the south over a strike length of 1 km. The apparent tectono-stratigraphic position of the Waterloo ultramafic rocks and mineralization, above a thick sequence of thin flow fractionated komatiites, is at variance with the classic Kambalda model, in which mineralization occurs at the base of the lowermost, most MgO-rich, flow. Although this configuration could reflect structural repetition, it shows that it is important to not be too model driven. The role of structure in the remobilization of nickel sulfide deposits has also been overlooked, largely because of the emphasis previously placed on volcanological controls on emplacement. The apparent stratigraphic position of Waterloo could, however, have been controlled by structure as much as volcanology and, together with the demonstrated remobilization of sulfides at a small scale within the Waterloo deposit, and the large scale detachment of sulfides to form the nearby shear-hosted Amorac deposit, this attests to the importance of a holistic approach in the development of models, targeting criteria, and exploration methodologies. The discovery of Waterloo, and Leinster-style stratigraphy, to the east of the Perseverance Fault has not only disproved the conventional wisdom used for area selection in the region, but has highlighted the potential for the discovery of further deposits in a previously unrecognized district. Finally, the discovery of Waterloo in an area of outcrop with previous drilling emphasizes the frailty of exploration, the sensitivity of the outcome to the methodology and mentality of the explorer, and the potential for finding more.

[1] LionOre Australia, Level 2, 10 Ord Street, West Perth, W.A. 6005, Australia

Introduction

The Thunderbox and Waterloo deposits are located about 700 km northeast of Perth and 300 km north of Kalgoorlie, adjacent to the Goldfields Highway some 40 km south of the township of Leinster (Bennett, 2003a). Both deposits are blind, with Thunderbox being concealed by a 25 m-thick lateritized Tertiary sedimentary cover sequence and recent alluvium, and Waterloo commencing at a depth of 100 m in an area of subcropping rock covered by a veneer of windblown sands derived from granite.

Thunderbox was discovered in 1999 through reconnaissance rotary air blast (RAB) drilling of a prospective trend concealed by lateritized Tertiary sediments and recent alluvium. The deposit comprises a resource of 27.8 Mt grading 2.25 g/t Au for more than 2 million contained ounces, and is open at depth beneath the present limit of drilling. Openpit mining commenced in 2002, with about 213 000 ounces of gold being produced in the first full year of production in 2003. The ore is processed through a conventional carbon-in-leach and carbon-in-pulp (CIL/CIP) plant at a nominal rate of 2.5 Mtpa for oxide ore and 2 Mtpa for primary ore. The openpit has an expected life of five years, and options for subsequent underground mining are currently being considered.

Waterloo is also a blind deposit, and was discovered in January 2002 in the first hole of a drilling program designed to test an electromagnetic conductor associated with a gossan derived from nickel sulfide and anomalous in platinum group elements (PGE), discovered earlier by LionOre in 1998. Delineation drilling proceeded throughout 2002 and 2003, and the deposit is currently subject to a pre-feasibility study.

Thunderbox gold deposit

Discovery and resources

The Thunderbox deposit was discovered in 1999 by reconnaissance RAB drilling beneath transported cover comprising lateritized Tertiary sediments and recent alluvium (Bennett et al., 2001; Bennett and Buck, 2001). The deposit was discovered in the last two holes of a RAB drilling program designed to test an area considered to be prospective for gold on the basis of various lines of general district-scale conceptual criteria and specific local-scale empirical evidence, as follows:

- recognition of its location within the southern pinchdown of the Yandal greenstone belt;
- recognition of a major throughgoing shear system, which appears to broadly control mineralization at Mount McClure to the north and Gwalia to the south;
- recognition of the presence of a granite batholith to the west and a felsic igneous complex to the east, which appear to constrain and focus deformation at this location;
- recognition of the presence of a widespread blanket of lateritized Tertiary sediments and recent alluvial cover where previous soil sampling was unlikely to have been effective;
- the occurrence of known gold mineralization at the Double A and Goanna Patch localities some 6 km along strike to the north;
- a lack of previous exploration in the immediate area, other than a single reconnaissance RAB traverse drilled some two years earlier;
- the presence of deep weathering and intense shearing in these RAB holes, indicating the presence of a major structure;
- the presence of coincident saprolitic gold and arsenic anomalism in one of these RAB holes, with one 4 m composite sample grading 1.4 g/t Au.

The weight of evidence was considered sufficiently compelling to drill two additional RAB traverses some 400 m to the north and 400 m south of the original reconnaissance traverse. The last two holes of this program (LWDR411 and 412), on the end of the northern traverse, proved to be the discovery holes by intersecting significant mineralization in what is now termed Zone A of the deposit. Key intercepts included 4 m at 11.7 g/t Au from 20 m and 5 m at 8.28 g/t Au from 47 m in LWDR411, and 4 m at 5.68 g/t Au from 69 m and 10 m at 4.93 g/t Au from 88 m in LWDR412. Mineralization was strongly associated with a visually distinctive yellowish-brown clay containing fragments of laminated silica and goethitic gossan, which appeared to be a weathered silica–sulfide-altered rock.

Three reverse circulation (RC) drillholes (LWDC025–027) were subsequently drilled to verify the RAB results, and determine the geometry and dip of mineralization. The deepest of these holes intersected fresh mineralization in the form of silica–arsenopyrite hydrothermal alteration. This was followed by several stages of RAB drilling along strike to scope out the strike extent of the oxide mineralization, which delimited Zone A to a strike length of 400 m (in the depth penetration range of RAB) and identified a minor zone (Zone B) to the north of Zone A. The last hole of this program (LWDR438) intersected the southern end of what is now termed Zone C. Intersections in this hole included 10 m at 4.19 g/t Au and 14 m at 2.4 g/t Au to the end of the hole. Subsequent RAB drilling confirmed the overall magnitude of Zone C, with wide zones of the distinctive goethitic clay being intersected. These zones, which are now known to be the main oxide ore position over Zone C, typically returned intersections of 40–70 m at 2–5 g/t Au in 80 × 40 m spaced drillholes over a 400 m strike length.

A major program of RC and diamond delineation drilling commenced in October 1999, and has since confirmed the internal integrity and downdip continuity of the deposit. The resource remains open at depth beneath the limit of drilling, some 400 m below surface.

Geological setting

The Thunderbox deposit is situated at the extreme southern end of the Yandal greenstone belt, in an area where several major intra-greenstone shear zones converge and join with the Perseverance Fault. This shear system continues south beyond the pinchout of the Yandal greenstone belt to the Leonora district, where it is associated with other major gold deposits such as Tarmoola and the Gwalia camp. The

Thunderbox Shear Zone forms the western boundary of this shear system and appears to be a major geological discontinuity, defining the boundary between two distinct geological domains:

- the Perseverance domain to the west, which is contiguous with the Wiluna – Mount Keith – Leinster – Mount Clifford sequence and characterized by classic deformed ultramafic- and mafic-dominated greenstone stratigraphy intruded by granitoid plutons;
- the Teutonic domain to the east, dominated by sedimentary rocks, bimodal felsic–mafic volcanic rocks and felsic intrusive complexes, and the Teutonic Bore volcanic-hosted massive sulfide (VHMS) prospective stratigraphy.

Geology

The Thunderbox deposit is a mesothermal lode gold deposit hosted largely within a thick lens of porphyritic dacite in the immediate hangingwall of a major shear zone, which is offset by late north-northeasterly striking faults displaying an apparent dextral displacement. The mineralization is strongly hostrock controlled and is coplanar with highly deformed stratigraphy, which strikes north-northwesterly and dips 70–75° to the west (Fig. 1). The deposit comprises two main mineralized zones, termed A and C, which are currently interpreted to be separated and offset by a late north-northeasterly fault. The bulk of the known mineralization occurs within Zone C, which has true widths of up to 75 m, a surface strike length of about 400 m, and plunges to the south. Zone A is narrower, having a true width of up to 25 m, but also has a strike length of about 400 m and plunges to the south.

The deposit is blind, being truncated by an unconformity that probably represents a Permian glacial peneplain, which is completely concealed by a 20–30 m-thick sequence of Tertiary sediments. The cover sequence comprises a mixture of quartz gravels, smectitic lacustrine clays, locally derived colluvium, and alluvial channel fills of unconsolidated ferruginous gravel. The entire Tertiary cover sequence, together with the uppermost parts of the Archaean basement, has been deeply lateritized and is, in turn, covered by a veneer of active alluvial sheetwash containing a surficial ferricrete layer known locally as Wiluna hardpan.

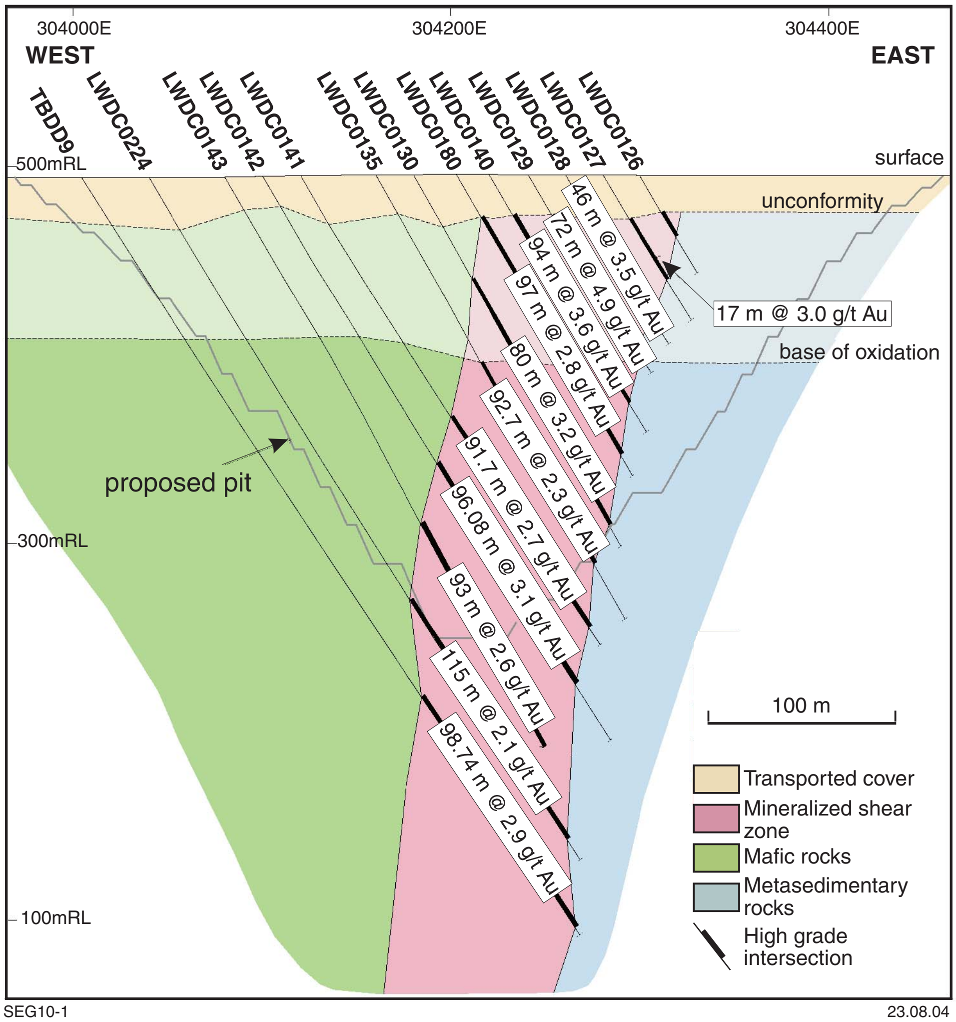

Figure 1. Cross section of the Thunderbox deposit at 6879880N showing simplified geology and mineralization, and location of drillholes

Mine tectono-stratigraphy

The footwall sequence comprises a relatively undeformed, upright facing, thick sequence of thinly bedded quartz to lithic wackes and epiclastic rocks. The footwall sequence is separated from the mineralized porphyry by a major steeply west-dipping shear zone occupied by an intensely foliated and crenulated chlorite–tremolite–carbonate–talc rock, which contains tectonic clasts of the mineralization itself. This unit is an intensely deformed and carbonated ultramafic rock, which appears to have acted as a preferential glide plane and fluid conduit during deformation. The presence of mineralized porphyry clasts within this shear zone indicates that movement, at least in part, postdates mineralization.

Mineralization is largely hosted within a well defined, intensely altered, and strongly deformed porphyritic dacite, which is currently interpreted to be a high level intrusion. Rare relict primary igneous fabrics comprise quartz, plagioclase, K-feldspar, and hornblende phenocrysts in a fine-grained quartzofeldspathic groundmass. The porphyry is, however, pervasively altered and severely deformed, exhibiting a variety of superimposed brittle and ductile deformation styles that vary locally from mylonitic, cataclastic, hydraulically brecciated, quartz veined, to folded, and are largely coplanar with the enclosing tectono-stratigraphic sequence.

Key structural features of the mineralization and adjacent rocks in the hangingwall sequence include the occurrence of two westerly dipping foliations, subhorizontal extensional veinlets, and south-plunging mineral stretching lineations, intersection lineations, and fold axes. These features are mutually consistent and suggest stretching along shallowly south-southeast-plunging fold axes, which could have formed by drag folding in the immediate hangingwall of a steep reverse shear system. This folding is also locally evident in the mineralization itself.

An unusual banded rock fringes the margins of the mineralized porphyry, and appears to be a tectonically hybridized rock comprising layers of altered porphyry, basalt, ultramafic rock, and wacke. The banded rock is modestly mineralized and is thickest along strike and downdip of the terminations of the main porphyry, where it interleaves with the porphyry. The configuration of the hybrid rock at hand specimen and deposit scales strongly suggests its derivation by tectonic transposition of various rock types, and that it has been squeezed into pressure shadows around the terminations of the relatively rigid, dacite porphyry body.

The hangingwall sequence comprises a thick sequence of strongly foliated chlorite-altered and calcite-veined basalts, which exhibit intense ductile deformation characteristics. The calcite veins in the hangingwall basalts are relatively early and have been transposed into the foliation. Petrographic studies (Du Puy, 2003) indicate that the basalt contains traces of a prograde hornblende–plagioclase–chlorite–calcite–ilmenite assemblage largely overprinted by a retrograde chlorite–quartz–albite–epidote–ankerite assemblage. Fluid inclusion studies (Du Puy, 2003) suggest a peak metamorphic temperature of 500 ± 50°C, close to the greenschist–amphibolite facies boundary.

The entire sequence is also dismembered by a series of later northeasterly to north-northeasterly striking faults, and is transected by an east–west joint set. Some of these joints have been intruded by late lamprophyre dykes, further suggesting that the shear zone is a deep crustal feature.

Mineralization

Beneath the unconformity, the deposit comprises an oxide zone, which extends downwards from the base of the cover sequence to a vertical depth of about 70 m, and a transitional zone, which extends to a vertical depth of 100 m. The oxide mineralization comprises orange-brown clays, which contain abundant fine-grained sugary quartz derived from the weathering of silica alteration and variable proportions of laminated quartz, vein quartz, and fragments of goethitic clays and gossanous iron oxides derived from the oxidation of sulfides. There is evidence of vertical leaching and supergene enrichment within the oxide profile. This is especially marked in the centre of Zone C, where an upper pallid leached zone containing quartz ribbons overlies a goethitic ferruginous clay zone with enriched gold grades.

In the primary zone, the porphyry is pervasively altered to a silica–albite–ankerite–dolomite–arsenopyrite–pyrrhotite assemblage, which is associated with much of the gold mineralization. Gold is intimately associated with recrystallized arsenopyrite and tends to occur on the grain boundaries. Much of this alteration is also affected by subsequent increments of deformation, and some of the silica has been annealed, indicating that much of the gold pre-dates peak metamorphism and deformation, and this free gold could have exsolved from an earlier As–Fe sulfide.

There is also free gold in veinlets of various generations, particularly in association with minor sphalerite and galena. Some of these quartz veinlets are boudinaged, folded, rotated, or a combination of these, into the penetrative ductile deformation fabric, and obviously predate much of the ductile deformation. Some are laminated and coplanar with the penetrative fabric, and appear to be coeval with the main deformation. Others are undeformed and flat, clearly crosscutting the penetrative ductile fabric. The latter, together with irregularly distributed hydraulic breccia lodes, clearly postdate much of the ductile deformation.

The common occurrence of features such as early folded quartz–arsenopyrite veins, layer-parallel ductile fabrics and laminated veins, later crosscutting quartz–gold veins, intact and dismembered hydraulic breccia lodes, folding of the ore, and clasts of mineralization within the footwall ultramafic shear zone, provides substantial evidence of mineralization being emplaced and perhaps mobilized in multiple incremental episodes before, during, and after peak metamorphism and ductile deformation events.

The gold mineralization is also overprinted by a later brittle vein set comprising small irregular quartz–calcite–

chlorite–pyrrhotite veins distributed throughout the deposit, and by a later alteration assemblage characterized by the presence of euhedral pyrite that is spatially associated with the late crosscutting and offsetting brittle faults.

Geological and genetic model

The intensity and complexity of deformation within the Thunderbox Shear Zone suggests that it is a major first-order shear zone and a significant control on mineralization. At the deposit scale, the hangingwall sequence west of the shear is strongly deformed and altered, and typical of upper greenschist to lower amphibolite facies metamorphosed greenstones, and the footwall sequence east of the shear comprises relatively undeformed rythmically graded quartz- and lithic wackes and epiclastic rocks. This contrast in the degree and nature of deformation mirrors the stratigraphic contrast observed at a district scale, suggesting that it is a domain-bounding structure. The occurrence of mineralized clasts within this structure does, however, indicate that at least some of the movement on this shear zone postdates mineralization, and therefore the mineralization is either relatively early or there is significant late-stage movement on the shear zone.

The mineralization is almost entirely hosted within a large lens of porphyritic dacite in the immediate hangingwall of the shear zone. The shear zone itself, being a zone of chlorite–tremolite–carbonate–talc rock, appears to have acted as a preferential glide plane and a strain buffer between the hangingwall sequence and the undeformed footwall sequence. In contrast to the deformed ultramafic rock in the footwall shear zone and the hangingwall basalts, the porphyry host rock apparently behaved in a more brittle manner, also containing various brittle fabrics such as flat quartz vein arrays, microveining, and hydraulic brecciation, as well as relatively steeply orientated ductile fabrics.

The exact timing relationships of the various brittle and ductile events are not yet understood, but the overall abundance of steeply orientated ductile planar fabrics, together with flatter brittle planar fabrics, and shallowly plunging fold axes are consistent with deformation within a compressive tectonic regime. The presence of annealed quartz, boudinaged quartz veins, folded quartz veins, layer-parallel laminated shear veins, exsolved gold associated with pre-peak metamorphic arsenopyrite, mesoscale folding of the deposit, dismembered hydraulic breccia lodes, late-stage undeformed hydraulic breccias and veins with free gold, flat extensional quartz veins, and clasts of mineralization within the footwall ultramafic shear zone indicate that mineralization occurred over a lengthy period, commencing relatively early in the tectonic and metamorphic history of the district, and continuing beyond peak metamorphism and deformation.

Waterloo nickel deposit

Discovery and resources

The Waterloo deposit is blind and was discovered in January 2002 as a result of drilling a subtle electromagnetic (EM) anomaly associated with a serpentinized ultramafic unit containing minor nickel and copper anomalism and a nearby gossan derived from nickel sulfide (Bennett, 2003b).

The ultramafic unit and the Ni–Cu anomalism was originally identified in drilling undertaken by Seltrust in the late 1970s, but the prospective basal contact of this unit was not tested. No further nickel exploration was undertaken until 1998, when LionOre identified a nickel sulfide gossan containing 3 g/t combined PGE during geological mapping. This gossan resembles a typical lateritic ferricrete and would not have been identified if not for systematic sampling, PGE analysis, and recognition of relict violaritized pentlandite textures in polished section. It was not immediately followed up due to the nearby discovery of the Thunderbox gold deposit in 1999, and the reprioritization of work programs.

Nickel exploration recommenced in 2001 with the reinterpretation of the Seltrust data, which indicated that the ultramafic sequence contained a thick serpentinized olivine cumulate unit with localized Ni–Cu anomalism in the weathered zone of this unit. A single line of three aircore holes, drilled to test the near-surface portion of the basal contact, intersected a Ni–Cu–PGE anomalous gossan on the basal contact of the serpentinite. Subsequent moving loop and fixed loop EM surveys also identified several EM anomalies within the ultramafic stratigraphy (Mutton and Peters, in press). LionOre personnel prioritized one of the weakest EM conductors based on its position midway between the PGE-bearing nickel gossan some 300 m along strike to the south, and the Ni–Cu anomalism identified in the previous Seltrust drilling and LionOre aircore drilling some 200 m along strike to the north. The first hole was drilled in January 2002 and intersected 10.68 m of disseminated, matrix, and massive sulfides grading 5.08% Ni.

Subsequent drilling has defined a south-plunging elongate ribbon of sulfide mineralization over a strike length of >1 km associated with the lower contact of the serpentinite unit. At the northern end, mineralization is a mere 10 m below the end of one of the Seltrust drillholes, which failed to reach the lower contact. While resource definition drilling was underway at Waterloo, drilling of a second EM conductor nearby led to the discovery of the Amorac deposit. This mineralization differs in style compared with Waterloo, and is structurally controlled within an undulating planar shear zone and not associated with any appreciable ultramafic stratigraphy.

Geological setting

The Waterloo nickel deposit is situated in an area previously viewed as unprospective, and consequently relatively unexplored. It is hosted by a folded remnant of ultramafic stratigraphy located within an enclave of greenstones at the southeastern margin of the Perseverance granitoid, which is itself situated at the confluence of two dominant geological trends within the northeastern Goldfields of the Yilgarn Craton — the southern extension of the nickel-prospective Agnew–Wiluna greenstone belt and the Perseverance Fault to the west, and the southern extension of the gold-prospective Yandal greenstone belt to the east.

A major regional shear zone east of the Waterloo locality defines the boundary between the eastern edge of the Perseverance granitoid and the western edge of the Yandal greenstone belt, and controls gold mineralization at Thunderbox and associated prospects. This structure, informally termed the Thunderbox Shear Zone, is a major deformation corridor and seems to represent a fundamental boundary between mafic–ultramafic-dominated stratigraphy analogous to that of the Agnew–Wiluna belt to the west, and stratigraphy to the east that is dominated by sedimentary and felsic volcanic rocks. On the basis of the degree of deformation associated with this structure, and the broad lithostratigraphic differences either side, it is interpreted to be a domain boundary.

To the west, the geology is dominated by the Perseverance granitoid, whose western margin is defined by the Perseverance Fault, which is a constituent of the so-called Keith–Kilkenny Lineament. Further west still, on the western side of the Perseverance Fault, are structurally attenuated ultramafic units that are interpreted to represent the southerly strike continuation of the Perserverance ultramafic stratigraphy of the Agnew–Wiluna nickel belt, and which continue further south to the Marshall Pool and Mount Clifford ultramafic sequences. The Agnew–Wiluna belt is the most richly endowed nickel belt in the Yilgarn Craton, and hosts the world's largest examples of komatiite-associated nickel sulfide deposits, including Mount Keith, Yakabindie, Perseverance, Rockys Reward, and Honeymoon Well. All these deposits, and their host ultramafic and greenstone sequences, are situated west of the Perseverance Fault, which has traditionally been regarded as being a fundamental delimiter of nickel sulfide prospectivity.

Waterloo is the first nickel deposit to be discovered east of the Perseverance Fault. This, together with the similarity of the Waterloo stratigraphy to that of the Mount Keith – Leinster area, suggests that the Thunderbox Shear Zone (to the east of Waterloo) is a more fundamental domain-bounding structure than the Perseverance Fault, and therefore the Perseverance Fault does not represent the easterly limit of nickel-prospective ultramafic stratigraphy in this region.

Geology

The Waterloo deposit primarily comprises a south-plunging elongate ribbon of matrix and disseminated style sulfide mineralization situated at the lower contact of a serpentinized ultramafic cumulate unit (Figs 2 and 3). The elongate geometry is pronounced — although the mineralization has a downplunge extent of over 1 km, the massive–matrix component rarely exceeds a thickness of 2–4 m and a cross-sectional dip extent of 50 m. At the northern end of the deposit, these sulfides have been thickened (up to 15 m) in the hinge zone of a south-plunging recumbent fold in the hangingwall of a subhorizontal shear zone, which truncates the lower limits of mineralization. All measured structural fabrics (including fold axes, mineral stretching lineations, and intersection lineations) plunge to the south at the same angle as the recumbent fold axis, and the deposit as a whole. Although there is considerable evidence attesting to localized structural remobilization, overall the deposit appears to be an intact magmatic sulfide deposit situated at the base of a komatiitic lava flow.

The sulfide assemblage comprises pyrrhotite–pentlandite in the primary zone, and both minerals are variably violaritized in the supergene zone. At a broad scale, the sulfides appear to be in situ, forming a classic massive–matrix–disseminated sequence on the lower contact of the serpentinite. At a detailed scale, however, the matrix and disseminated sulfides form a metamorphic sulfide–silicate intergrowth that has an incipient foliation, suggesting centimetric scale recrystallization and remobilization. Furthermore, most of the massive sulfide zones comprise tectonic breccias containing clasts of superjacent serpentinite and subjacent dacitic volcanic footwall rock, or are tectonically banded and recrystallized lenses of massive sulfides that have been mechanically remobilized. Many of the zones are interpreted to be related to flat shear zones that locally transect and disrupt the in situ sulfides. All sulfide styles are high tenor, which translates into high grades for the massive ore (10–17% Ni), matrix ore (5–10% Ni in ore containing 40–60% sulfide), and disseminated ore (1–3% Ni). The Waterloo deposit also contains unusually high levels of copper and PGE, with the copper content commonly exceeding 0.5% and total PGE (Pt, Pd, Os, Ir, Rh, and Ru) content commonly exceeding 1–2 g/t in the sulfide intersections.

The host serpentinite unit is at least 1 km long, varies from 20 m to 100 m in thickness, and is lenticular in cross section. Although the primary igneous fabric of the rock has been totally destroyed by metamorphism, its bulk rock chemistry and mineralogy suggest that it was originally an olivine mesocumulate or peridotite.

The stratigraphy enclosing the mineralization and the serpentinite is poorly understood, but appears to comprise (from base to top):

- a thick sequence of variably silicified dacitic felsic volcanic units;
- a sequence of thin flow fractionated komatiites with locally preserved A and B zones indicating upright facing;
- a dacitic felsic volcanic unit, which forms the immediate footwall to the serpentinite and sulfide mineralization;
- the serpentinite;
- a thick hangingwall sequence dominated by pillow basalts, mafic tuffs, and epiclastic rocks with minor komatiitic interflow units.

This sequence is variably disrupted by low angle shearing and associated folding, and the footwall dacites are intruded by a poikiloblastic pyroxenite. The pyroxenite displays intrusive relationships with the surrounding rocks, is relatively undeformed, and has been retrogressively metamorphosed into a tremolite–chlorite rock, suggesting that it was intruded into the sequence after peak deformation and before later stages of metamorphism.

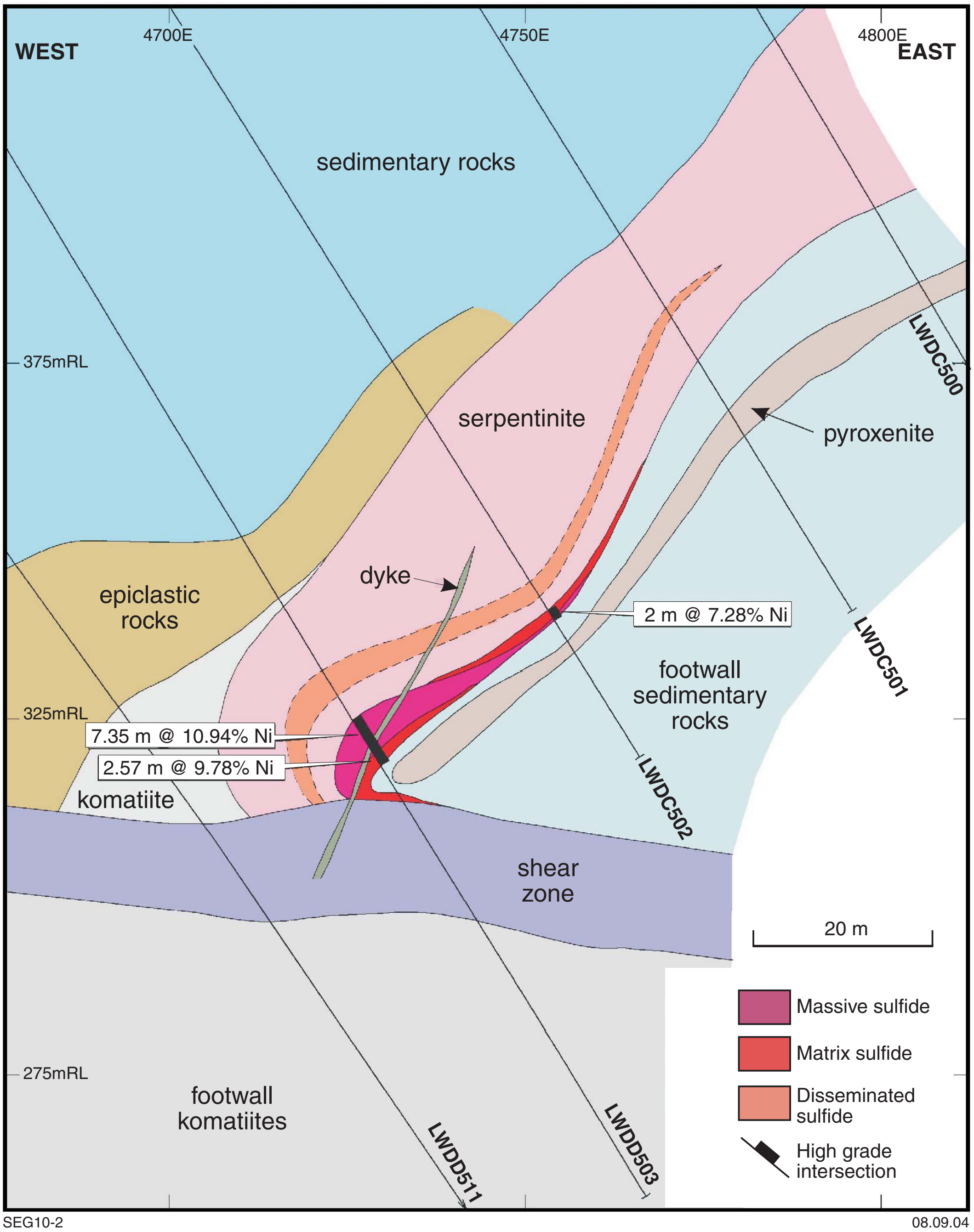

Figure 2. Cross section of the Waterloo deposit at 10020N (local mine grid) showing geology and mineralization, and location of drillholes

The position of the mineralized serpentinite above a thick sequence of thin flow fractionated komatiites apparently contradicts the classic Kambalda stratigraphic model, in which the thickest, highest MgO ultramafic flows (together with the strongest mineralization) occur at the stratigraphic base of the ultramafic sequence. It is not yet clear, however, to what extent the present apparent stratigraphic configuration reflects thrust repetition of the serpentinite over higher parts of the original stratigraphy.

Geological and genetic model

Current understanding of the geological and genetic controls on the Waterloo nickel deposit is only based on drilling data. Notwithstanding this, the current view is that:

- The Waterloo Ni–Cu–PGE mineralization formed at the basal contact of an olivine peridotite ultramafic lava erupted onto a substrate of dacitic felsic volcanic rocks, similar to elsewhere in the Mount Keith – Leinster district.

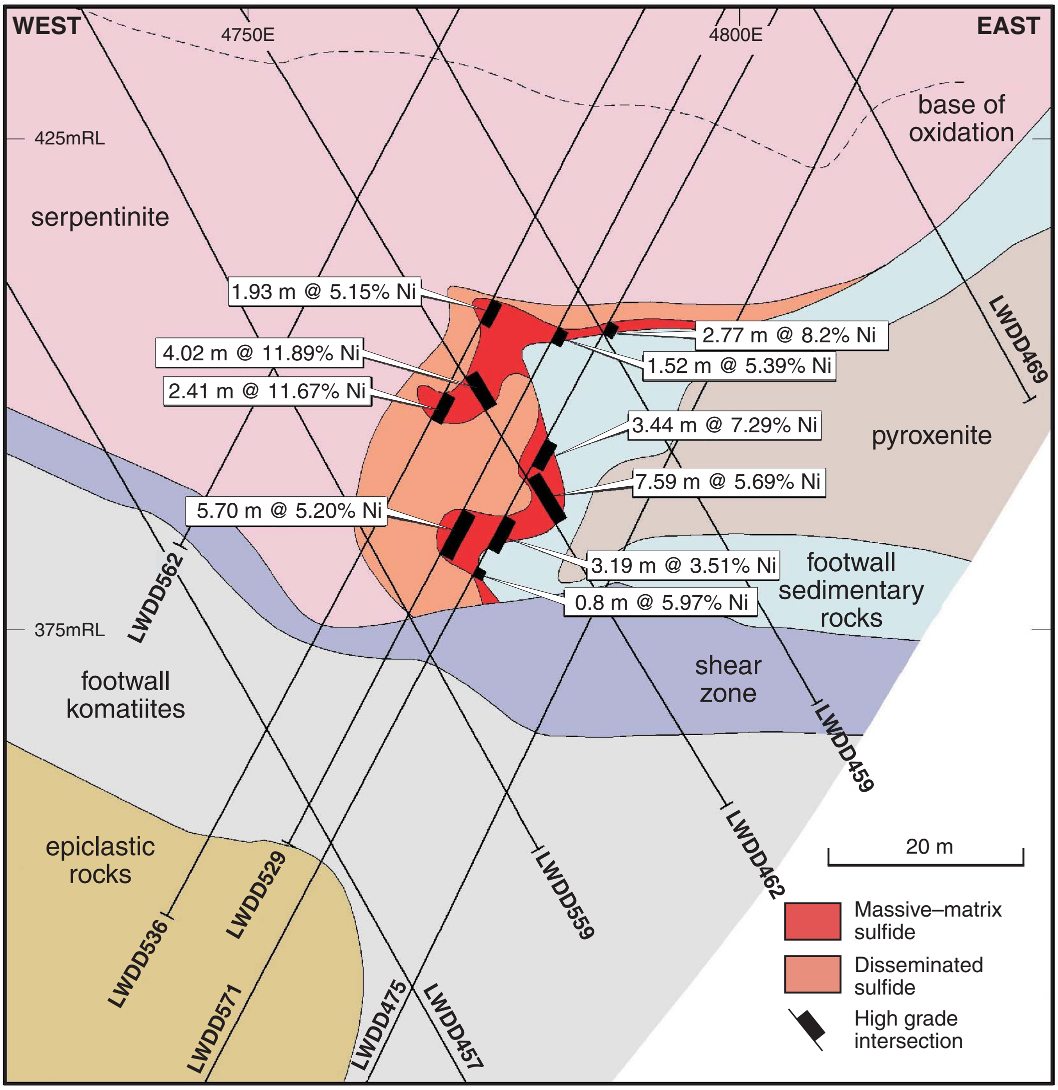

Figure 3. Cross section of the Waterloo deposit at 10340n (local mine grid) showing geology and mineralization, and location of drillholes

- This lava formed an elongate lenticular flow with relatively little high-Mg ultramafic lava occupying lateral flanking positions.
- Regional metamorphism resulted in the pervasive serpentinization and complete destruction of original igneous fabrics, and localized retrogressive talc–carbonation in this ultramafic unit.
- Ductile deformation events locally modified the geometry of the serpentinite and remobilized the sulfides, but have not greatly altered the original sulfide–hostrock relationships.
- Likewise, metamorphism modified fabrics at a small scale but has not greatly altered the original relationships. A localized exception to this is the remobilization and flushing of disseminated sulfides from the serpentinized ultramafic unit during the talc–carbonate metasomatism.
- The distribution of the mineralization and host serpentinite is mimicked by a pyroxenite, which appears to have intruded into the footwall after most of the deformation and before cessation of metamorphism. The spatial, temporal, and genetic relationship of this unit to the mineralization is enigmatic.
- The unusual position of the serpentinite above a thick sequence of thin flow fractionated komatiites suggests that the Waterloo mineralization and host flow have been thrust over the hangingwall sequence.
- The nearby Amorac deposit was structurally emplaced within a shear zone, with sulfides having been mechanically remobilized over a distance of at least several hundred metres from their parent ultramafic unit, which is as yet unidentified.

Significance of the Thunderbox gold and Waterloo nickel deposits in exploration models

Thunderbox is an atypical mesothermal gold deposit in several ways. Firstly, it is a wide, evenly mineralized deposit rather than a constrained lode style deposit, due largely to the shape and rheology of the dacite porphyry host rock. Secondly, it appears to be situated in a major first-order shear zone rather than a second- or third-order structure. Thirdly, many features of the deposit suggest that mineralization was emplaced in multiple incremental episodes over a protracted period, commencing relatively early in the tectonothermal history of the district. These features have implications for models of the formation of mesothermal gold deposits, and the targeting methodologies used in the search for them. The lack of an obvious geophysical and surface geochemical signature at the project–prospect scale also has implications for the methodologies selected at the exploration stage.

Thunderbox is one example of a number of recent discoveries such as Granny Smith, Kanowna Belle, Tarmoola, and Wallaby that, unlike most of the previously known gold deposits in the Yilgarn Craton, are not hosted by banded iron-formation (Hill 50, Mount Morgan) or differentiated mafic rocks (Golden Mile, Victory–Defiance, Junction, Wiluna). This new generation of discoveries has broadened the previous widely held belief that Fe-rich hostrocks are a critical ingredient as chemical triggers for gold deposition in hydrothermal systems in the Yilgarn. The location of Thunderbox in a major shear zone considered to be a first-order domain-bounding structure is also somewhat at odds with the conventional wisdom widely used in genetic models and targeting for mesothermal lode gold deposits. Furthermore, the features of the deposit that suggest that mineralization was emplaced in multiple increments over a long period commencing prior to peak deformation and metamorphism add weight to the growing evidence from other deposits (e.g. Golden Mile and Gwalia) that some of the Yilgarn deposits formed relatively early — a situation somewhat at odds with the continuum model of a single late-stage event. If Thunderbox is an example of an early formed deposit, and there are other early formed deposits, they will not be located using the logic developed for targeting late stage deposits, which is based on the assumption that the current structural architecture is essentially that existing at the time of gold emplacement — a so-called dilational jog in a late structure will have absolutely no bearing on the location of an early formed deposit. These observations have fundamental implications for the development of models and the application of targeting criteria.

Being concealed by lateritized sediments, the deposit does not have an obvious surface geochemical signature, which renders traditional surface-sampling techniques ineffective. It appears that even long-term stabilized, relatively thin cover can effectively render a deposit geochemically invisible. Also, being in a first-order structure, individual stratigraphic elements tend to parallel the overall structural grain and, consequently, it is very difficult to use datasets such as aeromagnetics to generate structural targets in these areas, rendering them invisible to conventional structural targeting of the sort routinely used in the Yilgarn.

Many features of the Waterloo deposit have implications for komatiite-hosted nickel sulfide exploration models, practical aspects of exploration, and exploration in the northeastern Eastern Goldfields in particular.

In a general sense, the discovery of nickel sulfides and fertile ultramafic rocks east of the Perseverance Fault attests to the high potential of an area previously disregarded, and demonstrates the danger of dogma in the process of area selection or exclusion. Also, the position of the Waterloo deposit with respect to the enclosing ultramafic stratigraphic column, demonstrates the potential for mineralization to occur at horizons other than those popularized by models such as those developed at Kambalda, irrespective of whether this is due to stratigraphic or structural processes.

Variations in the degree of remobilization within the Waterloo deposit itself, and between the Waterloo and Amorac deposits, also demonstrate the importance of a balanced, holistic approach to exploration in order to find the spectrum of deposits, ranging from intact magmatic deposits associated with the basal contacts of high-Mg ultramafic units to entirely remobilized deposits hosted by shear zones and breccia zones within genetically unrelated stratigraphic sequences. Although igneous and volcanological models are important at the area selection stage, it is vital to consider the role of deformation in the potential reconfiguration and redistribution of these deposits during the exploration stage (at the deposit scale), and subsequent evaluation (at the mining scale).

In detail, the discovery and the geology of the Waterloo deposit have also shown that:

- areally insignificant ultramafic units can be as prospective as more extensive, thicker sequences;
- previous exploration can leave vital clues;
- even densely drilled areas are not necessarily effectively explored;
- there is no substitute for mapping and systematic rockchip sampling.

Acknowledgements

This paper is the product of contributions from the geoscientists; field staff, support, and administration staff; management; and directors of LionOre. Their work has resulted in the discovery, development, and current understanding of the geology of the Thunderbox and Waterloo deposits and others yet to come. These people include Will Dox, Andy Thomspon, Mike Dunbar, Adrian McArthur, Bill Clayton, David Hutton, Neil Tomkinson, and Dann Stals. Their contributions and passion are gratefully acknowledged.

References

BENNETT, M. A., 2003a, The discovery of the Thunderbox gold mine and the Waterloo nickel deposit: AusIMM Bulletin, March/April 2003, p. 36–39.

BENNETT, M. A., 2003b, The Waterloo nickel deposit, Western Australia, *in* New frontiers in research on magmatic NiS–PGE mineralisation *edited by* W. E. STONE: Perth, Western Australia, The University of Western Australia, p. 95–101.

BENNETT, M. A., and BUCK, P. S., 2000, Discovery and geology of the Thunderbox gold deposit, Yandal Belt, *in* Yandal Greenstone Belt: Australian Institute of Geoscientists, Bulletin 32, p. 373–379.

BENNETT, M. A., BUCK, P. S., MASON, R. C, THOMPSON, A. J., DIX, W., DUNBAR, M., and CAIRNS, C., 2001, The discovery and delineation of the Thunderbox gold deposit, Western Australia *in* NewGenGold 2001, conference proceedings *edited by* K. YATES: Adelaide, South Australia, Australian Mineral Foundation, p. 185–198.

DU PUY, K., 2003, Descriptive hydrothermal alteration model for the Thunderbox gold deposit: insights into timing of gold mineralisation relative to deformation and metamorphism: The University of Western Australia, Honours thesis (unpublished).

MUTTON, P., and PETERS, W., in press, The Waterloo and Amorac nickel deposits, Western Australia: a geophysical case history: Exploration Geophysics.

Komatiite-hosted Ni–Cu–PGE deposits of the Agnew–Wiluna greenstone belt — an overview

by

S. W. Beresford[1] and N. M. Rosengren[1]

Introduction

The Agnew–Wiluna belt is an intensely mineralized Archaean greenstone belt that hosts some of the world's largest komatiite-hosted Ni–Cu(–PGE) deposits. It is a strongly attenuated greenstone belt and forms the northern third of the Norseman–Wiluna belt in the Yilgarn Craton (Fig. 1). The Agnew–Wiluna belt has an hourglass shape and four distinct domains. The northern domain is defined by the broadening of the belt near Wiluna and Honeymoon Well. The belt thins to the south parallel to the Keith–Kilkenny lineament, before widening in the Agnew and Marshall Pool – Mount Clifford areas. There is considerable variation in metamorphic grade and strain within the belt. Metamorphic grade varies from prehnite–pumpellyite facies at Wiluna to mid-amphibolite facies at Perseverance (Binns et al., 1976; Hill et al., 1990).

The Ni–Cu(–PGE) ore deposits in the Agnew–Wiluna belt have been inferred to be hosted by channelized komatiitic dunite lava flows along a corridor from 11 Mile Well to Honeymoon Well (Hill et al., 1995). The belt hosts the type areas for giant komatiitic dunite-hosted Ni–Cu(–PGE) ore deposits at Mount Keith and Perseverance (Barnes et al., 1988; Dowling and Hill, 1990). Nickel sulfide mineralization in the belt occurs as two distinct types (Barnes et al., 1999), as defined by variations in the sulfide content (disseminated versus massive) and location of sulfides (intra-unit versus basal contact). Type 1 mineralization is typified by contact massive sulfides at the base of komatiitic units (Perseverance, Cliffs, Cosmos, Waterloo, Wedgetail). Type 2 mineralization is typified by the large low-grade disseminated sulfides at Mount Keith. In the western part of the belt, the komatiitic units are barren of nickel sulfides but locally host structurally controlled mesothermal gold deposits, such as Agnew (Broome et al., 1998).

Komatiites occur in three distinct facies associations in the belt:

- komatiite – felsic volcanic rock;
- komatiite – black shale;
- komatiite–basalt.

Some of these associations are mineralized but it is unclear whether there is a relationship between mineralization and the nature and sulfide content of the footwall.

Although the komatiites in the belt are intensely mineralized, there are domains that are known to be poorly mineralized and even barren. The corridor of komatiites that extends from 11 Mile Well to Honeymoon Well is variably mineralized, but the komatiites north of Honeymoon Well are barren of nickel sulfide mineralization.

Ore deposit diversity and stratigraphic relationships

The stratigraphy and mineralization in the Agnew–Wiluna belt is best characterized by the Mount Keith area. This area is located in the most attenuated portion of the Agnew–Wiluna greenstone belt, about 80 km south of Wiluna, where it has a maximum thickness of about 6 km (Fig. 2). The belt is bound to the west and east by voluminous Archaean granitoids. The greenstone sequence in the Mount Keith area includes three ultramafic horizons, locally designated the Eastern, Central, and Western Ultramafic units (Dowling and Hill, 1990). The ultramafic horizons can be traced 30 km north of Mount Keith to the Honeymoon Well nickel deposit, and 9 km south to the Cliffs–Charterhall nickel deposit. Beyond these limits, definition of the belts is uncertain due to structural complexities.

The Western and Central Ultramafics contain well developed spinifex-textured komatiites with Kambalda-style basal accumulations of massive sulfide (Type 1) occurring sporadically at the base of the Central Ultramafic, notably in the Cliffs–Charterhall area. The Eastern Ultramafic differs substantially from the other ultramafic horizons in three fundamental respects:

1. lack of spinifex-textured komatiites that are demonstrably contiguous with and not in structural contact with cumulate rocks anywhere along its strike extent (Rosengren et al., in press);
2. presence of thick (>500 m) coarse-grained olivine

[1] Department of Earth Sciences, Monash University, Victoria 3800, Australia

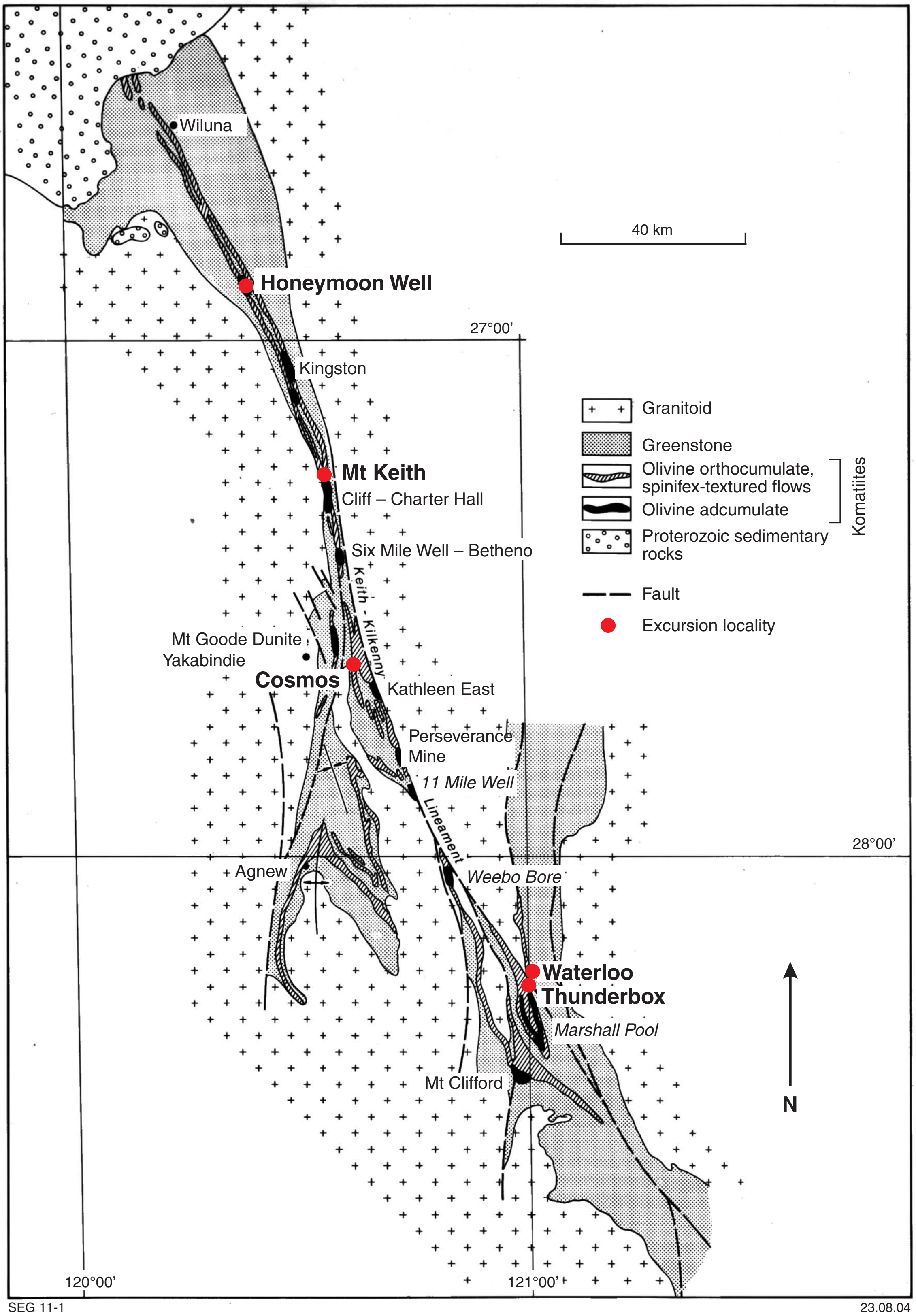

Figure 1. Geological map of the Agnew–Wiluna belt (adapted from Hill et al., 1990)

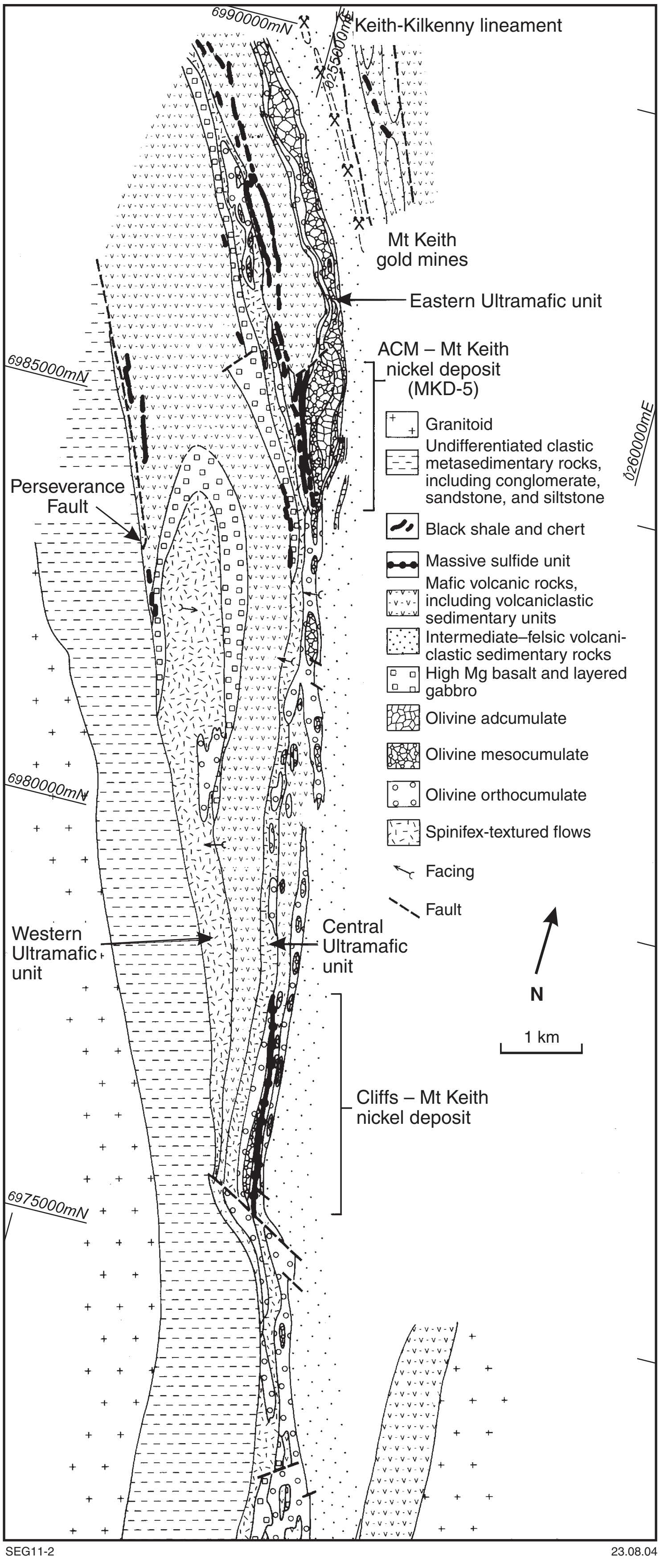

Figure 2. Geological map of Mount Keith area (adapted from Grgruric, 2002)

cumulate rocks (adcumulate and mesocumulate peridotite) with olivine crystals up to 2.5 cm in size (Dowling and Hill, 1990);

3. presence of extremely coarse grained, internally discordant olivine pegmatoids with crystals up to 4 cm in size (Dowling and Hill, 1990).

All three ultramafic units dip steeply (and locally subvertically) to the west. Igneous textures and geochemical trends indicate a west-facing orientation for the Eastern and Central Ultramafics (Naldrett and Turner, 1977; Dowling and Hill, 1990). Local easterly facings and shallow dips within the Western Ultramafic are attributed to shallowly plunging, tight to isoclinal synclinal folding (Bongers, 1994).

The giant MKD5 nickel deposit is a Type 2 nickel deposit and is hosted in a komatiitic dunite–peridotite pod that forms part of a zone of substantial thickening in the Eastern Ultramafic. The pod was completely serpentinized and talc–carbonate altered during a retrograde fluid infiltration event following metamorphism to mid-greenschist facies (Barrett et al., 1977; Rödsjö and Goodgame, 1999). Nickel sulfides are interstitial to former olivine grains with an abundance of 3–5%. The typical sulfide mineralogy comprises pentlandite, pyrrhotite, pyrite and minor millerite, hypogene violarite, godlevskite, and heazlewoodite (Grguric, 2002).

Within the Mount Keith area, the three ultramafic units are enclosed by a sequence of variably deformed and altered felsic and mafic rocks. The footwall to the Eastern Ultramafic comprises monotonous coherent to in situ fragmented, dacitic, phenocryst- and vesicle-rich lithological units (Rosengren et al., in press). The dacitic units are associated with breccia horizons comprising clasts of the coherent material. The jigsaw fit of the clasts and curviplanar nature of their edges indicates they are hyaloclastites caused by quench fragmentation of lavas upon contact with cold seawater. On this basis, the dacitic units are interpreted as submarine, autobrecciated to quench-fragmented lavas. Heptinstall (1991) and Palich (1994) identified lateral and vertical facies variations. The hangingwall rocks of the Eastern Ultramafic just north of the MKD5 deposit, and near Shed Well and Sarahs Find, consist of dacitic rocks that are geochemically and texturally identical to those of the footwall sequence. The hangingwall to the Eastern Ultramafic at the MKD5 deposit consists of a thin pyritic chert-like unit, overlain by fine-grained foliated mafic units and then the Central Ultramafic. The Central Ultramafic is in faulted contact with the Eastern Ultramafic in the southern part of the MKD5 pit, and at several locations along strike between the MKD5 and Cliffs–Charterhall deposit.

To the north of MKD5, the footwall and hangingwall rocks are compositionally and texturally identical, representing the same coherent to in situ fragmented dacitic to andesitic phenocryst-rich rocks present in the footwall at MKD5. This relationship has also been recognized south of the MKD5 deposit towards Shed Well and Golgotha (Hepinstall, 1991; Palich, 1994). Primary contact relationships indicate that this stratigraphy (dacitic lavas and associated fragmental facies) represents the primary sequence into which the Eastern Ultramafic was emplaced. Near the MKD5 pit, the hangingwall sequence to the Eastern Ultramafic is complicated by faulting that apparently juxtaposed the original felsic hangingwall sequence with the more mafic rocks. The mafic and felsic sequences in the hangingwall are separated by a layer of highly deformed pyritic chert, which appears to be the detachment locus for faulting.

References

BARNES, S. J., GOLE, M., and HILL, R. E. T. 1988, The Agnew nickel deposit, Western Australia: Part I. Structure and stratigraphy: Economic Geology, v. 83, p. 524–536.

BARNES, S. J., HILL, R. E. T., PERRING, C. S., and DOWLING, S. E., 1999, Komatiite flow fields and associated Ni–sulphide mineralisation with examples from the Yilgarn Block, Western Australia, *in* Dynamic processes in magmatic ore deposits and their applications in mineral exploration *edited by* R. R. KEAYS, C. M. LESHER, P. C. LIGHTFOOT, and C. E. G. FARROW: Geological Association of Canada, Short Course no. 13, p. 159–194.

BARRETT, F. M., BINNS, R. A., GROVES, D. I., MARSTON, R. J., and McQUEEN, K. G., 1977, Structural history and metamorphic modification of Archean volcanic-type nickel deposits, Yilgarn Block, Western Australia: Economic Geology, v. 77, p. 1195–1223.

BINNS, R. A., GUNTHORPE, R. J., and GROVES, D. I., 1976, Metamorphic patterns and development of greenstone belts in the Yilgarn Block, Western Australia, *in* The Early history of the Earth *edited by* B. F. WINDLEY: New York, U.S.A., Wiley, p. 303–313.

BONGERS, E. A., 1994, A structural interpretation of the Mt. Keith region, Western Australia: Flinders University, BSc Honours thesis (unpublished).

BROOME, J., JOURNEAUX, T., SIMPSON, C., DODUNSKI, N., HOSKEN, J., DE VITRY, C., and PILAPIL, L., 1998, Agnew gold deposits, *in* Geology of Australian and Papua New Guinea mineral deposits *edited by* D. A. BERKMAN and D. H. MacKENZIE: The Australasian Institute of Mining and Metallurgy, Monograph 22, p. 161–166.

DOWLING, S. E., and HILL, R. E. T., 1990, Rivers of fire: the physical volcanology of komatiites in the Mount Keith region, Norseman–Wiluna greenstone belt, Western Australia: CSIRO Restricted Investigation Report EG103R (unpublished).

GRGURIC, B. A., 2002, Hypogene violarite of exsolution origin from Mount Keith, Western Australia: field evidence for a stable pentlandite–violarite tie line: Mineralogical Magazine, v. 66, p. 313–326.

HEPTINSTALL, A. J., 1991, The nature of felsic volcanism and its association with sulfide mineralisation in the Shed Well area, Mt Keith, W.A.: Curtin University of Technology, BSc Honours thesis (unpublished).

HILL, R. E. T., BARNES, S. J., GOLE, M. J., and DOWLING, S. E., 1990, Physical volcanology of komatiites (2nd edition): Geological Society of Australia, W.A. Division, Excursion Guide no. 1, 101p.

HILL, R .E. T., BARNES, S. J., GOLE, M. J., and DOWLING, S. E., 1995, The volcanology of komatiites as deduced from field relationships in the Norseman–Wiluna Greenstone belt, Western Australia: Lithos, v. 34, p. 159–188.

NALDRETT, A. J., and TURNER, A. R., 1977, The geology and petrogenesis of a greenstone belt and related nickel sulfide mineralization at Yakabindie, Western Australia: Precambrian Research, v. 5, p. 43–103.

PALICH, B. M., 1994, The stratigraphy and volcanology of the Archean felsic volcanic succession in the Norseman–Wiluna greenstone belt at Mt Keith, Western Australia: Monash University, BSc Honours thesis (unpublished).

RÖDSJÖ, L., and GOODGAME, V. R., 1999, Alteration of the Mt Keith nickel sulfide deposit, *in* Mineral deposits: processes to processing *edited by* C. J. STANLEY: Rotterdam, The Netherlands, A. A. Balkema, p. 779–782.

ROSENGREN, N. M., BERESFORD, S. W., GRGURIC, B. A., and CAS, R. A. F., in press, An intrusive origin for the giant, komatiitic MKD5 nickel deposit, Mount Keith, Western Australia: Economic Geology.

MKD5 nickel sulfide deposit, Mount Keith

by

B. A. Grguric[1] and N. M. Rosengren[1]

Abstract

The low grade, high tonnage MKD5 orebody at Mount Keith in central Western Australia is currently the largest nickel producer in Australia. The orebody comprises disseminated Ni–Fe sulfides hosted in a series of cumulate dunite and peridotite units that form part of the Eastern Ultramafic unit, in the northern Agnew–Wiluna greenstone belt. The Archean cumulate sequence is of komatiitic affinity and has been variously interpreted as an intrusive dyke or sill, or, more recently, as the product of a giant komatiite lava river. Nickel sulfide mineralization is interpreted to have formed by cotectic crystallization of olivine cumulus crystals and a sulfide melt phase following sulfur saturation of the komatiitic melt phase. Subsequent hydrothermal serpentinization and talc–carbonate alteration of the ultramafic sequence have resulted in modifications to sulfide phase relations.

Introduction

The giant, low grade, MKD5 nickel sulfide orebody at Mount Keith in the northeastern Eastern Goldfields of Western Australia is currently the largest nickel producer in Australia. Owned and operated by WMC Resources, nickel has been produced since 1994 and currently stands at 377 000 t of Ni metal in concentrate to the end of 2003. Disseminated nickel sulfide mineralization extends over a strike length of 2 km and continues downward to at least 600 m depth (current base of drilling). The bulk of economic mineralization is in the grade range 0.4–1.2% Ni, with typical head grades of current mill feed in the range 0.5–0.8% Ni. The deposit is mined as a single-staged cutback pit using conventional opencut methods. It is a 50 Mtpa operation, of which 11.2 Mtpa is mill feed. The ore is processed by froth flotation, yielding a sulfide concentrate containing 18–27% Ni, depending on ore mineralogy. Minor byproducts include Co, Cu, and platinum group elements (PGE).

Discovery and resources

The name Mount Keith comes from the sheep station on which the deposit is located (later incorporated into Albion Downs Station), which, in turn, was named after a small hill several kilometres to the north of the current opencut.

[1] WMC Resources Limited, Post Office Box 91, Belmont, W.A. 6104, Australia

The resident managers of Mount Keith Station in the 1960s were Jim and Eileen Jones. Jim Jones was a keen amateur prospector and, following WMC's discovery of nickel sulfides in Kambalda in 1966, was alert to signs of possible nickel mineralization. In November 1968, he unsuccessfully attempted to use a small water-boring rig to test an outcrop of weathered ultramafic rock in which he'd previously found some gossanous material. Fortuitously, a driller friend arrived at the station at this time with a reverse circulation (RC) drill rig that required repair work. Jim agreed to perform the repairs in exchange for a single RC hole being drilled. The hole was collared 3 m from the site of his abortive water drill attempt, and struck disseminated nickel sulfides at 70 m depth. It is believed that this discovery occurred at the present-day Golgotha prospect in the Central Ultramafic unit and not in the adjacent Eastern Ultramafic, which hosts the MKD5 orebody (Fletcher, M., 1998, pers. comm.)*. Samples of the drill cuttings were passed to geologists from Metals Exploration NL who were working in the Kingston area north of Mount Keith at the time. On returning positive assay results, Metals Exploration, in joint venture with Freeport of Australia, acquired the Mount Keith mineral claims through purchase and pegging, and, in January 1969, commenced a detailed exploration program, targeting both massive sulfides in basal contact positions and broad, low-grade disseminated mineralization. The

* Drilling in the same area in 1998 confirmed the presence of preserved sulfides at unusually shallow depths relative to the rest of the Mount Keith area (where sulfides are not usually seen at less than 100 m), suggesting the initial recovery was indeed fortuitous.

very poor outcrop and deep weathering profile necessitated reliance on magnetic data to define ultramafic unit boundaries. Initially, 39 000 m of percussion drilling (1296 holes) was carried out. A diamond drilling program followed in July 1969 and, in November of the same year, drillhole MKD5 intersected 176 m at 0.60% Ni, proving the economic potential of the prospect. The first indicated ore reserve for the MKD5 orebody, of 195 Mt at 0.60% Ni, was announced in 1971. A series of joint ventures and changes in ownership followed, together with additional drilling programs, but mining was delayed for over two decades as a consequence of low metal prices and metallurgical problems (principally low Ni recoveries and poor concentrate quality). WMC acquired full ownership of Mount Keith in 1993 and, following commissioning of the metallurgical plant in 1994, began nickel production in October of that year. Current (2003) ore reserves are 308 Mt at 0.56% Ni with an ore resource (inclusive of reserves) of 505 Mt at 0.56% Ni. The projected mine life is in the order of 25–30 years, based on an average annual processing rate of about 11 Mtpa.

Geological setting

The MKD5 orebody is in the Agnew–Wiluna greenstone belt in the Archean Yilgarn Craton of Western Australia (Hill et al., 1990). The belt trends north-northwesterly and is constrained by large- to terrane-scale faults and granitoid bodies (Fig. 1). The belt is most attenuated in the Mount Keith area, with a maximum thickness of 6 km, and changes strike about the Mount Keith position, possibly reflecting an underlying primary structural control. This section of the belt is bound to the west and east by voluminous Archaean granitoids (Barrett et al., 1977). The greenstone sequence in the Mount Keith area includes three ultramafic horizons, locally designated the Eastern, Central, and Western Ultramafic units (Fig. 1; Dowling and Hill, 1990). The ultramafic horizons can be traced 30 km north of Mount Keith to the Honeymoon Well nickel deposit, and 9 km south to the Cliffs–Charterhall nickel deposit. Beyond these limits, definition of the belts is uncertain due to structural complexities. There are well developed spinifex-textured komatiites in the Western and Central Ultramafic units, with sporadic Kambalda-style basal accumulations of massive Ni–Fe sulfide at the base of the Central Ultramafic, notably in the Cliffs–Charterhall deposit area. The Eastern Ultramafic lacks the development of spinifex-textured komatiite anywhere along its strike extent, and contains giant accumulations of extreme olivine-cumulate rocks (dunite and mesocumulate peridotite) with olivine grainsizes up to 2.5 cm. All three ultramafic units dip steeply (and locally subvertically) to the west. Igneous textures and

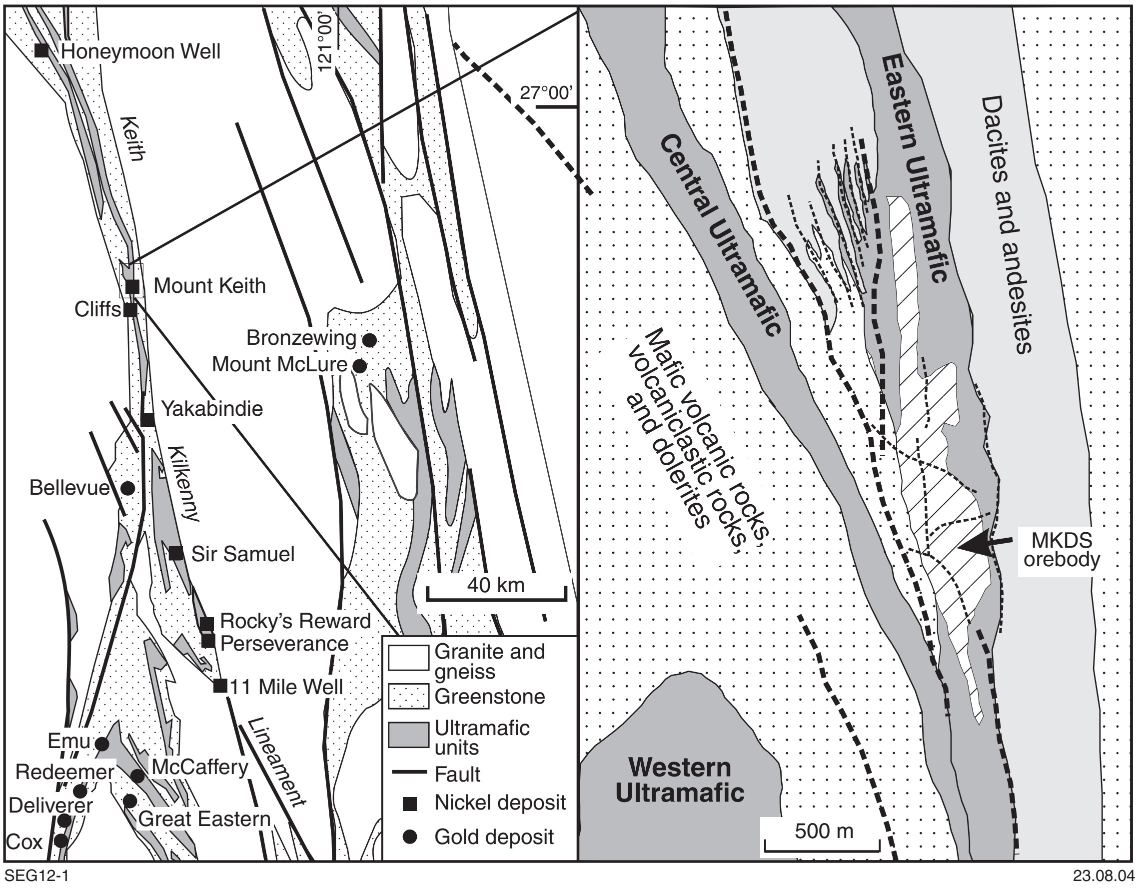

Figure 1. Regional geology of the Agnew–Wiluna belt and the Mount Keith area showing the relationship between the Western Ultramafic, Central Ultramafic, and Eastern Ultramafic units hosting the MKD5 orebody

geochemical trends indicate a west-facing direction for the Eastern and Central Ultramafic units (Naldrett and Turner, 1977; Dowling and Hill, 1990). Local east facings and shallow dips within the Western Ultramafic are attributed to shallowly plunging, tight to isoclinal synclinal folding (Bongers, 1994). The genetic relationship between the three ultramafic horizons has been controversial, but recent work by Rosengren et al. (in press) described preserved upper contacts between the Eastern Ultramafic and hangingwall dacites. These upper contacts preserve features such as incorporation of dacite xenoliths by the Eastern Ultramafic and apophyses of ultramafic rock into the hangingwall dacite, indicating an intrusive origin for the unit. Volcanic textures indicate the Western and Central Ultramafic units are subaqueous extrusive sequences.

In the Mount Keith area, the three ultramafic horizons are enclosed by a sequence of variably deformed and altered intermediate and mafic rocks. The Central and Western Ultramafic units are broadly enclosed by mafic units of basaltic bulk composition that are generally fine grained and deformed (Fig. 1). The footwall to the Eastern Ultramafic consists of monotonous, coherent to in situ, fragmented, dacitic to andesitic, phenocryst-rich lavas (Fig. 1), within which lateral and vertical facies variations have previously been identified by Heptinstall (1991), Palich (1994), and recently reinterpreted by Rosengren (2004). The hangingwall rocks of the Eastern Ultramafic just north of the MKD5 deposit, and near Shed Well and Sarahs Find, consist of dacitic to andesitic rocks, identical to those of the footwall sequence (Rosengren, 2004). The hangingwall to the Eastern Ultramafic at the MKD5 deposit consists of a thin, structurally emplaced, pyritic, chert unit overlain by fine-grained foliated mafic units, which are, in turn, overlain by the Central Ultramafic. The Central Ultramafic is in faulted contact with the Eastern Ultramafic in the southern portion of the MKD5 pit, and at several locations along strike between the MKD5 and Cliffs–Charterhall deposits. The giant MKD5 orebody is a Type IIB nickel deposit, as defined by Lesher (1989), and is hosted in a komatiitic dunite–peridotite body that forms part of a zone of substantial thickening in the Eastern Ultramafic.

State of knowledge of the deposit

Previous work on the general geology and mineralization style of the MKD5 orebody was carried out by Burt and Sheppy (1975), Groves and Keays (1978), Dowling and Hill (1990, 1993), and Hopf and Head (1998), with a more detailed examination of the alteration systematics undertaken by Rödsjö (1999), and Rödsjö and Goodgame (1999). More recently, the igneous geology of the Agnew–Wiluna belt has been the subject of an AMIRA project (P710), led by Dr Steve Beresford of Monash University. Work as part of this project in the Mount Keith area has led to a reinterpretation of the contact relations and emplacement history of the Eastern Ultramafic (Rosengren et al., in press), a facies model for the enclosing dacitic sequence (Rosengren, 2004), and a refinement of the igneous stratigraphy of the Eastern Ultramafic (Rosengren, 2004). The current understanding of the igneous stratigraphy and alteration overprint is a culmination of this work and that of WMC exploration and mining geoscientists since the commencement of mining in the mid-1990s.

Primary lithology

The Mount Keith ultramafic complex hosting the MKD5 orebody can be subdivided into a series of seven primary igneous units (Fig. 2), the boundaries of which are generally parallel to the regional trend of the Eastern Ultramafic. From east to west, the steeply west-dipping units generally become more magnesian and closer-packed olivine cumulates increase in abundance, indicating a westward facing direction for the complex, which is consistent with observations throughout the Eastern Ultramafic (Naldrett and Turner, 1977; Dowling and Hill, 1990).

The lowermost Unit 101, which is in sheared contact with the footwall dacitic sequence, is denoted the Millerite Orthocumulate Domain by local mine geologists, and consists of a former olivine orthocumulate (Ooc on Fig. 3) peridotite that is essentially barren of sulfide mineralization. Unit 102 (Millerite Adcumulate Domain of local mine geologists) lies stratigraphically above, and consists of extreme olivine adcumulate dunite (EOAD on Fig. 3) with subordinate horizons of orthocumulate and pyroxenite, particularly near the base of the unit. Former olivine crystals in the dunite are 0.5–2 cm long, and are typically elongated and aligned in a well-defined igneous fabric. The dunite contains pods and horizons of disseminated magmatic sulfide mineralization, but, for the most part, is sulfide poor. Unit 102 thickens in the northern portion of the complex. Unit 104 (Pentlandite Adcumulate Domain of mine geologists), which overlies Unit 102, consists of olivine adcumulate (Oad on Fig. 3) dunite to mesocumulate (Omc on Fig. 3) peridotite, and is notable for containing a generally uniform distribution of magmatic sulfide mineralization. Former olivine grains tend to be more rounded in this unit, and the presence of lobate intercumulus chromite is conspicuous by the pink–magenta colour of its alteration products; stichtite and woodallite. In the southern and central portions of the complex, Unit 104 is at its widest, with intersections of up to 300 m (true width) containing ore-grade mineralization. These large intersections of economic mineralization have driven the geometry of the openpit mine design. A thin (<10 m) discontinuous zone of unusual olivine rocks is common between the base of Unit 104 and top of Unit 102. Denoted the Porphyritic Olivine Rock Domain (Unit 103; POR on Fig. 3), it locally contains serpentine pseudomorphs after very large olivine crystals (up to 5 cm; Seymon, 1996). Textures are often distinctly amoeboid harrisitic, and a characteristic feature is the presence of brown 'bastite' replacing pyroxene, together with flakes of phlogopite. The bulk chemistry is typically similar to that of an orthocumulate (e.g. Al_2O_3 >0.8% and locally as high as 10%; Table 1). There can be very coarse segregations (up to 10 cm) of sulfides, but these are typically of very low Ni tenor. Pegmatoidal gabbroic segregations containing elevated levels of elements incompatible with ultramafic rocks (e.g. Zr, P, Ti) are

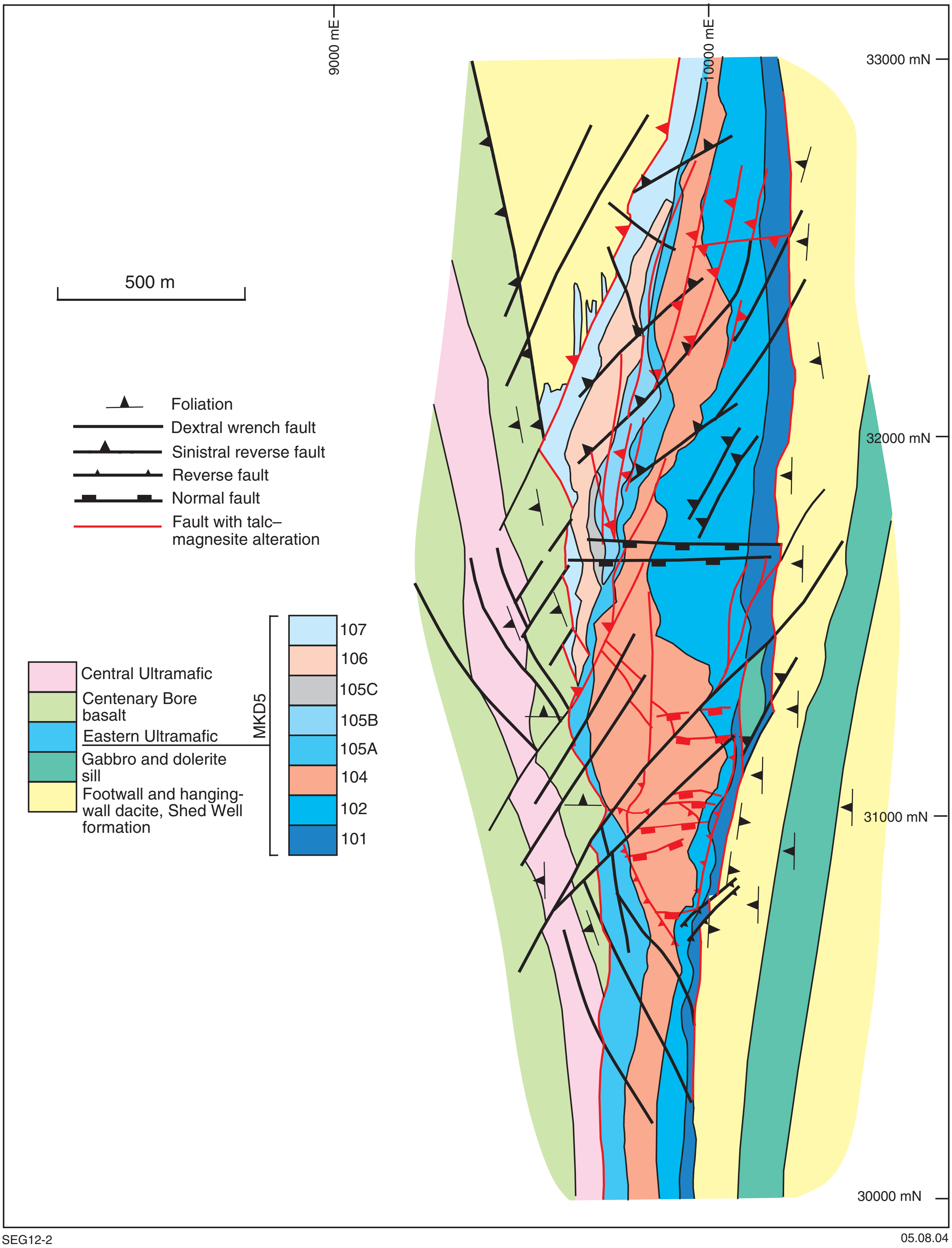

Figure 2. **Schematic plan view showing primary rocks of the Mount Keith ultramafic complex. Plan is constructed at 400RL (ground surface is at 544RL). Explanation of primary stratigraphy is given in the text. Diagram from Rosengren (2004) using structural data from Hayward (2004). Local grid is rotated 4° east from GDA94**

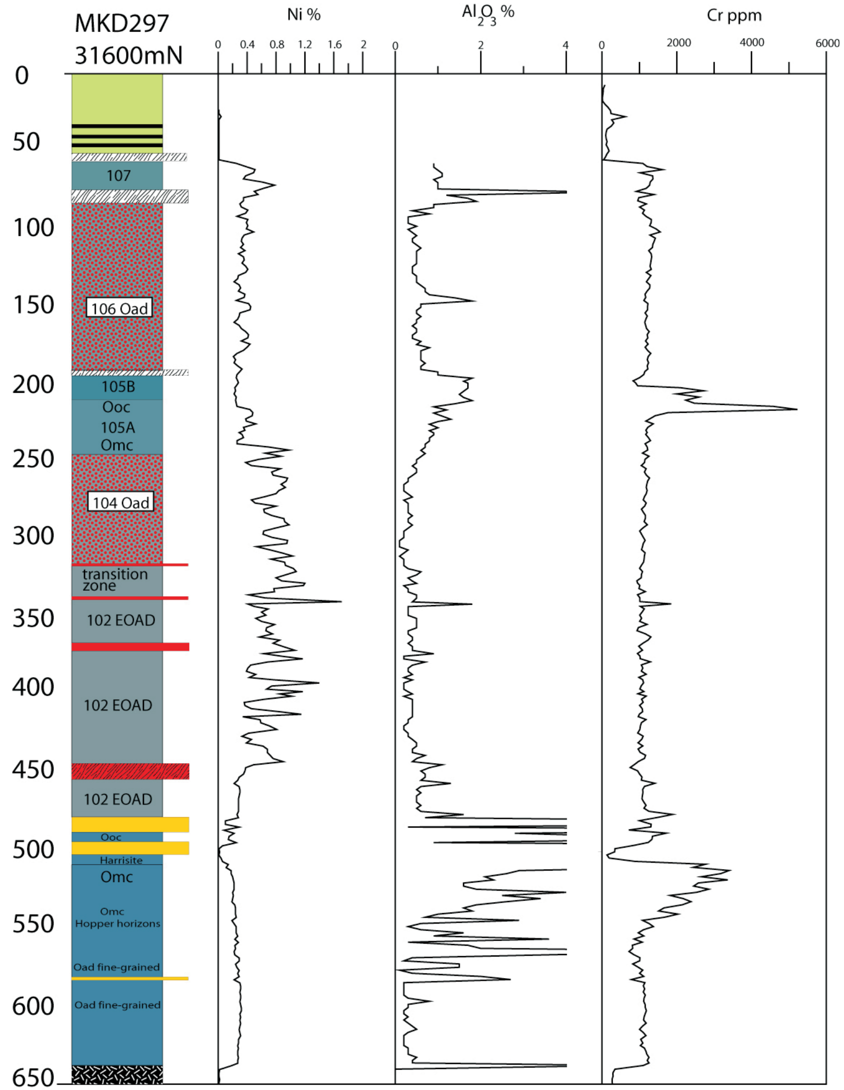

Figure 3. **Downhole geochemical plots for Ni, Al_2O_3, and Cr in diamond drillhole MKD297, with schematic igneous stratigraphy and textural descriptions. Units 101–107 and abbreviations are explained in the text. Drillhole is oriented east–west and located along 31600N on Figure 2**

Table 1. Whole rock analyses of MKD5 samples

	1	*2*	*3*	*4*	*5*
			Percentage		
MgO	39.2	40.2	41.2	34.6	38.7
SiO	34.5	34.0	33.3	34.9	36.3
Al Ô	0.3	0.4	0.1	1.1	1.8
Fe$^{2\ \ 3}$	4.6	3.9	4.7	5.3	5.6
CaO	0.33	0.15	0.20	4.4	0.8
Ni	0.65	0.26	0.53	0.38	0.41
S	1.03	0.01	0.3	0.4	0.3
			Parts per million		
Cr	781	835	1 217	1 355	1 853
Co	160	60	127	112	126
Cu	270	5	25	34	23
As	15	35	10	7	9
			Parts per billion		
Ru	14	1	7	na	na
Rh	6	1	4	na	na
Pd	34	1	22	na	na
Os	11	6	7	na	na
Ir	9	4	9	na	na
Pt	13	1	6	na	na

NOTES:
1 Medium grade ore. Lizardite–brucite-altered dunite from central Unit 104 (MKD153 556–558 m)
2 Antigorite–magnesite-altered dunite from upper Unit 102, containing no macroscopic sulfides (MKD153 697–699 m)
3 Sample from ore-grade pod in Unit 102. Antigorite–magnesite-altered dunite (MKD219 512–514 m)
4 Unit 107 serpentine–chlorite-altered orthocumulate peridotite containing trace sulfides (MKD297 64–66 m)
5 Unit 103 serpentine–magnesite–chlorite-altered amoeboid harrisite, containing trace sulfides (MKD297 339.3 – 340.8 m)
na not available

associated with Unit 103, and could represent some type of late-stage melt segregation.

In the northern portion of the ultramafic complex, the Unit 104 adcumulate dunite grades into an essentially barren mesocumulate peridotite unit with an orthocumulate peridotite top, known locally as the Mesocumulate Domain (Unit 105). This unit contains localized pods of pyroxenite, bladed and amoeboid harrisites, and pegmatoidal gabbroic segregations. The upper part of the mesocumulate (sensu stricto) unit is particularly elevated in Cr, with typical levels of 2500 ppm, peaking locally to 6000 ppm (Fig. 3), and is mainly orthocumulate peridotite. Unit 104 in the central and southern portions of the complex is directly overlain by a thin orthocumulate peridotite horizon (Unit 107), which contains some localized pods of ore-grade sulfide mineralization. This unit is in sheared contact with hangingwall rocks, notably the aforementioned pyritic chert unit.

In the northwestern portion of the complex, a body of ad- to mesocumulate dunite (Unit 106) overlies Unit 105 (Fig. 2). Locally denoted the Western Mineralized Domain, it appears to represent a late-stage injection of fresh, uncontaminated magma. Nickel–Fe sulfides are present in the form of relatively coarse intercumulus blebs, characteristically of low Ni tenor. The western margin of this unit consists of orthocumulate peridotites and subordinate harrisites, pyroxenites, and gabbro horizons.

In defining and modelling these units in the ultramafic complex, particular importance is placed on whole-rock major and trace element chemistry, which can be used to define lithological boundaries in areas where hydrothermal alteration has obliterated primary textures, and identify subtle changes in lithology that are not readily noted during conventional core logging. Components such as Al_2O_3 and TiO_2 are useful in this regard, owing to their relative immobility during alteration and relative incompatibility in olivine. Their abundance thus mirrors that of the intercumulus component. Examples of downhole geochemical profiles are given in Figure 3, and representative whole-rock analyses are presented in Table 1.

Alteration overprint

The host dunites and peridotites in the Mount Keith ultramafic complex have been completely serpentinized and locally talc–carbonate altered after deformation and metamorphism to mid-upper greenschist facies (Barrett et al., 1977; Rödsjö; 1999; Rödsjö and Goodgame, 1999). The retrograde serpentinization–carbonation event was initiated by infiltration of H_2O–CO_2-rich fluids, which exploited early contact-parallel and crosscutting (D_2) faults and shears as conduits (Rödsjö, 1999; Widdup, 2000; Hayward, 2004). The geochemical signature of the altering fluids (as indicated by wall-rock chemistry) is consistent with regional Archean gold fluids, i.e. H_2O–CO_2 dominant, As-bearing, and containing low levels of Au, Te, and reduced S (Rödjsö, 1999). Infiltrating fluids reacted with the ultramafic wallrock to produce a talc–magnesite assemblage proximal to the structural conduits, with enveloping antigorite–magnesite haloes. The most distal manifestation of this alteration process is a lizardite–brucite assemblage. The relatively low temperature fluid infiltration (<320°C) has resulted in high levels (up to 20% in run of mine ore) of hydrotalcite group minerals, particularly in areas of low fluid–rock interaction, such as lizardite–brucite alteration zones. Of these, the most common species are iowaite [$Mg_6Fe_2(OH)_{16}Cl_2.4H_2O$], pyroaurite [$Mg_6Fe_2(OH)_{16}CO_3.4H_2O$], and stichtite [$Mg_6Cr_2(OH)_{16}CO_3.4H_2O$], with the last mentioned forming replacements of magmatic chromite grains (Grguric et al., 2001; Grguric, 2004). In addition, the MKD5 orebody is the type locality for woodallite (the chlorine analogue of stichtite; Grguric et al., 2001) and mountkeithite (a mineral related to pyroaurite; Hudson and Bussell, 1981). This sequence of alteration assemblages resembles that described by Eckstrand (1975) in the Dumont serpentinite complex, Quebec, except that no original igneous olivine is preserved in MKD5, and hydrotalcite group minerals are apparently absent in Dumont. Magnesian chlorite appears as an alteration mineral where aluminium levels in the ultramafic rocks are elevated (e.g. in orthocumulate rocks, and adjacent to hanging- and footwall contacts). Late-stage, pegmatoidal, gabbroic bodies within the ultramafic complex are typically rödingitized, particularly when enclosed by ultramafic units that were formerly rich in calcium, such as pyroxenites or orthocumulate peridotites.

Alteration is extremely important from a mineral processing point of view, principally because processing of talc–magnesite-altered ores results in poor quality concentrates. Talc, being a free-floating mineral, reports to final concentrate, which results in unacceptably high MgO levels in this product. In addition, the highest levels of arsenic occur within talc–magnesite zones, and this element is generally upgraded during beneficiation. Lizardite–brucite ores present the least metallurgical problems, with the exception that chlorine levels in final concentrates can be high due to the presence of the aforementioned hydrotalcite group minerals (Grguric, 1999).

Ore mineralogy

Intercumulus sulfide blebs range in size from 40 µm to 1.5 mm (average 0.5 mm) and are usually situated at the triple point junctions of former olivine grains. These blebs consist of aggregates of Ni–Fe sulfide grains surrounded by a corona of magnetite, the outer margins of which are partially replaced by iowaite, chlorian pyroaurite(–tochilinite), or ferroan magnesite in most cases. A coarse network of magnetite 'crossbars' is typically present within the blebs (Fig. 4a). Sulfide abundances in ore grade material are usually in the 1–5% range. Such sulfide–gangue textures are representative of the bulk of the nickel mineralization in MKD5. The distribution of ore mineral assemblages is now well defined following an extensive mineral mapping and microanalytical study by the senior author in 2001 (representative microprobe analyses are given in Table 2). A distinctive feature of the deposit is the zonation of sulfide assemblages. This zonation is interpreted to be a consequence of:

- primary variations in sulfur saturation during segregation of sulfides from the primary magma and subsequent cooling (resulting in variations in sulfide to silicate proportions);
- most improtantly, modifications to sulfide–oxide subsolidus phase relations as a result of contrasting oxygen and sulfur fugacity conditions during later hydrothermal alteration.

The main ore zone in MKD5 comprises a pentlandite–pyrrhotite assemblage in Unit 104. Partial to complete hypogene replacement of pyrrhotite by a lamellar intergrowth of pyrite–marcasite–magnetite is extremely common in this unit (Fig. 4a). Owing to a relatively coarse bleb size (locally up to 3 mm), these ores generally yield the highest Ni recoveries during processing. On the margins of the Unit 104, the sulfide assemblage grades to dominant pentlandite with subordinate pyrite, hypogene violarite, or both, with the violarite present as exsolution lamellae in pentlandite grains (Fig. 4b; Grguric, 2002). The adjacent Unit 102 is characterized by a more 'poddy' distribution of ore grade material, with ore pods and shoots separated by low grade zones averaging 0.30–0.35% Ni and lacking macroscopically visible blebs. Sulfides are present in the low grade zones as essentially unrecoverable, micron-sized dustings within former olivine grains. This low grade mineralization contains virtually no detectible Cu or PGE, and reflects the alteration of dunite containing no magmatic sulfides*. Sulfide assemblages in the ore pods are sulfur poor relative to Unit 104, and Fe sulfide phases are absent. Assemblages are dominated by high-Ni pentlandite, millerite (Fig. 4c), godlevskite, and hypogene violarite, which have developed as a consequence of elevated fluid fO_2 associated with antigorite–magnesite alteration of the host dunites (Grguric, 2002, 2004). In the northern part of Unit 102, less intense alteration has resulted in contrasting extremely low fluid fO_2, with the consequence that heazlewoodite is stabilized.

The other significant ore domain is Unit 106, the adcumulate–mesocumulate dunite unit in the northwest of the orebody. This unit is characterized by relatively Fe-rich sulfide assemblages with pyrrhotite (partly or completed replaced by lamellar pyrite–marcasite) present in equal or larger proportions to pentlandite. Supergene alteration of the sulfide assemblages are common in this unit due to the presence of late-stage structures that have acted as conduits for supergene fluids.

Within talc–carbonate altered zones, the fO_2 and fS_2 of fluids attending talc–magnesite alteration have resulted in the stabilization of pyrite. Existing pyrrhotite–pentlandite assemblages are usually preserved, with the addition of some hydrothermal pyrite. Magnetite coronas and crossbars on blebs are completely replaced by ferroan magnesite (Fig. 4d). Locally, there is extensive alteration of pyrrhotite and pentlandite along the [0001] plane of pyrrhotite and [111] plane of pentlandite. The result is a distinctive lamellar texture in which relict sulfide lamellae (1–5 µm thick) are interleaved with talc and magnesite. Owing to deformation, these lamellae can be kinked or bent. Although Cu is not elevated in talc zones, modified phase relations have resulted in the formation of minor chalcopyrite associated with Ni and Fe–Ni sulfides (Fig. 4d). Most talc-altered ore contains elevated levels of As (30–6500 ppm) as a consequence of the As content of the alteration fluid. At low levels of whole rock As (<500 ppm), Fe and Fe–Ni sulfide minerals apparently host As in solid solution or as submicroscopic inclusions. At higher As levels, discrete As-bearing opaque minerals such as gersdorffite (NiAsS), nickeline (NiAs), cobaltite (CoAsS), and maucherite ($Ni_{11}As_8$) are common, typically replacing pre-existing pyrrhotite and pentlandite.

Supergene alteration is developed as a subhorizontal zone below the oxide zone and persists to a vertical depth of about 100 m, with some deeper perturbations of the supergene–primary surface along late-stage brittle structures. The supergene zone is defined by the presence of secondary violarite after pentlandite or millerite (Fig. 4e), and an elevated non-sulfide Ni content relative to the protore. There is no significant supergene enrichment of total Ni or Co in this zone. Sulfide minerals associated with secondary violarite include secondary millerite, pyrite, marcasite, and relict pentlandite (Butt and Nickel, 1981). Both the textural characteristics (Figs. 4b and 4e) and mineral chemistry (Table 2) of secondary violarite are markedly different to those of its hypogene

* The Ni grade of this material reflects the fact that natural forsteritic olivines can contain up to 4000 ppm Ni in solid solution. Subsequent serpentinization–carbonation of olivine by fluids containing reduced sulfur results in exsolution of Ni in the form of fine sulfide particles.

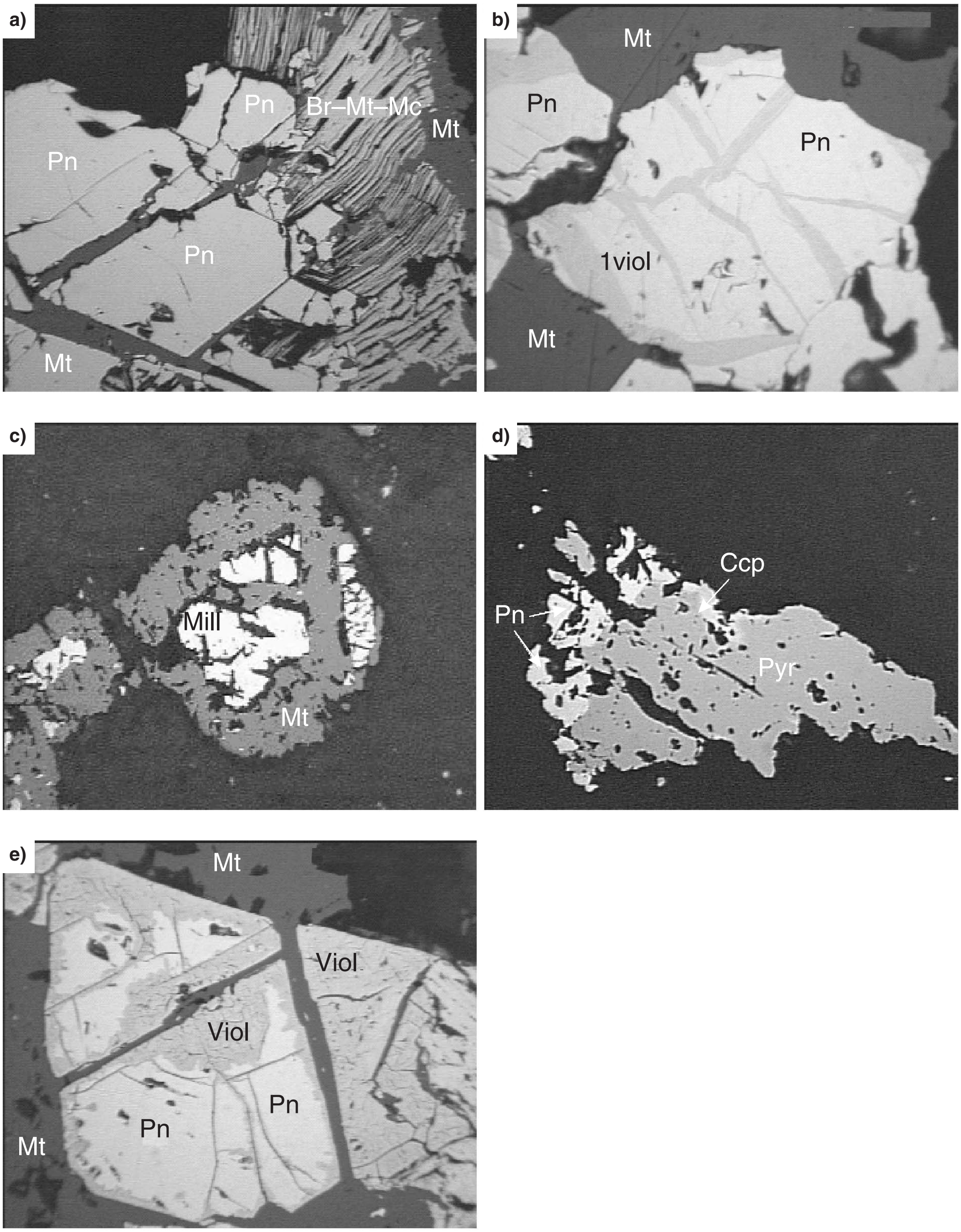

Figure 4. Reflected light micrographs of MKD5 ore textures: a) Detail of a sulfide bleb from Unit 104 showing coarsely crystalline pentlandite (Pn) with magnetite (Mt) rims and crossbars, and associated with a distinctive lamellar intergrowth of bravoitic pyrite, magnetite, and marcasite (Br–Mt–Mc); intergrowth is a hypogene alteration product of pyrrhotite; field of view 600 µm. b) Sulfide bleb from the eastern margin of Unit 104, consisting of pentlandite (Pn) with hypogene violarite (1viol) exsolution lamellae surrounded by a corona of magnetite (Mt); field of view 250 µm; from Grguric (2002). c) Millerite (Mill) bleb from Unit 102 with thick magnetite corona; millerite formed by replacement of pre-existing pentlandite as evident from the relict triangular cleavage; field of view 500 µm. d) Typical sulfide bleb from a talc–magnesite-altered zone in Unit 104 consisting of pyrrhotite (Pyrr), pentlandite (Pn), and minor chalcopyrite (Ccp); note complete absence of magnetite rims or crossbars; field of view 600 µm. e) Sulfide bleb from the supergene zone showing replacement of hypogene pentlandite (Pn) by porous supergene violarite (Viol) along grain boundaries and microfractures; field of view 250 µm; from Grguric (2002)

Table 2. Microprobe analyses of MKD5 ore minerals using wavelength dispersive spectrometers (WDS)

	1	*2*	*3*	*4*	*5*	*6*	*7*
				Percentage			
Co	1.51	0.26	6.23	1.32	0.97	1.13	13.05
Fe	29.85	24.73	17.70	16.77	0.24	8.79	5.00
Ni	35.90	41.86	33.36	39.64	63.02	58.03	14.28
As	0.00	0.09	0.05	0.00	0.11	0.08	47.37
S	32.66	32.84	41.90	38.18	35.25	31.80	19.17
Total	**99.94**	**99.80**	**99.27**	**96.10**	**99.68**	**99.88**	**99.20**

NOTES:
1 Pentlandite from pentlandite–pyrrhotite assemblage, Unit 104 (MKD261 200.0 m)
2 Pentlandite from pentlandite – hypogene violarite assemblage, lowermost Unit 104 (MKD33 220.0 m)
3 Hypogene violarite from pentlandite – hypogene violarite assemblage, Unit 104 (MKD27 498.0 m)
4 Supergene violarite associated with supergene pyrite and relict pentlandite, Unit 104 transition zone (MKD100 140.0 m)
5 Millerite from millerite-only assemblage, Unit 102 (MKD146 270.3 m)
6 Godlevskite from godlevskite–millerite assemblage, Unit 102 (MKD16 252.0 m)
7 Cobaltian gersdorffite from talc–magnesite-altered zone, Unit 104 (MKD34 330.1 m)

equivalent in the MKD5 orebody (Grguric, 2002). Owing to incipient oxidation of sulfide mineral surfaces in the supergene zone, Ni flotation recoveries are significantly lower when treating supergene ores relative to hypogene ores of the same head grade.

Geological and genetic models for the deposit

Large dunite and peridotite bodies of komatiitic affinity containing disseminated NiS mineralization occur in several localities worldwide. Examples additional to MKD5 include the Goliath and Six Mile Well complexes at Yakabindie in Western Australia (Burt and Sheppy, 1975; Naldrett and Turner, 1977; Dowling and Hill, 1990, 1993); Dumont in the Abitibi Province, Canada (Eckstrand, 1975; Duke, 1986); and Hunters Road, Zimbabwe (Prendergast, 2001). These low-grade deposits (Type IIB classification of Lesher, 1989) are significantly different to the more widespread basal massive sulfide deposits, as exemplified by the Kambalda orefield system (Type I classification of Lesher, 1989). The latter are associated with well-developed spinifex-textured komatiites, and are interpreted as products of komatiitic lava flow fields (Gresham and Loftus-Hills, 1981; Lesher et al., 1984; Cowden, 1988).

In contrast to Type I deposits, the emplacement mode of Type II dunite bodies was originally interpreted as either horizontally emplaced sills (e.g. Dumont: Eckstrand, 1975; Duke, 1986) or vertically emplaced dyke complexes (e.g. MKD5: Burt and Sheppy, 1975; Six Mile Well: Naldrett and Turner, 1977). Later work by Barnes et al. (1988), Dowling and Hill (1990), and Hill et al. (1990) reinterpreted the dunite complexes of the Agnew–Wiluna belt as the product of giant lava channels capable of thermomechanically eroding their substrate. The lava channels were interpreted to represent the more proximal facies of Kambalda-style komatiite flow fields. However, the mode of emplacement of Type II deposits in the Agnew–Wiluna belt has been reinvestigated as part of the P710 AMIRA project, and the recognition of preserved upper contacts (Rosengren et al., in press), indicates that an extrusive model for the Eastern Ultramafic in the Mount Keith region is not tenable. A model involving shallow level intrusion into a submarine felsic volcanic sequence is now the preferred interpretation for the emplacement of the Eastern Ultramafic, with the Central Ultramafic possibly representing a comagmatic subaqueous extrusive analogue.

The style and grade of mineralization in Type IIB deposits is worth considering since sulfide mineralized zones in these deposits characteristically have grade distributions centred around 0.6 % Ni and very high Ni/Cu ratios (20–300; Groves and Keays, 1979). The regular distribution of sulfides as intercumulus blebs is interpreted to result from cotectic precipitation or crystallization of olivine cumulus crystals and a sulfide melt phase following sulfur saturation of the komatiitic melt phase (Duke and Naldrett, 1978; Duke, 1986). Although requiring a significant flux of undepleted magma within the ore-forming system, the sulfide formation process itself is relatively static in contrast to the dynamic sulfide entrainment and depositional processes invoked for the formation of massive and matrix sulfide segregations in Type I systems. The centring of the grade distribution at 0.6% Ni is interpreted to reflect the equilibration of the sulfide phase with surrounding cumulus olivine crystals carrying about 4000 ppm Ni and sulfur-saturated komatiitic silicate melt carrying about 2000 ppm Ni (Duke and Naldrett, 1978). The sulfur saturation state of the system depends on parameters such as the aFeO, $a\mathrm{SiO_2}$, $f\mathrm{S_2}$, $f\mathrm{O_2}$, temperature, and pressure of the melt phase (Naldrett, 1989), and variations in these parameters during the formation of the cumulate pile apparently controlled the distribution of sulfide mineralization throughout the MKD5 orebody. Rare occurrences of matrix and massive sulfides, notably in Unit 103, point to deviations from the equilibrium cotectic crystallization process and could reflect highly localized zones of more dynamic (Type I style) sulfide deposition. In contrast to Type I ores, Cu contents of the disseminated mineralization are low (typically 200–300 ppm in ore containing 0.6% Ni), which is consistent with formation via sulfur saturation and sulfide phase precipitation from relatively unfractionated, high-Mg melts (Duke and Naldrett, 1978). Likewise, PGE contents are low (110 ppb combined PGE in ore containing 0.6% Ni; see Table 1).

It is proposed that the starting composition of the intercumulus sulfide blebs was a simple, single phase *mss*. Slow, subsolidus cooling led to exsolution of magnetite in the form of well defined, coarse lamellae (‘crossbars’) and possible solid-state diffusive Ni exchange with host olivine grains. Further cooling below 600 ± 10°C resulted in exsolution of pentlandite from *mss* (see Naldrett et al., 1967). The low-temperature hydrothermal alteration resulted in conversion of some (or, in some cases, all) of the Fe component in the sulfide phases to one or more of the phases magnetite, ferroan magnesite, iowaite, tochilinite–valleriite, ferroan brucite, in the form of distinctive coronas on the blebs. Local fluid compositions and oxidation state dictate the phase that forms. The overall effect of converting a magmatic *mss*-type phase to millerite or heazlewoodite plus one of the abovementioned Fe-bearing gangue phases is a reduction in the particle size of the relict sulfide phase (assuming local scale Ni–Fe mass balance). This grainsize reduction naturally has implications for sulfide liberation during processing, hence, as a general rule, high tenor assemblages in Type IIB orebodies show lower sulfide recoveries relative to lower tenor (pentlandite–pyrrhotite) assemblages.

Regional greenschist facies metamorphism and deformation of the MKD5 deposit were probably not significant in modifying or redistributing nickel sulfide mineralization. During prograde deformation, the unserpentinized dunitic body apparently behaved rigidly, with strain being principally partitioned into surrounding wallrocks. Syn- and post-serpentinization deformation was accommodated by 'block shuffling' of ultramafic lithons along sheared and slickensided surfaces (Widdup, 2000). There is no strong evidence in the MKD5 deposit for hydrothermal remobilization of Ni beyond grain scales; apparent Ni depletion in talc–carbonate zones can be explained by the increase in the specific gravity of the host rock.

Importance of deposit in exploration models

Given current mining technology and metal prices, low-grade, high-tonnage deposits of the Mount Keith style generally need to be near surface and suitable for openpitting to be economic. The number of similar prospects lying within a 50 km radius of Mount Keith (Six Mile, Goliath, Honeymoon Well, Betheno) that, at the time of writing, are still unexploited >20 years after their discovery, is a testament to the narrow economic margins associated with mining and processing these types of deposits. Although all these deposits have large amounts of contained metal, the economics of mining and processing are highly sensitive to open-pit strip ratio, grade distribution, metallurgical parameters of the ore (particularly the proportion of mineralization affected by talc–carbonate and supergene alteration), and proximity to existing processing facilities. The large size and near-surface requirements for these deposits naturally limits exploration targeting options, and in a relatively well defined and heavily explored greenstone terrain, such as the Yilgarn Craton, the chances of a large, near-surface, Mount Keith analogue remaining undiscovered are relatively slim. However, this does not discount the possibility that undiscovered analogues could still remain in ultramafic complexes that are less well explored. Given their inherent low grade (with whole rock Ni contents only 2–3 times greater than those of typical unmineralized dunites), geochemical exploration for Type IIB deposits in highly weathered terrains presents special problems, which have been highlighted by Butt and Sheppy (1975), and Brand and Butt (2001).

From the viewpoint of brownfields exploration, it is perhaps worthwhile emphasizing the potential for some associated massive sulfide mineralization. It has been generally assumed that Type IIB deposits are not associated with massive sulfide segregations (Lesher, 1989), but recent drilling and mining at Mount Keith have shown that massive and matrix sulfide pods, albeit small (tens of tonnes), do occur in these systems.

Acknowledgements

This work represents a revision of the abstract given by the senior author at The University of Western Australia (UWA) Nickel Short Course in February 2003. The authors acknowledge the contributions of Metals Ex, CSIRO, and academic workers, together with WMC geoscientific colleagues (past and present), whose efforts and advice have resulted in the current detailed understanding of the geology of the Mount Keith ore system. In addition, we acknowledge the excellent contributions by research students, such as Leif Rödsjö (UWA), and the Monash University and UWA members of the current AMIRA P710 project team. The original manuscript was proofread by Jon Hronsky, Dave Chapman, and Peter Bewick (WMC).

References

BARNES, S. J., HILL, R. E. T., and GOLE, M. J., 1988, The Perseverance ultramafic complex, Western Australia: the product of a komatiitic lava river. Journal of Petrology, v. 29, p. 305–331.

BARRETT, F. M., BINNS, R. A., GROVES, D. I., MARSTON, R. J., and McQUEEN, K. G., 1977, Structural history and metamorphic modification of Archean volcanic-type nickel deposits, Yilgarn Block, Western Australia: Economic Geology, v. 77, p. 1195–1223.

BONGERS, E. A. 1994, A structural interpretation of the Mt Keith region, Western Australia: Flinders University, BSc Honours thesis (unpublished).

BRAND, N. W., and BUTT, C. R. M., 2001, Weathering, element distribution and geochemical dispersion at Mt Keith, Western Australia: implications for nickel sulphide exploration: Geochemistry: Exploration, Environment, Analysis v. 1, p. 391–407.

BURT, D. R. L., and SHEPPY, N. R., 1975, Mount Keith nickel sulphide deposit, *in* Economic geology of Australia and Papua New Guinea *edited by* C. L. KNIGHT: The Australasian Institute of Mining and Metallurgy, Monograph 5, v. 1, p. 159–168.

BUTT, C. R. M., and NICKEL, E. H., 1981, Mineralogy and geochemistry of the weathering of the disseminated nickel sulfide deposit at Mt Keith, Western Australia: Economic Geology, v. 76, p. 1736–1751.

BUTT, C. R. M., and SHEPPY, N. R., 1975, Geochemical exploration problems in Western Australia exemplified by the Mt Keith area, *in* Geochemical Exploration 1974. Developments in economic geology *edited by* I. L. ELLIOT and W. K. FLETCHER: Amsterdam, The Netherlands, Elsevier, p. 391–415.

COWDEN, A. C., 1988, Emplacement of komatiite lava flows and associated nickel sulfides at Kambalda, Western Australia: Economic Geology, v. 83, p. 436–442.

DOWLING, S. E., and HILL, R. E. T., 1990, Rivers of fire: the physical volcanology of komatiites in the Mount Keith region, Norseman–

Wiluna greenstone belt, Western Australia: CSIRO Restricted Investigation Report EG103R (unpublished).

DOWLING, S. E., and HILL, R. E. T., 1993, The Mount Keith ultramafic complex and the Mount Keith nickel deposit, *in* Crustal evolution, metallogeny and exploration of the Eastern Goldfields *edited by* P. R. WILLIAMS and J. A. HALDANE: Australian Geological Survey Organisation, Record 1993/54, p. 165–170.

DUKE, J. M., 1986, The Dumont nickel deposit: a genetic model for disseminated magmatic sulphide deposits of komatiitic affinity, *in* Metallogeny of basic and ultrabasic rocks *edited by* M. J. GALLAGHER, R. A. IXER, C. R. NEARY, and H. M. PRICHARD: London, United Kingdom, The Institution of Mining and Metallurgy, p. 151–160.

DUKE, J. M., and NALDRETT, A. J., 1978, A numerical model of the fractionation of olivine and molten sulfide from komatiite magma: Earth and Planetary Science Letters, v. 39, p. 255–266.

ECKSTRAND, O. R., 1975, The Dumont serpentinite: a model for control of nickeliferous opaque mineral assemblages by alteration reactions in ultramafic rocks: Economic Geology, v. 70, p. 183–201.

GRESHAM, J. J., and LOFTUS-HILLS, G. D., 1981, The geology of the Kambalda nickel field: Economic Geology, v. 76, p. 1373–1416.

GRGURIC, B. A., 1999, Chlorine in the MKD5 nickel deposit, Mount Keith, Western Australia: mineralogy, distribution and implications for mineral processing, *in* MINSA Mini-Symposium, 1999, extended abstracts *edited by* U. W. REIMOLD and M. CLOETE: Pretoria, South Africa, Mineralogical Association of South Africa, p. 78–82.

GRGURIC, B. A., 2002, Hypogene violarite of exsolution origin from Mount Keith, Western Australia: field evidence for a stable pentlandite–violarite tie line: Mineralogical Magazine, v. 66, p. 313–326.

GRGURIC, B. A., 2004, Minerals of the MKD5 nickel deposit. Mount Keith, Western Australia: Australian Journal of Mineralogy, v. 9, p. 55–71.

GRGURIC, B. A., MADSEN, I. C., and PRING, A., 2001, Woodallite, a new chromium analogue of iowaite from the Mount Keith nickel deposit, Western Australia: Mineralogical Magazine, v. 65, p. 427–436.

GROVES, D. I., and KEAYS, R. R., 1979, Mobilisation of ore-forming elements during alteration of dunites, Mt Keith–Betheno, Western Australia: Canadian Mineralogist, v. 17, p. 373–389.

HAYWARD, N., 2004, Structural geology of the Mt Keith Mine Area: WMC Resources Ltd (unpublished).

HEPTINSTALL, A. J., 1991, The nature of felsic volcanism and its association with sulphide mineralisation in the Shed Well area, Mt Keith, W.A.: Curtin University of Technology, BSc Honours thesis (unpublished).

HILL, R. E. T., BARNES, S. J., GOLE, M. J., and DOWLING, S. E., 1990, The physical volcanology of komatiites in the Norseman–Wiluna belt, *in* Third International Archean Symposium, Perth 1990, excursion guidebook *edited by* S. E. HO, J. E. GLOVER, J. S. MYERS, and J. R. MUHLING: Perth, Western Australia, Geoconferences (WA) Inc., p. 362–397.

HOPF, S., and HEAD, D. L., 1998, Mount Keith nickel deposit, *in* Geology of Australian and Papua New Guinean mineral deposits *edited by* D. A. BERKMAN and D. H. MacKENZIE: The Australasian Institute of Mining and Metallurgy, Monograph 22, p. 307–314.

HUDSON, D. R., and BUSSELL, M., 1981, Mountkeithite, a new pyroaurite-related mineral with an expanded interlayer containing exchangeable $MgSO_4$: Mineralogical Magazine, v. 44, p. 345–350.

LESHER, C. M., 1989, Komatiite-associated nickel sulphide deposits, *in* Ore deposition associated with magmas *edited by* J. A. WHITNEY and A. J. NALDRETT: Reviews in Economic Geology, no. 4, p. 44–101.

LESHER, C. M., ARNDT, N. T., and GROVES, D. I., 1984, Genesis of komatiite-associated nickel sulphide deposits at Kambalda, Western Australia: a distal volcanic model, *in* Sulphide deposits in mafic and ultramafic rocks *edited by* D. L. BUCHANAN and M. J. JONES: London, United Kingdom, The Institution of Mining and Metallurgy, p. 70–80.

NALDRETT, A. J., 1989, Sulfide melts — crystallization temperatures, solubilities in silicate melts, and Fe, Ni and Cu partitioning between basaltic magmas and olivine, *in* Ore deposition associated with magmas *edited by* J. A. WHITNEY. and A. J. NALDRETT: Reviews in Economic Geology, no. 4, p. 5–20.

NALDRETT, A. J., CRAIG, J. R., and KULLERUD, G., 1967, The central portion of the Fe–Ni–S system and its bearing on the pentlandite exsolution in iron–nickel sulfide ores: Economic Geology, v. 62, p. 826–847.

NALDRETT, A. J., and TURNER, A. R., 1977, The geology and petrogenesis of a greenstone belt and related nickel sulfide mineralization at Yakabindie, Western Australia: Precambrian Research, v. 5, p. 43–103.

PALICH, B. M., 1994. The stratigraphy and volcanology of the Archean felsic volcanic succession in the Norseman–Wiluna greenstone belt at Mt Keith, Western Australia: Monash University, BSc Honours thesis (unpublished).

PRENDERGAST, M. D., 2001, Komatiite-hosted Hunters Road nickel deposit, central Zimbabwe: physical volcanology and sulfide genesis: Australian Journal of Earth Sciences, v. 48, p. 681–694.

RÖDSJÖ, L., 1999, The alteration history of the Agnew–Wiluna Greenstone Belt, Western Australia, and the impacts on nickel sulphide mineralisation: The University of Western Australia, PhD thesis (unpublished).

RÖDSJÖ, L., and GOODGAME, V. R., 1999, Alteration of the Mt. Keith nickel sulphide deposit, *in* Mineral deposits: processes to processing *edited by* C. J. STANLEY: Rotterdam, The Netherlands, A. A. Balkema, p. 779–782.

ROSENGREN, N. M., 2004, Architecture and emplacement of an Archaean komatiitic dunite and associated Ni-sulphide mineralisation: Mt Keith, Agnew–Wiluna greenstone belt, Yilgarn Craton, Western Australia: Monash University, PhD thesis (unpublished).

ROSENGREN, N. M., BERESFORD, S. W., GRGURIC, B. A., and CAS, R. A. F., in press, An intrusive origin for the giant, komatiite-hosted MKD5 nickel deposit, Mount Keith, Western Australia: Economic Geology.

SEYMON, A. R., 1996, The petrology and geochemistry of porphyritic olivine-rich rocks within the Mount Keith komatiite-hosted nickel sulphide deposit, Western Australia: Monash University, BSc Honours thesis (unpublished).

WIDDUP, H., 2000, Structural geology of the Mt Keith Ultramafic Complex: University of Melbourne, BSc Honours thesis (unpublished).

Honeymoon Well Nickel Project

by

A. Goode[1] and N. Castleden[1]

Introduction

The Honeymoon Well Nickel Project is located at the northern end of the Agnew–Wiluna greenstone belt, about 45 km south of Wiluna (Fig. 1). This portion of the belt hosts significant nickel and gold mineralization, including the Mount Keith, Cosmos, Perseverance, and Six Mile nickel deposits, and the Wiluna gold deposits. Mineralization at Honeymoon Well was first identified in the early 1970s, and subsequent resource evaluation by CRA from that period to the late 1990s led to the definition of five disseminated deposits and one associated massive sulfide deposit.

Ownership

The Honeymoon Well tenements were recently acquired by MPI Nickel Pty Ltd, is a joint venture between MPI Mines Ltd (80%) and the OM Group (20%), which owns and operates the Cawse Laterite Project. MPI Nickel also operates the Black Swan nickel mine northeast of Kalgoorlie. The company has established access to the contiguous Albion Downs and Honeymoon Well tenements in the Wiluna region, which comprise a 43 km strike length of the Agnew–Wiluna greenstone belt. Drilling activity commenced in September 2003, and included exploration and resource drill evaluation of massive sulfide deposits in conjunction with re-evaluation of all previous disseminated sulfide studies. Scope exists for depth extensions to existing resources, as well as discovery of new massive sulfide mineralization.

The previous owners of the Honeymoon Well project established an endowment of more than 1 Mt of nickel contained within four major disseminated deposits over a total strike length of 12 km. They committed some A$60 million on exploration and feasibility work to establish this endowment, using data from over 800 drillholes.

The 2004 program at Honeymoon Well includes A$5 million on exploration and A$3 million on feasibility studies. Most of this expenditure is focused on Wedgetail, with continuing exploration for further massive sulfide resources at Harrier and elsewhere along the contact zone. Exploration targets within the Honeymoon Well ultramafic rocks have been defined, and will be explored by surface and downhole electromagnetic (EM) surveys, and follow-up drilling.

Geological setting

In the Honeymoon Well project area, the greenstone belt is some 6–7 km wide and contains an ultramafic sequence varying up to 3.0 km in width. The sequence contains a complex suite of metamorphosed and structurally modified komatiites similar to the Mount Keith sequence and comprising olivine orthocumulates, mesocumulates, and adcumulates, and spinifex-textured rocks.

There is minimal outcrop in the project area, and early exploration was achieved by ground magnetometer surveys combined with shallow rotary percussion drilling to depths of 30 m. Multi-element geochemistry from drill samples provided an important tool for geological and mineralization discrimination. Early drilling programs initially planned to test the entire extent of the ultramafic body but, reportedly on the basis of early results combined with the discovery of the Perseverance deposit at Agnew, the program was modified to focus on the margins of the body.

Over the life of the project, diverse geophysical techniques have been used to help identify geological and mineralization boundaries, with mixed success. Detailed aeromagnetic imagery has been particularly useful for the broad-scale identification and targeting of footwall ultramafic positions. However, the use of traditional surface electrical geophysical methods such as transient EM (TEM) has been hindered by geophysically noisy cover materials, and saline groundwater within the saprock profile, at least over parts of the tenement area.

The ultramafic succession at Honeymoon Well has undergone multiple phases of deformation to result in the present arrangement, whereby a mainly thin-flow mineralised sequence is distributed around the periphery of a volumetrically larger and unmineralized dunite. The overall geometry is reminiscent of a south-plunging synform that has been complicated by thrust repetition and later strike faulting.

[1] MPI Mines Ltd, Level 1, 28 Kings Park Road, West Perth, W.A. 6005, Australia

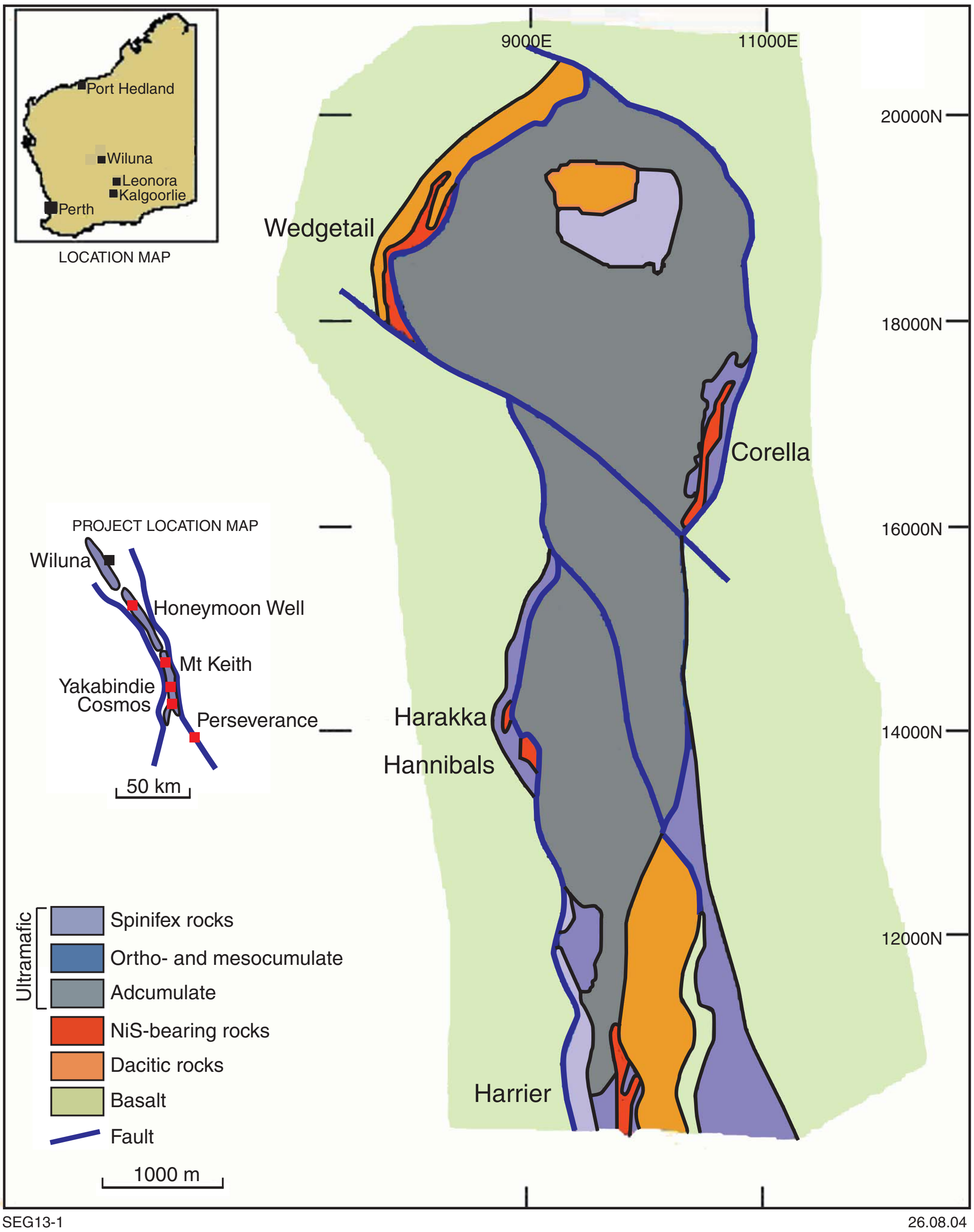

Figure 1. Location and geology of the Honeymoon Well project (local grid)

The surrounding rocks are dominantly andesitic to dacitic volcanic and volcanoclastic units separated by thin black shale and reworked volcanosedimentary horizons. The sequence has been intruded by dolerite, gabbro, and, locally, felsic dykes and sills.

All rocks have undergone lower greenschist facies regional metamorphism. Ultramafic rocks preserve evidence of sea-floor metasomatic processes, and local talc–carbonate–magnesite alteration along structures. In places, surrounding felsic volcanic rocks have focused a later gold-related silica–sericite–pyrite–arsenopyrite alteration event.

The ultramafic package generally dips steeply to the east and facing directions, documented in spinifex-textured komatiite flows, are generally to the west, suggesting that much of the belt is overturned. At the Wedgetail deposit, facing within the mineralized flow package is clearly to the west and, therefore, presents an intriguing and much-discussed spatial relationship with the massive sulfide distributed along the adjacent western felsic contact.

Mineralization

Nickel mineralization comprises mainly disseminated sulfides and lesser massive sulfide occurrences, in addition to extensive laterite deposits developed over many of the ultramafic rocks. Most of the previous drilling programs were testing for disseminated sulfides suitable for open

Table 1 Mineral resources as outlined by previous owners in 1995 feasibility study document

	Million tonnes	*Ni %*	*Ni tonnes*
Indicated Mineral Resources			
Hannibals	27.1	0.77	–
Harrier	37.5	0.65	–
Wedgetail	23.4	1.06	–
Corella	43.1	0.65	–
Total Indicated Resources	**131.5**	**0.75**	**986 000**
Inferred Mineral Resources			
Harraka	3.7	0.8	–
Total Inferred Resources	**3.7**	**0.8**	**30 000**

pit mining, similar to the Mount Keith deposit. As such, deeper drilling to test extensions to the mineralizing systems has not been systematically carried out. The mineralogy of the nickel sulfides is mainly pentlandite, with lesser amounts of millerite, violarite, and heazlewoodite.

Disseminated mineralization has been outlined in four main deposits — Hannibals, Harakka, Harrier, Corella, and Wedgetail. Economic studies by previous owners outlined a total Indicated Mineral Resource of 132 Mt at 0.75% Ni using a 0.5% cutoff (Table 1). Recent drilling by MPI Nickel has defined a separate massive sulfide resource at Wedgetail comprising Indicated and Inferred Mineral Resources of >1 Mt at 6.9% Ni. A feasibility study of the Wedgetail resource is ongoing.

Exploration

Exploration activity aims to infill and extend the Wedgetail massive sulfide resource, as well as explore for new sulfide targets elsewhere in the tenements.

The massive sulfide resource definition drill program at Wedgetail is targeted at defining an Indicated Mineral Resource to support a final feasibility study for a potential underground operation. Good lateral continuity has been demonstrated within several subhorizontal, massive sulfide channel horizons. Additional, structurally modified, high nickel tenor sulfide accumulations are developed locally along the channel flanks.

Some of the better results include 5.3 m at 10.12% Ni in 04HWD880; 9.7 m at 5.50% Ni in 04HWD890; 7.7 m at 5.54% Ni in 04HWD902; and 6.0 m at 9.43% Ni in 04HWD904. Significant mixed disseminated, vein, and matrix sulfide intercepts included 29.0 m at 2.51% Ni above massive sulfide in 04HWD880; and 19.0 m at 3.86% Ni in 04HWD889.

Drilling is now focused on testing the down-plunge continuity of defined channels, with success achieved at several locations (Fig. 2). Massive sulfide intercepts of 4.3 m at 7.2% Ni from 372 m, and 2.1 m at 11% Ni from 450 m have been made. A result of 0.2 m at 12.6% Ni from 527 m was returned from one of the deepest holes at 100 m step-out intervals, and strong downhole

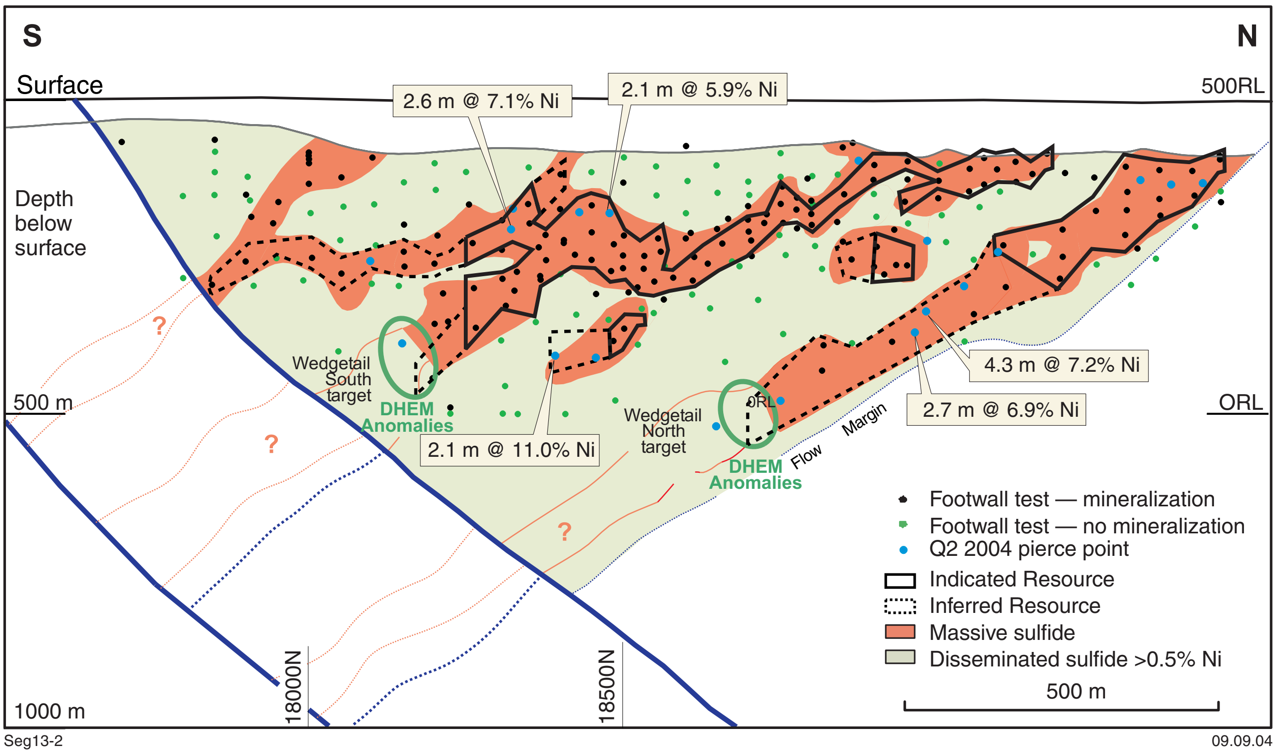

Figure 2. Schematic long section of Wedgetail showing higher grade drill intercepts as at June 2004

geophysical support was demonstrated. Indications are that additional massive sulfide resources will be defined as drilling progresses.

Trial EM surveys were carried out at Wedgetail to develop more effective depth penetration in the soil-covered portions of the Honeymoon Well and Albion Downs tenements, and this testwork continues. Exploration targets elsewhere at Honeymoon Well are being assessed, with several targets earmarked for drilling and downhole EM surveys.

Cosmos Nickel Project, Kathleen Valley

by

P. Langworthy[1]

Abstract

The Cosmos and Cosmos Deeps deposits together comprise the Cosmos Nickel Project, which is owned and operated by Sir Samuel Mines NL, a wholly owned subsidiary of Jubilee Mines NL. These two discrete, high grade, massive Ni–Fe sulfide deposits have a total Mineral Resource of 961 000 t at 8.2% Ni. Minor by-products include Cu, Co, and platinum group elements (PGE).

Cosmos is a typical Kambalda-style, komatiite-associated, massive sulfide deposit located close to surface, whereas the Cosmos Deeps deposit is a massive sulfide deposit that is interpreted to have been at least partly structurally remobilised, and is now hosted within the felsic volcanic rocks that form the footwall to the Cosmos deposit. Open pit mining of the Cosmos deposit is completed, and the Cosmos Deeps deposit is an underground mining operation using a combination of longhole open stopes and mechanized cut and fill.

Introduction

The Cosmos Nickel Project is located in the Kathleen Valley area, about 40 km north of Leinster in Western Australia (Fig. 1). It is located on the SIR SAMUEL (SG 51-13) 1:250 000 scale map sheet at latitude 27°36'04"S and longitude 120°34'28"E, about 700 km northeast of Perth and 700 km north of the port of Esperance.

In August 1997, routine evaluation of a prospective greenstone belt using a combination of geological, geochemical, and geophysical exploration techniques resulted in the discovery of the Cosmos deposit. Before mining commenced, the deposit contained a Mineral Resource of 401 000 t at 8.2% Ni. Openpit mining of the Cosmos deposit commenced in October 1999, with about 10 000 t of nickel metal in concentrate being produced per year, and production continued until mid-2003.

The Cosmos Deeps deposit was discovered in February 2000, following the drilling and geophysical testing of a conceptual geological target. The deposit has a Mineral Resource of 560 000 t at 8.2% Ni. Development of the underground mine commenced in December 2001, and ore production commenced in mid-2003.

[1] Jubliee Mines NL, 3rd Floor, 24 Outram Street, West Perth, W.A. 6005, Australia

The ore is processed through the Cosmos flotation plant at a rate of 400 t per day. To February 2004, 520 000 t of ore at a grade of 8.51% Ni has been processed, yielding about 217 000 t of sulfide concentrate grading about 20% Ni, with nickel recoveries averaging 95.3%. The product is exported to Canada via the port of Esperance. Based upon current ore reserves, and maintaining the current rate of nickel production, the Cosmos Nickel Project has an expected mine life until at least 2008.

Discovery and resources

The discovery of the Cosmos orebody in September 1997 was a turning point in Jubilee's evolution. The mine's rapid development, which culminated with first concentrate production in April 2000, marked Jubilee's transformation from explorer to miner and producer in just over two years.

During this period, the company negotiated native title agreements with indigenous claimant groups, clearing the way for the project to go ahead, completed a bankable feasibility study, signed a life of mine off-take agreement with Inco Limited of Canada, let major contracts to selected tenderers, and obtained a full debt finance package. Construction commenced in October 1999 and the Cosmos treatment plant was commissioned in April 2000.

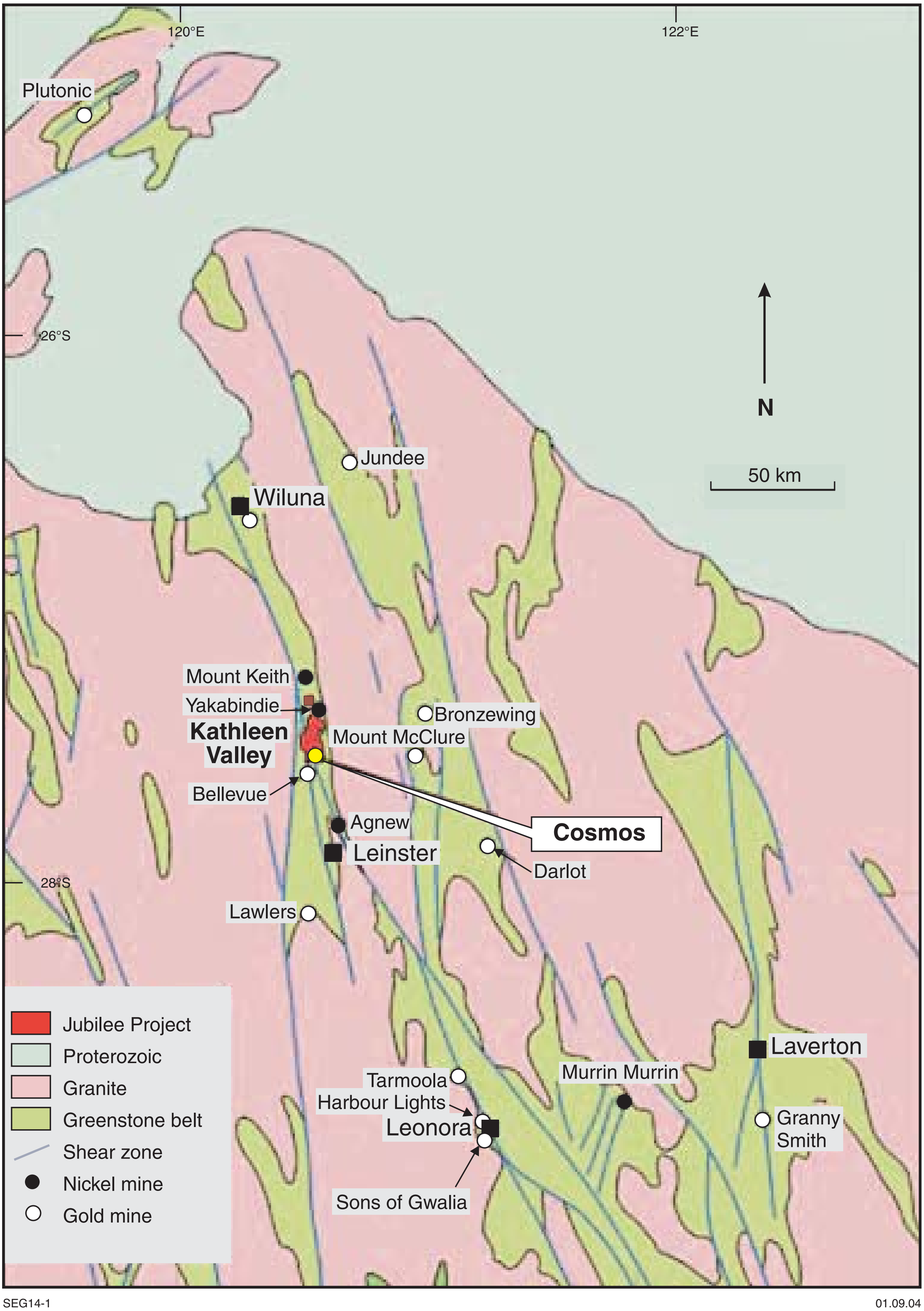

Figure 1. Location and regional geology of the Cosmos Nickel Project in the Kathleen Valley area

In early 1997, Jubilee made the decision to broaden its exploration focus to other commodities apart from gold, and this included sulfide nickel. The company recognized that its project areas within the Sir Samuel district contained a portion of the ultramafic units that elsewhere in the district host significant nickel sulfide resources, and therefore Jubilee's properties also had the potential to be prospective for this commodity type.

The Sir Samuel district has been explored intermittently for sulfide nickel since the late 1960s. The area around Cosmos was first explored by Anaconda Australia Inc. in 1970–72, and was known as the Mount Goode project. An ultramafic unit was identified and early reconnaissance work confirmed its prospectivity. This was drill tested with widely spaced lines of shallow rotary holes, several deep percussion holes, and several diamond drillholes. Many of the rotary holes returned elevated Ni values (up to 4–5% Ni), associated with high Cu values, from the weathered zone, and the follow-up percussion and diamond drillholes intersected several zones of disseminated nickel sulfide mineralization. It is now known that one of these diamond drillholes was located only about 100 m south of the Cosmos deposit, with the others located some 200–400 m north of Cosmos. At the end of the 1972 field season, Anaconda decided to work elsewhere in the district, and the Mount Goode project was terminated. Later, in the 1970s, WMC undertook some minor exploration but no significant results were obtained, and nickel exploration in this area lapsed until Jubilee commenced work in 1997.

Discovery of Cosmos

Jubilee commenced exploration in the vicinity of Anaconda's Mount Goode project, which was situated within the southern part of Jubilee's property. Initially, a reconnaissance rotary airblast (RAB) drilling program outlined a large zone of coincident near-surface Ni and Cu anomalism, thus confirming the earlier Anaconda results, and the prospect was named 'Cosmos'. This was followed by a reverse circulation (RC) drilling program, which intersected disseminated nickel sulfide mineralization.

The next phase of exploration comprised a multipronged geophysical approach involving a detailed moving loop electromagnetic (EM) survey, and a follow-up fixed loop EM survey. The EM surveys defined a very strongly conductive body about 150–200 m long and 100–150 m deep, commencing 50 m below surface. A line of RAB holes was drilled across the peak of the EM response, and one hole intersected strongly anomalous Ni, Cu, and PGE values.

The prospective geology, highly anomalous geochemistry, and the presence of disseminated nickel sulfide mineralization justified a decision to commence diamond drilling to test the modelled bedrock conductor. The geophysical component of this exploration program is discussed in detail by Craven et al. (2000).

The first diamond drillhole, JCD001, was drilled in August 1997 and intersected a 3 m-wide zone of massive sulfide mineralization grading at 7.5% Ni. The second drillhole was collared 40 m to the south, and intersected 22.3 m at 9.3% Ni in massive pentlandite–pyrrhotite mineralization. Some four months, 82 holes, and about 16 000 m of drilling later, the drill-out phase of the Cosmos deposit was completed. In February 1998, the Mineral Resource for the Cosmos deposit was announced as 401 000 t at 8.2% Ni. Upon completion of a feasibility study in June 1998, an Ore Reserve of 420 000 t at 7.5% Ni was announced.

Discovery of Cosmos Deeps

Soon after the commencement of open pit mining of the Cosmos deposit, continued exploration led to the discovery of the Cosmos Deeps deposit in January 2000 (Figs 2 and 3). Based upon a conceptual geological study that investigated the potential for repetitions of the Cosmos mineralization at depth, four 600 m-deep diamond drillholes were drilled beneath and along strike from the openpit. Spaced at 200 m intervals, these holes were designed to test the basal contact of the Cosmos ultramafic unit and its adjacent footwall zone, and provide EM coverage of the downdip extensions of the Cosmos mine sequence. Downhole EM surveys were carried out and one conductor was detected.

The target was subsequently drill tested and the first hole, JCD100, passed through the target horizon (base of ultramafic unit) without intersecting any nickel sulfide mineralization. However, when extending the hole into the felsic footwall in order to provide EM coverage of the target horizon, the hole passed through 5 m of massive sulfide mineralization grading at 8.8% Ni. During the next eight months, 65 diamond drillholes totalling about 23 200 m were drilled. In September 2000, the Mineral Resource for the Cosmos Deeps was announced as 560 000 t at 8.2% Ni. Upon completion of a feasibility study in April 2001, an Ore Reserve of 520 000 t at 7.2% Ni was announced.

Geological setting

Cosmos is situated within the Agnew–Wiluna portion of the Norseman–Wiluna greenstone belt, in the northeastern Eastern Goldfields Province of Western Australia. This is Australia's premier nickel sulfide producing district, containing the Mount Keith and Leinster mines, and the undeveloped deposits of Yakabindie, Cliffs, and Honeymoon Well. This portion of the belt is strongly attenuated, and characterized by large scale faults, complex folding, and typically steep dips. The greenstone sequence is bounded to the east and west by large granitoid bodies. The Cosmos project area is near the junction of the northwesterly trending regional Keith–Kilkenny Tectonic Zone and the northerly trending Miranda Shear. The junction is characterized by intense shearing and deformation, which has resulted in major local structural complexities.

Locally, the project area is divided into three geological zones, locally termed the Western, Central, and

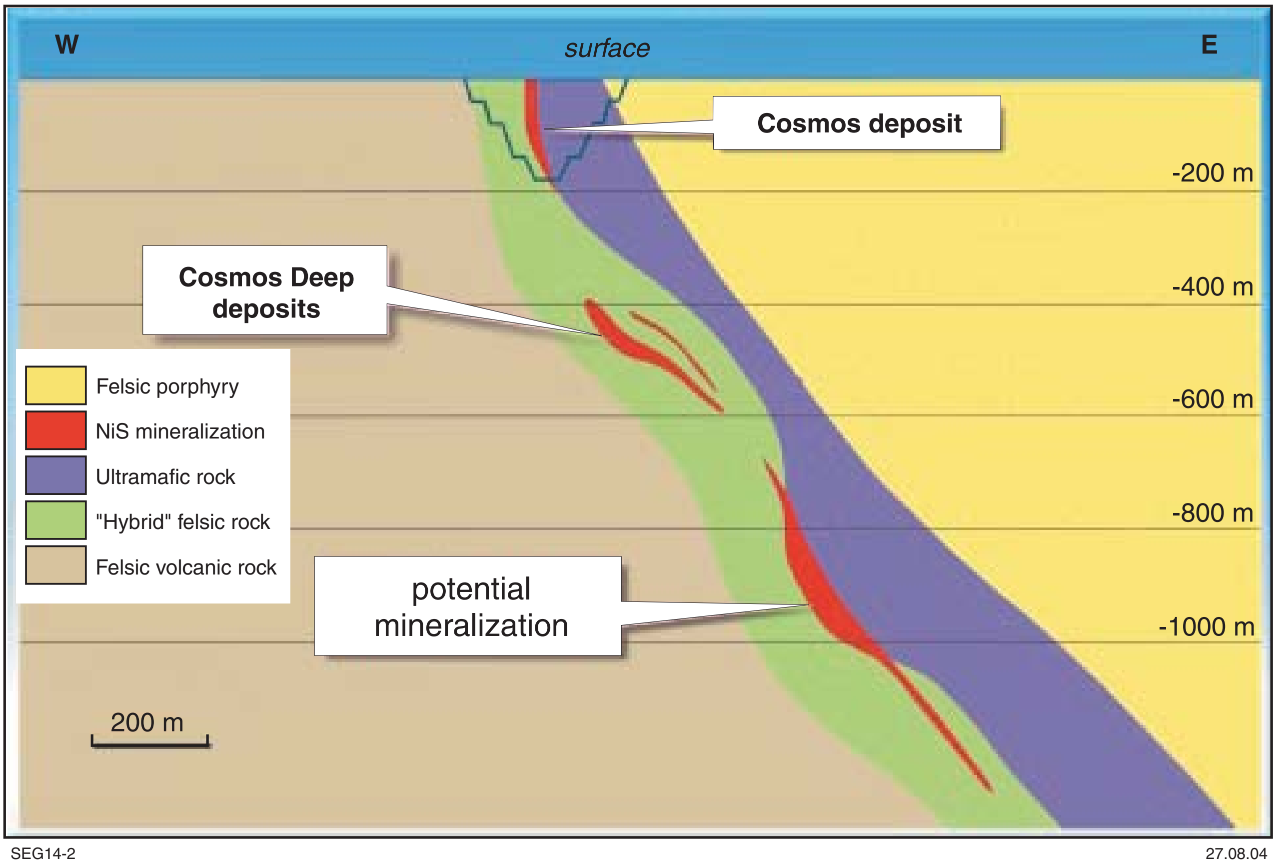

Figure 2. Geological cross section showing the geological setting of the Cosmos and Cosmos Deeps deposits

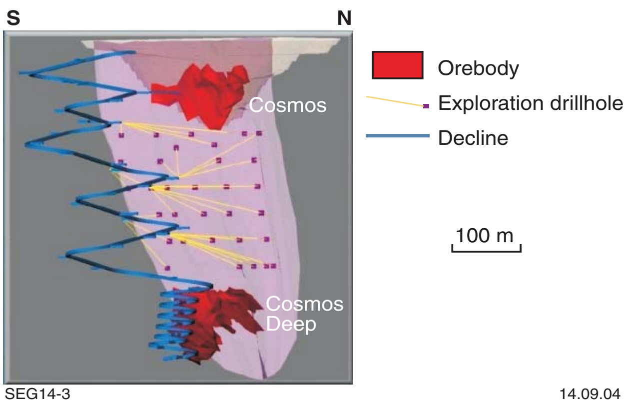

Figure 3. Three-dimensional illustration showing open pit development of the Cosmos deposit and underground development of the Cosmos Deep deposit

Eastern Zones. The Western Zone consists of a northeasterly striking and southeast-facing sequence of tholeiitic lavas, differentiated gabbroic sills, and ultramafic chloritic schists, metamorphosed to upper greenschist facies. The Eastern Zone comprises a northerly striking, east-dipping sequence of felsic, mafic and ultramafic volcanic and sedimentary rocks, with an upper greenschist to mid-amphibolite metamorphic grade. The ultramafic rocks consists of a series of komatiitic lava flows containing primary igeneous textures, including spinifex and cumulate textures, which have been variably hydrothermally altered. The ultramafic rocks in the Eastern Zone contain the nickel sulfide deposits at Leinster, Yakabindie, Mount Keith, and Honeymoon Well, and, before the discovery of Cosmos, were historically the target for most nickel exploration in the district.

The Western and Eastern Zones are separated by the Central Zone, which is a mixed package of rocks comprising the heterogeneous Jones Creek Conglomerate; felsic, mafic, and ultramafic volcanic rocks; felsic volcanoclastic sedimentary rocks; and doleritic and felsic porphyry intrusions. The Cosmos and Cosmos Deeps deposits are hosted within the Central Zone.

State of knowledge of the deposits

Local geology

The Cosmos deposits represent an essentially in situ accumulation of primary magmatic Ni–Fe sulfides. Mineralization is dominated by massive and semi-massive (breccia and stringer), Ni–Fe sulfides located at the base of an ultramafic unit hosted within the Central Zone. The ultramafic unit strikes north, is east facing, and dips between 50° east and vertical. It is structurally attenuated, varies up to 200 m in width, and is scattered within the Cosmos property over a distance of about 15 km. The ultramafic unit is strongly hydrothermally altered, serpentinized, and subsequently metamorphically recrystallized, and primary igneous textures are rarely preserved.

Around Cosmos, rocks are strongly weathered to a depth of about 30 m, the level of a cavernous silica layer. Beneath this, sulfide mineralization commences at about 40–60 m below surface. Before mining started, there were minor exposures of a gossan representing the weathered surface expression of the Cosmos sulfide mineralization.

At the southern end of the property, to the east, and overlying the ultramafic unit is a quartz–feldspar porphyry intrusion that is, in turn, overlain by the Jones Creek Conglomerate. The lower contact of the porphyry strikes northwest, potentially crosscutting and truncating the ultramafic unit in places. The porphyry is interpreted to terminate the Cosmos mineralization at the northern end of the pit, but drilling indicates that some ultramafic rocks remain along this contact and are mineralized in places. To the north, the ultramafic sequence widens again until terminated by what is interpreted to be an offsetting northeasterly trending fault.

Underlying the ultramafic unit and, in most areas, forming the footwall to the Cosmos massive sulfide mineralization is a mixed sequence of felsic breccia, volcanic and sedimentary rocks, and porphyries. The Cosmos Deeps mineralization, which consists of several zones of massive, breccia, and stringer Ni–Fe sulfides, is contained entirely within this package of rocks.

Recent structural studies of the Cosmos Deeps deposit have demonstrated that the contact between the footwall rocks and massive sulfides is most likely primary. Mineralization is fully enclosed in this footwall package of felsic breccia, volcanic and sedimentary rocks, and porphyries (with few ultramafic rocks), suggesting that that the hangingwall rocks have been thrust over the mineralization, thereby removing the ultramafic host. Additional information is being gathered to test this interpretation and develop the concept.

Further minor sulfide mineralization is present throughout the deposit as Fe, Ni, Cu, Pb, and Zn sulfides, as disseminated grains, fracture fillings, or within quartz veinlets. A dolerite dyke intrudes the ultramafic and felsic footwall in the southern part of the Cosmos area. The dyke commences about 40 m below surface, and is up to 50 m wide (east–west), 140 m long (north–south), and open at depth. It is massive, with no obvious signs of jointing or shearing, and has a fine-grained reaction rim at the contact with surrounding rocks. The upper surface plunges at about 50° to the north, and forms the footwall to the massive sulfide mineralization in the central part of the Cosmos deposit.

The Cosmos district is mostly covered by a veneer of alluvial sand and a few metres of residual lateritic soils. Bedrock exposures are rare and usually consist of small, isolated outcrops or subcrops of weathered felsic porphyry and felsic volcanic rocks. The area is cut by wide shallow creeks, which only flow occasionally and are mostly filled with sand. Vegetation consists of widely scattered shrubs, with the thickest growth in the drainage channels.

Cosmos mineralization

The Cosmos deposit comprises one discrete zone of massive and semi-massive sulfides that extends over a strike length of some 240 m, and has a vertical depth extent of about 120 m. The body has an average true width of about 7 m, with a maximum of 20 m. Mineralization is stratabound between the overlying ultramafic unit and the underlying dolerite and felsic volcanic rocks. There are sharp, relatively undeformed, contacts on both the hanging- and footwalls. Continuity of grade and width of mineralization are strong, both along strike and downdip. The massive sulfide domain is the most common ore type. It is defined as consisting of 81–100% sulfides containing moderate to abundant inclusions of felsic footwall rock and ultramafic hangingwall rock. Locally, there are minor disseminated sulfides within the ultramafic inclusions and the ultramafic rocks directly overlying massive and semi-massive mineralization.

From the surface to the base of complete oxidation (about 40 m deep), the sulfide body has weathered to a vuggy goethite–silicate rock. Sporadic outcrops of gossan were exposed prior to commencement of mining. Geochemically, this gossan contained elevated values of Ni, Cu, PGE, and other pathfinder elements.

The supergene and transitional zones are below 40 m depth, and are characterized by an alteration assemblage of violarite–pyrite–marcasite after pentlandite–pyrrhotite. With increasing depth, the proportion of pentlandite–pyrrhotite increases until about 60 m below surface, where the mineral assemblage is mostly primary.

Within the primary zone, the mineralization consists of intergrowths of equal proportions of pentlandite and pyrrhotite with subsidiary chalcopyrite. Pentlandite is the dominant Ni-bearing sulfide species, with only scattered grains of other nickel sulfide minerals being observed petrologically. Accessory sulfides include pyrite, sphalerite, and galena. Much of the primary ore consists of coarse pentlandite crystals, up to 2 cm in diameter, in a matrix of finely intergrown pentlandite and pyrrhotite. Less commonly, there are alternating pentlandite- and pyrrhotite-rich bands up to a few centimetres thick. Chalcopyrite forms fine to coarse blebs through the massive sulfide, particularly near the base of the body, and also rims silicate inclusions.

Cosmos Deeps mineralization

The Cosmos Deeps deposit consists of several bodies of massive, breccia, and stringer nickel sulfide mineralization contained entirely within the felsic footwall to the Cosmos ultramafic unit. These bodies have been termed the Main Zone and Hangingwall Zones. The Main Zone is a large coherent body of massive sulfides that contains over 90% of the total nickel endowment of the deposit, and has been defined in the Measured and Indicated Mineral Resource categories. It demonstrates excellent internal geological and grade continuity, and, consequently, most of the Mineral Resource was converted to the Proved and Probable Ore Reserve categories. The Hangingwall Zones consist of several discrete ribbons of sulfide mineralization located 10–30 m stratigraphically above the Main Zone. Their widths vary and, as there is a high degree of internal dilution, they have poor grade continuity. Consequently, the Hangingwall Zones have been assigned to the Inferred Mineral Resource category, and have not been converted to an ore reserve. The Hangingwall Zones will be further explored and delineated from underground.

The Main Zone begins about 450 m below surface and extends to at least 600 m in depth. It is about 120 m long, has a maximum thickness of 20 m, and dips to the northeast at about 35°. The mineralization has a very sharp footwall contact and an erratic, feathery hangingwall contact, and remains open both along strike and downdip. The Cosmos Deeps mineralization is mineralogically similar to that of the Cosmos deposit, with coarse grained pentlandite crystals in a fine grained matrix of intergrown pentlandite–pyrrhotite mineralization, with equivalent amounts overall of pentlandite and pyrrhotite. The nickel content of the 100% massive sulfides is almost always greater than 12% Ni, although the grade of mineralization depends on the volume of inclusions. Medium to fine grained chalcopyrite is common near the margins of the mineralization and rimming felsic inclusions. There are some significant differences, however, between the Cosmos and Cosmos Deeps deposits.

The Cosmos Deeps mineralization contains:

- large cubes of pyrite (up to 15 cm) scattered randomly through the massive ore;
- felsic, ultramafic, and dolerite clasts up to 1 m across;
- significant accumulations of massive sphalerite and galena, which are present on the northern footwall.

Geological and genetic models for the deposits

Cosmos

The Cosmos mineralization occurs as a massive nickel sulfide deposit typical of the Type 1 style of mineralization as defined by Dowling and Hill (1998). Examples additional to Cosmos include Kambalda, Silver Swan, Perseverance, and Rocky's Reward. Cosmos is a syngenetic deposit located along the basal contact of a komatiitic lava channel. The presence of partially rounded felsic footwall inclusions suggests that there was partial melting and thermal erosion of the sulfide-rich felsic substrate. However, the absence of matrix and disseminated mineralization directly above the deposit suggests that the sulfide body was decoupled from the primary komatiite liquid. Subsequent structural activity has resulted in the sequence being tilted into a steeply east-dipping and east-facing position. Metamorphism has recrystallized pentlandite into coarse grained granoblasts within a fine grained, mixed sulfide matrix, with localized mineralogical banding produced by a low intensity ductile tectonic regime.

Cosmos Deeps

The Cosmos Deeps deposit has, until recently, been interpreted as a body of massive nickel sulfide mineralization that was structurally remobilized from the Cosmos deposit into a dilational zone within the felsic footwall.

Supporting evidence for this model includes:

- similar sulfide mineralogies and geochemical signatures of the two mineralized bodies;
- distinct breccia and recrystallization textures within the sulfide mineralization;
- eclectic mixture of different wallrock clast types present within the sulfide mineralization;
- encapsulation of the orebody within a footwall rock package at least 60 m beneath the base of the ultramafic unit;
- presence of en echelon extensional fractures filled with sulfides, including pentlandite, hosted within the footwall rock package and oriented parallel to the main ore horizon;

- location of the Cosmos Deeps mineralization where there is a significant change in the orientations of the bounding structures and the geological units.

As discussed above, an alternative model is being developed following a detailed structural review based on mapping of underground exposures. The new model suggests that the basal contact of the sulfides is largely in situ, with little or no structural modification. Evidence that the hangingwall is comprised of the same rock package and little ultramafic unit remains in contact with the sulfides is explained by thrusting of the hangingwall package over the massive sulfides, and structural removal of the ultramafic unit. Minor remobilization of the sulfides along thrust planes has resulted in the development of the hangingwall lodes and incorporation of country rock into the sulfide body. Detailed evaluation of this model is underway.

Significance of the Cosmos Deposits in exploration models

There are several significant aspect of the Cosmos and Cosmos Deeps deposits that have implications for the exploration for such bodies.

1. Prior to these discoveries, all known nickel sulfide occurrences in this district were contained within the ultramafic units of the eastern part of the greenstone belt. The Cosmos and Cosmos Deeps deposits are in the Western Ultramafic unit (Dowling and Hill, 1990) and, to date, are the only nickel sulfide deposits to have been discovered in this unit. This has opened up a new area of nickel sulfide prospectivity.
2. The location of Cosmos Deeps within the footwall stratigraphy has similarities with many other deposits (Rockys Reward, Maggie Hays, and 1A Shoot). It continues to highlight the need to focus nickel exploration within the footwall sequences of ultramafic sequences as well as throughout the ultramafic rocks.
3. These discoveries have demonstrated that very high grade nickel sulfide deposits, similar to Silver Swan and some at Kambalda, can and do occur in the Agnew–Wiluna district. The extremely high unit value of this type of deposit makes them an attractive exploration target.
4. The Cosmos deposit is close to the surface, and gossan was present at surface, indicating that undiscovered nickel sulfide deposits can and probably still do exist in Western Australia, even in areas that have undergone significant levels of previous exploration.

Mine production

The Cosmos Nickel Project is based on both openpit and underground (underneath the Cosmos pit) mining. Mining commenced in October 1999 using conventional selective openpit techniques. Openpit mining was completed in July 2003.

Development of the Ilias decline, to access the Cosmos Deeps orebody, commenced in December 2001. The decline was developed at a gradient of 1 in 7 down, to intersect the orebody some 500 m below surface. The first ore was produced from Cosmos Deeps in June 2003, with production from the mineable reserve of 520 000 t at 7.2% Ni (containing 37 000 t of nickel metal) expected to continue until 2008.

The project uses conventional processing technology developed by the world's major nickel producers over the past 40–50 years. The plant comprises a crusher, semi-autogenous grinding (SAG) mill, flotation plant, cyclones, thickener, and filter, and is designed to annually process 150 000 t of ore to produce 10 000 t nickel in concentrate. Considerable effort has been expended in optimizing the performance of the plant, and recoveries in excess of 97% are being achieved on a regular basis.

The concentrate is dispatched by road to Leonora and then by rail to Esperance for shipping to Inco under an off-take agreement that included the first 30 000 t of nickel metal from the Cosmos Deeps project. Based on current reserves, Cosmos will be a profitable producer until at least 2008.

Mine production

This paper is an updated and edited version of a paper prepared by Tony Rovira. There have been additions and deletions to reflect new information. As previously acknowledged by Tony, I thank all Jubilee Mine's geoscientific colleagues (past and present) whose fieldwork, research, and advice have resulted in the current detailed understanding of the geology of the Cosmos and Cosmos Deeps ore deposits. There has also been significant input from various consultants and academic workers. The manuscript was proofread by Karyn Lyons, Steve Vallance, and Peter Thompson, whose suggestions were gratefully received.

References

CRAVEN, B., ROVIRA, A., GRAMMER, T., and STYLES, M., 2000, The role of geophysics in the discovery and delineation of the Cosmos nickel sulphide deposit, Leinster area, Western Australia: Exploration Geophysics, v. 31, p. 201–209.

DOWLING, S. E., and HILL, R. E. T., 1990, Rivers of fire: the physical volcanology of komatiites in the Mount Keith region, Norseman–Wiluna greenstone belt, Western Australia: CSIRO Restricted Investigation Report EG103R (unpublished).

DOWLING, S. E., and HILL, R. E. T., 1998, Komatiite-hosted nickel sulphide deposits, Australia: AGSO Journal of Australian Geology and Geophysics, v. 17, p. 121–127.

NEUMAYR et al.

Gold and nickel deposits in the Archaean Norseman–Wiluna greenstone belt, Yilgarn Craton, Western Australia — a field guide

SEG 2004 EXCURSION GUIDE

RECORD 2004/16

Further details of geological publications and maps produced by the Geological Survey of Western Australia can be obtained by contacting:

Information Centre
Department of Industry and Resources
100 Plain Street
East Perth WA 6004
Phone: (08) 9222 3459   Fax: (08) 9222 3444
www.doir.wa.gov.au/gswa/onlinepublications